REV LTR

THE BOEING COMPANY

AIRPLANE DIVISION
P.O. BOX 707
RENTON, WASHINGTON 98055

CODE IDENT. NO. 81205

NUMBER D6-15000

NASA CR-62036

TITLE: Large Transport Landing Characteristics as Simulated in Flight and on the Ground

FOR LIMITATIONS IMPOSED ON THE USE OF THE INFORMATION CONTAINED IN THIS DOCUMENT AND ON THE DISTRIBUTION OF THIS DOCUMENT, SEE LIMITATIONS SHEET.

MODEL 367-80 CONTRACT NAS2-3224

ISSUE NO. 26 ISSUED TO: Nasa Ames

PREPARED BY J. W. Kerrigan — J. W. Kerrigan — 2/4/66

PREPARED BY R. G. Root — R. G. Root — 2/4/66

SUPERVISED BY _____ — L. G. Kimbrel — _____

APPROVED BY _____ — H. C. Higgins — _____

APPROVED BY _____ (DATE)

ACTIVE SHEET RECORD

SHEET NUMBER	REV LTR	ADDED SHEETS				SHEET NUMBER	REV LTR	ADDED SHEETS			
		SHEET NUMBER	REV LTR	SHEET NUMBER	REV LTR			SHEET NUMBER	REV LTR	SHEET NUMBER	REV LTR
Title Page						VI-43					
1						VI-44					
ii						VI-45					
iii						VI-46					
iv						VI-47					
2						VI-48					
3						VI-49					
I-4						VI-50					
II-5						VI-51					
III-6						VI-52					
III-7						VI-53					
III-8						VI-54					
III-9						VI-55					
IV-10						VI-56					
IV-11						VI-57					
IV-12						VII-58					
IV-13						VII-59					
IV-14						VII-60					
V-15						VII-61					
V-16						VII-62					
VI-17						VII-63					
VI-18						VII-64					
VI-19						VII-65					
VI-20						VII-66					
VI-21						VII-67					
VI-22						VII-68					
VI-23						VII-69					
VI-24						VII-70					
VI-25						VII-71					
VI-26						VII-72					
VI-27						VII-73					
VI-28						VII-74					
VI-29						VII-75					
VI-30						VII-76					
VI-31						VII-77					
VI-32						VII-78					
VI-33						VII-79					
VI-34						VII-80					
VI-35						VII-81					
VI-36						VII-82					
VI-37						VII-83					
VI-38						VII-84					
VI-39						VII-85					
VI-40						VII-86					
VI-41						VII-87					
VI-42						VII-88					

ACTIVE SHEET RECORD

SHEET NUMBER	REV LTR	ADDED SHEETS				SHEET NUMBER	REV LTR	ADDED SHEETS			
		SHEET NUMBER	REV LTR	SHEET NUMBER	REV LTR			SHEET NUMBER	REV LTR	SHEET NUMBER	REV LTR
VII-89						IX-135					
VII-90						X-136					
VII-91						X-137					
VII-92						X-138					
VII-93						X-139					
VII-94						X-140					
VII-95						X-141					
VII-96						X-142					
VII-97						X-143					
VII-98						X-144					
VII-99						X-145					
VII-100						X-146					
VII-101						X-147					
VIII-102						A1-1					
VIII-103						A1-2					
VIII-104						A1-3					
VIII-105						A1-4					
VIII-106						A1-5					
VIII-107						A1-6					
VIII-108						A1-7					
VIII-109						A1-8					
VIII-110						A1-9					
VIII-111						A1-10					
VIII-112		VIII-112A				A1-11					
VIII-113						A1-12					
VIII-114						A1-13					
VIII-115						A1-14					
VIII-116						A1-15					
VIII-117						A1-16					
VIII-118						A1-17					
VIII-119						A1-18					
VIII-120						A1-19					
VIII-121						A1-20					
VIII-122						A1-21					
IX-123						A1-22					
IX-124						A1-23					
IX-125						A2-1					
IX-126						A2-2					
IX-127						A2-3					
IX-128						A2-4					
IX-129						A2-5					
IX-130						A2-6					
IX-131						A2-7					
IX-132						A2-8					
IX-133						A2-9					
IX-134						A2-10					

ACTIVE SHEET RECORD

SHEET NUMBER	REV LTR	ADDED SHEETS				SHEET NUMBER	REV LTR	ADDED SHEETS			
		SHEET NUMBER	REV LTR	SHEET NUMBER	REV LTR			SHEET NUMBER	REV LTR	SHEET NUMBER	REV LTR
A3-1											
A3-2											
A4-1											
A4-2											
A4-3											
A4-4											
A4-5											
A4-6											
A4-7											
A4-8											
A4-9											
A4-10											
A4-11											
A4-12											
A5-1											
A5-2											
A5-3											
A5-4											
A5-5											
A5-6											
A5-5											
A5-6											
A6-1											
A6-2											
A6-3											

REVISIONS			
REV SYM	DESCRIPTION	DATE	APPROVAL

Table of Contents

Table of Contents (cont'd)

I. SUMMARY

32624

The stability and control characteristics during low speed landing approaches of various Ames large transport configurations were evaluated using the Boeing 367-80 airplane and the Ames moving base analog simulator. This report documents comparisons of the 367-80 and the moving base simulators to the theoretically calculated characteristic responses of the large transport configurations. For all maneuvers performed the simulation accuracy was satisfactory. AUTHOR

II References

1. D6-19860. 367-80 Airplane Variable Stability Simulation System (NASA Ames Large Transport Simulation Program). (NASA CR-62037)

2. Etkin, Bernard; Dynamics of Flight. John Wiley & Sons, Inc., 1962.

III. LIST OF ILLUSTRATIONS

IV. SYMBOLS

Coefficients and Derivatives

C_D	Drag Coefficient, Drag/qS_w
C_L	Lift Coefficient, Lift/qS_w
C_l	Rolling Moment Coefficient, Rolling Moment/$qS_w b$
C_m	Pitching Moment Coefficient, Pitching Moment/$qS_w \bar{c}$
C_n	Yawing Moment Coefficient, Yawing Moment/$qS_w b$
C_y	Side Force Coefficient, Side Force/qS_w
$C_{D_{\alpha=0}}$	Drag Coefficient at $\alpha = 0$
C_{D_α}	Drag-Curve Slope, $\partial C_D/\partial \alpha$
$C_{L_{\alpha=0}}$	Lift Coefficient at $\alpha = 0$
C_{L_α}	Lift-Curve Slope, $\partial C_L/\partial \alpha$
$C_{L_{\dot{\alpha}}}$	Lift Coefficient Due to Angle-of-Attack Rate $\partial C_L/\partial \dot{\alpha}$
C_{L_δ}	Lift Coefficient Due to Surface Deflection $\partial C_L/\partial \delta$
$C_{L_{i_H}}$	Lift Coefficient Due to Horizontal Stabilizer Incidence $\partial C_L/\partial i_H$
C_{L_q}, $C_{L_{\dot{\theta}}}$	Lift Coefficient Due to Pitch Rate, $\partial C_L/\partial q$
C_{l_β}	Effective Dihedral Derivative, $\partial C_l/\partial \beta$
C_{l_δ}	Roll Control Derivative, $\partial C_l/\partial \delta$
C_{l_p}, $C_{l_{\dot{\phi}}}$	Rolling Moment Due to Roll Rate, $\partial C_l/\partial p$
C_{l_r}, $C_{l_{\dot{\psi}}}$	Rolling Moment Due to Yaw Rate, $\partial C_l/\partial r$
$C_{m_{\alpha=0}}$	Pitching moment Coefficient at $\alpha = 0$
C_{m_α}	Static Longitudinal Stability Derivative, $\partial C_m/\partial \alpha$
$C_{m_{\dot{\alpha}}}$	Pitching Moment Coefficient Due to Angle-of-Attack Rate, $\partial C_m/\partial \dot{\alpha}$

C_{m_δ}	Pitch Control Power Derivative, $\partial C_m / \partial \delta$
$C_{m_{i_H}}$	Pitching Moment Due to Horizontal Stabilizer Incidence, $\partial C_m / \partial i_H$
C_{m_q}, $C_{m_{\dot{\theta}}}$	Pitching Moment Coefficient Due to Pitch Rate, $\partial C_m / \partial q$
C_{n_β}	Static Directional Stability Derivative, $\partial C_n / \partial \beta$
C_{n_δ}	Yawing Moment Coefficient Due to Surface Deflection, $\partial C_n / \partial \delta$
C_{n_p}, $C_{n_{\dot{\phi}}}$	Yawing Moment Coefficient Due to Roll Rate, $\partial C_n / \partial p$
C_{n_r}, $C_{n_{\dot{\psi}}}$	Yawing Moment Coefficient Due to Yaw Rate, $\partial C_n / \partial r$
C_{Y_β}	Side-Force Derivative, $\partial C_Y / \partial \beta$
C_{Y_δ}	Side-Force Coefficient Due to Surface Deflection, $\partial C_Y / \partial \delta$
C_{Y_p}, $C_{y_{\dot{\phi}}}$	Side-Force Coefficient Due to Roll Rate, $\partial C_Y / \partial p$
C_{Y_r}, $C_{y_{\dot{\psi}}}$	Side-Force Coefficient Due to Yaw Rate, $\partial C_Y / \partial r$
C_μ	BLC Blowing Coefficient
$\dot{(\ )}$	Time derivative $d(\ ) / dt$

General

a.c.	Aerodynamic Center
a_y	Side Acceleration Normal to the Flight Path
a_z	Vertical Acceleration Normal to the Flight Path (positive downward)
b	Wing Span
c	Chord
$\bar{c}$	Mean Aerodynamic Chord

F	Control Force
g	Gravitational Constant, 32.2 feet/second^2
GW	Gross Weight
h	Altitude
I	Moment of Inertia Slug-feet^2
IRIG	Clock Time
i_H	Horizontal Stabilizer Incidence Relative to the Wing Chord Plane
L	Rolling Acceleration, $C_{l_\delta} \delta_{MAX}\ qSb/I_{xx}$ Lift Acceleration, a_z/V, $\frac{C_{L_\alpha} \alpha qS}{mv}$, $\frac{C_{L_\delta} \delta qS}{mv}$
m	Mass
M	Pitching Acceleration $\frac{C_{m_\delta} \delta_{max} q S \bar{C}}{I_{yy}}$
MAC or m.a.c.	Mean Aerodynamic Chord
M_{CG}	Pitching Moment about CG
n, n_z	Load Factor, g's (body axis)
P	Damped Period
p	Rolling Velocity
q	Dynamic Pressure, Pitching Velocity
r	Yawing Velocity
S	Area
T, TH	Thrust
$T_{1/2}$, $t_{1/2}$	Time to Half Amplitude
$t_{\delta a\ max}$	Time to maximum aileron
U	Change in Velocity
V_e	Equivalent Airspeed
V_i	Indicated air speed

V_S	Velocity at Stall
V_T	True Airspeed
W	Weight
α	Angle of Attack of Horizontal Reference Line
α_W	Angle of Attack of the wing mean chord
β	Sideslip Angle
β_{NB}	Sideslip Angle measured at nose boom
δ	Surface Deflection
γ	Flight Path Angle
ζ	Damping Ratio
θ	Angle between the Horizontal Reference Line and the Horizon
τ	Time Constant
ϕ	Roll Angle
ψ	Yaw Angle
$\lvert\phi\rvert/\lvert\beta\rvert$	Roll Angle to Sideslip Ratio
ω_d	Dutch Roll Undamped Natural Frequency
ω_n	Undamped Natural Frequency
ω_D	Damped Natural Frequency

Subscripts

a, A	Aileron
a.c.	Aerodynamic Center
C	Thrust modulator clamshell door
CG	Center of Gravity
Col	Column
d	Dutch Roll
e, E	Elevator
H	Horizontal Stabilizer
MAX	Maximum
N	Net
O	Reference, Free Stream
P	Pedal
r, R	Rudder, Roll mode
s	Spoiler
SB	Speed Brake
S.P.	Short Period
ss	Steady State
trim	Trim Condition
W, WH	Wheel
XX, YY, ZZ, XZ,	Moment of Inertia Designation

V. INTRODUCTION

Large transport airplanes of the type capable of making shortfield landings at 500,000 lb gross weight were evaluated using the Boeing 367-80 in-flight dynamic simulator in conjunction with the Ames Moving Base Transport Simulator, during late 1965 (7 September to 14 December). Stability and control characteristics in the landing approach were evaluated by NASA/Ames pilots. The ground based simulation was used to investigate a large number of configurations while the in-flight simulation was used to substantiate the results.

The purpose of this report is to describe and document the configurations evaluated on the 367-80 and the ground-based simulators. The accuracy and validity of the simulations are shown in Section VI where response characteristics are presented in detail for basic or typical configurations. Response characteristics of other important configurations are shown in Sections VII, VIII and IX along with a tabulation of dynamic characteristics for all of the configurations evaluated. Section IX presents the response characteristics of the Boeing 367-80 with boundary layer control, one of the configurations evaluated. Section X compares the inflight and ground based simulations of several configurations. The documentation maneuvers performed to measure these characteristics are described in Appendix 6.

The Boeing 367-80 airplane (707 prototype) is shown in Fig. 1. Its description as a five-degree-of-freedom variable stability airplane for in-flight dynamic simulation of a large transport airplane is detailed in Reference 1. A description of the Ames moving base transport simulation system is given in Appendix 5.

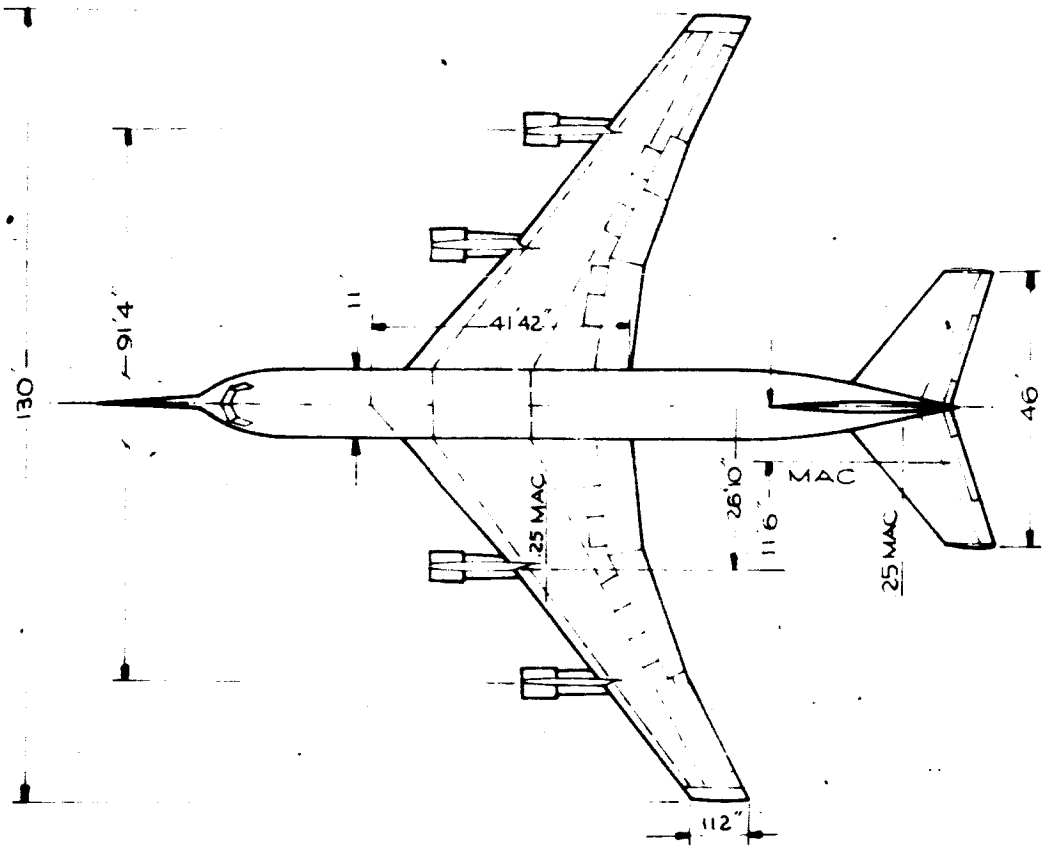

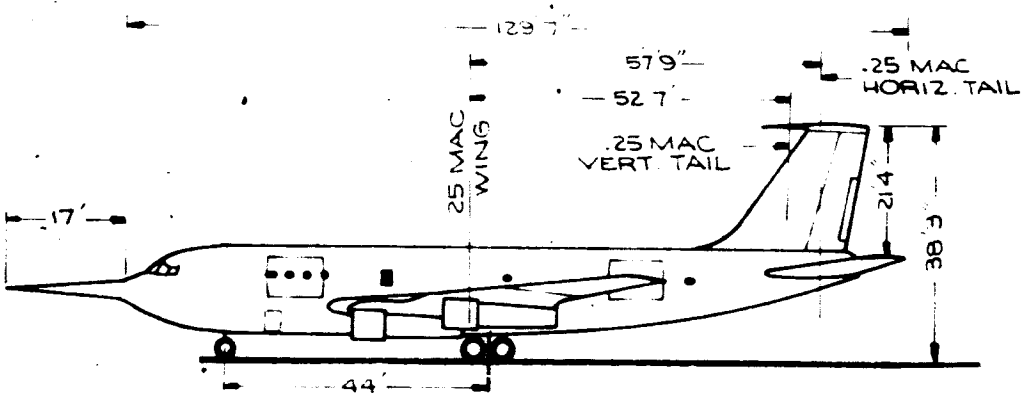

WING:		HORIZONTAL TAIL:		VERTICAL TAIL	
AREA	2821.36FT²	AREA	625FT²	AREA	312 FT²
ASPECT RATIO	6.0	ASPECT RATIO	3.37	ASPECT RATIO	1.46
SWEEP @ .25$\bar{c}$	35.0°	SWEEP @ .25$\bar{c}$	35.0°	SWEEP @ .25$\bar{c}$	31.0°
INCIDENCE	2.0°	TAPER RATIO	.421	TAPER RATIO	.45
DIHEDRAL	7.0°	DIHEDRAL	7.0°	$\bar{V}_V$	.0447
MAC	20.05FT	$\bar{V}_H$	.638		

CALC			REVISED	DATE	367-80 CHARACTERISTICS	D6-1[illegible]
CHECK						FIG. 1
APR.					THE BOEING COMPANY RENTON, WASHINGTON	PAGE V 16
APR.						

VI. Documentation of the Basic Configuration

A. Airborne Simulation

The characteristics of the basic longitudinal configuration (designated 101A) and the basic lateral configuration (designated 1209) for a large transport aircraft are presented in Figs. 2 to 21. The maneuvers performed to determine the aerodynamic characteristic are listed below along with brief comments on the agreement between flight test data and theory. The theoretical characteristics shown are derived in Appendix 4.

Longitudinal:

Maneuver	Comments
Pitch Rate Reversal	Fig. 2. The 367-80 accurately simulated the basic 101A configuration for a pitch rate reversal. An example of how the data was obtained is shown in Fig. 3.
Column Step	Fig. 4. A time lag is evident in the flight test time history when compared to a theoretically calculated column step. This is probably caused by aerodynamic and control surface lags which are not included in the theory. The column step was usually reversed prematurely before the peak load factor was reached.
Wind Up Turn	Figs. 5 & 6. The wind up turn flight test data agrees quite well with theory when the data are shifted to allow for mis-trim during the flight test.
Speed Stability	Fig. 7. The flight test data shows a slight mis-trim but otherwise agrees quite well with theory for configuration 101A.

PITCH RATE REVERSAL

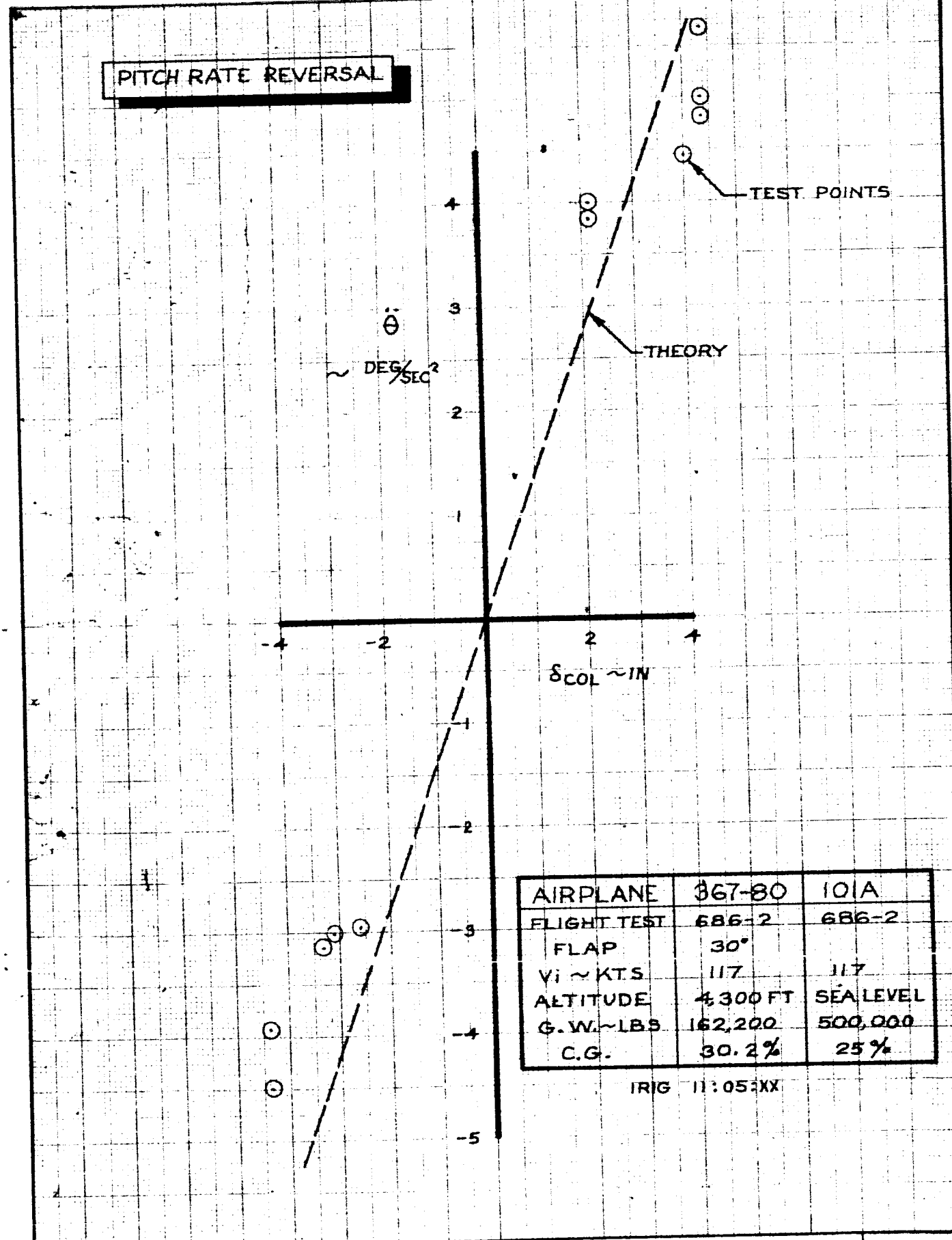

AIRPLANE	367-80	101A
FLIGHT TEST	686-2	686-2
FLAP	30°	
V_i ~ KTS	117	117
ALTITUDE	4,300 FT	SEA LEVEL
G.W.~LBS	162,200	500,000
C.G.	30.2%	25%

IRIG 11:05:XX

CALC			REVISED	DATE
CHECK				
APR				
APR				

PITCH RATE REVERSAL
FLIGHT TEST 686-2
CONFIGURATION 101A

367-80

FIG. 2

THE BOEING COMPANY D6-15000

TD 461 C-R4

PITCH RATE REVERSALS

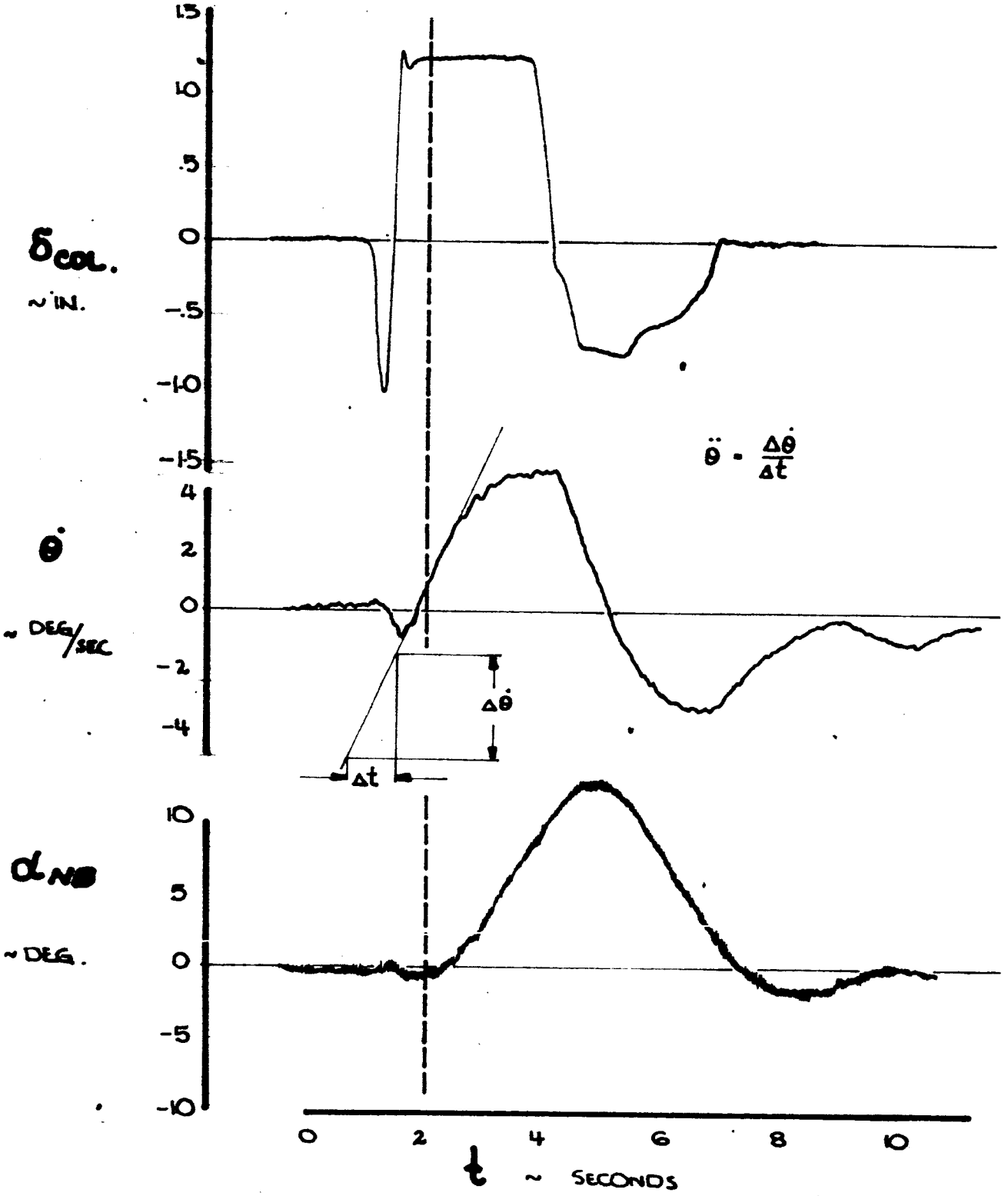

ENGR.			REVISED	DATE	SAMPLE OF FLIGHT TEST DATA FOR PITCH RATE REVERSALS	D6-15000
CHECK						FIG. 3
APR						
APR					THE BOEING COMPANY RENTON, WASHINGTON	VI-19

AD 1017-R6

6-7000

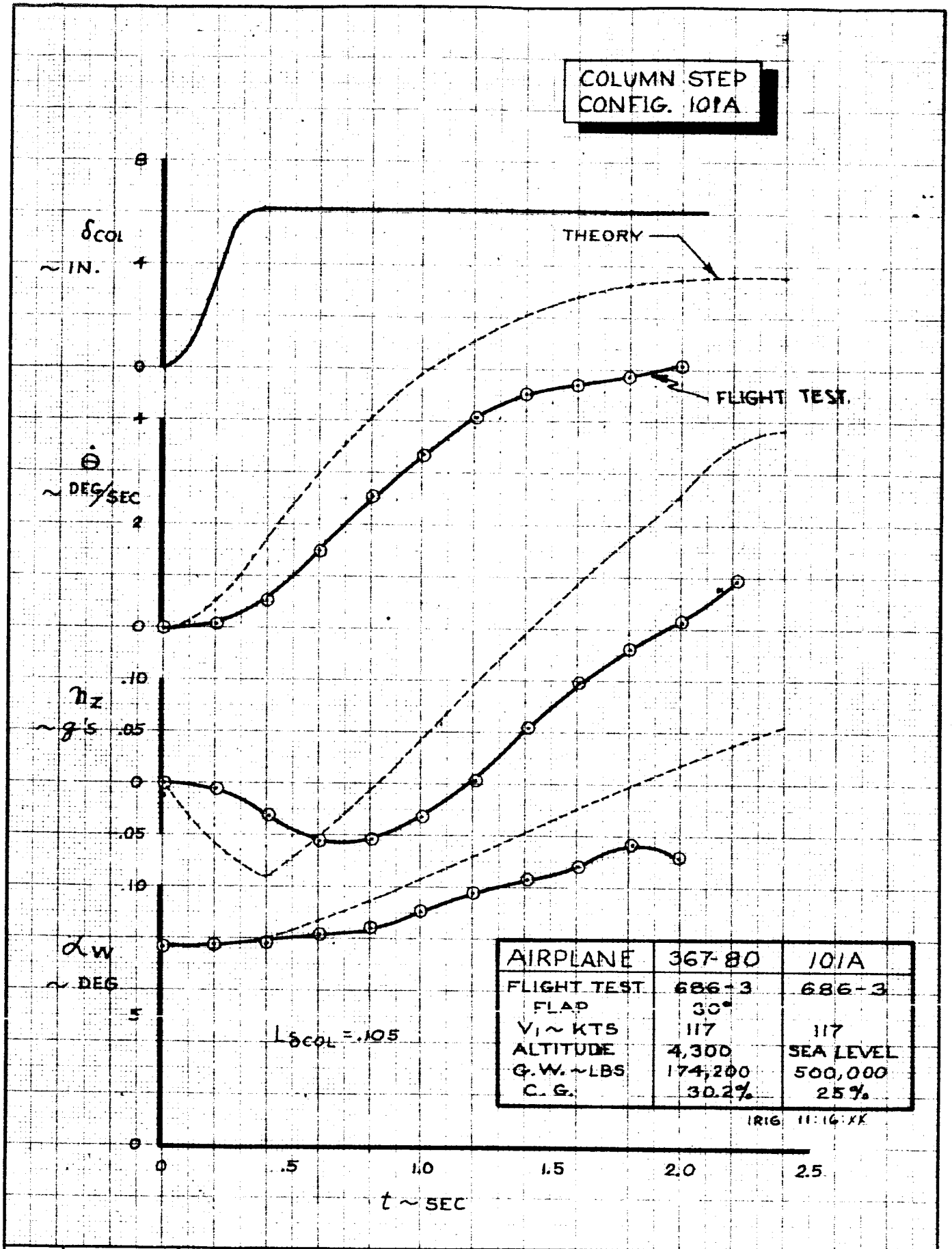

AIRPLANE	367-80	101A
FLIGHT TEST	686-3	686-3
FLAP	30°	
V_I ~ KTS	117	117
ALTITUDE	4,300	SEA LEVEL
G.W. ~ LBS	174,200	500,000
C. G.	30.2%	25%

CALC			REVISED	DATE
CHECK				
APR				
APR				

COLUMN STEP
FLIGHT TEST 686-3
CONFIGURATION 101A

367-80

FIG. 4

THE BOEING COMPANY D6-15000

PAGE VI-20

TD 461 C-R4

WINDUP TURN

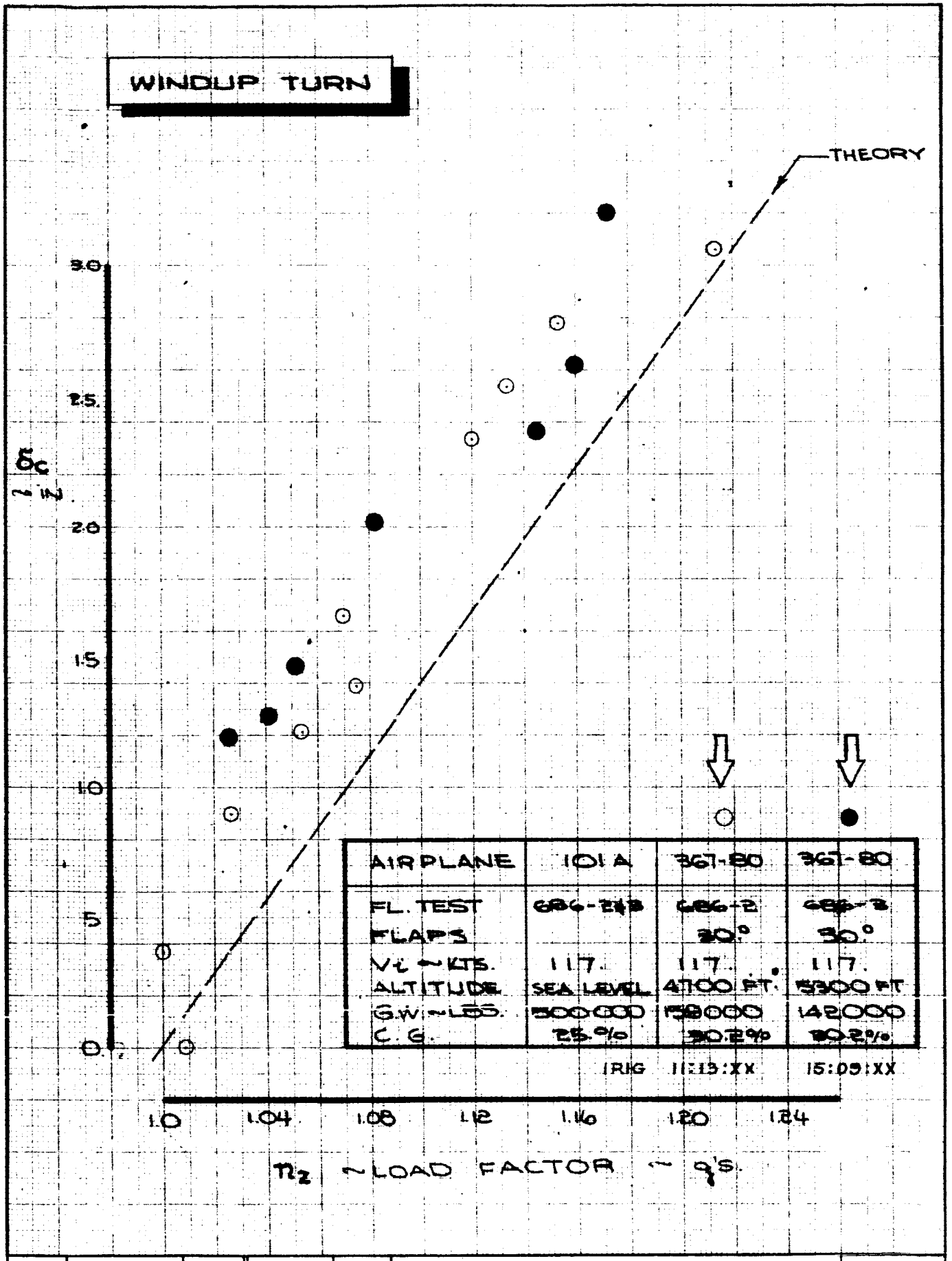

AIRPLANE	101A	367-80	367-80
FL. TEST	686-2&3	686-2	686-3
FLAPS		20°	30°
V_i ~ KTS.	117.	117.	117.
ALTITUDE	SEA LEVEL	4700 FT.	5300 FT
G.W ~ LBS.	500000	458000	442000
C. G.	25%	30.2%	30.2%
	IRIG	11:13:XX	15:09:XX

CALC			REVISED	DATE	WINDUP TURN FL. TEST: 686-2 & -3 CONFIG.: 101A
CHECK					
APR					
APR					
					THE BOEING COMPANY D6-15000

367-80

FIG. 5

PAGE VI-21

TD 461 C-R4

WINDUP TURN

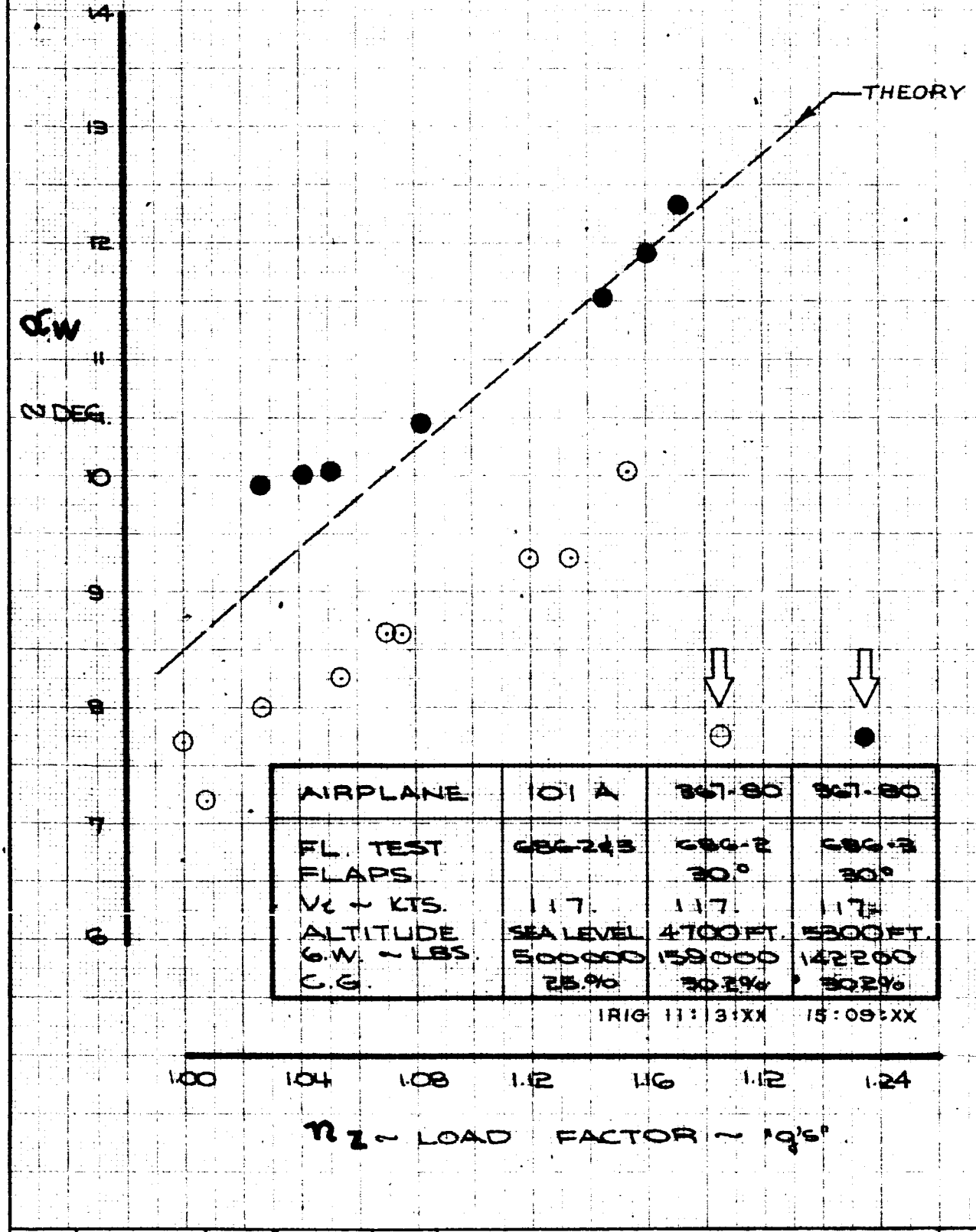

AIRPLANE	101 A	367-80	367-80
FL. TEST	G86-2&3	G86-2	G86-3
FLAPS		30°	30°
V_c ~ KTS.	117.	117.	117.
ALTITUDE	SEA LEVEL	4700 FT.	5300 FT.
G.W. ~ LBS.	500000	159000	142200
C.G.	25.%	30.2%	30.2%
		IRIG 11:31:XX	15:09:XX

CALC			REVISED	DATE	WINDUP TURN	367-80
CHECK					FL. TEST G86-2 & 3	FIG. 6
APR					CONFIG. : 101A	
APR					THE BOEING COMPANY D6-15000	PAGE VI-22

TD 461 C-R4

CALC			REVISED	DATE	SPEED STABILITY 367-80
CHECK					FL. TEST: 686-2 FIG. 7
APPD.					CONFIG. 101A
APPD.					THE BOEING COMPANY D6-15000 PAGE VI-23

TD 1053-R5

±7 KTS
130
125
120
115
110
105
100
V_t
KTS
0
4
8
12
16
20
24
$\Delta\psi$
DEG

Phugoid	Fig. 8. The measured period of the phugoid agrees very well with the theoretical while the measured damping ratio is approximately 40% of the theoretical value. The damping ratio, however, is very difficult to measure accurately since only one cycle of the phugoid was recorded.
Pitch Attitude	Fig. 9. Approximately 3 seconds are required for a change in pitch attitude of 8 degrees.
Elevator Pulse	Fig. 10. The 367-80 simulated the elevator pulse of the basic configuration accurately.

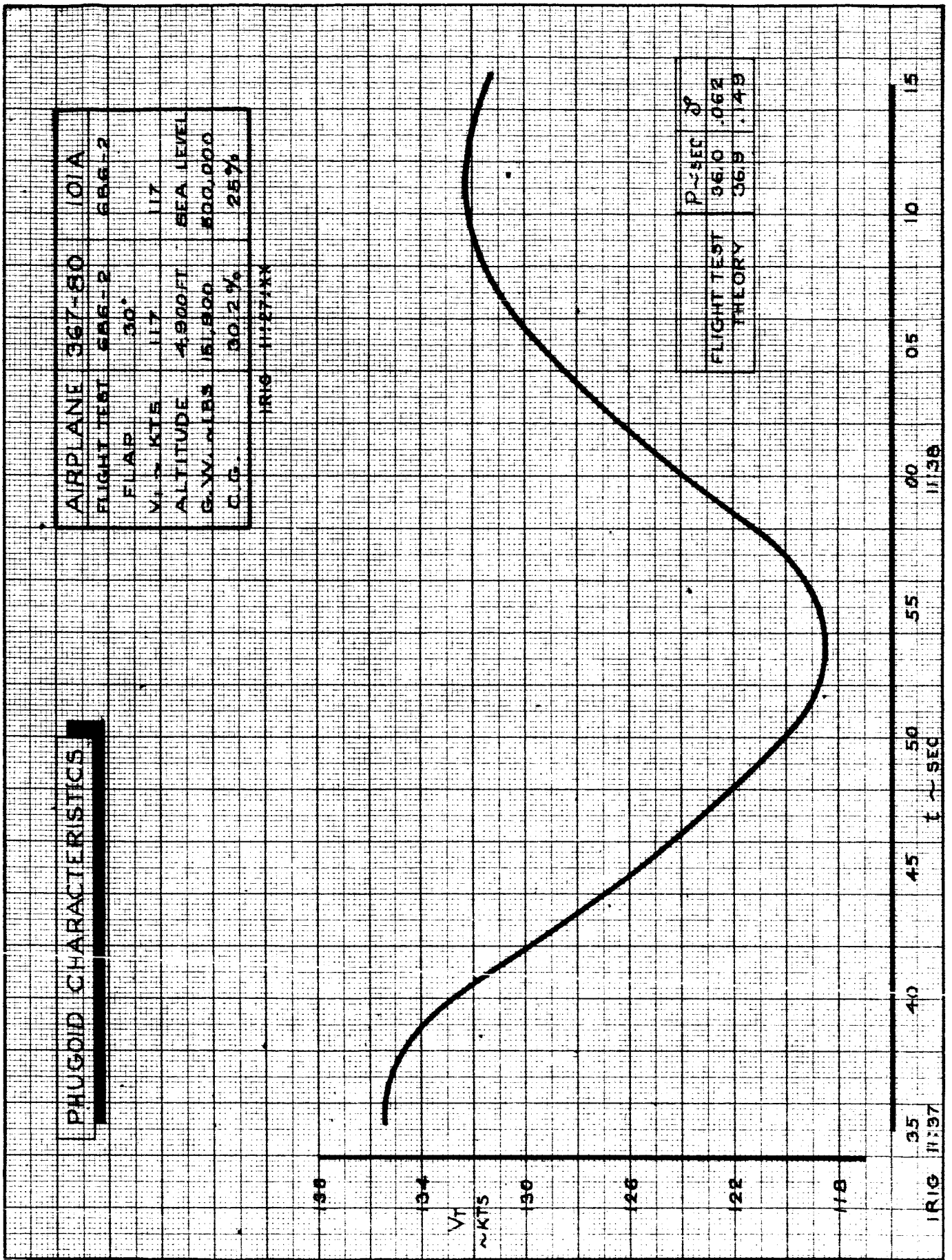

CALC			REVISED	DATE	PHUGOID CHARACTERISTICS FLIGHT TEST 686-2 COFIGURATION 101A	367-80
CHECK						FIG. 8
APR					THE BOEING COMPANY D6-15000	PAGE VI-25
APR						

TD 461 C-R4

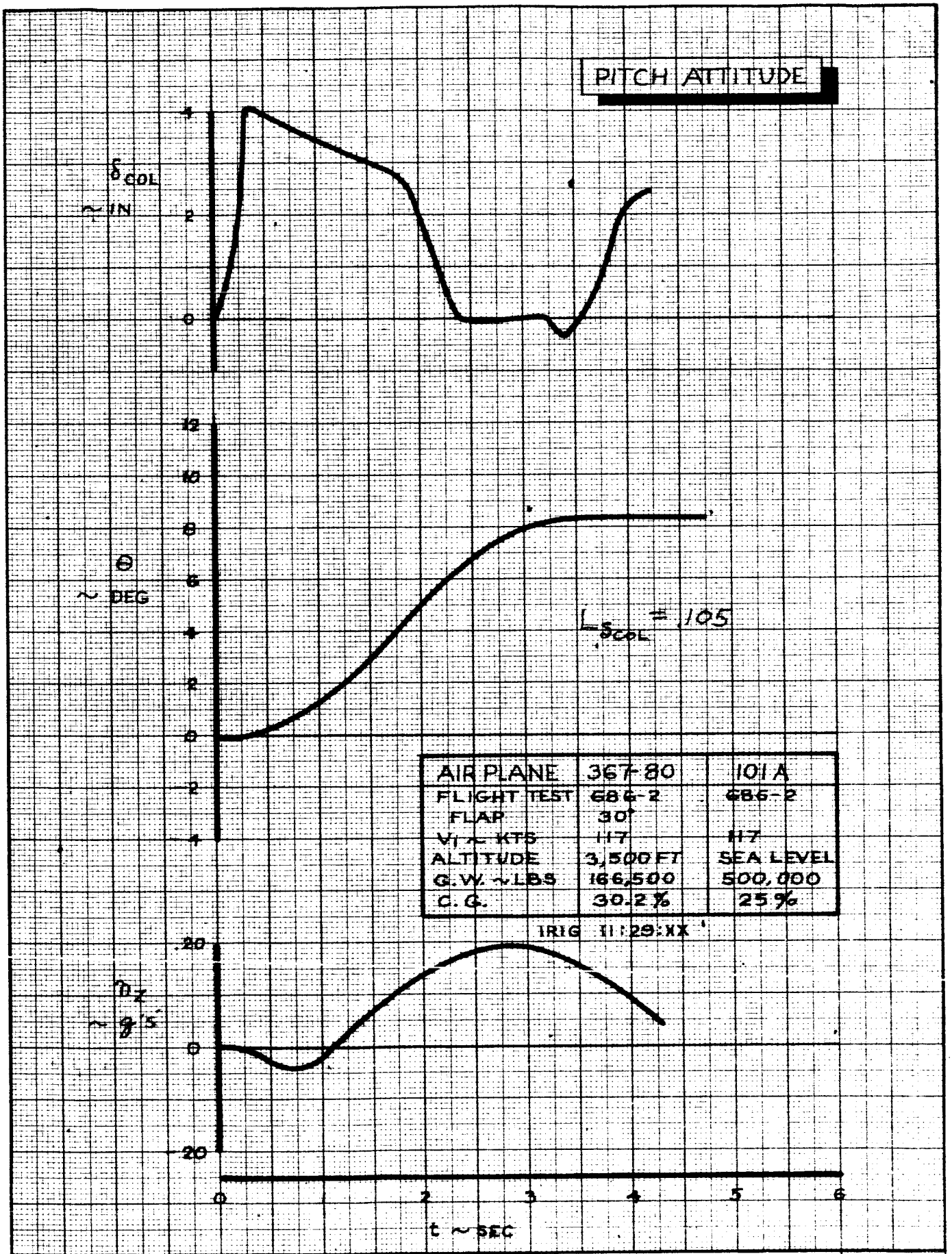

			REVISED	DATE	PITCH ATTITUDE FLIGHT TEST 686-2 CONFIGURATION 101A	367-80
CALC						FIG. 9
CHECK						
APR					THE BOEING COMPANY D6-15000	PAGE VI-26
APR						

TD 461 C-R4

CALC			REVISED	DATE	ELEVATOR PULSE FLIGHT TEST 686-2 CONFIGURATION 101A
CHECK					
APPD.					
APPD.					
					THE BOEING COMPANY D6-15000

367-80

FIG. 10

PAGE VI-21

TD 1053-R5

30

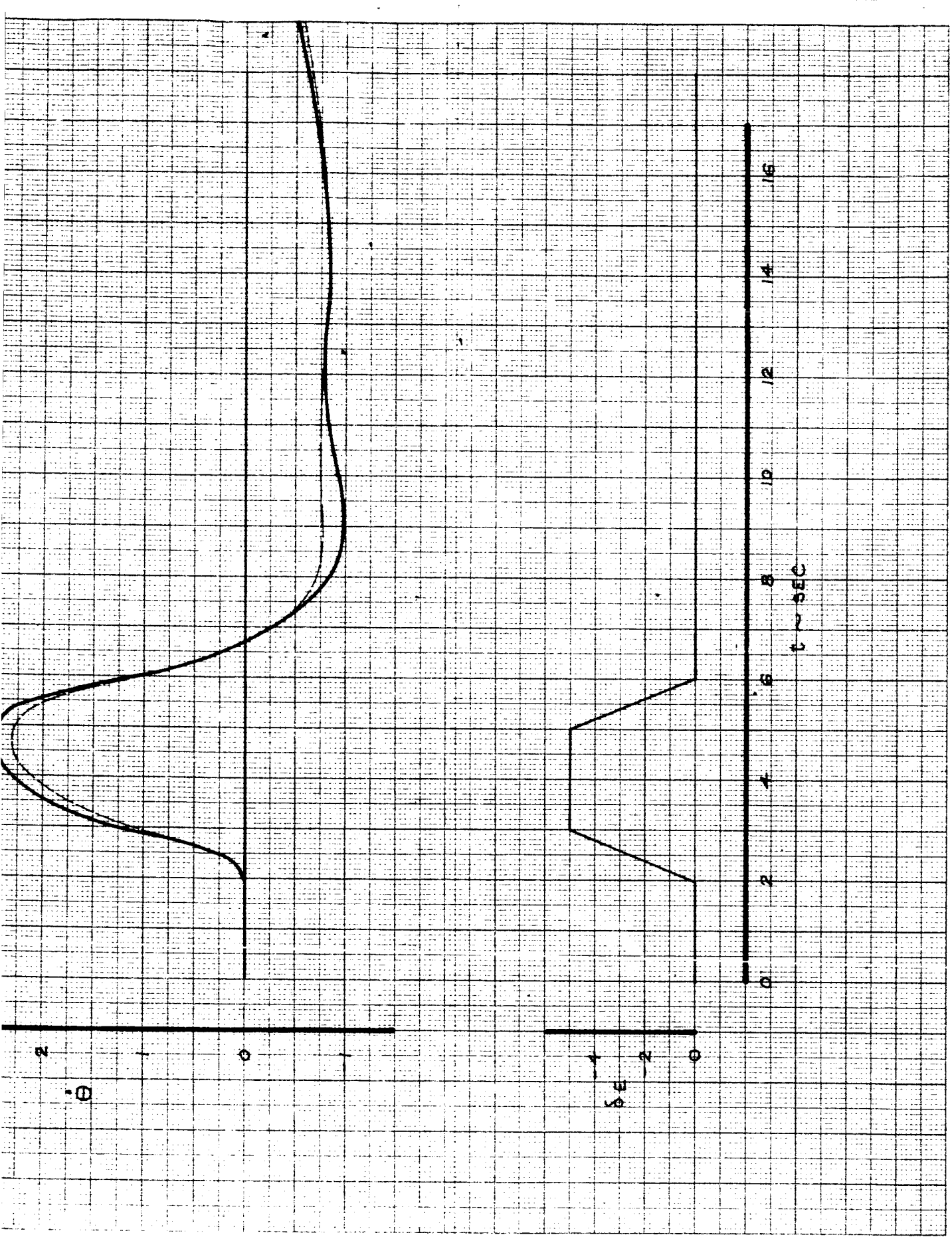

VI-27.2

Lateral:

Maneuver	Comments
Steady Roll Rate	Fig. 11. The Steady State roll rate characteristics of the 367-80 were nonlinear whereas the theory is linear. The maximum roll rate achieved in flight was somewhat less than theory predicts. A sample of how the flight test data was reduced is shown in Fig. 12.
Roll Rate Reversal	Fig. 13. The 367-80 accurately simulated the basic 1209 configuration roll acceleration. Fig. 14 shows how the flight data were reduced.
Yaw Rate Reversal	Fig. 15. The yaw acceleration was slightly larger than predicted by the theory. Fig. 16 shows how flight data were reduced.
Steady Sideslip	Fig. 17. The 367-80 exhibited a low lateral control deflection to balance the sideslip angles generated,
Spiral Stability	Fig. 18. Theory gives the time to half amplitude as 18.3 seconds. Flight Test data indicated a time to half amplitude on the order of 100 seconds.
20° Heading Change	Fig. 19. A 20° heading change was accomplished in approximately 10.5 seconds. Opposite wheel is required to stop the roll at the desired bank angle.

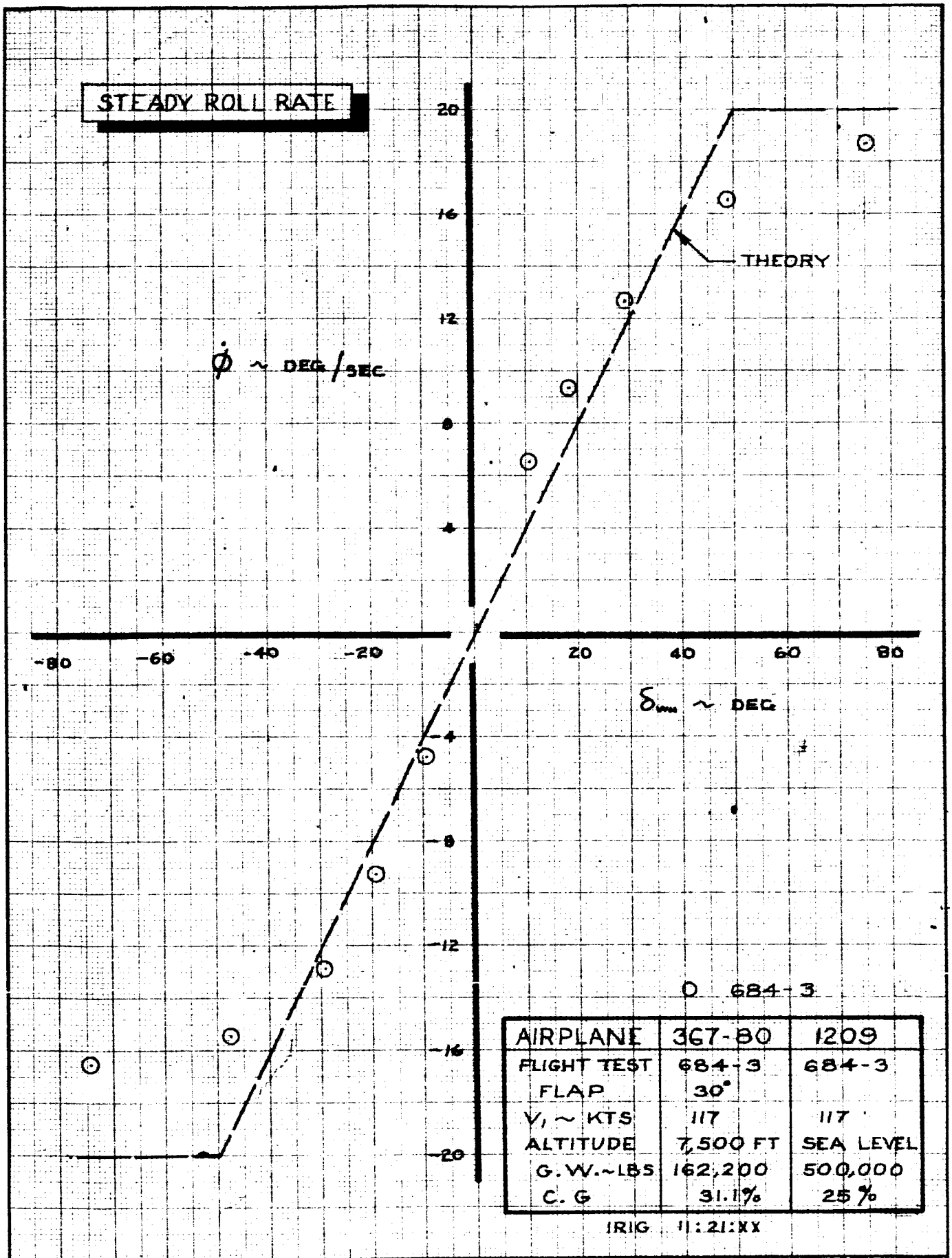

CALC			REVISED	DATE
CHECK				
APR				
APR				

STEADY ROLL RATE
FLIGHT TEST 684-3
CONFIGURATION 1209

367-80

FIG. 11

THE BOEING COMPANY D6-15000

TD 461 C-R4

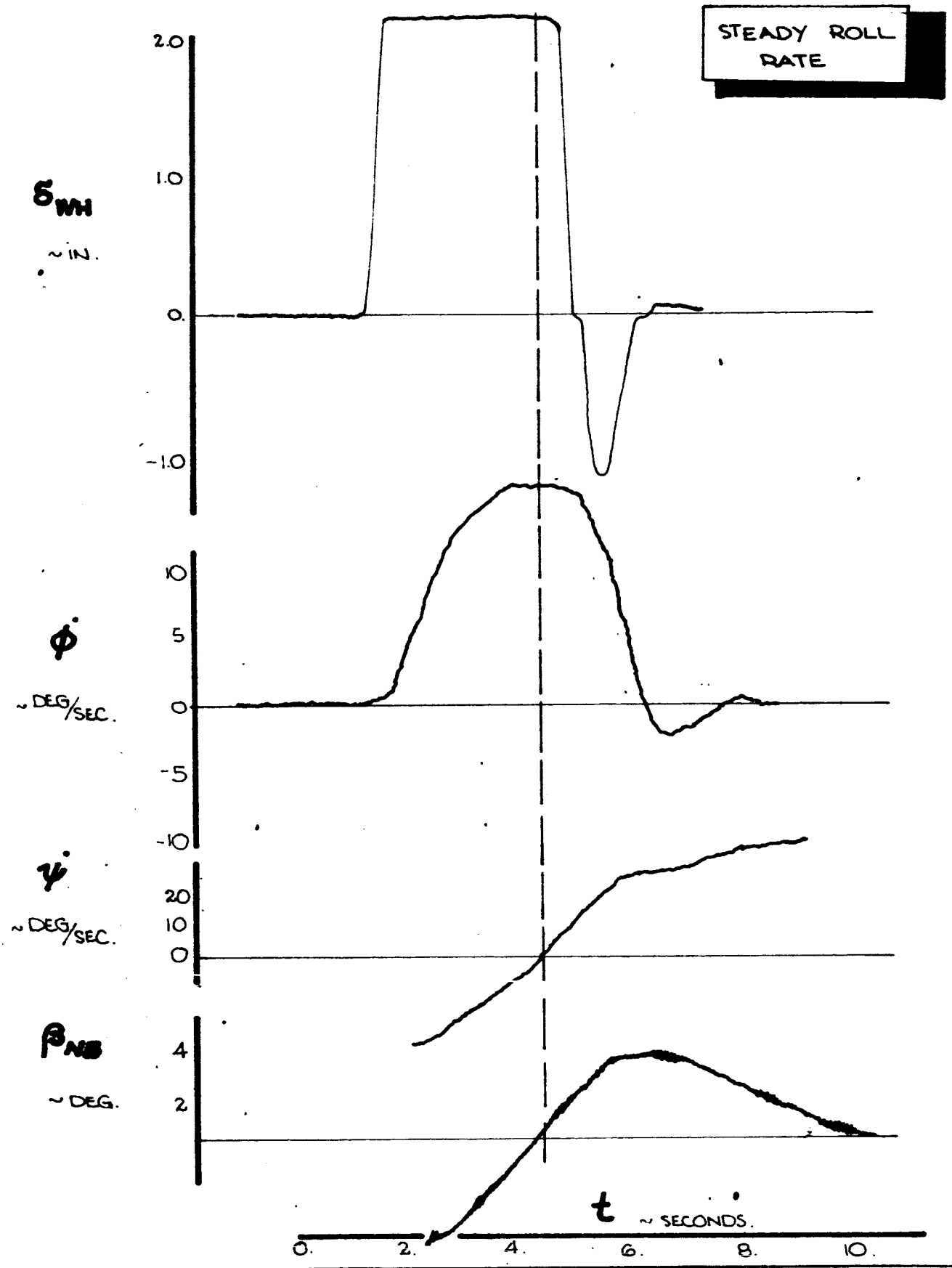

ENGR.			REVISED	DATE	SAMPLE OF FLIGHT TEST DATA FOR STEADY ROLL RATE.	D6-15000
CHECK						FIG. 12
APR						
APR					THE BOEING COMPANY RENTON, WASHINGTON	VI-30

ROLL RATE REVERSAL

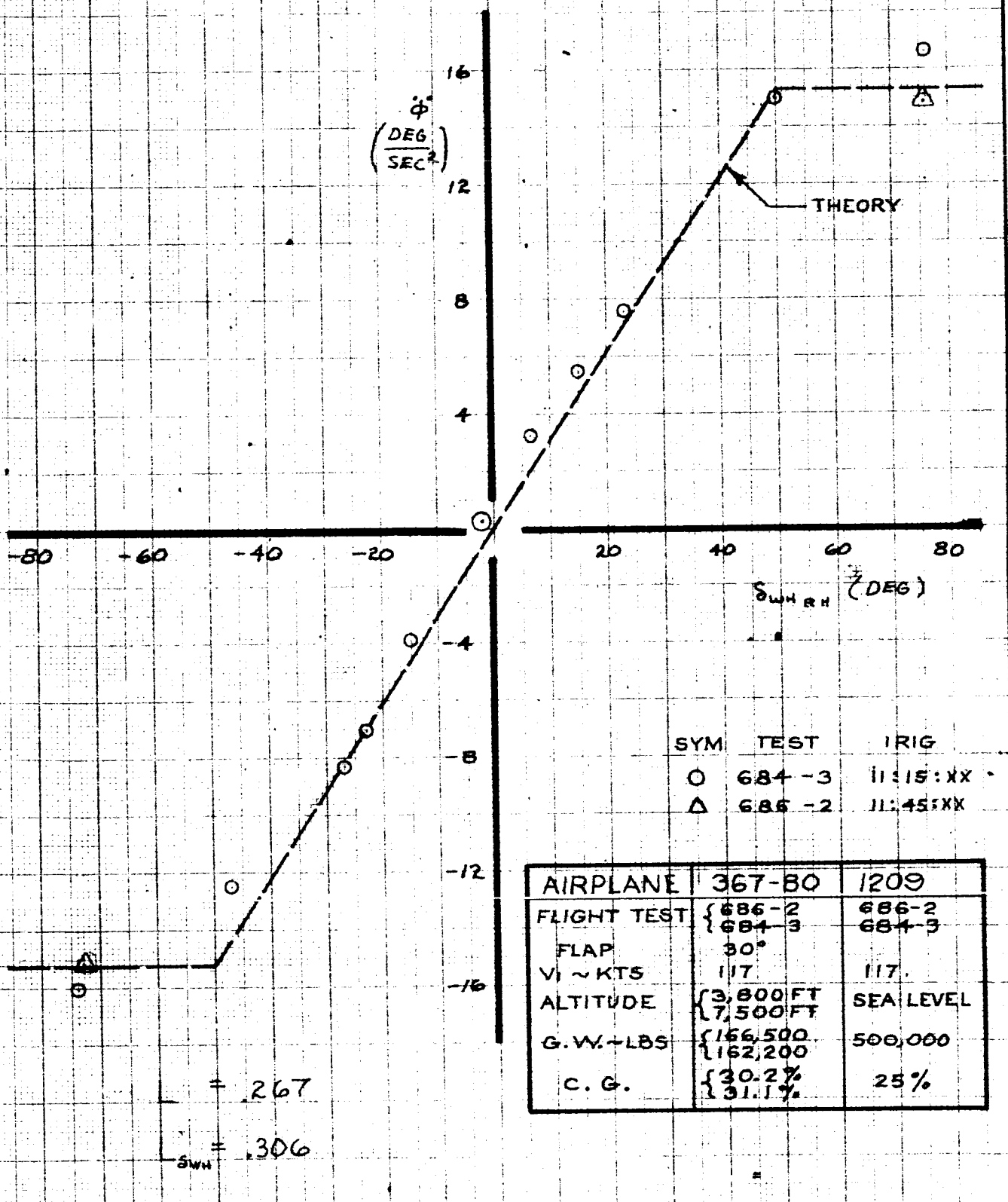

SYM	TEST	TRIG
○	684-3	11:15:XX
△	686-2	11:45:XX

AIRPLANE	367-80	1209
FLIGHT TEST	{686-2 {684-3	686-2 684-3
FLAP	30°	
V_i ~ KTS	117	117
ALTITUDE	{3,800 FT {7,500 FT	SEA LEVEL
G.W.-LBS	{166,500 {162,200	500,000
C.G.	{30.2% {31.1%	25%

			REVISED	DATE
CALC				
CHECK				
APR				
APR				

ROLL RATE REVERSAL
FLIGHT TEST 686-2 & 684-3
CONFIGURATION 1209

367-80

FIG. 13

THE BOEING COMPANY D6-15000

TD 461 C-R4

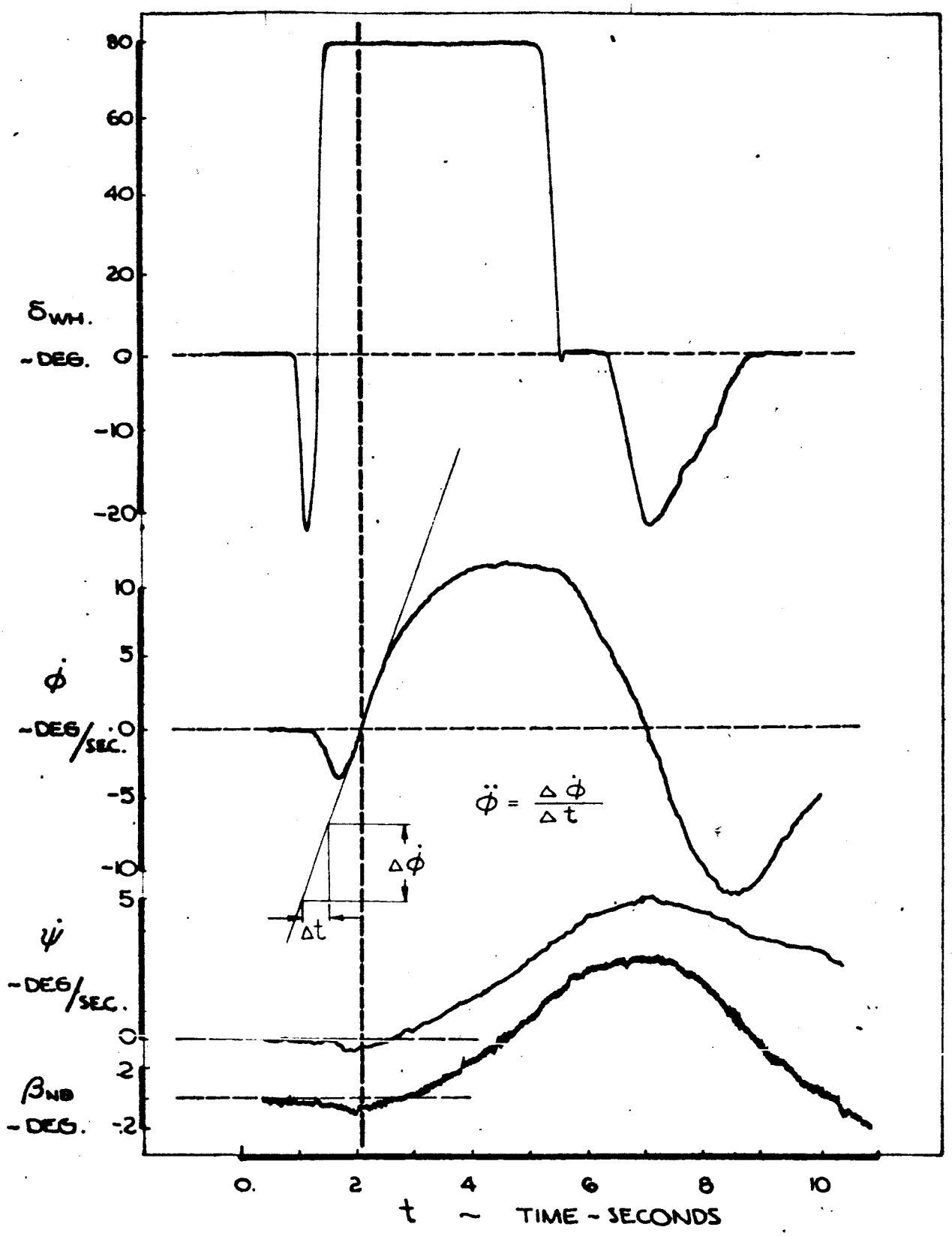

ENGR.			REVISED	DATE	SAMPLE OF FLIGHT TEST DATA FOR ROLL RATE REVERSAL.	367-80
CHECK						FIG. 14
APR						
APR					THE BOEING COMPANY RENTON, WASHINGTON D6-15000	VI-32

YAW RATE REVERSAL

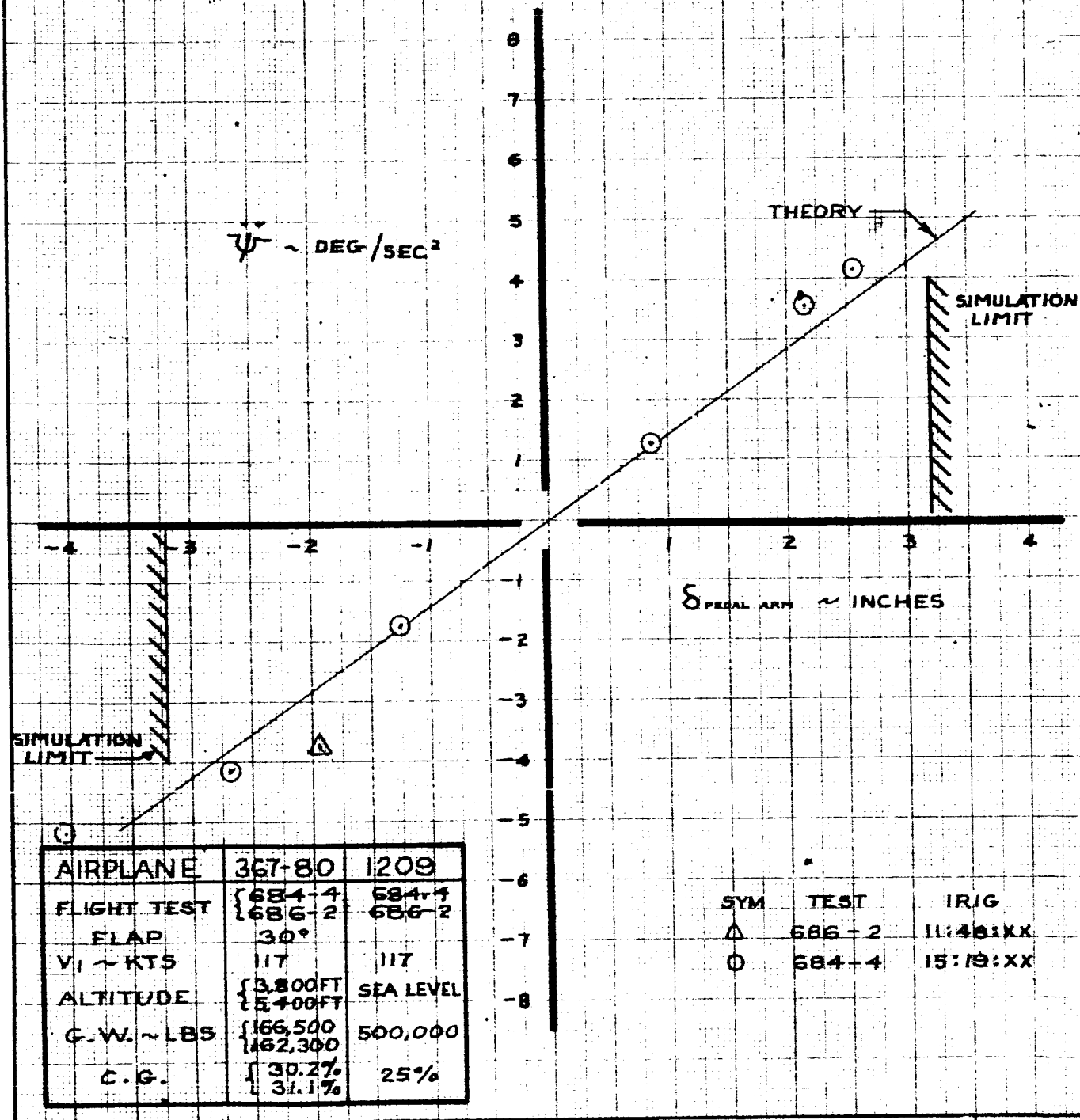

AIRPLANE	367-80	1209
FLIGHT TEST	{684-4 {686-2	684-4 686-2
FLAP	30°	
V_i ~ KTS	117	117
ALTITUDE	{3,800 FT {5,400 FT	SEA LEVEL
G.W. ~ LBS	{166,500 {162,300	500,000
C.G.	{30.2% {31.1%	25%

SYM	TEST	IRIG
△	686-2	11:48:XX
○	684-4	15:19:XX

			REVISED	DATE
CALC				
CHECK				
APR				
APR				

YAW RATE REVERSAL
FLIGHT TEST 684-4 & 686-2
CONFIGURATION 1209

367-80

FIG. 15

THE BOEING COMPANY D6-15000

TD 461 C-R4

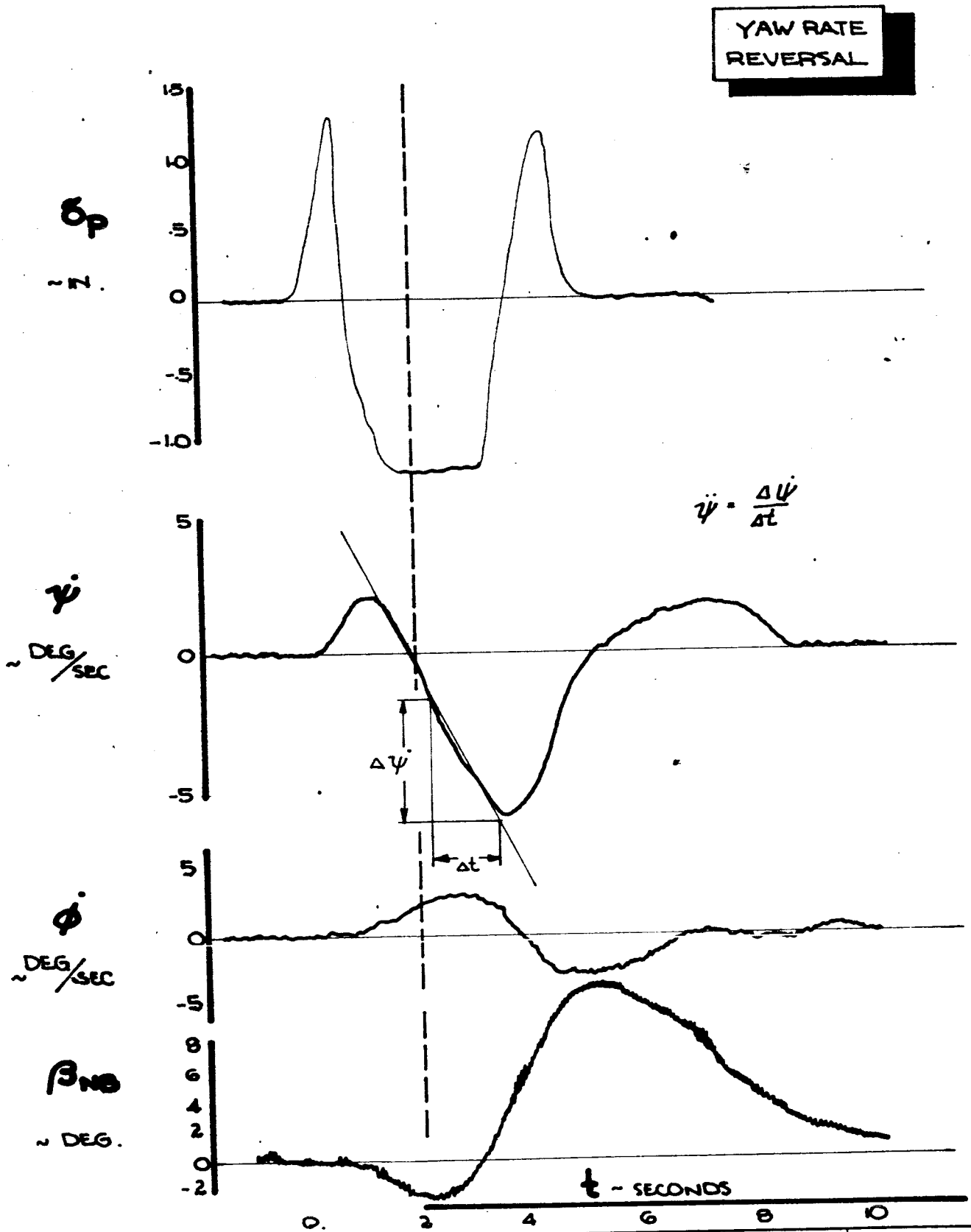

ENGR.			REVISED	DATE	SAMPLE OF FLIGHT TEST DATA FOR YAW RATE REVERSALS.	D6-15000
CHECK						FIG. 16
APR						
APR					THE BOEING COMPANY RENTON, WASHINGTON	VI-34

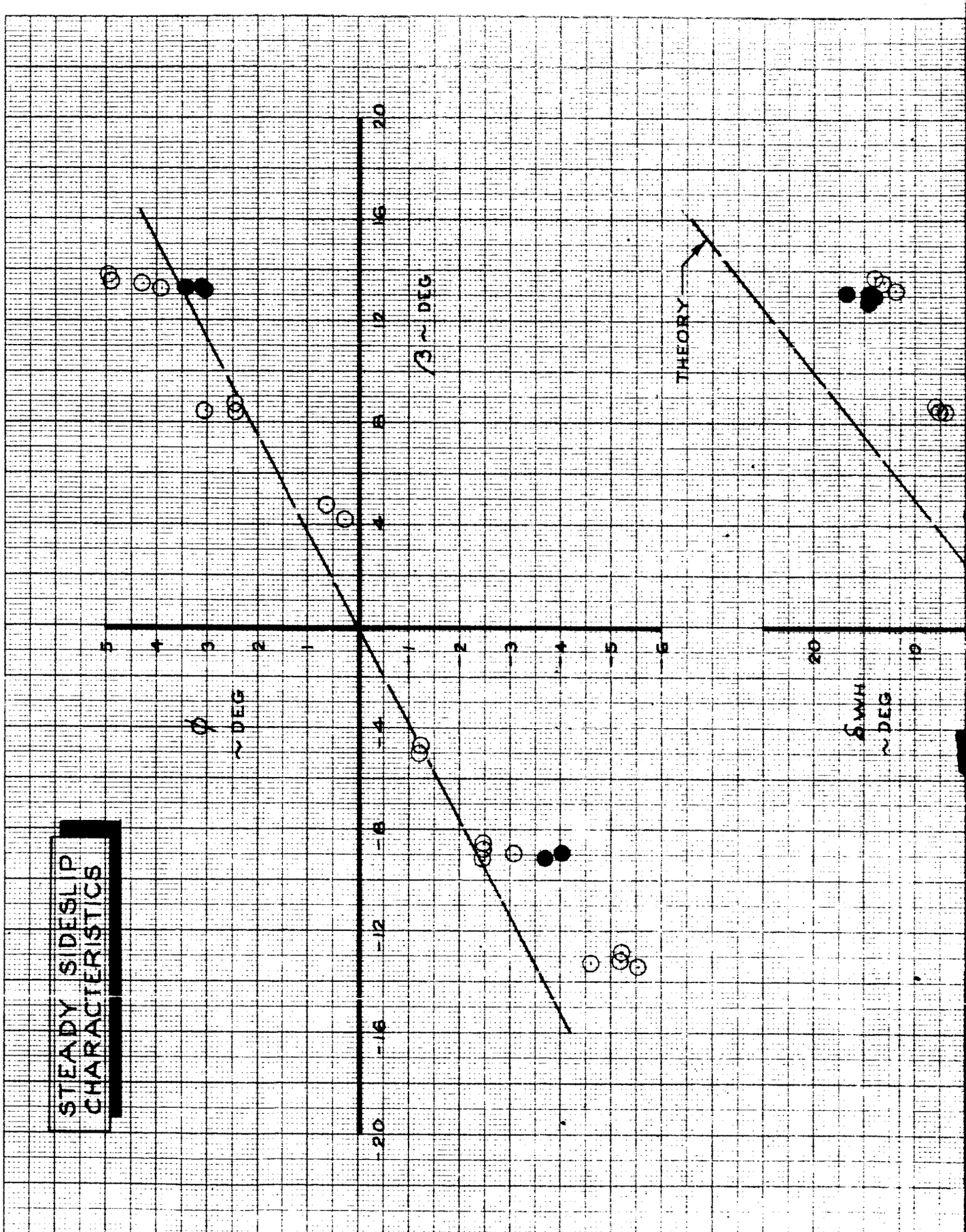

			REVISED	DATE
CALC				
CHECK				
APPD.				
APPD.				

STEADY SIDESLIP CHARACTERISTICS
FLIGHT TEST 684-2, 686-2
CONFIGURATION 1209

367-80

FIG. 17

THE BOEING COMPANY D6-15000

TD 1053-R5

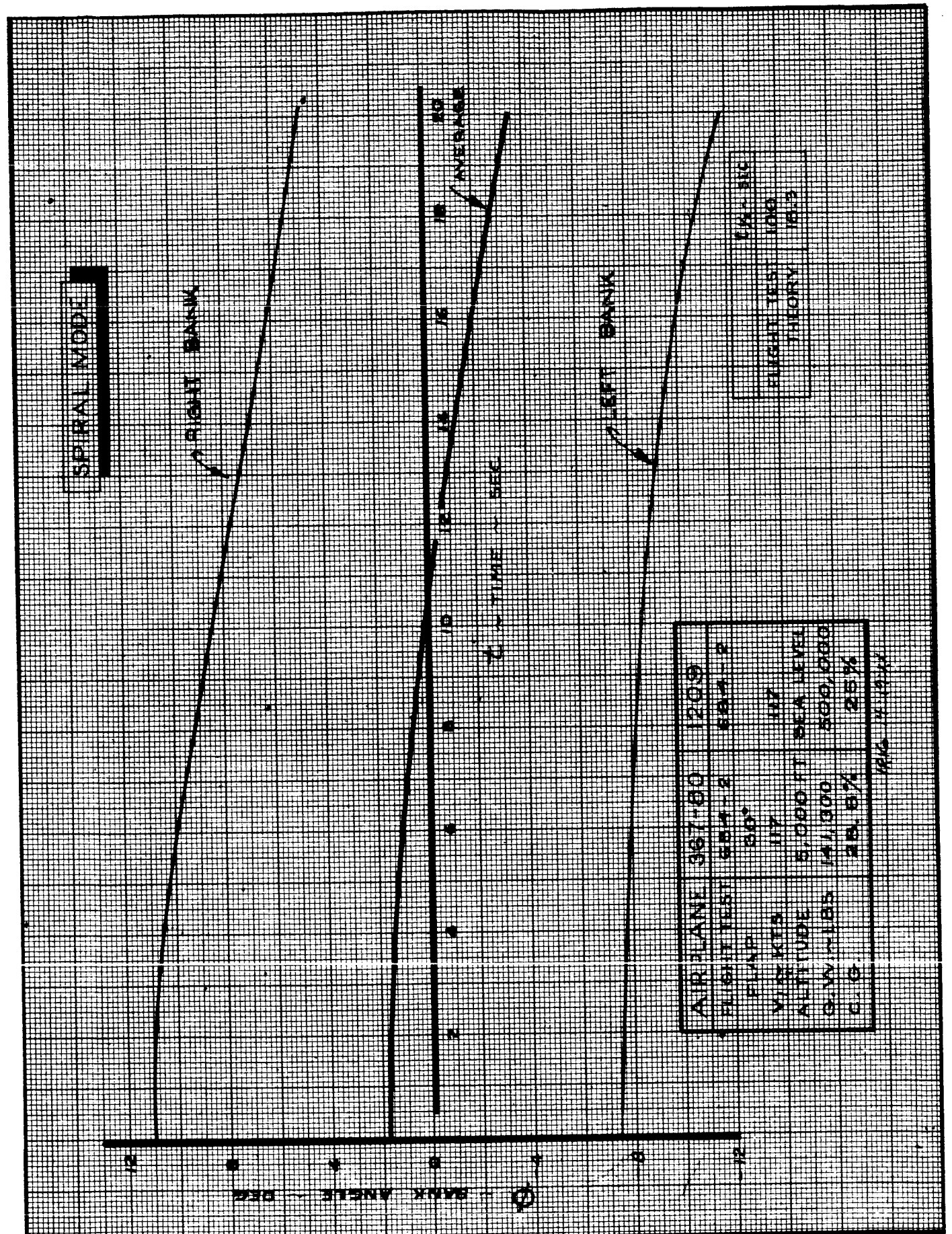

CALC			REVISED	DATE
CHECK				
APR				
APR				

SPIRAL STABILITY
FLIGHT TEST 684-2
CONFIGURATION 1209

367-80

FIG. 18

THE BOEING COMPANY D6-15000

PAGE VI-36

TD 461 C-R4

K&E ALBANENE® TRACING PAPER

AIRPLANE 367-80 1209 367-80
FLIGHT TEST 684-2 686-2
FLAP 30° 30
Vi ~ KTS 117 117
ALTITUDE 4,900 FT SEA LEVEL 4,900 FT
G.W.-LBS 141,200 590000 149,400
C.G. 28.8% 25% 30.2%
IRIG 14:24:XX 11:42:XX
β ~ DEG
δp ~ IN
β ~ DEG

VI-35-2

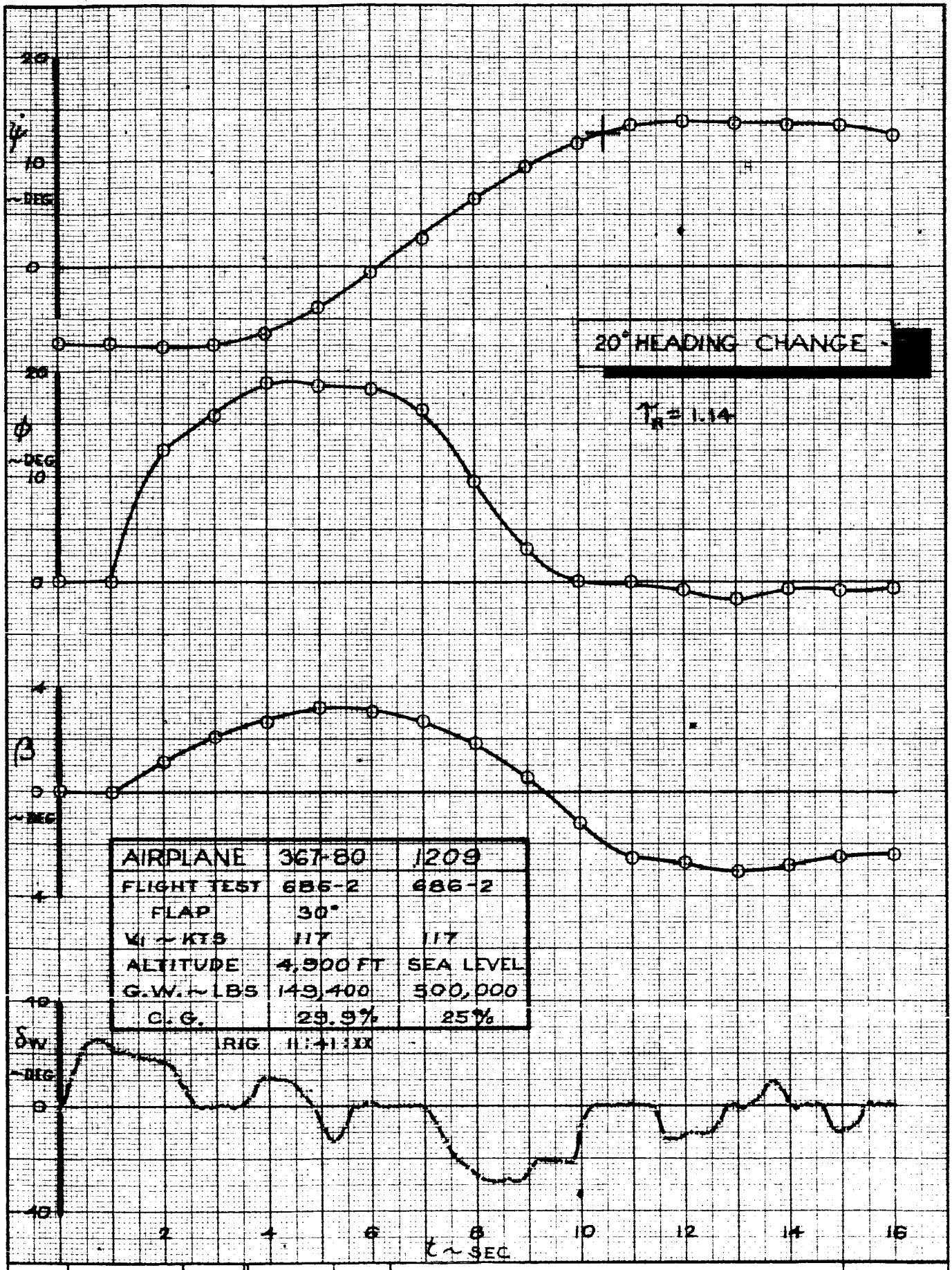

AIRPLANE	367-80	1209
FLIGHT TEST	686-2	686-2
FLAP	30°	
V_i ~ KTS	117	117
ALTITUDE	4,900 FT	SEA LEVEL
G.W. ~ LBS	149,400	500,000
C. G.	29.9%	25%
RIG	11:41:XX	

			REVISED	DATE
CALC				
CHECK				
APR				
APR				

20° HEADING CHANGE
FLIGHT TEST 686-2
CONFIGURATION 1209

367-80

FIG. 19

THE BOEING COMPANY
D6-15000

PAGE VI-37

TD 461 C-R4

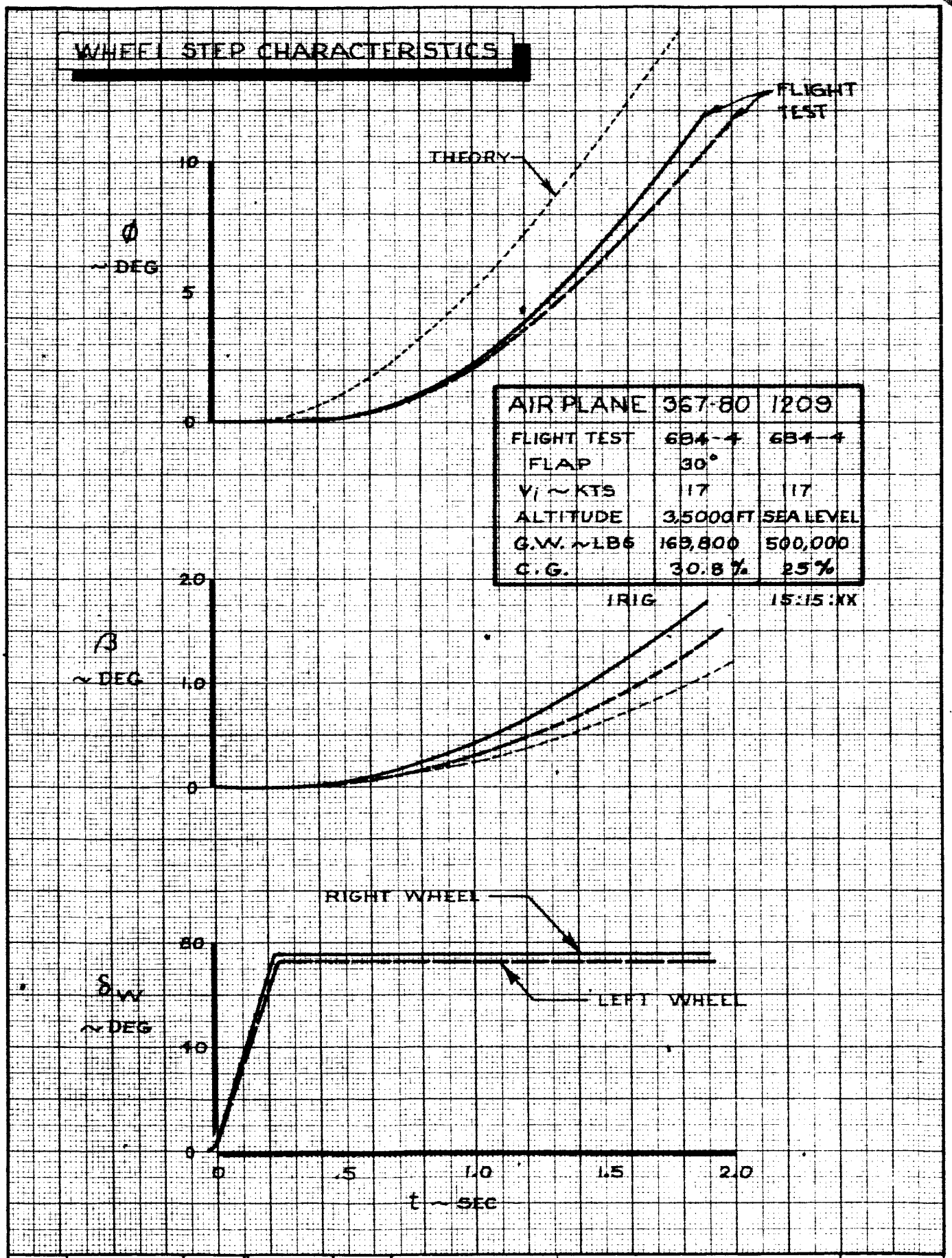

			REVISED	DATE	WHEEL STEP CHARACTERISTICS FLIGHT TEST 684-4 CONFIGURATION 1209	367-80
CALC						
CHECK						FIG. 20
APR						
APR					THE BOEING COMPANY D6-15000	PAGE VI-38

TD 461 C-R4

Wheel Step	Fig. 20. Flight test roll angle data lags behind the six degree of freedom digital computer values for the wheel step shown. This is probably due to the aerodynamic and control surface lags which are not incorporated into the digital computer program.
Wheel Pulse	Fig. 21. Flight test data shows a good correlation with the theory for the basic 1209 configuration with the exception of sideslip angle.
Rudder Pulse	Fig. 22. Good correlation is evident with the exception of sideslip angle at the first reversal.

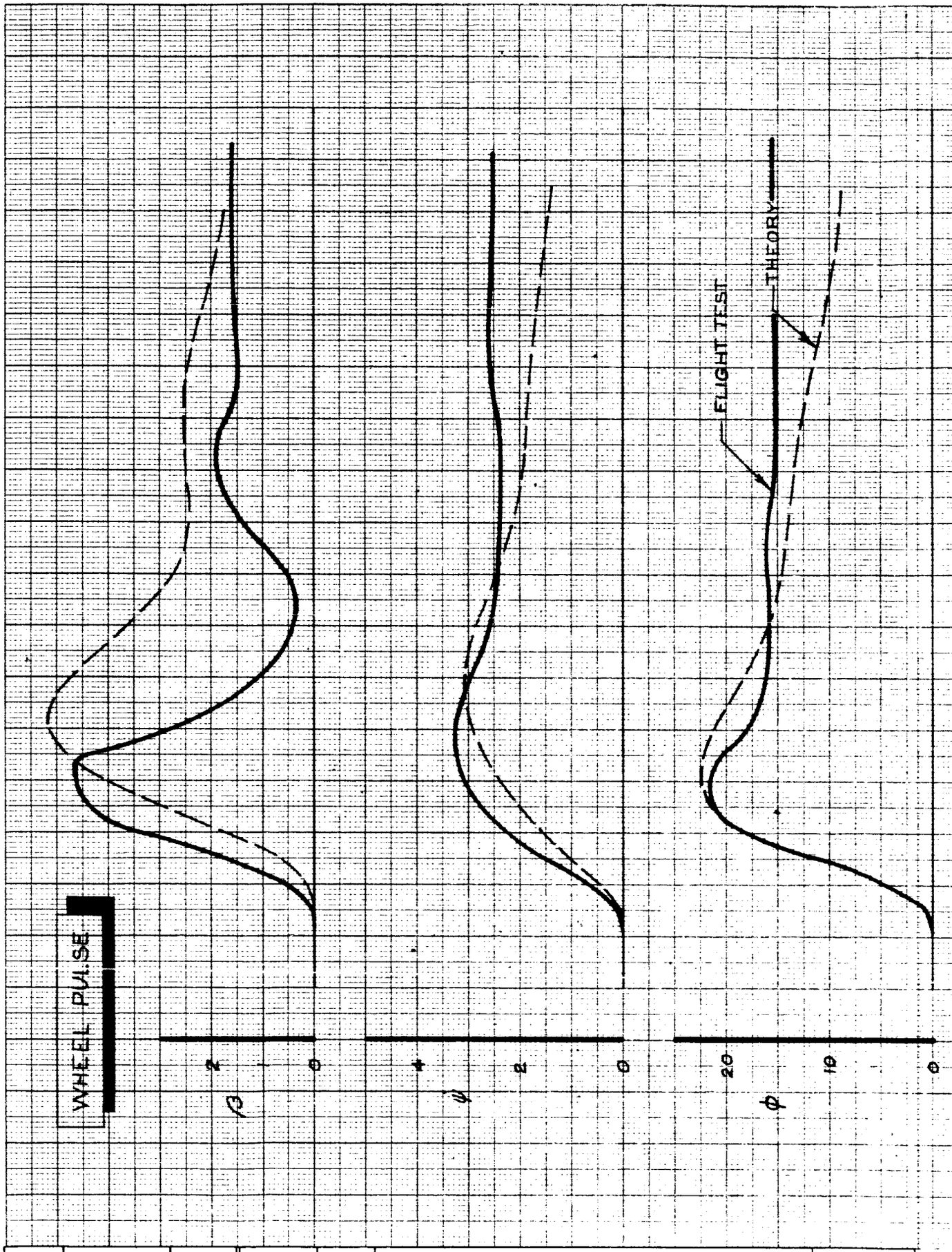

CALC			REVISED	DATE	WHEEL PULSE FLIGHT TEST 686-5 CONFIGURATION: 1209
CHECK					
APPD.					
APPD.					
					THE BOEING COMPANY D6-15000

367-80

FIG. 21

TD 1053-R5

Fig. 10.2

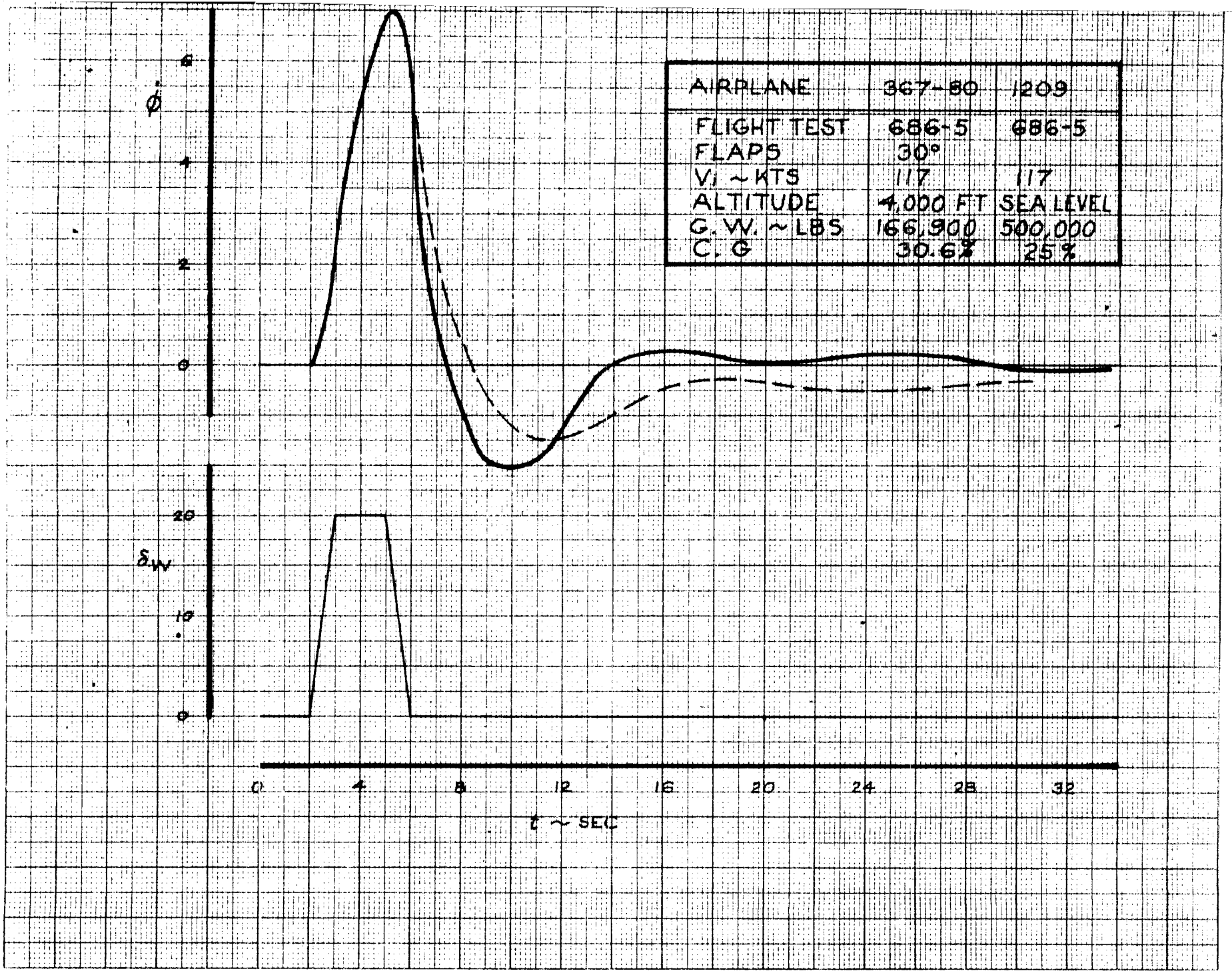
AIRPLANE 367-80 1209
FLIGHT TEST 686-5 686-5
FLAPS 30°
Vi ~ KTS 117 117
ALTITUDE 4,000 FT SEA LEVEL
G. W. ~ LBS 166,900 500,000
C. G 30.6% 25%
φ̇
6
4
2
0
δ_W
20
10
0
0
4
8
12
16
20
24
28
32
t ~ SEC

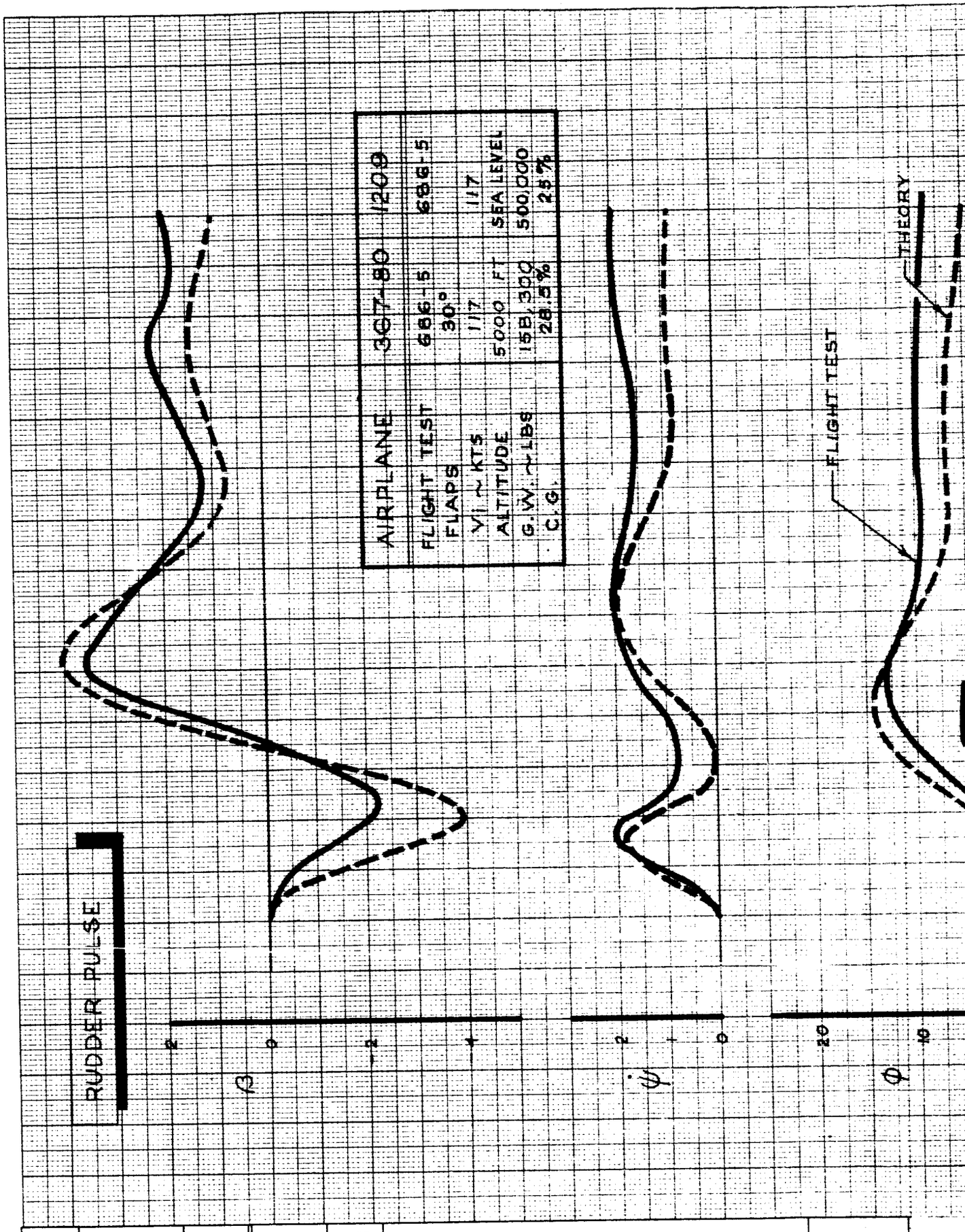

			REVISED	DATE	RUDDER PULSE FLIGHT TEST 686-5 CONFIGURATION: 1209	D6-15000 FIG. 22
CALC						
CHECK						
APPD.					THE BOEING COMPANY	PAGE VI-41
APPD.						

TD 1053-R5

VI-41
-2

B. Ground Based Simulation

The characteristics of a typical longitudinal configuration (G 100) and lateral directional configuration (G1202A), are presented in Figs. 23 thru 36. The theoretical characteristics shown are derived using the methods of Appendix 4. The parameters presented in these figures were used to validate the accuracy of the ground based simulation. Figs. 23 thru 36 indicate that the simulation was an accurate representation of the desired configurations.

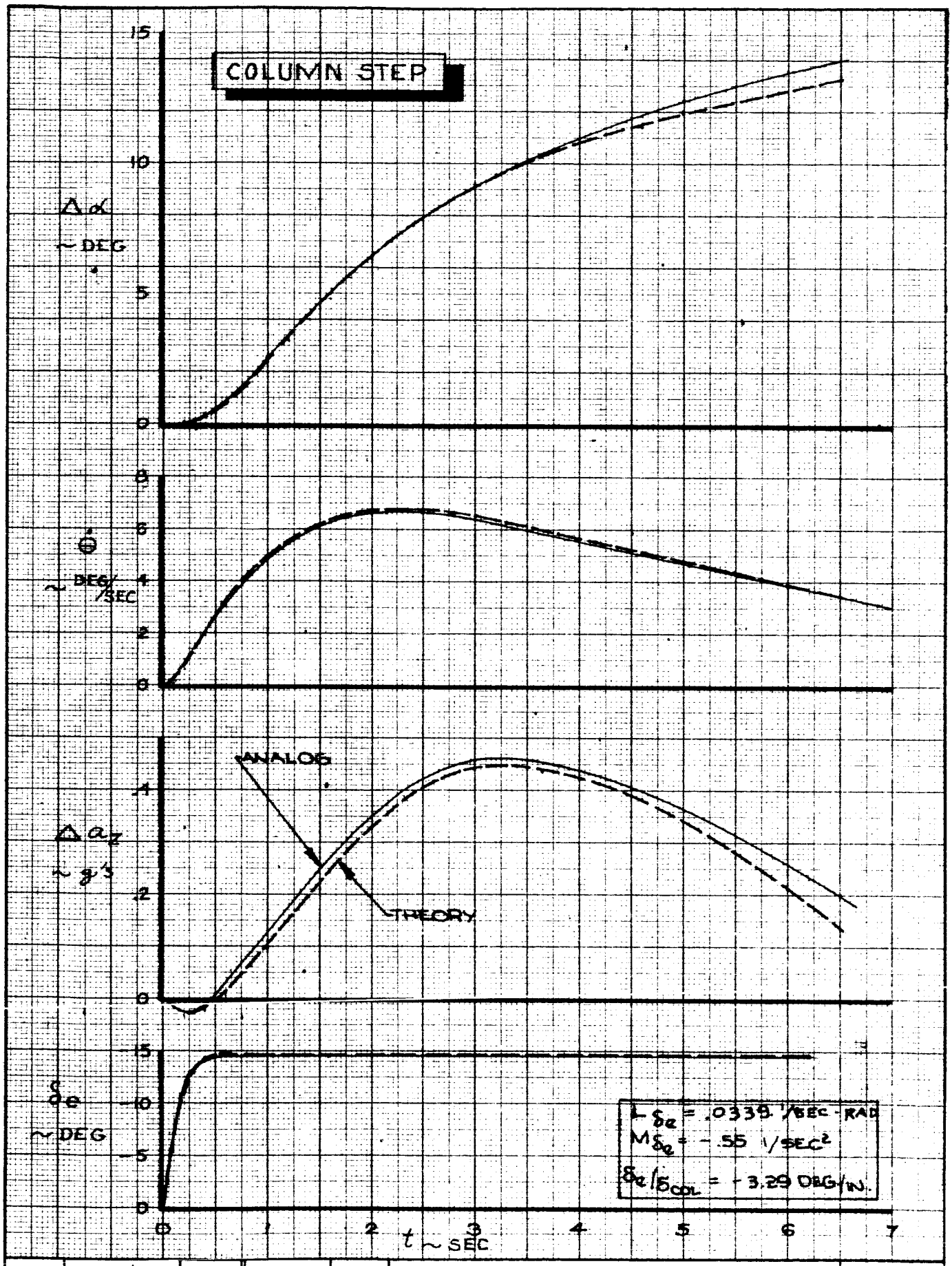

CALC	R. Root	2-2-66	REVISED	DATE	COLUMN STEP GROUND BASED SIMULATOR CONFIGURATION G101A
CHECK					
APR					
APR					
					THE BOEING COMPANY

D6-15000
FIG. 23
PAGE VI-43

TD 461 C-R4

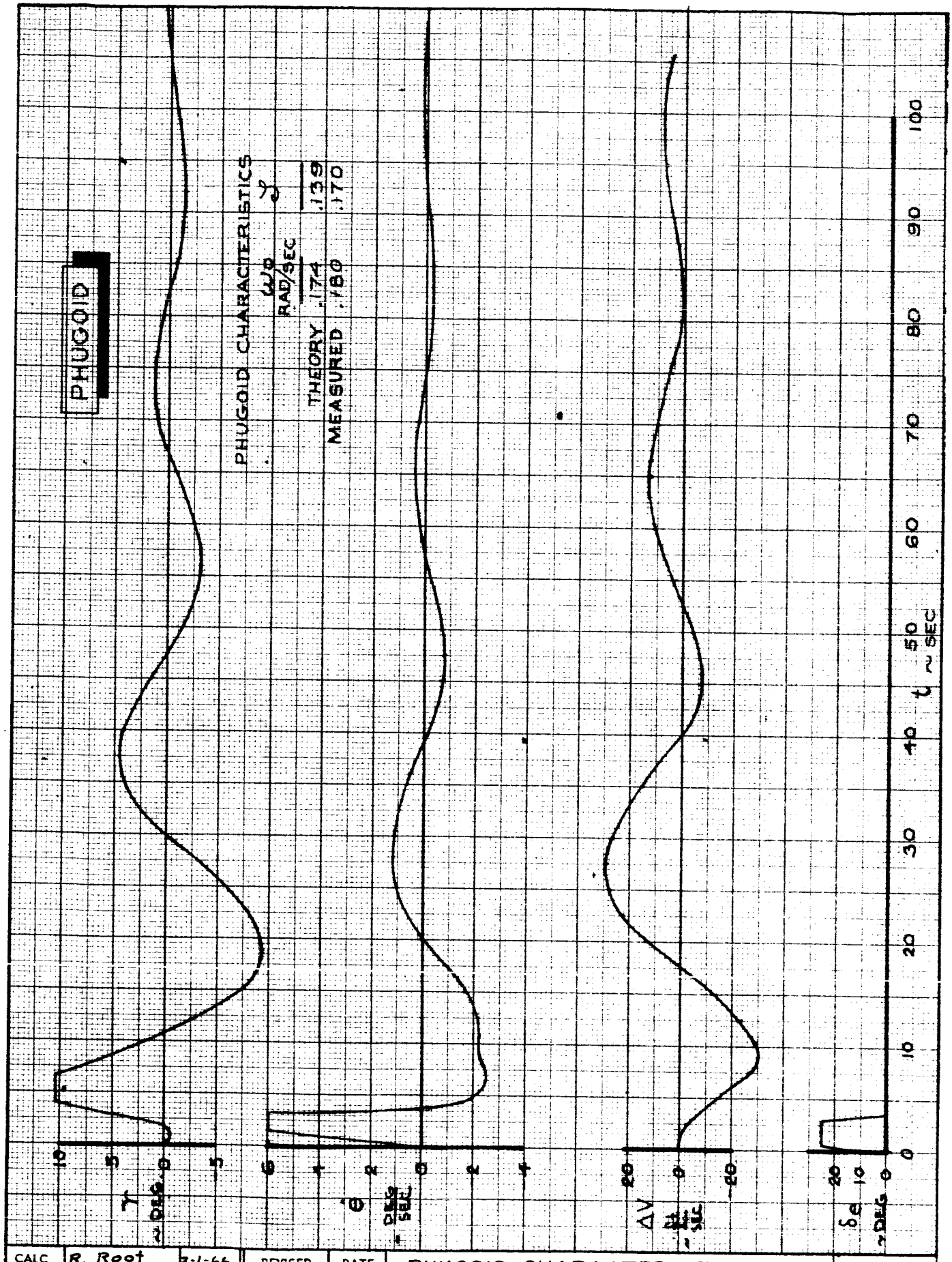

CALC	R. Root	2-1-66	REVISED	DATE	PHUGOID CHARACTERISTICS GROUND BASED SIMULATOR CONFIGURATION G100
CHECK					
APR					
APR					
					THE BOEING COMPANY

D6-15000

FIG. 24

PAGE VI-44

TD 461 C-R4

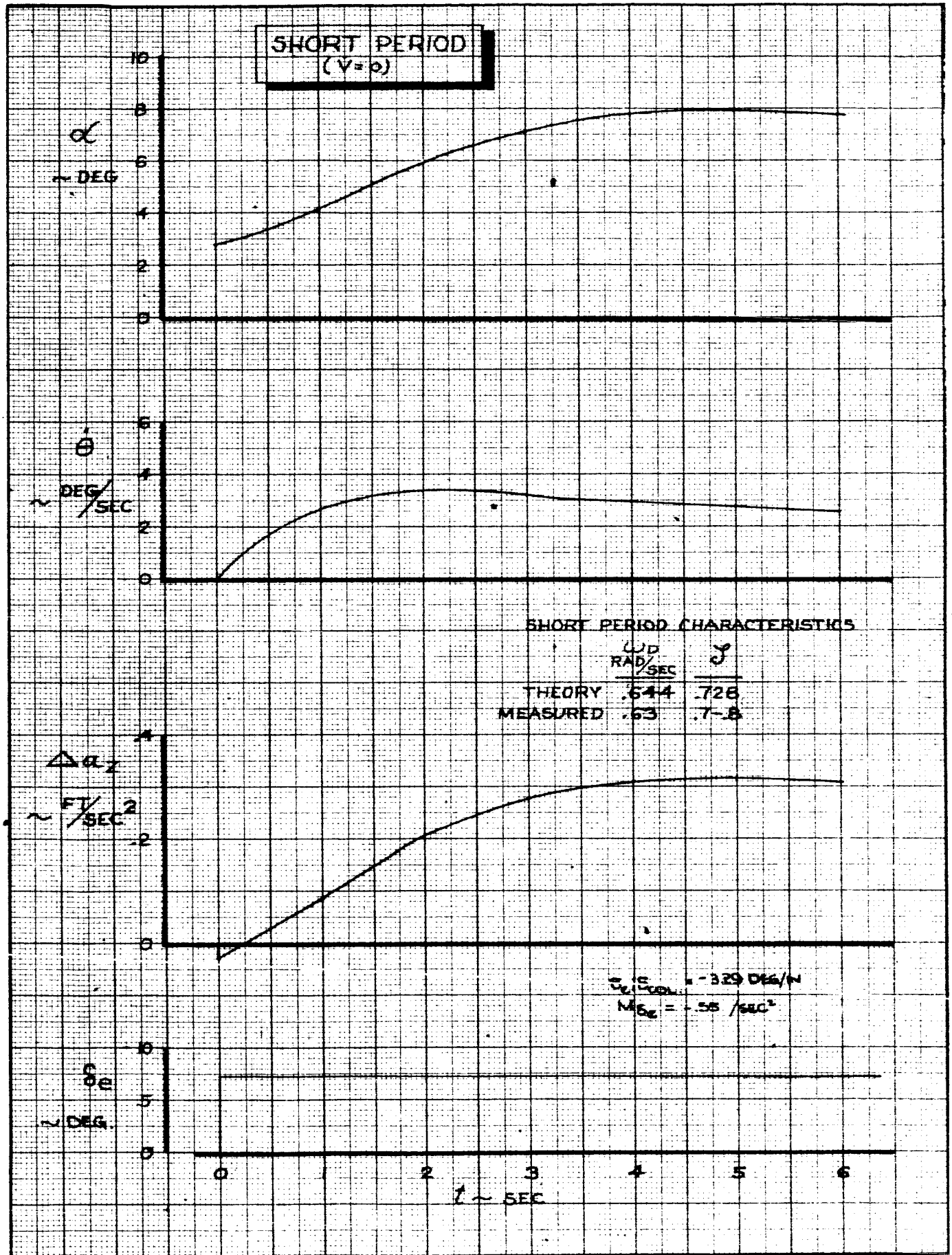

CALC	R. Root	2-1-66	REVISED	DATE	SHORT PERIOD CHARACTERISTICS GROUND BASED SIMULATOR CONFIGURATION GIOIA
CHECK					
APR					
APR					
					THE BOEING COMPANY

D6-15000
FIG. 25
PAGE VI-45

TD 461 C-R4

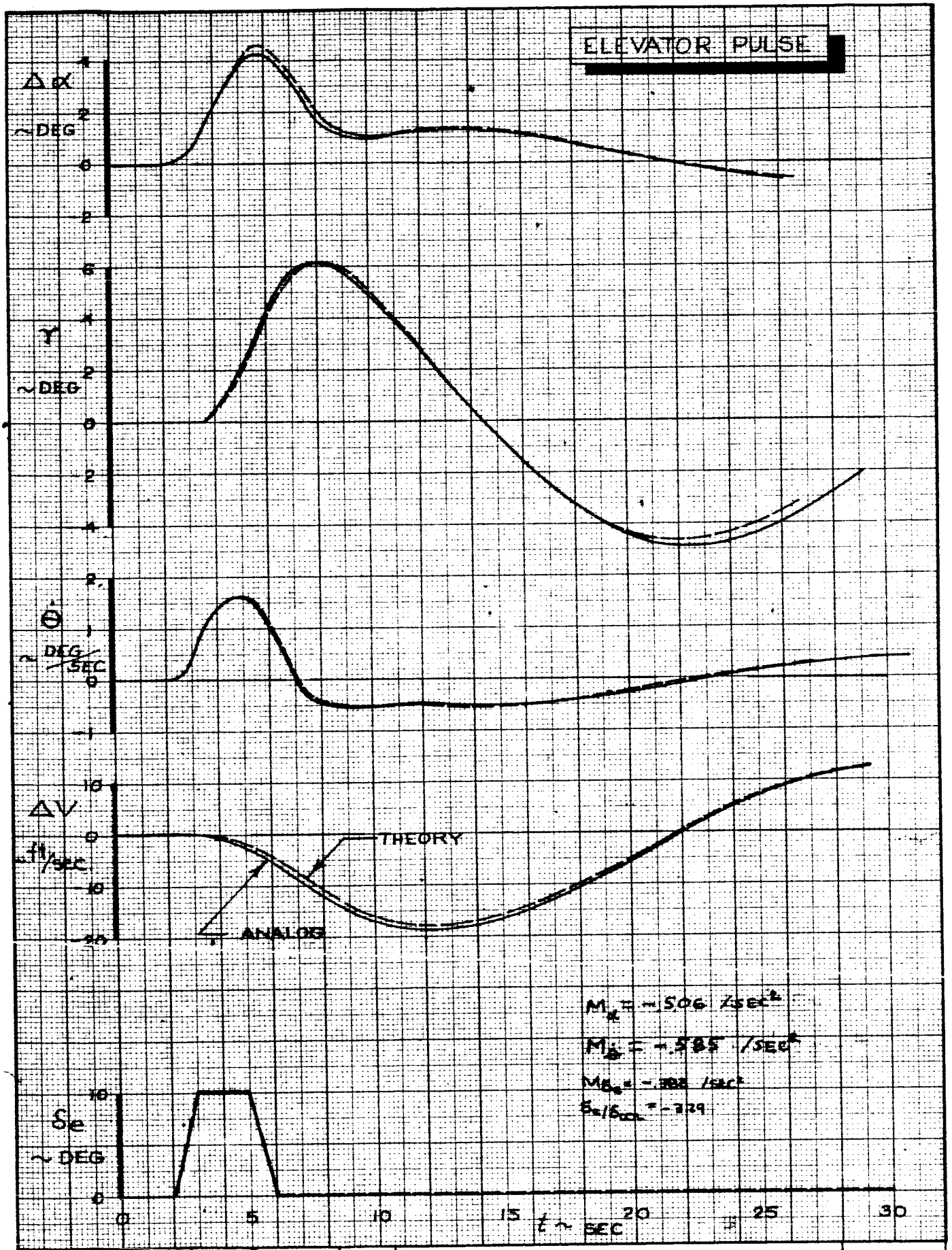

CALC	R. Root	2-2-66	REVISED	DATE	ELEVATOR PULSE GROUND BASED SIMULATOR CONFIGURATION G100
CHECK					
APR					
APR					
					THE BOEING COMPANY

D6-15000

FIG. 26

PAGE VI-46

TD 461 C-R4

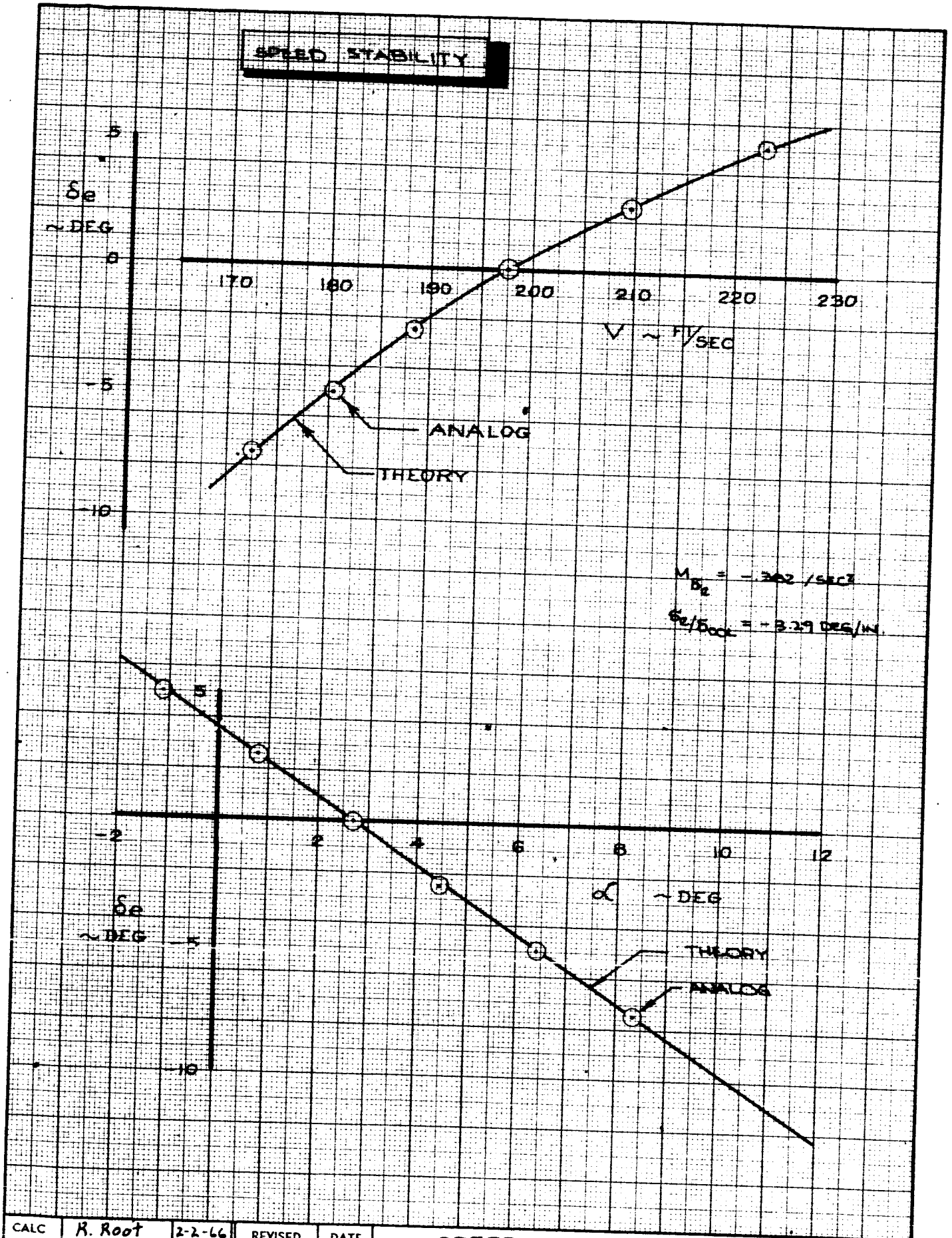

CALC	R. Root	2-2-66	REVISED	DATE	SPEED STABILITY GROUND BASED SIMULATOR CONFIGURATION G100
CHECK					D6-15000
APR					FIG. 27
APR					THE BOEING COMPANY
					PAGE VI-47

TD 461 C-R4

50

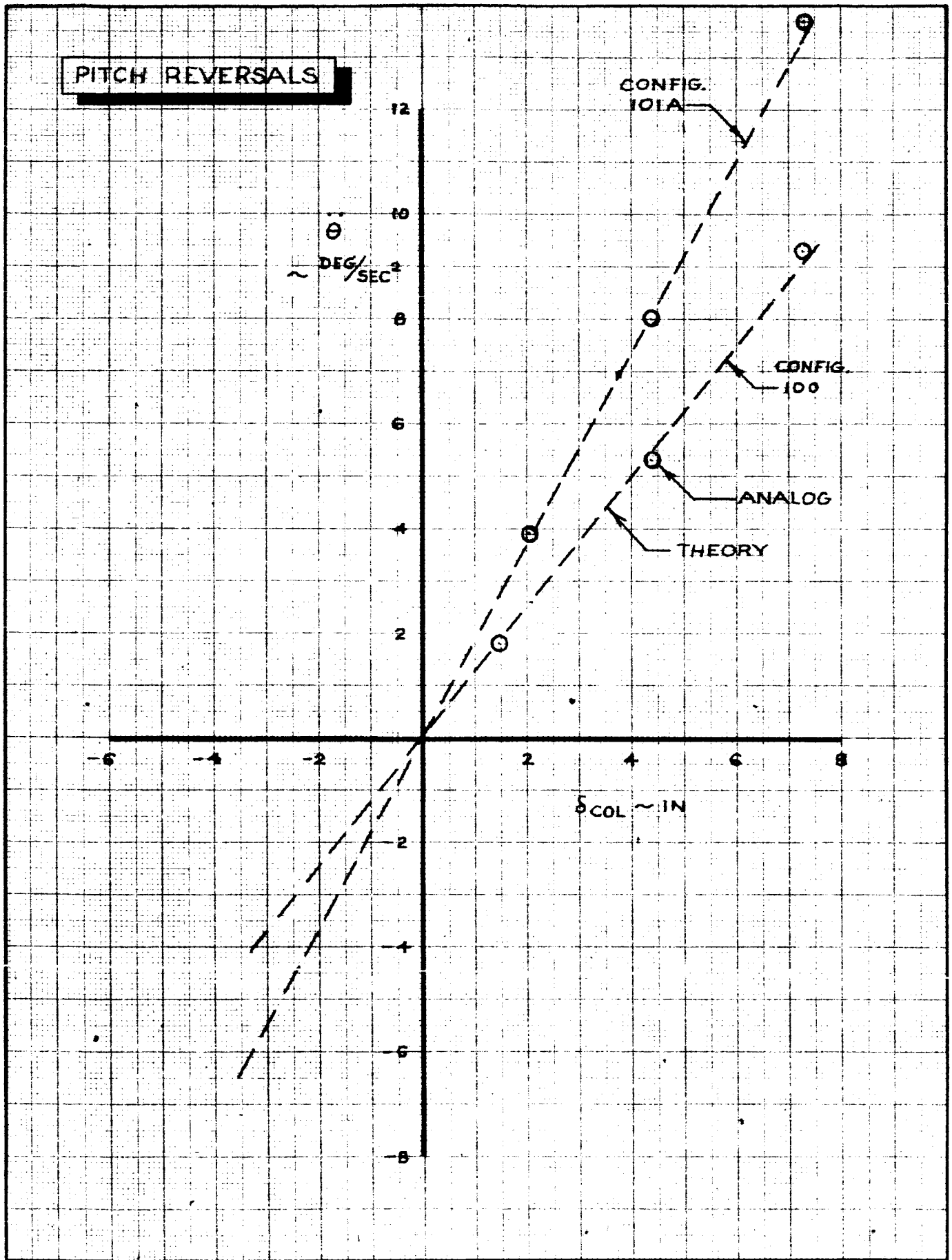

CALC	R. Root	2-2-66	REVISED	DATE	PITCH REVERSALS GROUND BASED SIMULATOR CONFIGURATION G100 & G101A
CHECK					D6-15000
APR					FIG. 28
APR					THE BOEING COMPANY
					PAGE VI-48

TD 461 C-R4

WHEEL REVERSAL

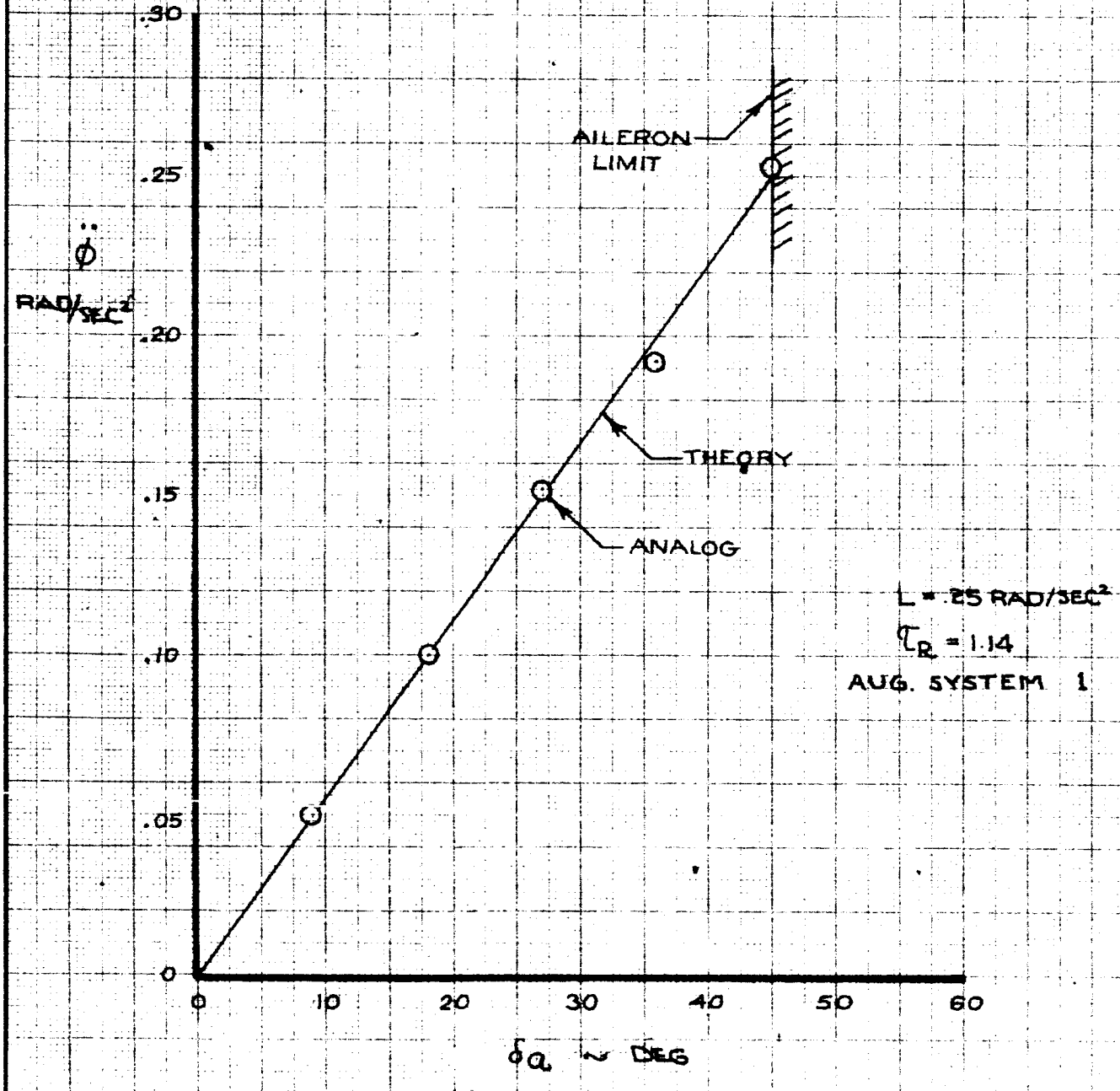

CALC	R. Root	2-2-66	REVISED	DATE	WHEEL REVERSAL GROUND BASED SIMULATOR CONFIGURATION G1202A	D6-15000
CHECK						FIG. 29
APR					THE BOEING COMPANY	PAGE VI-49
APR						

TD 461 C-R4

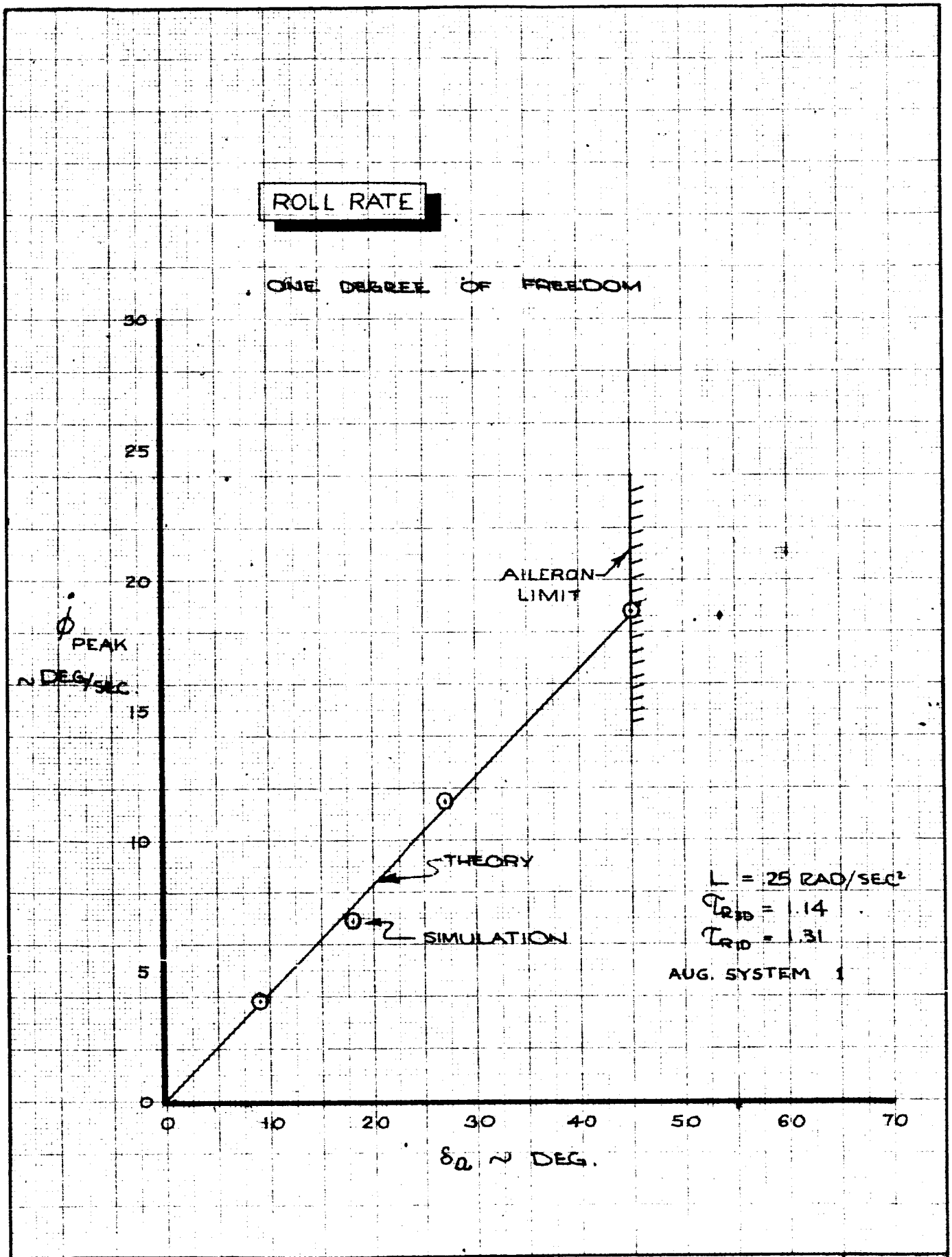

CALC	R. Root	2-2-66	REVISED	DATE	ROLL RATE GROUND BASED SIMULATOR CONFIGURATION G1202A	D6-15000
CHECK						FIG. 30
APR					THE BOEING COMPANY	PAGE VI-50
APR						

TD 461 C-R4

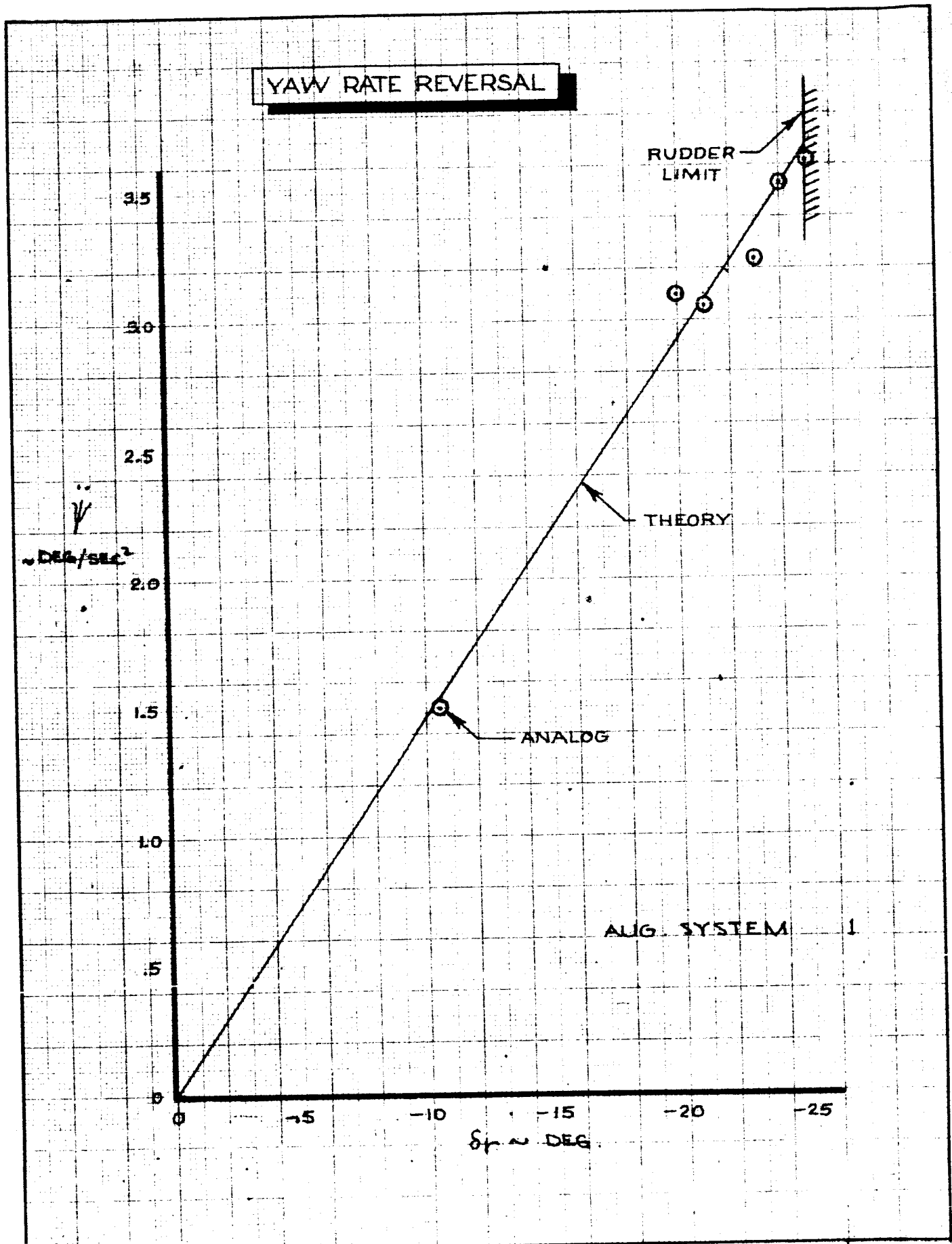

CALC	R. Root	2-2-66	REVISED	DATE	YAW RATE REVERSAL GROUND BASED SIMULATOR CONFIGURATION G1202A	D6-15000
CHECK						FIG. 31
APR						
APR					THE BOEING COMPANY	PAGE VI-51

TD 441 C-84

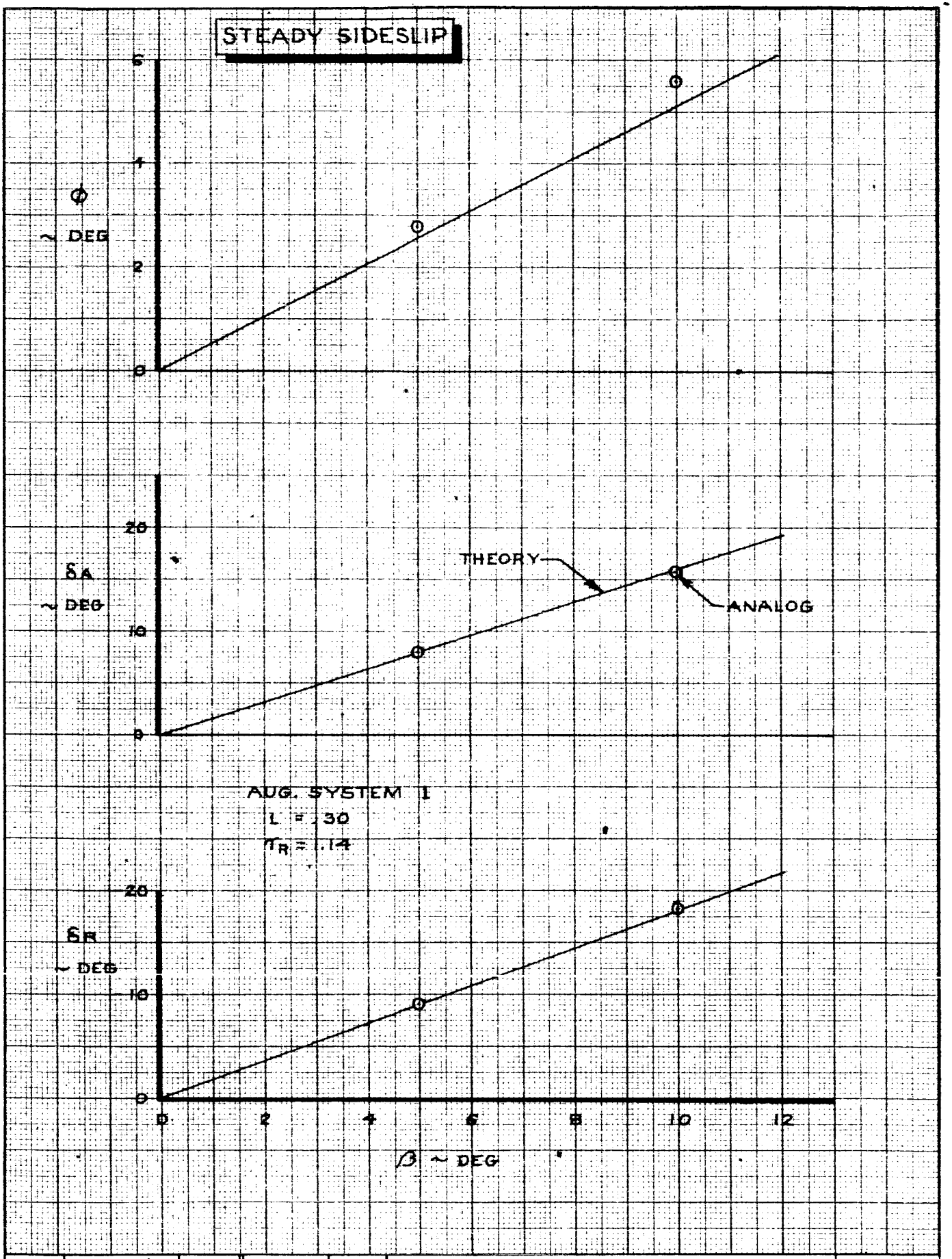

CALC	R. Root	2-2-66	REVISED	DATE	STEADY SIDESLIP CHARACTERISTICS GROUND BASED SIMULATOR CONFIGURATION G1202	D6-15000
CHECK						FIG. 31A
APR					THE BOEING COMPANY	PAGE VI-52
APR						

TD 461 C-R4

55

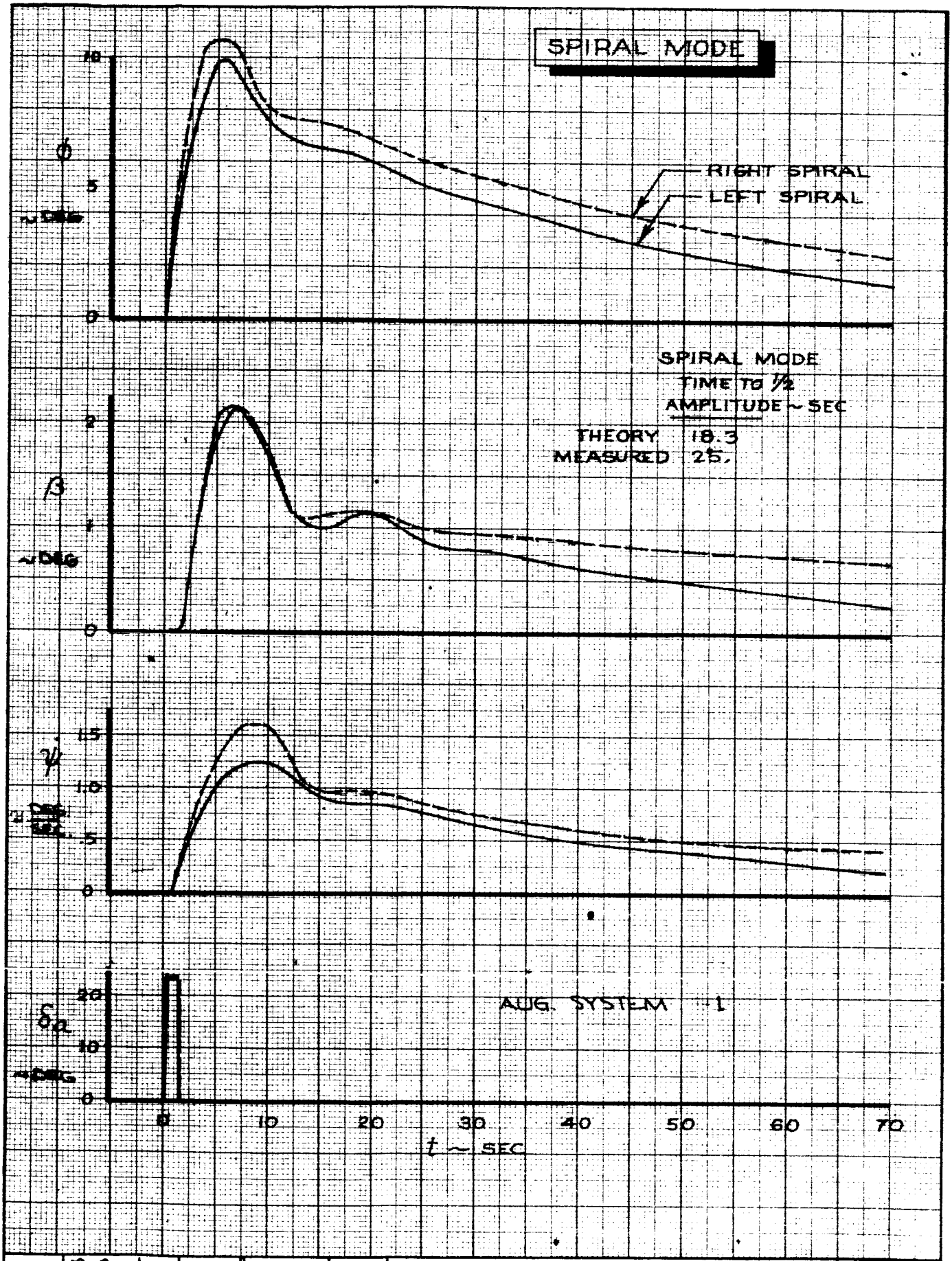

CALC	R. Root	2-2-66	REVISED	DATE	SPIRAL MODE GROUND BASED SIMULATOR CONFIGURATION G1202A	D6-15000
CHECK						FIG. 32
APR					THE BOEING COMPANY	PAGE VI-53
APR						

TD 461 C-R4

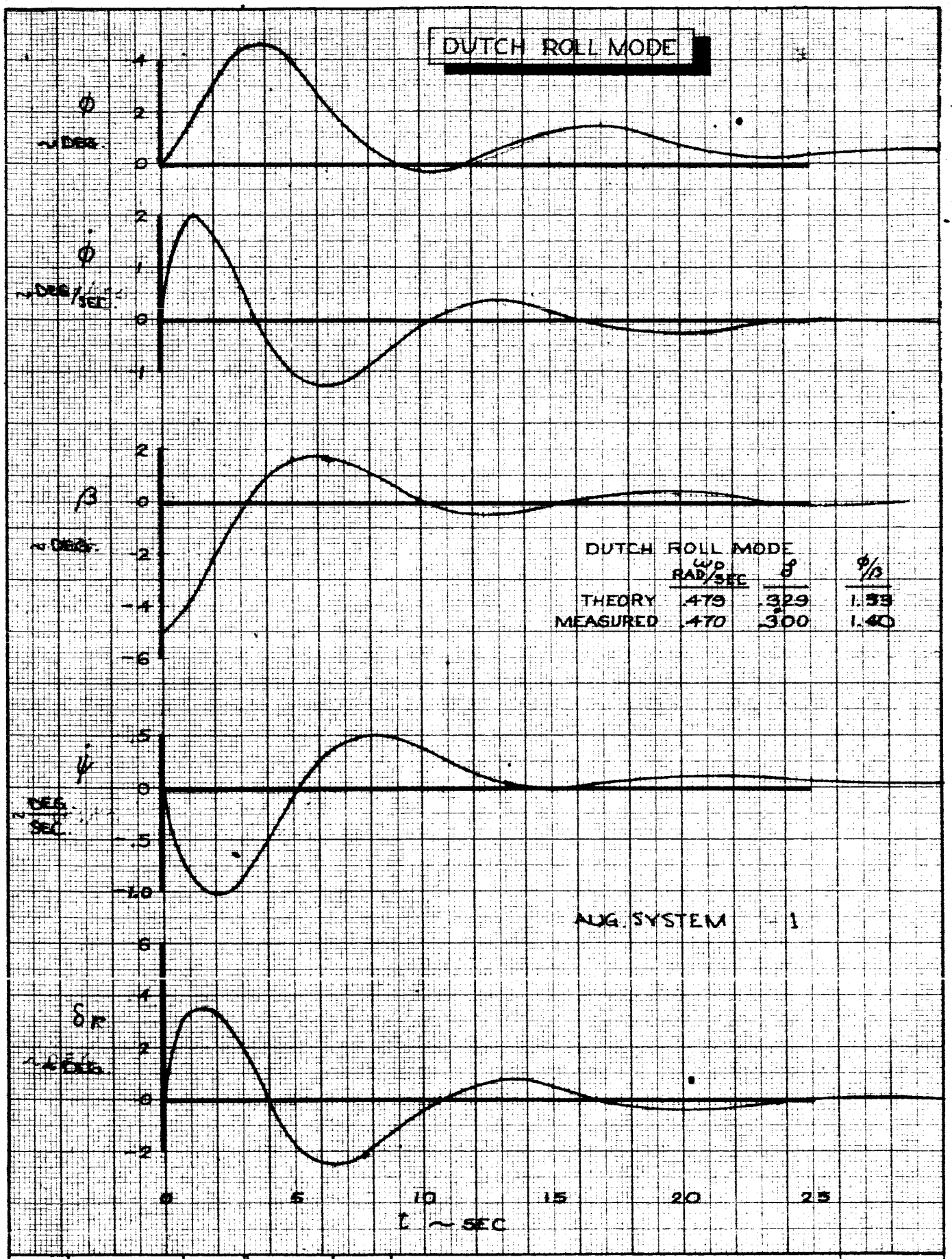

CALC	R. Root	2-2-66	REVISED	DATE	DUTCH ROLL MODE GROUND BASED SIMULATOR CONFIGURATION G1202A
CHECK					
APR					
APR					
					THE BOEING COMPANY

D6-15000

FIG. 33

PAGE VI-54

TD 461 C-R4

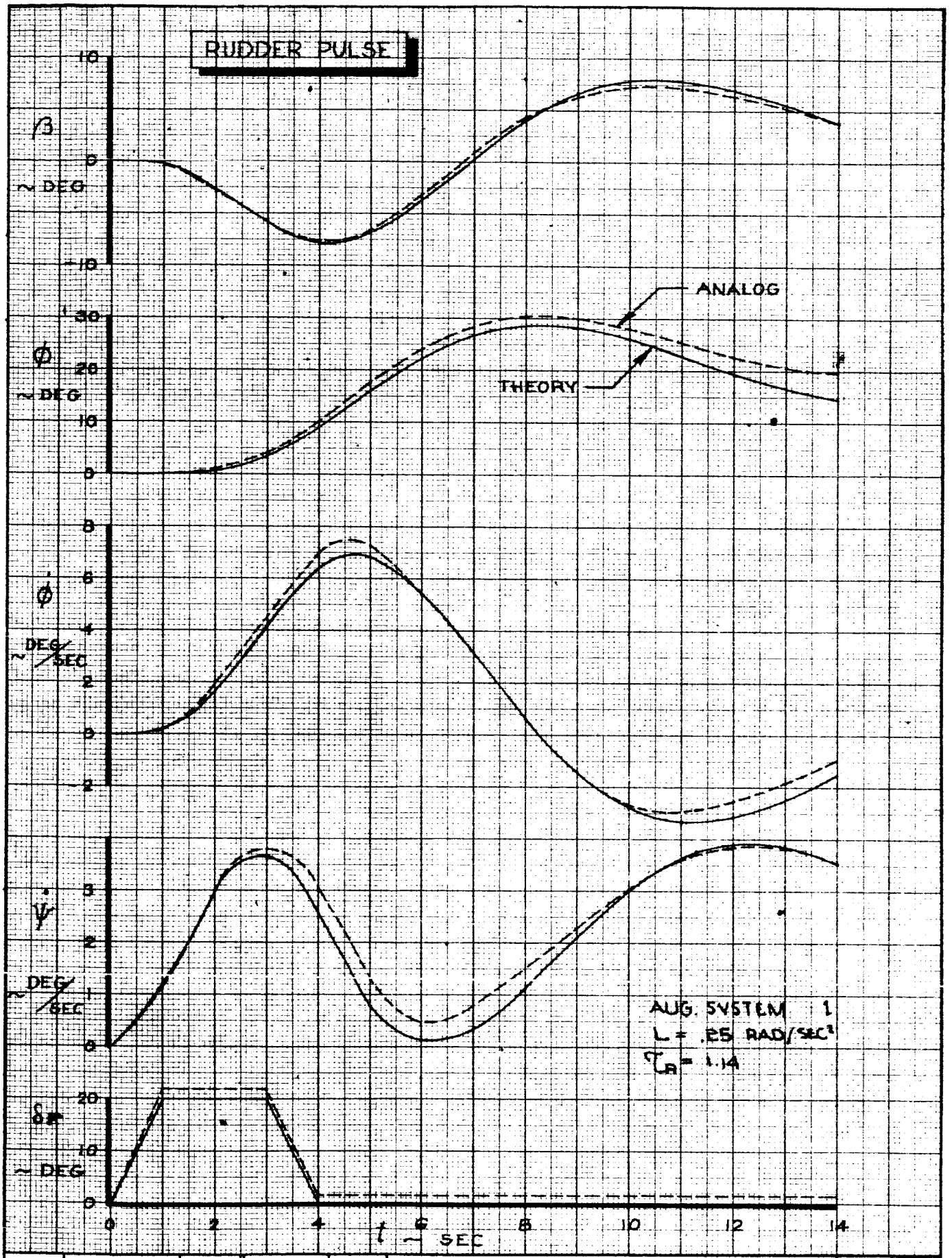

CALC	R. Root	2-2-66	REVISED	DATE	RUDDER PULSE GROUND BASED SIMULATOR CONFIGURATION G1202A
CHECK					
APR					
APR					
					THE BOEING COMPANY

D6-15000

FIG. 34

PAGE VI-55

TD 461 C-R4

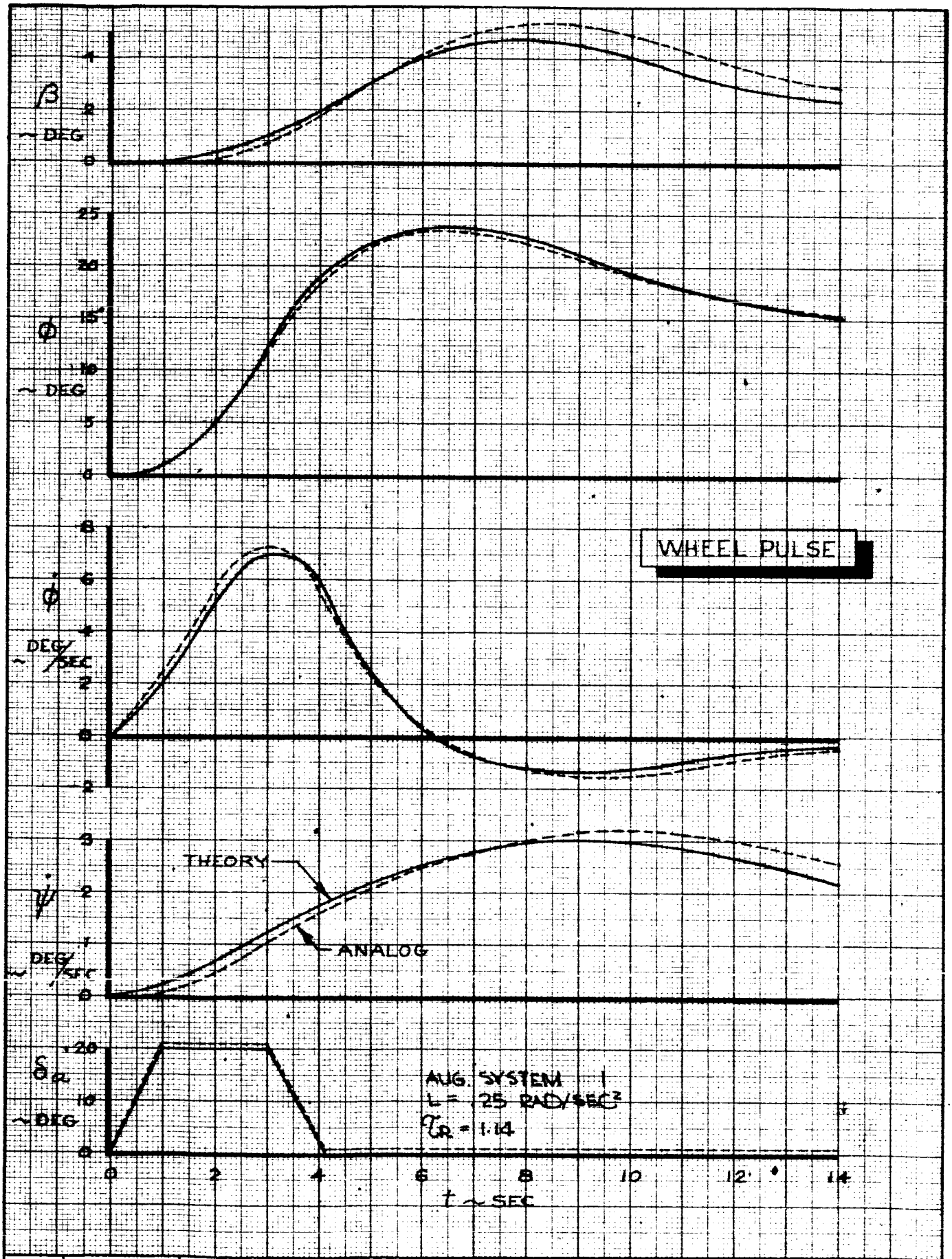

CALC	R. Root	2-2-66	REVISED	DATE	WHEEL PULSE GROUND BASED SIMULATOR CONFIGURATION G1202A
CHECK					
APR					
APR					
					THE BOEING COMPANY

D6-15000

FIG. 35

PAGE VI-56

TD 461 C-R4

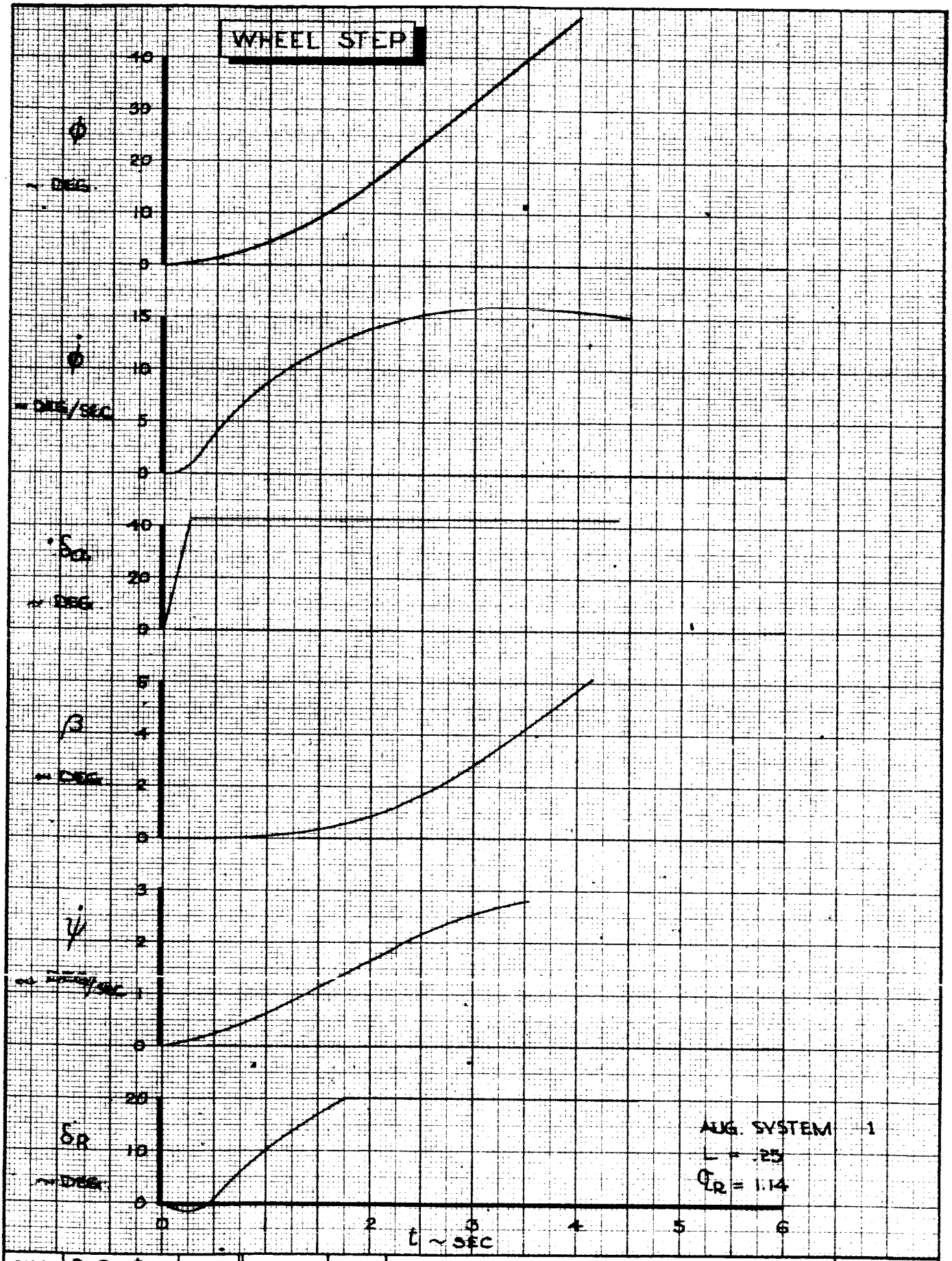

CALC	R. Root	2-2-66	REVISED	DATE	WHEEL STEP GROUND BASED SIMULATOR CONFIGURATION G1202A
CHECK					
APR					
APR					THE BOEING COMPANY

D6-15000

FIG. 36

PAGE VI-57

TD 461 C-R4

VII. LONGITUDINAL CONFIGURATION

A. Airborne Simulation

Eight variations of the basic longitudinal configuration are discussed in this section. The documentation maneuvers performed with each configuration are summarized in a single Figure or Table whenever possible. They are eliminated entirely when the response does not change significantly from that of the basic configuration. For the purposes of evaluating and documenting the longitudinal mode the lateral configuration was always the basic 1209.

Table 1 contains a summary of the longitudinal configurations evaluated on the Airborne Simulation. The numbers shown are theoretical values equivalent to the theoretical lines shown on the Figures. The longitudinal aerodynamic coefficients used to obtain these characteristics are listed in Appendix 1.

27

AD 1017-R6

ENGR.	CHECK	APR	APR

DATE	REVISED

AIRBORNE SIMULATION
LONGITUDINAL RUN LOG

THE BOEING COMPANY
RENTON, WASHINGTON

TABLE 1
D6-15000
VII-59

CONFIG.	L_α /SEC-RAD	M_α 1/SEC²	$L_{\delta COL.}$ 1/SEC-IN	$M_{\delta COL.}$ RAD/SEC²/IN	$M_{\dot\alpha}$ 1/SEC	$L_{\dot\alpha}$ 1/RAD	SHORT PERIOD ω_n RAD/SEC	SHORT PERIOD ζ –	PHUGOID ω_n RAD/SEC	PHUGOID ζ –	COMMENTS INCREASED (+) DECREASED (–)
101A	.521	-.506	-.00313	.0252	-.587	.0516	.907	.7033	.1720	.1490	BASIC
100	↓	↓	+.00262	.0167	↓	↓	↓	↓	↓	↓	– SENSITIVITY
105A	↓	↓	-.00625	.0504	↓	↓	↓	↓	↓	↓	+ SENSITIVITY – LIFT WITH δ COL.
105 *	↓	↓	+.00792	↓	↓	↓	↓	↓	↓	↓	+ SENSITIVITY – – LIFT WITH δ COL.
151B	↓	↓	+.00010	.0252	↓	↓	↓	↓	↓	↓	+ + LIFT WITH $\delta_{COL.}$
151C	↓	↓	+.00164	↓	↓	↓	↓	↓	↓	↓	+ LIFT WITH $\delta_{COL.}$
151D	↓	↓	+.00020	.0504	↓	↓	↓	↓	↓	↓	+ SENSITIVITY + + LIFT WITH δ COL.
158A	.552	-1.012	+.00635	↓	-1.174	.0984	1.330	.7205	.1693	.1845	+ SENS. – LIFT WITH δ COL. + DAMPING + STATIC STABILITY
159A	.521	-.506	+.00316	.0252	-1.174	.0984	1.071	.8647	.1446	.2352	+ DAMPING
159B	.521	-.506	+.00635	.0504	-1.174	.0984	1.071	.8647	.1446	.2352	+ SENS. – LIFT WITH δ COL. + DAMPING
161B	.497	-.128	+.00635	↓	-.587	.0516	.650	.9423	.1200	.3320	+ SENS – LIFT WITH $\delta_{COL.}$ – STATIC STAB.
-80 BLC	.459	-.469	+.00278	.0641	-.125	0	1.347	.5245	.1352	.1244	+ DAMPING + STATIC STABILITY

A summary of pitch rate reversals for all configurations is shown in Fig. 37 normalized to the pitch control sensitivity of the basic 101A configuration. This curve shows some scatter in the data but generally good agreement with the theoretical for all configurations.

Column steps are shown in Figs. 38 & 39 for two configurations, 151B and 151C, which point out changes in lift due to column deflection when compared to the basic 101A configuration (Fig. 4). A lag is apparent in the flight test data that does not show up in the theoretical results. This could be due to an aerodynamic lag or a lag in the lift control (spoilers) which does not appear in the theory.

The wind up turn data is shown for all configurations in Figs. 40 through 55 and matches the theoretical calculations accurately.

Speed stability tests were performed and correlation with the theoretical static characteristics was good. Results are shown in Figs. 56 through 63.

A summary of phugoid characteristics for all configurations is shown in Table 2. The damping ratios were difficult to measure accurately since only one cycle of the phugoid was recorded and they do not compare accurately with the theoretical. The period, on the other hand, was easily determined and agrees closely with theory.

TABLE 2

PHUGOID CHARACTERISTICS

CONFIGURATION	PERIOD (SEC)		DAMPING RATIO	
	Flight Test	Theory	Flight Test	Theory
-80B	40.9	46.5	.140	.1244
100	36.6	36.9	.078	.1490
101A	36.0	36.9	.062	.1490
105*	29.6	36.9	.058	.1490
105A	30.0	36.9	.063	.1490
151B	26.2	36.9	.093	.1490
151C	31.2	36.9	.070	.1490
158A	35.8	37.8	.102	.1845
159A	40.8	44.5	.128	.2352
161B	31.3	55.5	.090	.3320

A pitch attitude change is shown for configuration 158A in Fig. 64. Comparison with the basic 101A configuration (Fig. 9) shows the effect of changing lift with column deflection.

Elevator pulses are shown in Figs. 65 thru 67 for three configurations, 158A, 159A and 161B. Comparison of these pulses with the 101A configuration (Fig. 10) and with one another shows the effect static stability and pitch damping.

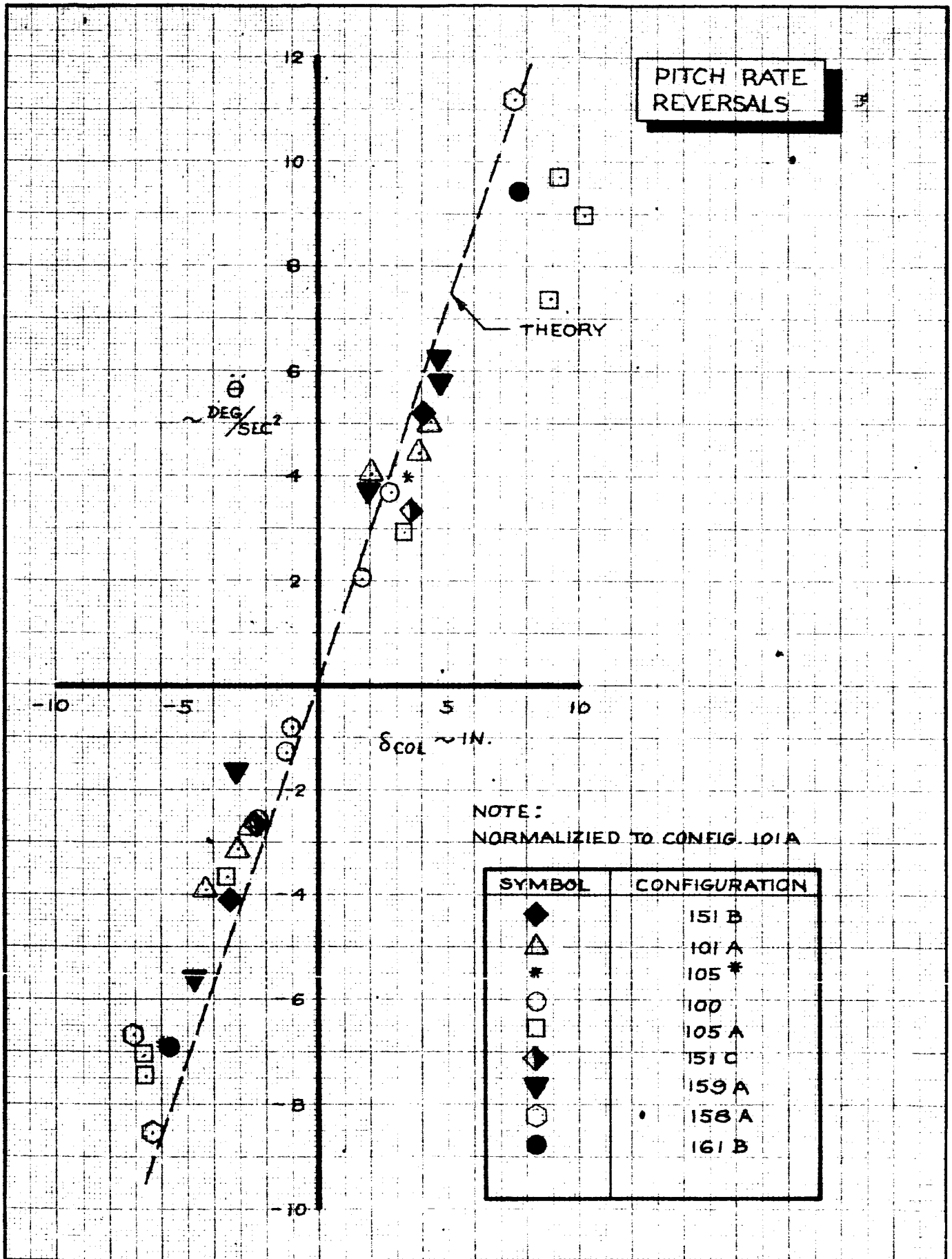

CALC			REVISED	DATE	NORMALIZIED PITCH RATE REVERSALS - SUMMARY
CHECK					
APR					
APR					

367-80

FIG. 37

THE BOEING COMPANY D6-15000

PAGE VII-62

TD 461 C-R4

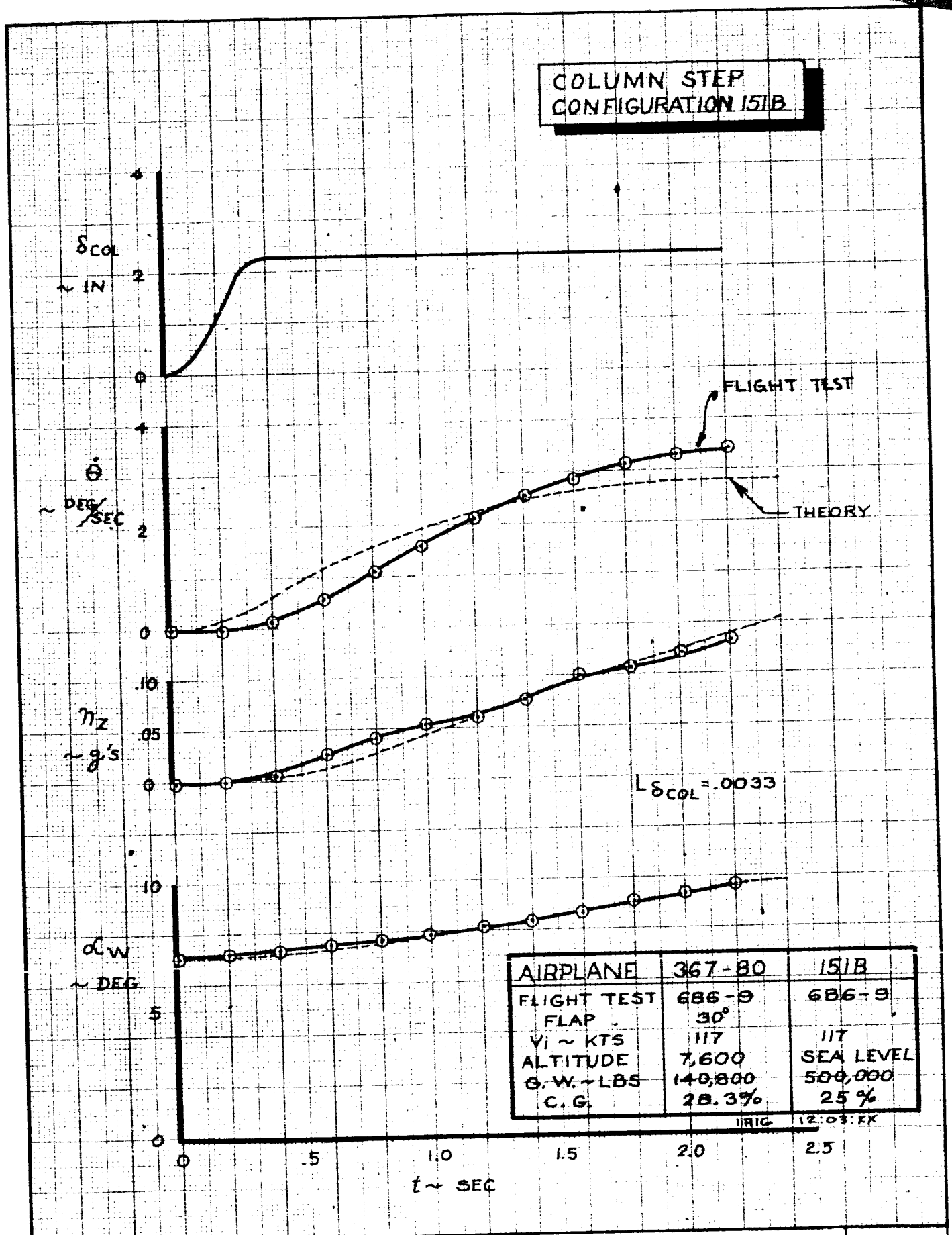

AIRPLANE	367-80	151B
FLIGHT TEST	686-9	686-9
FLAP	30°	
Vi ~ KTS	117	117
ALTITUDE	7,600	SEA LEVEL
G.W. ~ LBS	140,800	500,000
C.G.	28.3%	25%

IRIG 12:03:FK

CALC			REVISED	DATE
CHECK				
APR				
APR				

COLUMN STEP
FLIGHT TEST 686-9
CONFIGURATION 151 B

367-80

FIG. 38

THE BOEING COMPANY D6-15000

PAGE VII-63

TD 461 C-84

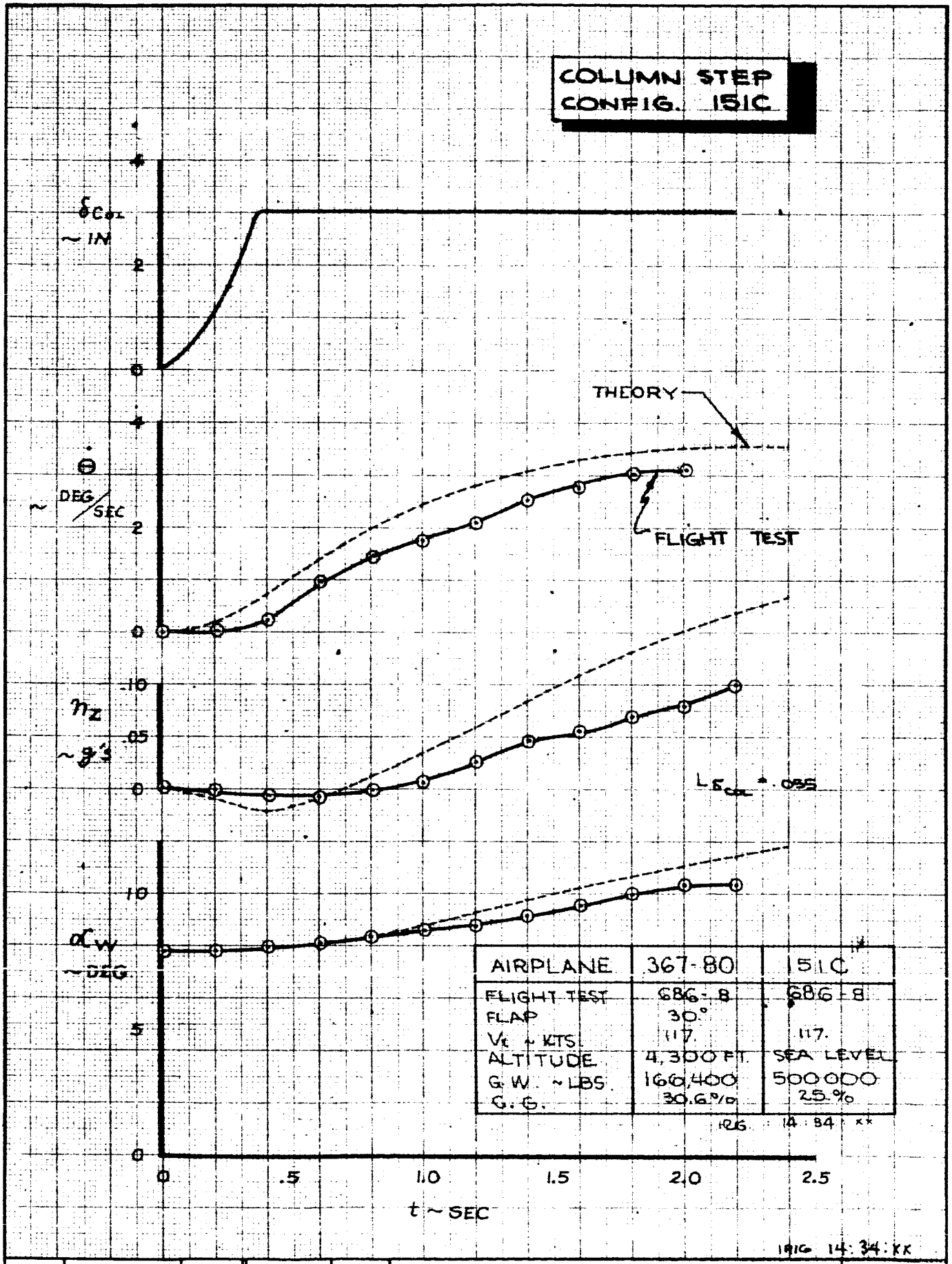

			REVISED	DATE		
CALC					COLUMN STEP FLIGHT TEST 686-8 CONFIGURATION 151C	367-80
CHECK						FIG. 39
APR						
APR					THE BOEING COMPANY DG-15000	PAGE VII-64

TD 461 C-R4

WINDUP TURN

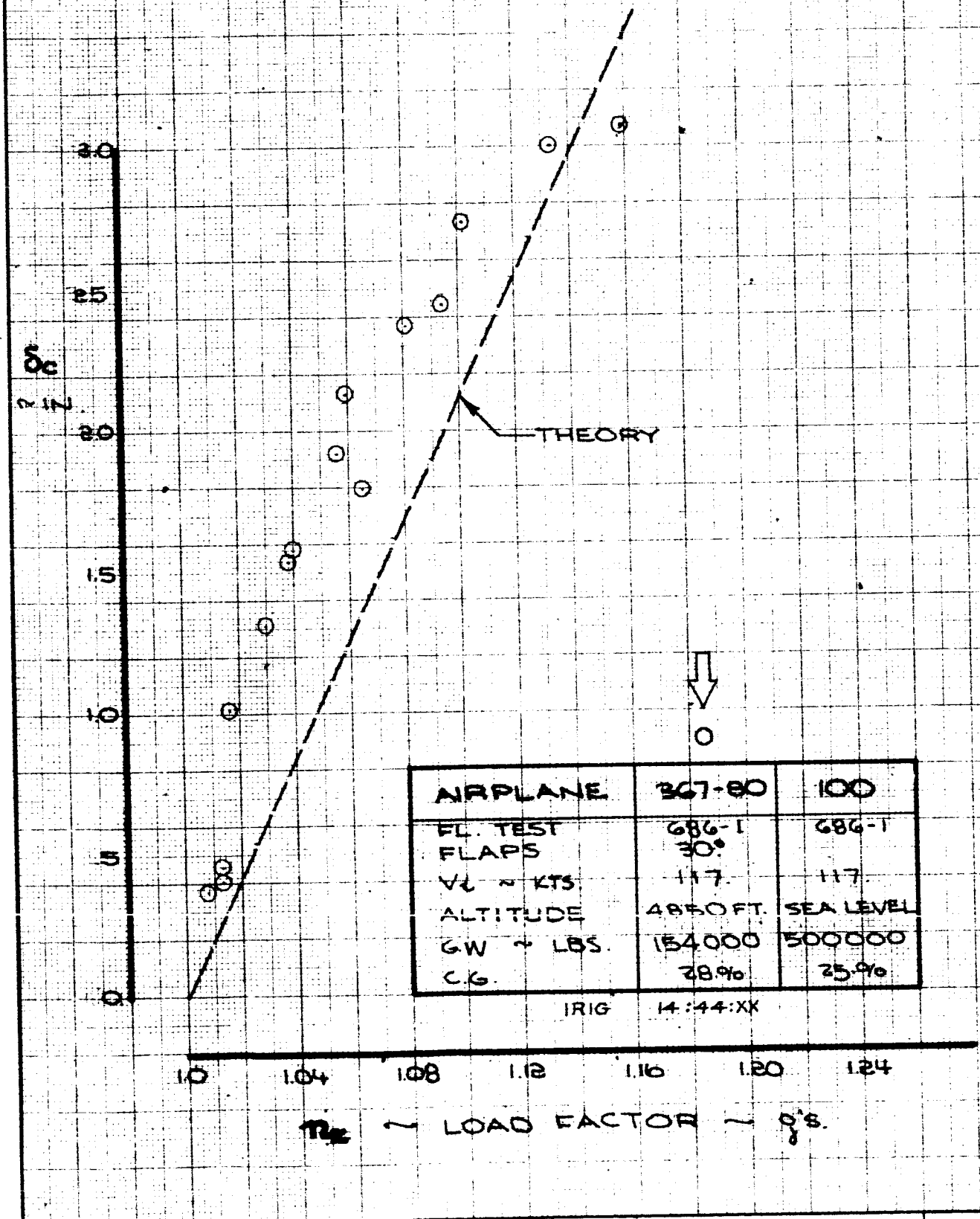

AIRPLANE	367-80	100
FL. TEST	686-1	686-1
FLAPS	30°	
V_i ~ KTS.	117.	117.
ALTITUDE	4850 FT.	SEA LEVEL
GW ~ LBS.	154000	500000
C.G.	28%	25.9%

IRIG 14:44:XX

			REVISED	DATE
CALC				
CHECK				
APR				
APR				

WINDUP TURN
FL. TEST : 686-1
CONFIG. : 100

367-80

FIG. 40

THE BOEING COMPANY D6-15000

PAGE VII-65

TD 461 C-R4

WINDUP TURN

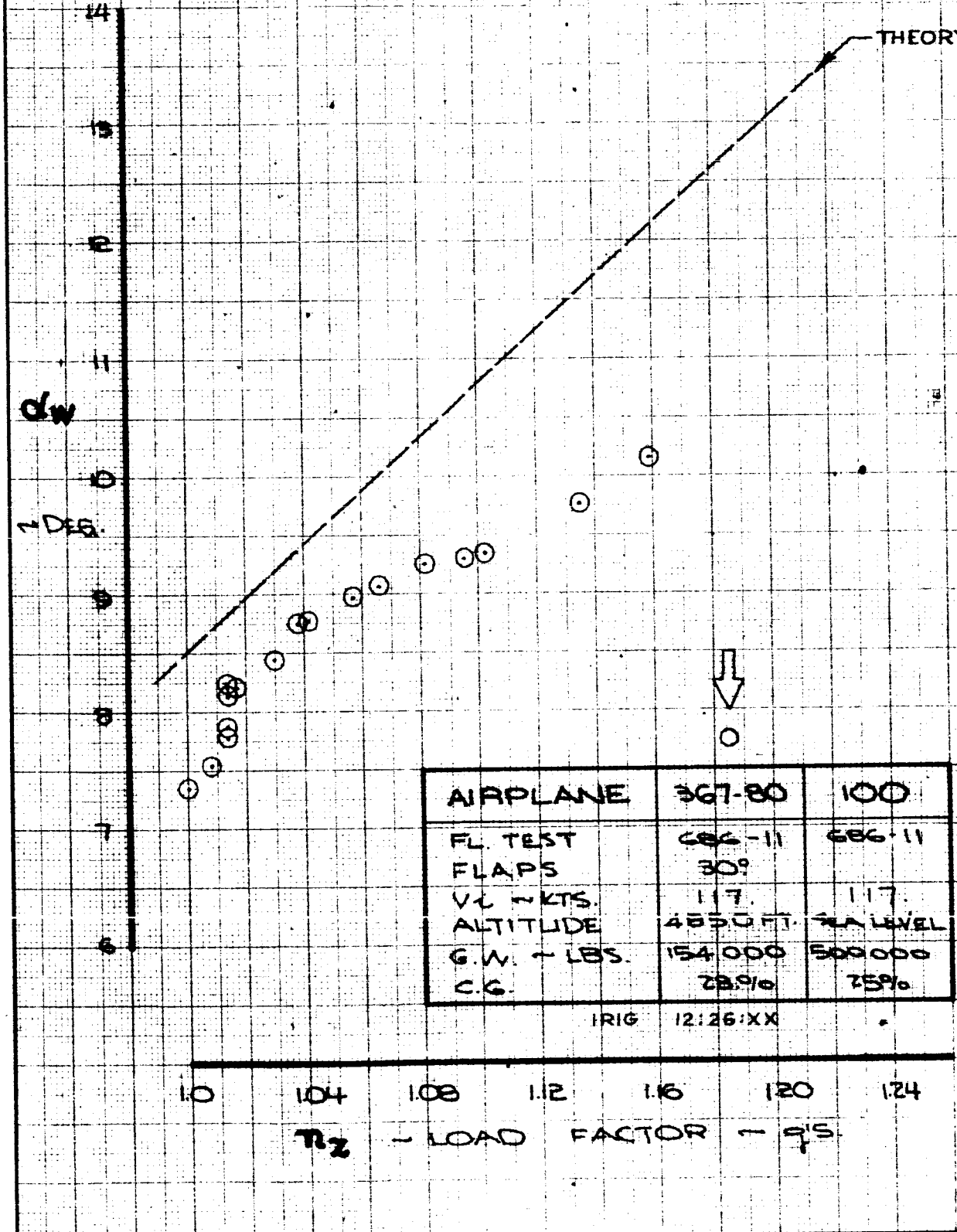

AIRPLANE	367-80	100
FL. TEST	686-11	686-11
FLAPS	30°	
V_L ~ KTS.	117.	117.
ALTITUDE	4850 FT.	SEA LEVEL
G.W. ~ LBS.	154000	500000
C.G.	28.9%	25%
	IRIG 12:26:XX	

			REVISED	DATE	WINDUP TURN FL. TEST : 686-11 CONFIG. : 100	367-80 FIG. 41
CALC						
CHECK						
APR						
APR					THE BOEING COMPANY D6-15000	PAGE VII-66

WINDUP TURN

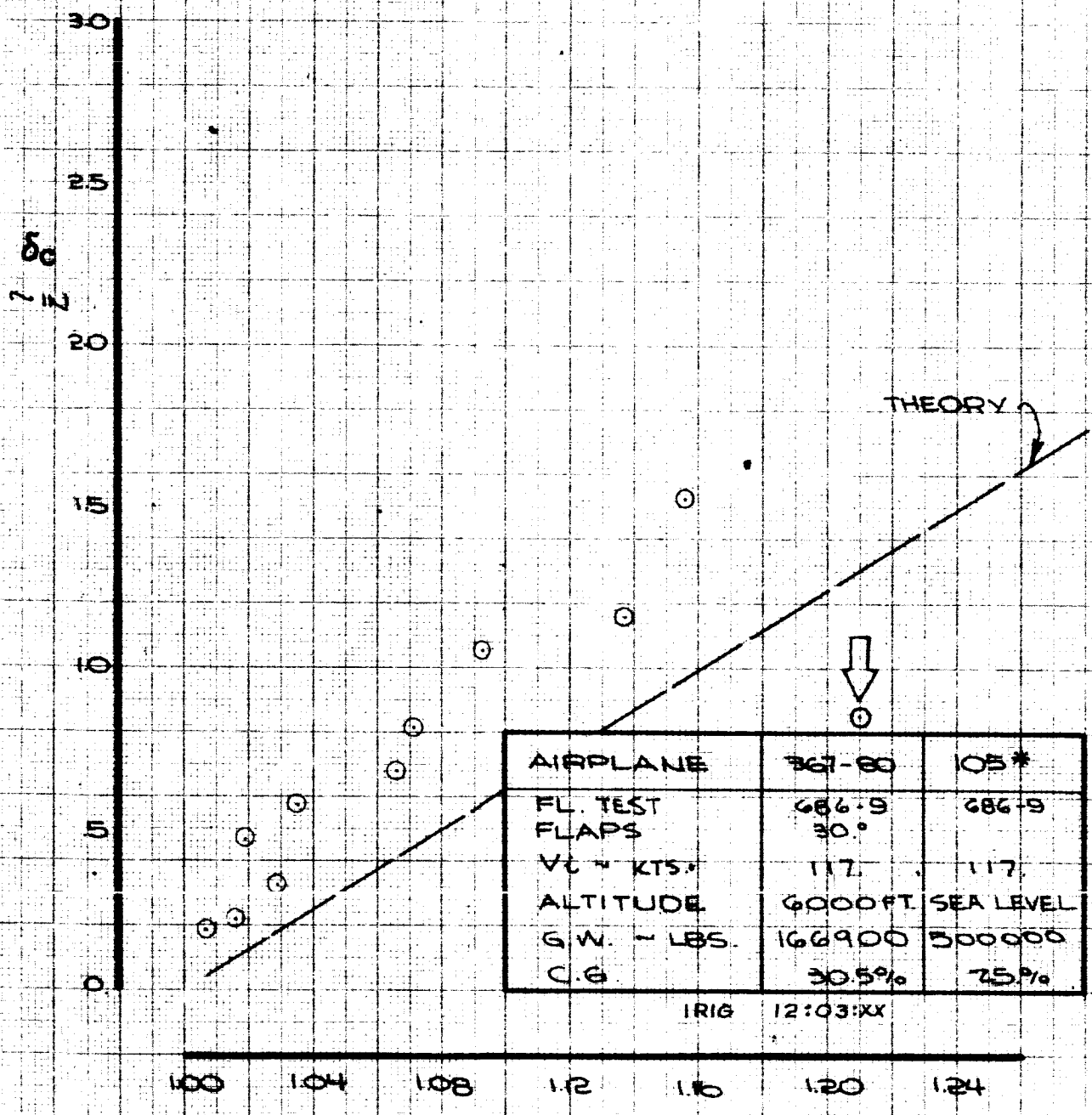

AIRPLANE	367-80	105*
FL. TEST	686-9	686-9
FLAPS	30°	
V_t ~ KTS.	117.	117.
ALTITUDE	6000 FT.	SEA LEVEL
G.W. ~ LBS.	166900	500000
C.G	30.5%	25%
	IRIG	12:03:XX

			REVISED	DATE	WINDUP TURN	367-80
CALC					FL. TEST : 686-9 .	
CHECK					CONFIG. 105*	FIG. 42
APR					THE BOEING COMPANY D6-15000	PAGE VII-67
APR						

TD 461 C-R4

WINDUP TURN

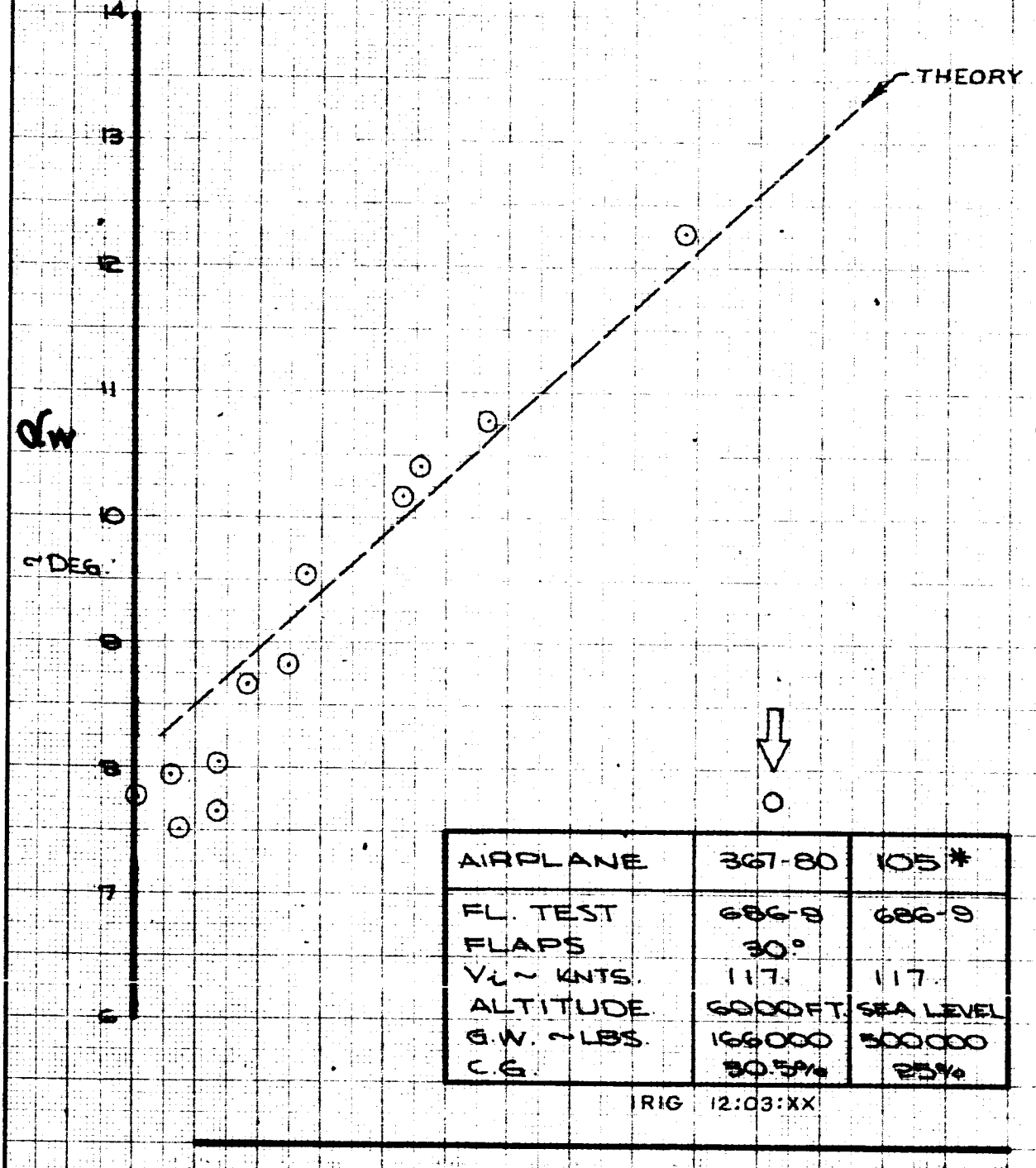

AIRPLANE	367-80	105*
FL. TEST	686-8	686-9
FLAPS	30°	
V_i ~ KNTS.	117.	117.
ALTITUDE	6000 FT.	SEA LEVEL
G.W. ~ LBS.	166000	300000
C.G.	30.5%	25%

IRIG 12:03:XX

CALC			REVISED	DATE	WINDUP TURN FL. TEST: 686-9 CONFIG. : 105*	367-80
CHECK						FIG. 43
APR						
APR					THE BOEING COMPANY D6-15000	PAGE VII-68

TD 461 C-R4

WINDUP TURN

AIRPLANE	367-80	105A
FL. TEST	686-7	686-7
FLAPS	30°	
V_C ~ KTS.	117.	117.
ALTITUDE	4500 FT.	SEA LEVEL
G.W. ~ LBS.	162000	500000
C.G.	30.7%	25.%

IRIG 11:50:XX

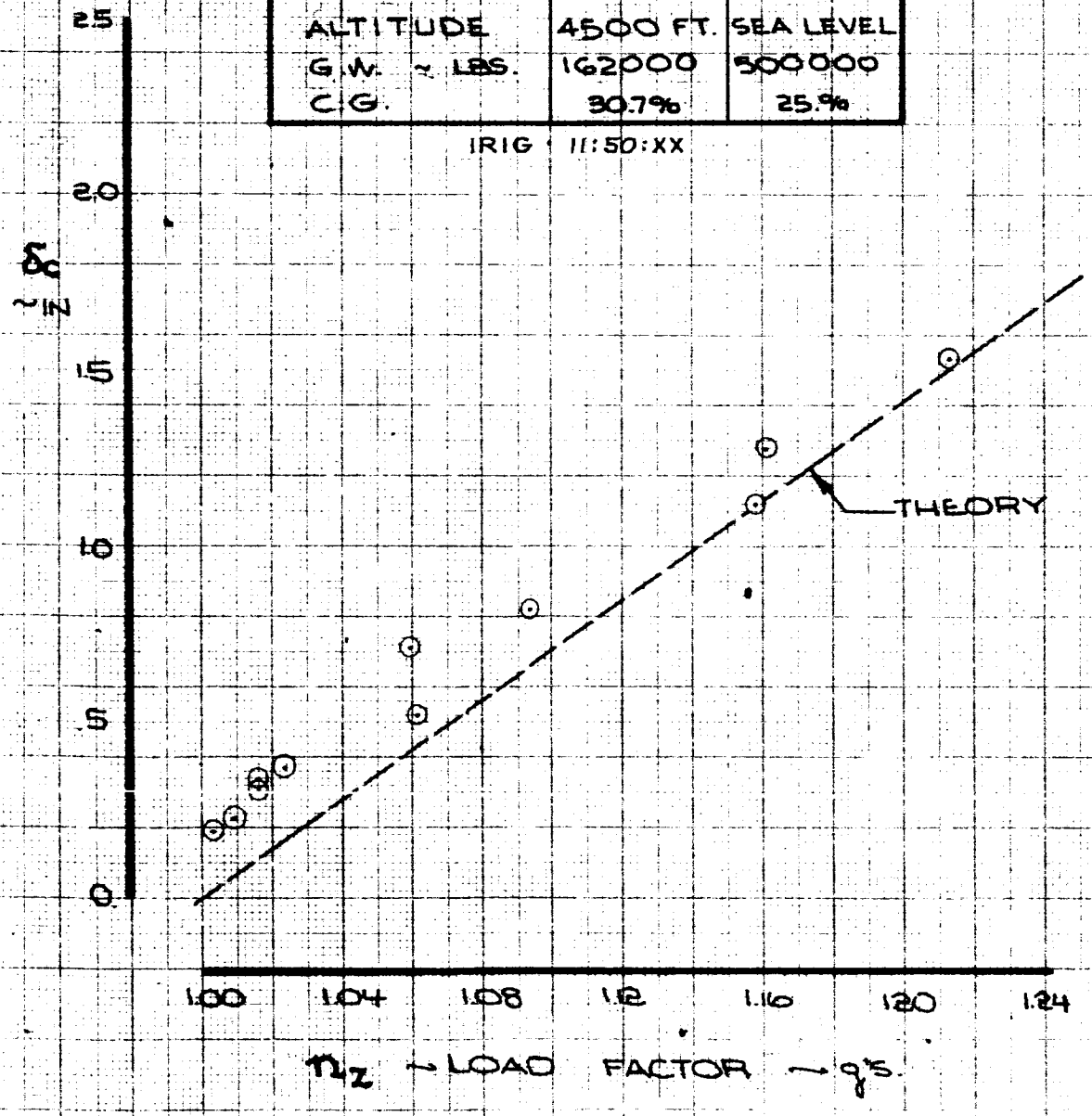

CALC			REVISED	DATE	WINDUP TURN	367-80
CHECK					FL. TEST : 686-7	
APR					CONFIG.: 105A	FIG. 44
APR					THE BOEING COMPANY D6-15000	PAGE VII-69

TD 461 C-R4

72

WINDUP TURN

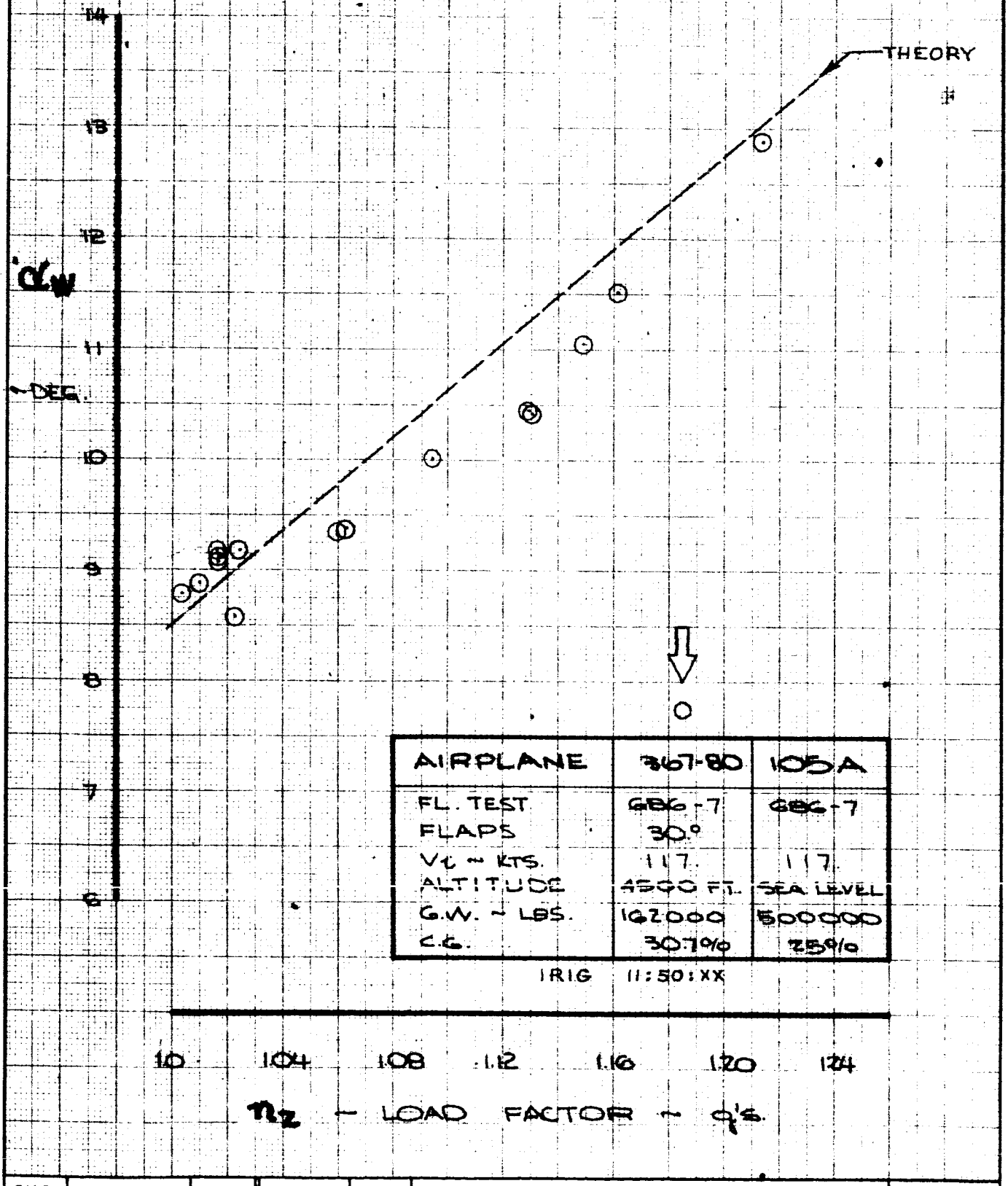

AIRPLANE	367-80	105A
FL. TEST	686-7	686-7
FLAPS	30°	
V_i ~ KTS.	117.	117.
ALTITUDE	4500 FT.	SEA LEVEL
G.W. ~ LBS.	162000	500000
C.G.	30.7%	25%
IRIG	11:50:XX	

			REVISED	DATE		
CALC					WINDUP TURN	105A
CHECK					FL. TEST : 686-7	
APR					CONFIG. : 105A	FIG. 45
APR					THE BOEING COMPANY D6-15000	PAGE VII-70

TD 461 C-R4

WINDUP TURN

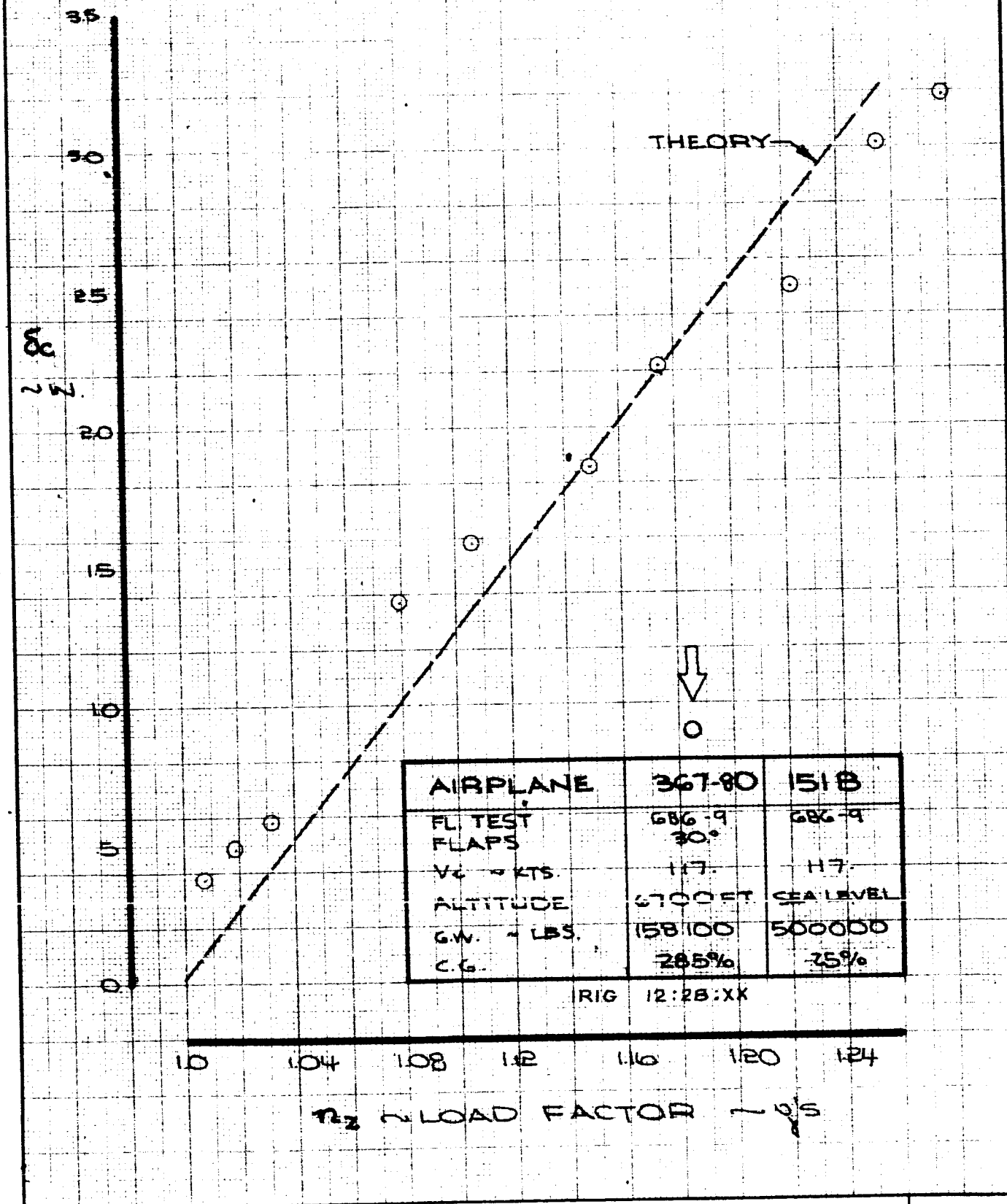

AIRPLANE	367-80	151B
FL. TEST	686-9	686-9
FLAPS	30°	
V_c ~ KTS.	117.	117.
ALTITUDE	6700 FT.	SEA LEVEL
G.W. ~ LBS.	158100	500000
C.G.	28.5%	25%

RIG 12:28:XX

			REVISED	DATE
CALC				
CHECK				
APR				
APR				

WINDUP TURN
FL. TEST: 686-9
CONFIG. 151B

THE BOEING COMPANY D6-15000

367-80
FIG. 46
PAGE VII-71

TD 461 C-R4

WINDUP TURN

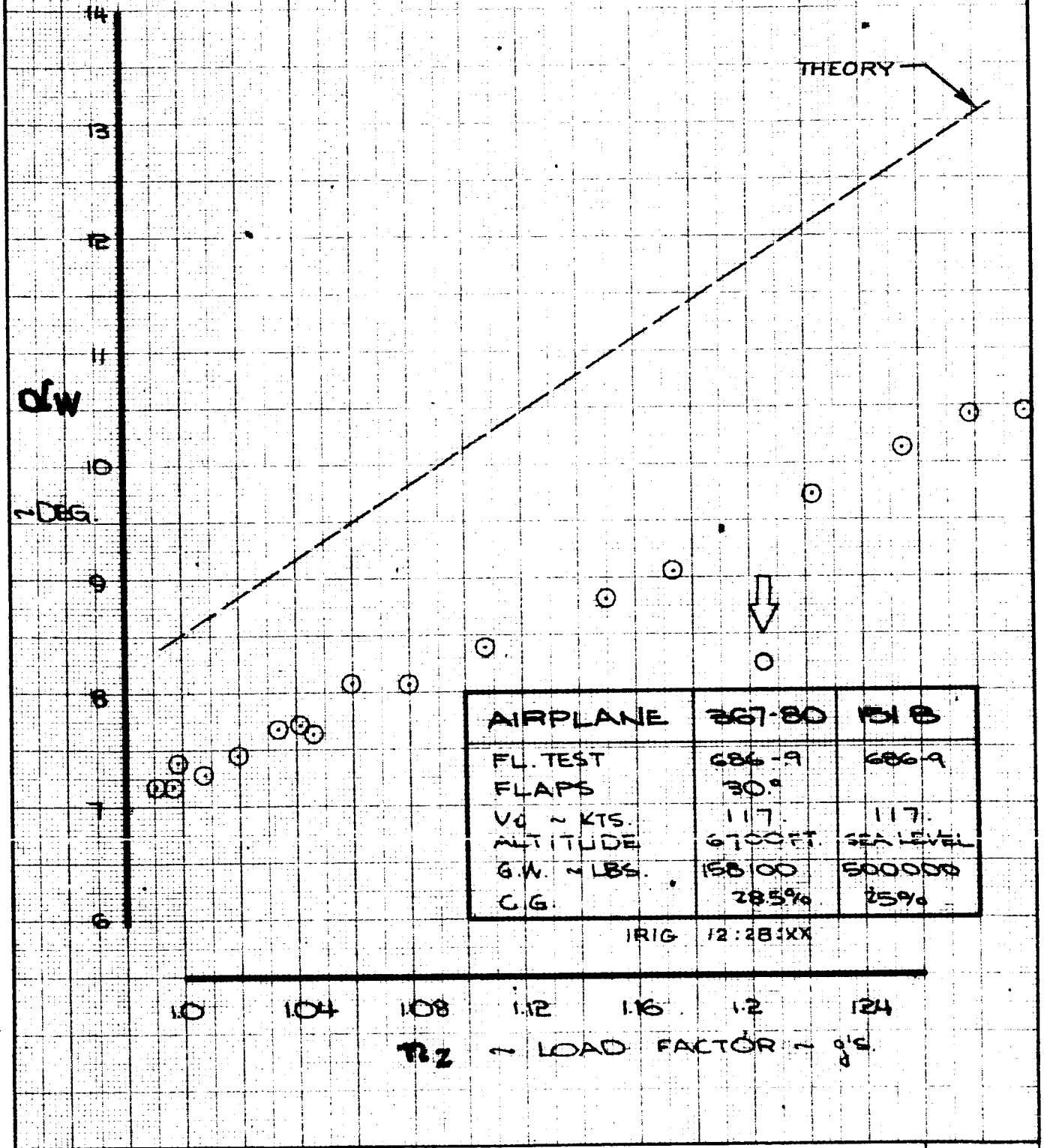

AIRPLANE	367-80	151 B
FL. TEST	686-9	686-9
FLAPS	30°	
Vc ~ KTS.	117.	117.
ALTITUDE	6700 FT.	SEA LEVEL
G.W. ~ LBS.	158100	500000
C.G.	28.5%	25%

IRIG 12:28:XX

CALC			REVISED	DATE	WINDUP TURN FL. TEST : 686-9 CONFIG. : 151B
CHECK					
APR					
APR					

151-B

FIG. 47

THE BOEING COMPANY D6-15000

PAGE VII-72

TD 461 C-R4

WINDUP TURN

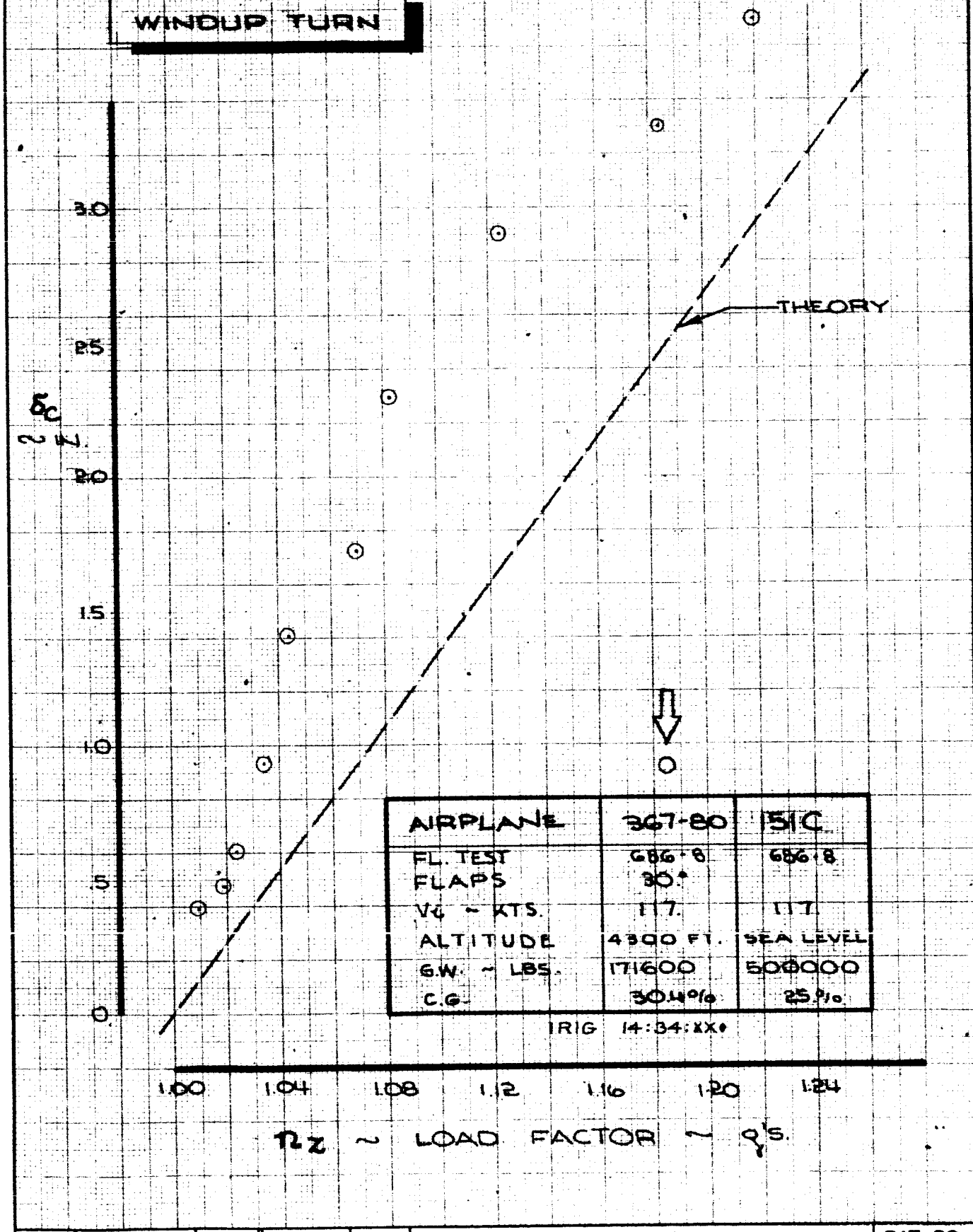

AIRPLANE	367-80	151C
FL. TEST	686-8	686-8
FLAPS	30°	
V_i ~ KTS.	117.	117.
ALTITUDE	4300 FT.	SEA LEVEL
G.W. ~ LBS.	171600	500000
C.G.	30.4%	25.%

IRIG 14:34:XX

			REVISED	DATE
CALC				
CHECK				
APR				
APR				

WINDUP TURN
FL. TEST. : 686-8
CONFIG. 151C

367-80

FIG. 48

THE BOEING COMPANY D6-15000

PAGE VII-73

TD 461 C-R4

WINDUP TURN

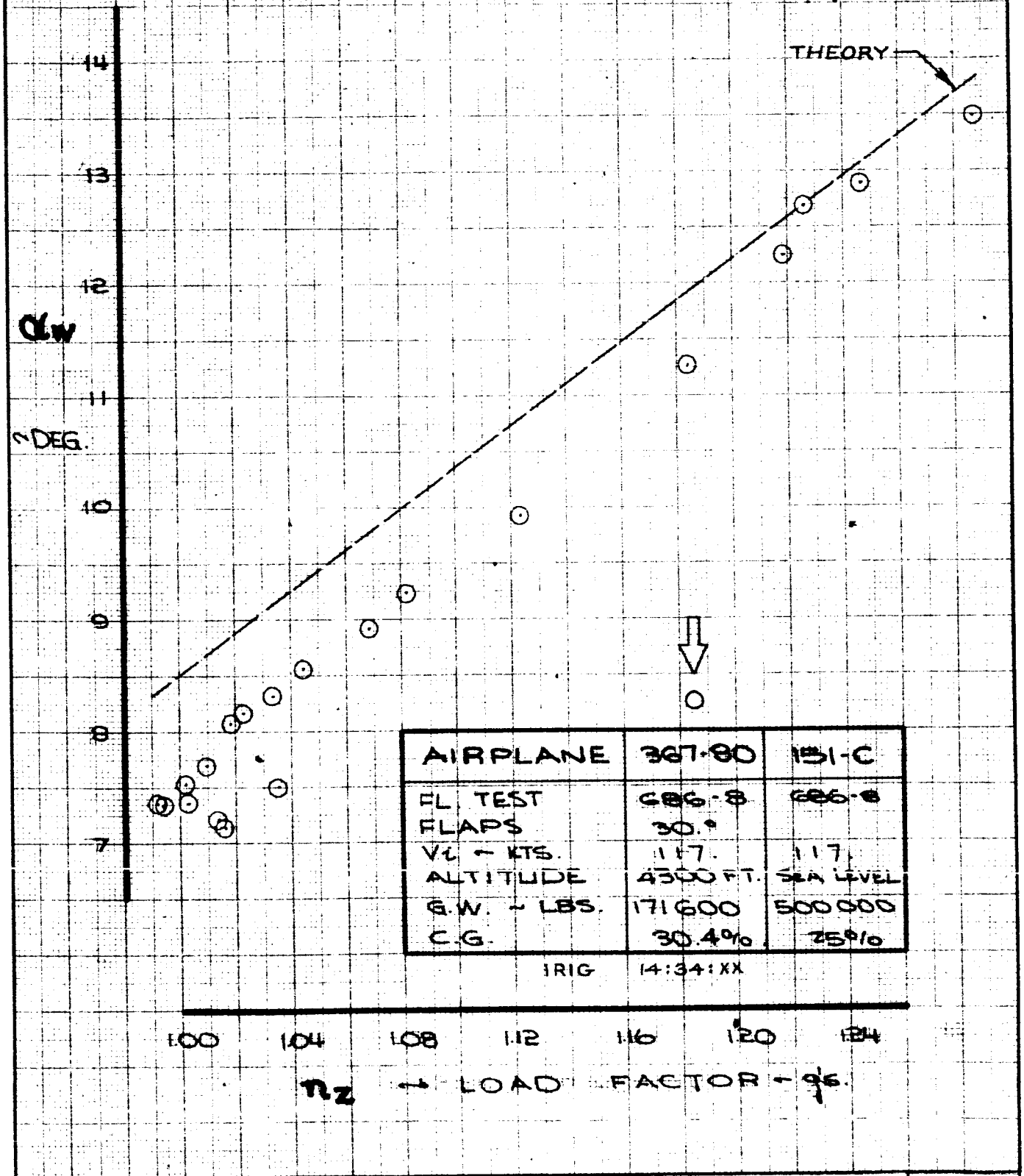

AIRPLANE	367-80	151-C
FL. TEST	686-8	686-8
FLAPS	30.°	
Vi ← KTS.	117.	117.
ALTITUDE	4500 FT.	SEA LEVEL
G.W. ← LBS.	171600	500000
C.G.	30.4%	25%
	IRIG	14:34:XX

			REVISED	DATE
CALC				
CHECK				
APR				
APR				

WINDUP TURN
FL. TEST : 686-8
CONFIG. : 151-C

151-C

FIG. 49

THE BOEING COMPANY
D6-15000

PAGE VII-74

TD 461 C-R4

77

WINDUP TURN

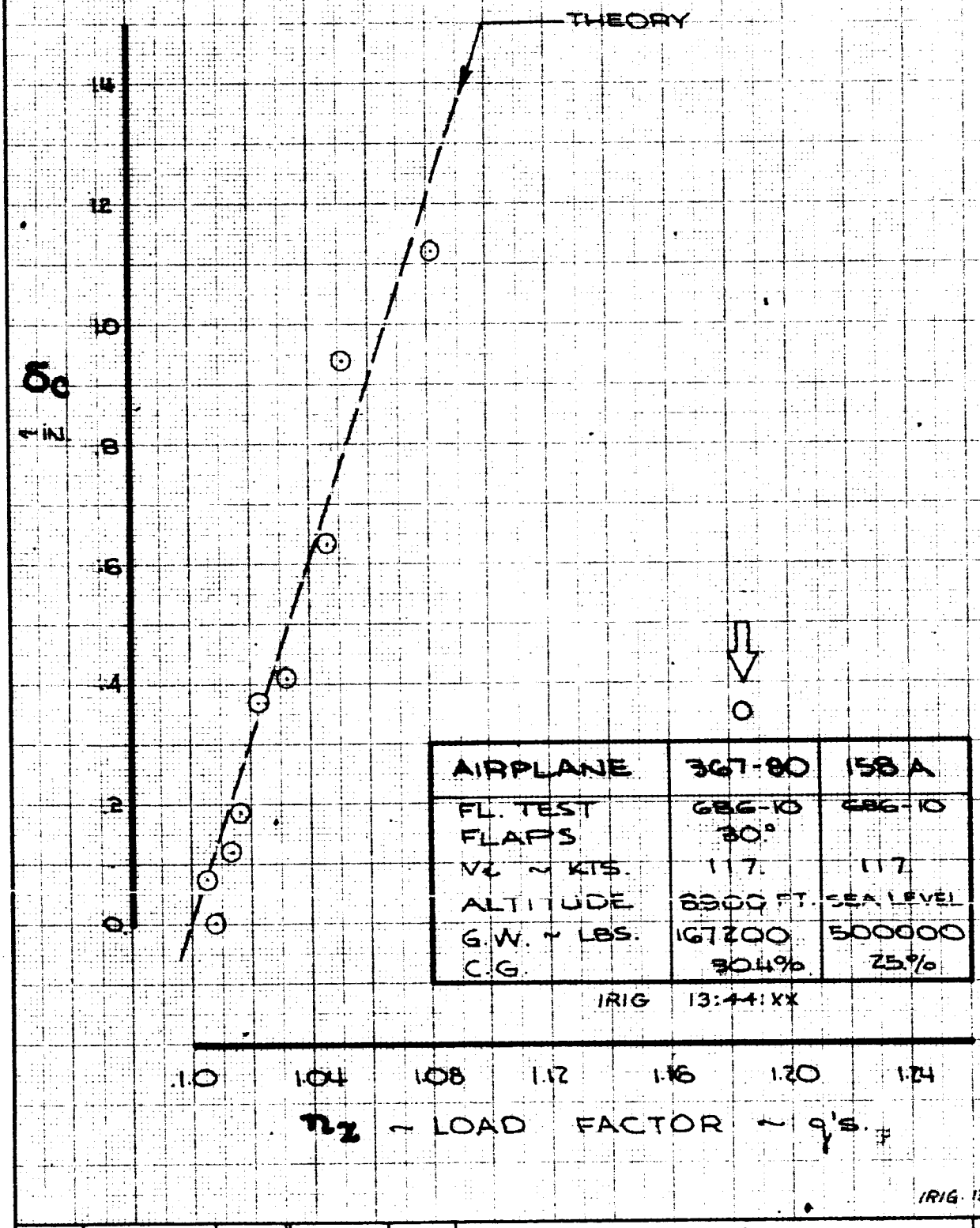

AIRPLANE	367-80	158 A
FL. TEST	686-10	686-10
FLAPS	30°	
Vc ~ KTS.	117.	117.
ALTITUDE	8500 FT.	SEA LEVEL
G.W. ~ LBS.	167200	500000
C.G.	30.4%	25%
IRIG	13:44:XX	

IRIG 13-44-18

			REVISED	DATE	WINDUP TURN	367-80
CALC					FL. TEST: 686-10	
CHECK					CONFIG. : 158A	FIG. 50
APR						
APR					THE BOEING COMPANY D6-15000	PAGE VII-75

TD 461 C-R4

WINDUP TURN

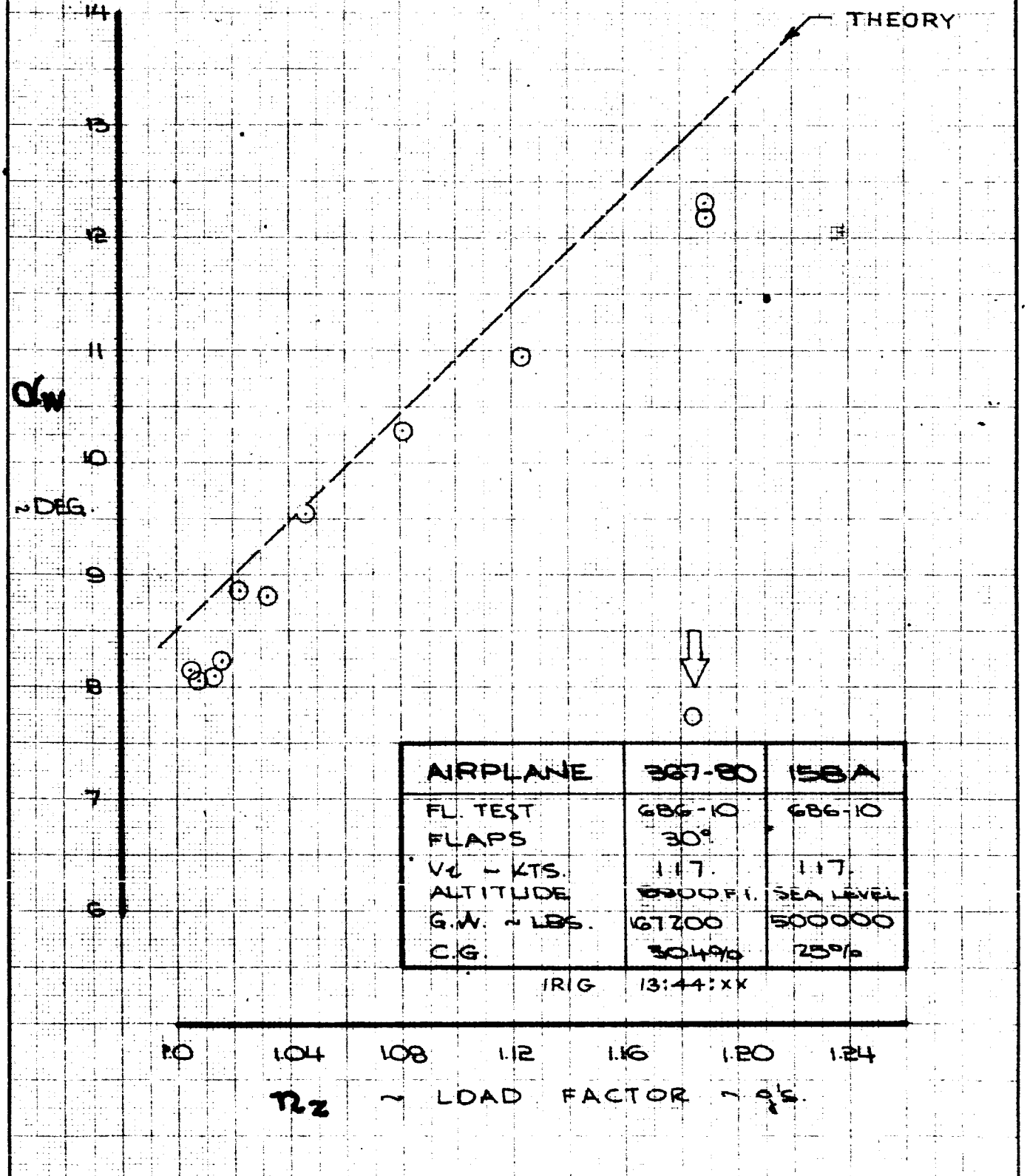

AIRPLANE	367-80	158A
FL. TEST	686-10	686-10
FLAPS	30°	
V_i ~ KTS.	117.	117.
ALTITUDE	10000 F.T.	SEA LEVEL
G.W. ~ LBS.	167200	500000
C.G.	30.4%	25%
	IRIG	13:44:XX

CALC			REVISED	DATE	WINDUP TURN FL. TEST. 686-10 CONFIG. : 158A
CHECK					
APR					
APR					

158A

FIG. 51

THE BOEING COMPANY D6-15000

PAGE VII-76

TD 461 C-R4

WINDUP TURN

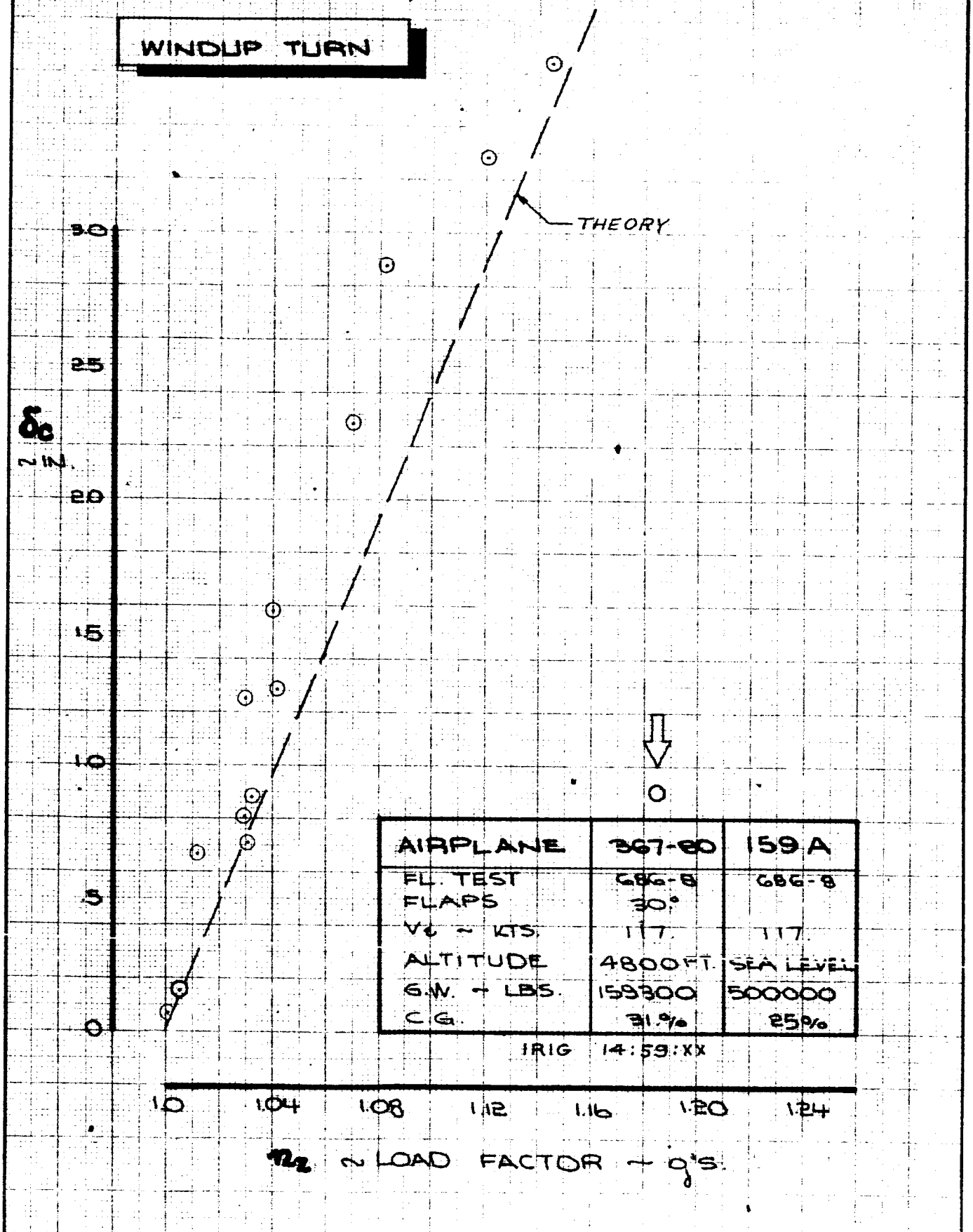

AIRPLANE	367-80	159A
FL. TEST	686-8	686-8
FLAPS	30°	
V_C ~ KTS.	117.	117.
ALTITUDE	4800FT.	SEA LEVEL
G.W. ~ LBS.	159300	500000
C.G.	31%	25%
	IRIG 14:59:XX	

			REVISED	DATE		
CALC					WINDUP TURN	367-80
CHECK					FL. TEST : 686-8	
APR					CONFIG. 159A	FIG. 52
APR					THE BOEING COMPANY D6-15000	PAGE VII-77

TD 461 C-R4

WINDUP TURN

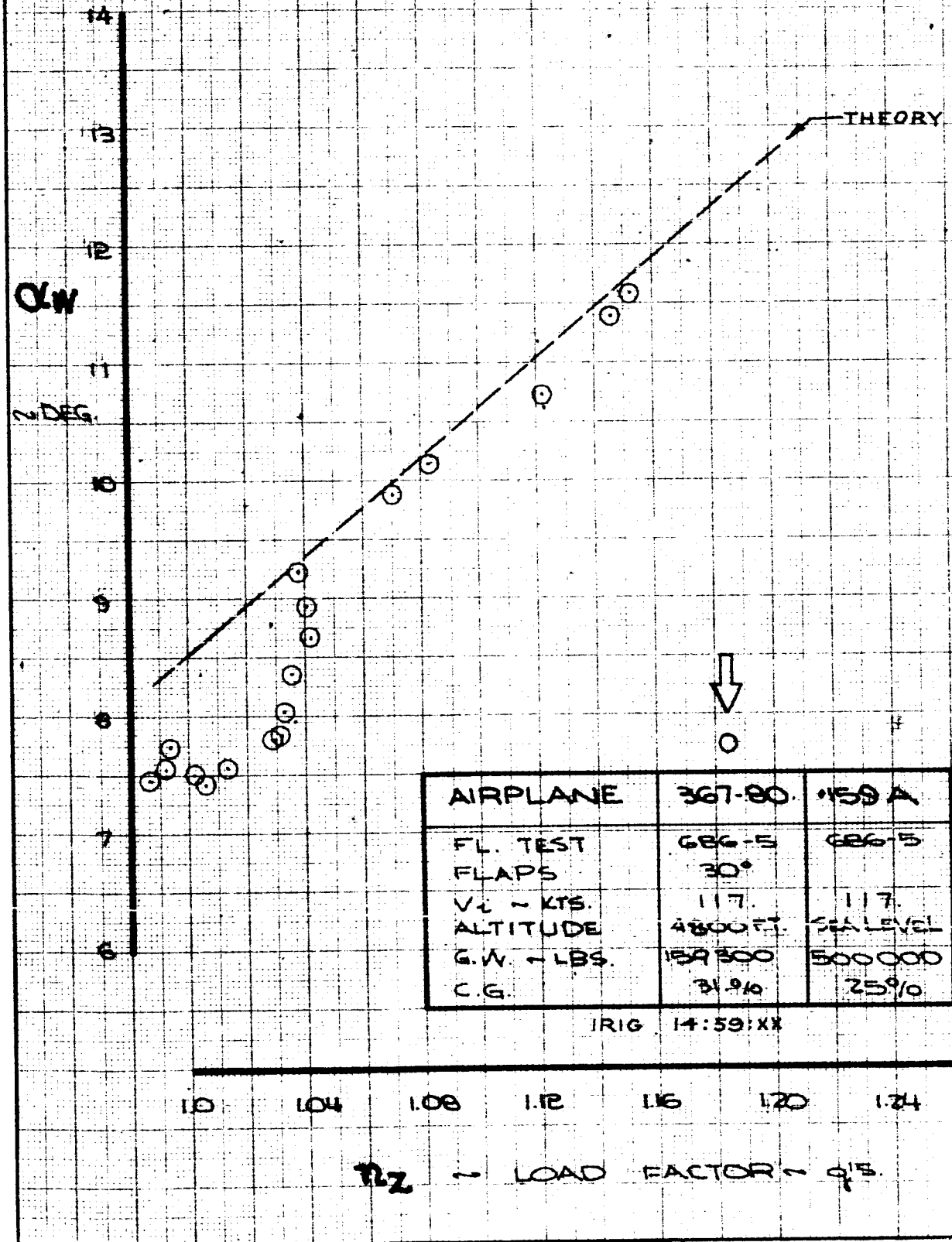

AIRPLANE	367-80	159A
FL. TEST	686-5	686-5
FLAPS	30°	
V_i ~ KTS.	117.	117.
ALTITUDE	4800 FT.	SEA LEVEL
G.W. ~ LBS.	159300	500000
C.G.	31.9%	25%

IRIG 14:59:XX

			REVISED	DATE	WINDUP TURN	159A
CALC					FL. TEST : 686-5	FIG. 53
CHECK					CONFIG. : 159A	
APR					THE BOEING COMPANY	PAGE VII-78
APR					DG-15000	

TD 461 C-R4

WINDUP TURN

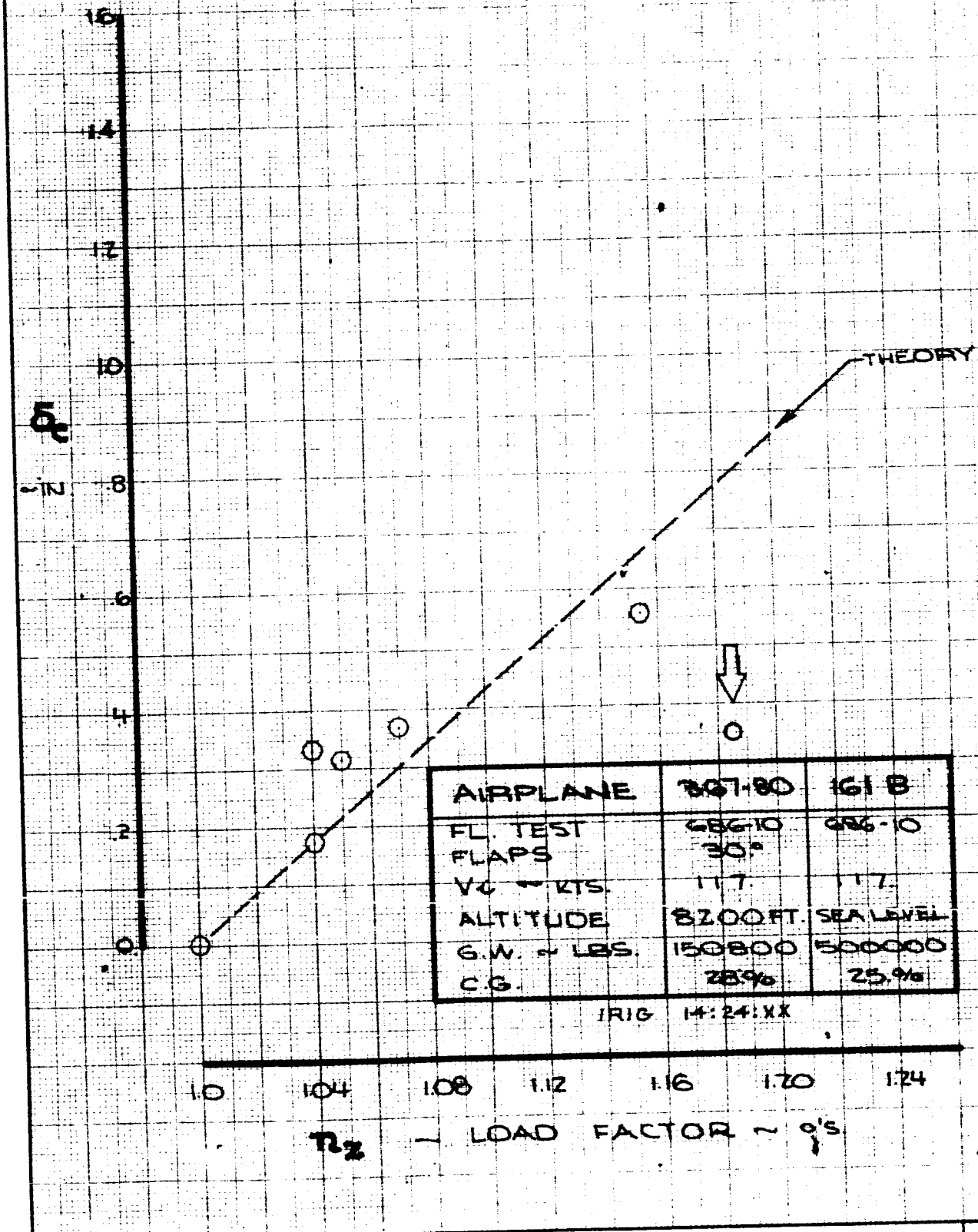

AIRPLANE	367-80	161 B
FL. TEST	GBG-10	GBG-10
FLAPS	30°	
Vc ~ KTS.	117.	117.
ALTITUDE	8200 FT.	SEA LEVEL
G.W. ~ LBS.	150800	500000
C.G.	28%	25.9%
	IRIG	14:24:XX

			REVISED	DATE	WINDUP TURN	367-80
CALC					FL. TEST : GBG-10	FIG. 54
CHECK					CONFIG. : 161B	
APR					THE BOEING COMPANY D6-15000	PAGE VII-79
APR						

WINDUP TURN

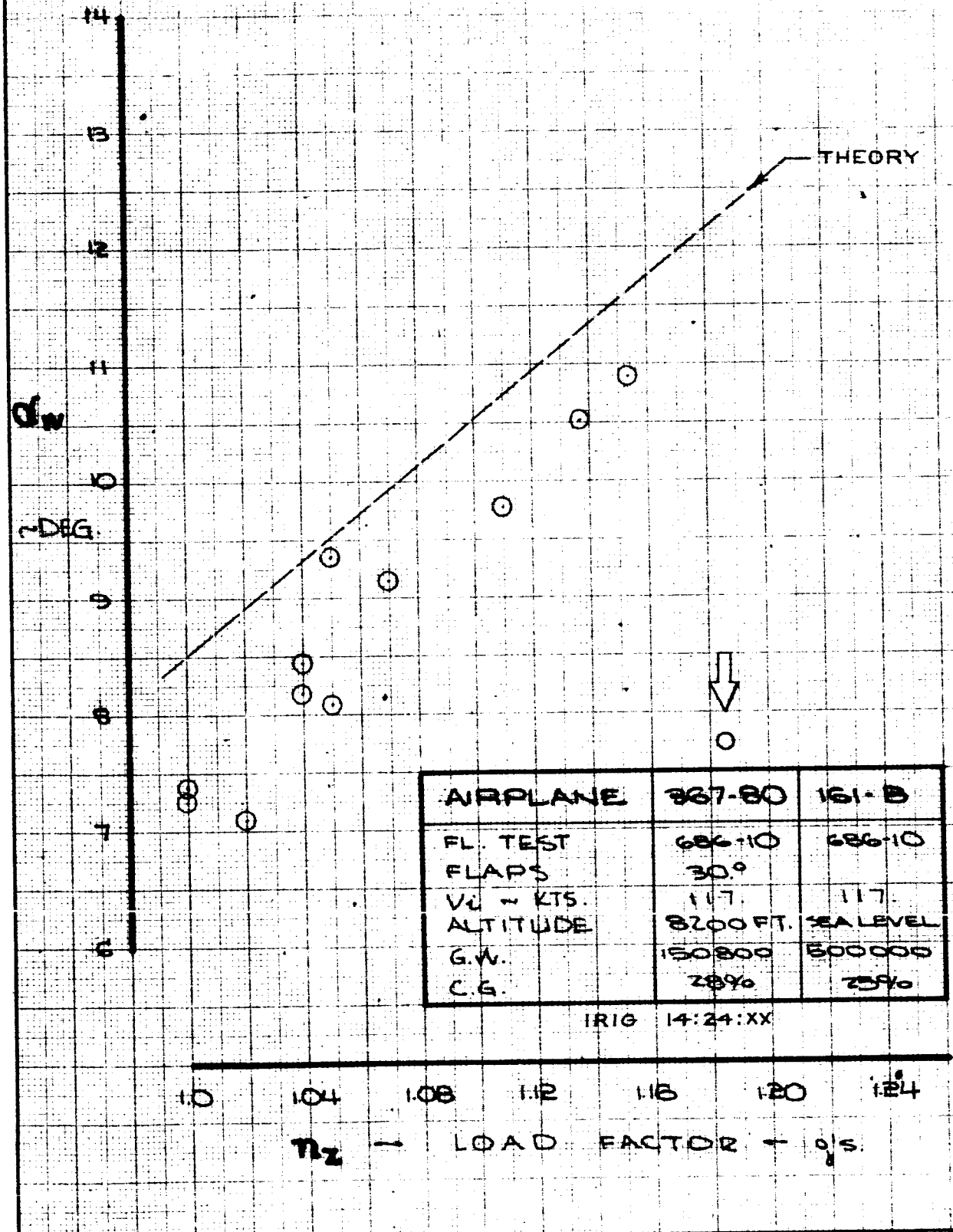

AIRPLANE	367-80	161-B
FL. TEST	686-10	686-10
FLAPS	30°	
V_i ~ KTS.	117.	117.
ALTITUDE	8200 FT.	SEA LEVEL
G.W.	150800	600000
C.G.	28%	25%
IRIG	14:24:XX	

			REVISED	DATE		
CALC					WINDUP TURN	161 B
CHECK					FL. TEST : 686-10	FIG. 55
APR					CONFIG. : 161B	
APR					THE BOEING COMPANY D6-15000	PAGE VII-80

TD 461 C-R4

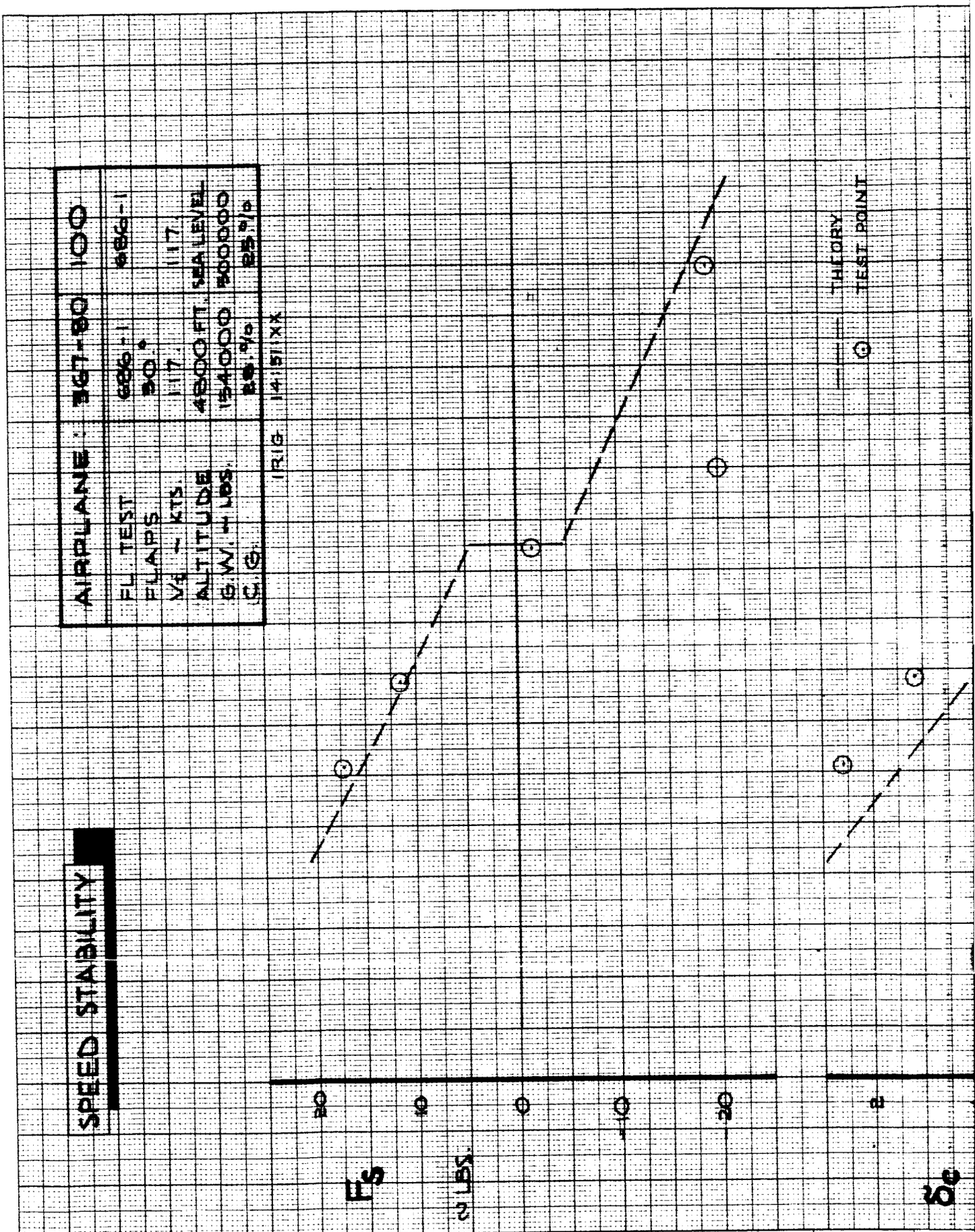

			REVISED	DATE
CALC				
CHECK				
APPD.				
APPD.				

SPEED STABILITY
FL. TEST : 686-1
CONFIG. : 100

367-80
FIG. 56
PAGE VII-31

THE BOEING COMPANY D6-15000

TD 1053-R5

V_i, KTS
100
105
110
115
120
125
130
Ω_W, DEG
0
1
2
3
4
5
6
7
2π
11.7 KTS

VII-8½

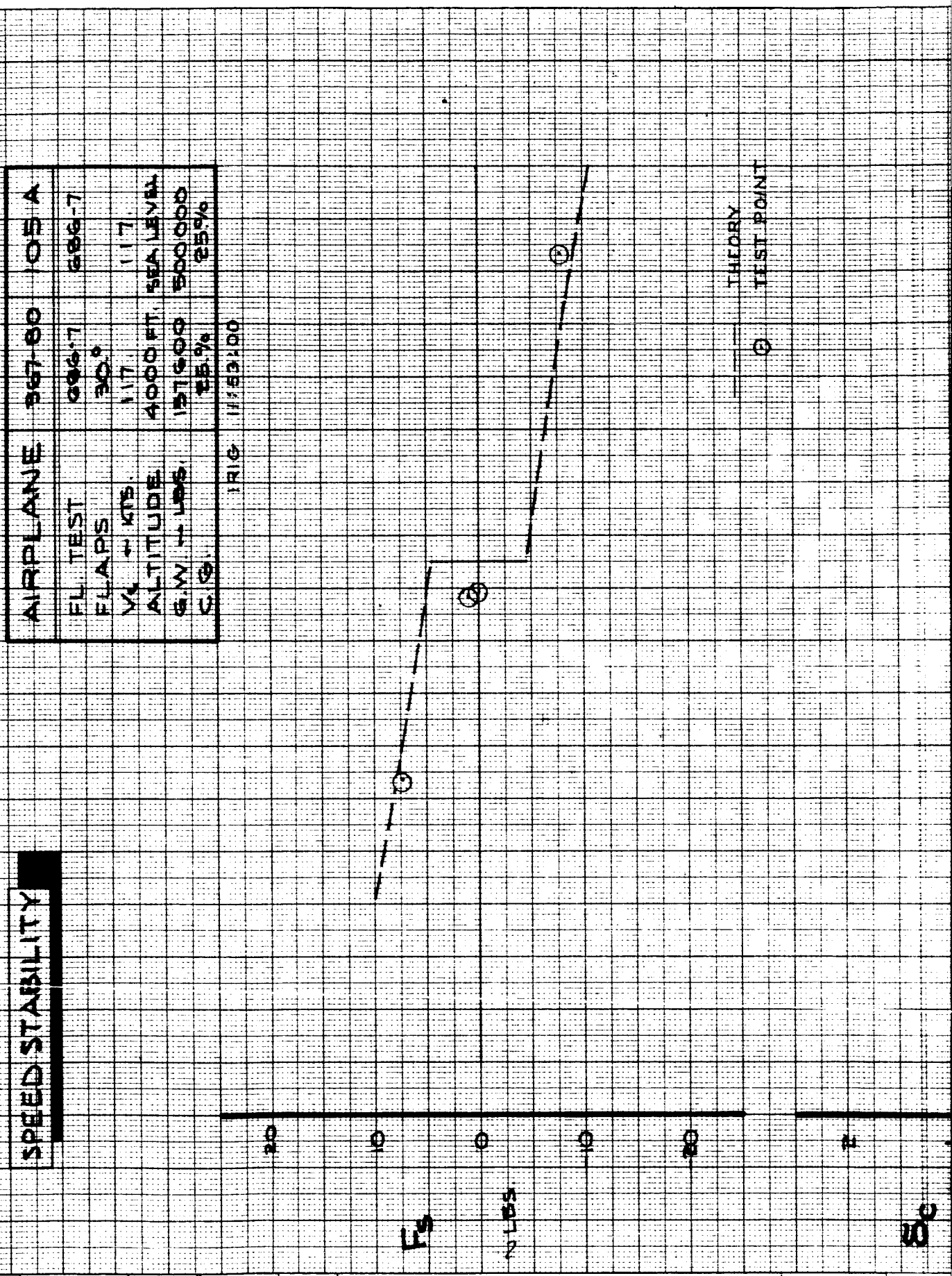

			REVISED	DATE	SPEED STABILITY	367-80
CALC					FL. TEST : 686-7	FIG. 57
CHECK					CONFIG. 105-A	
APPD.					THE BOEING COMPANY D6-15000	PAGE VII-32
APPD.						

TD 1053-R5

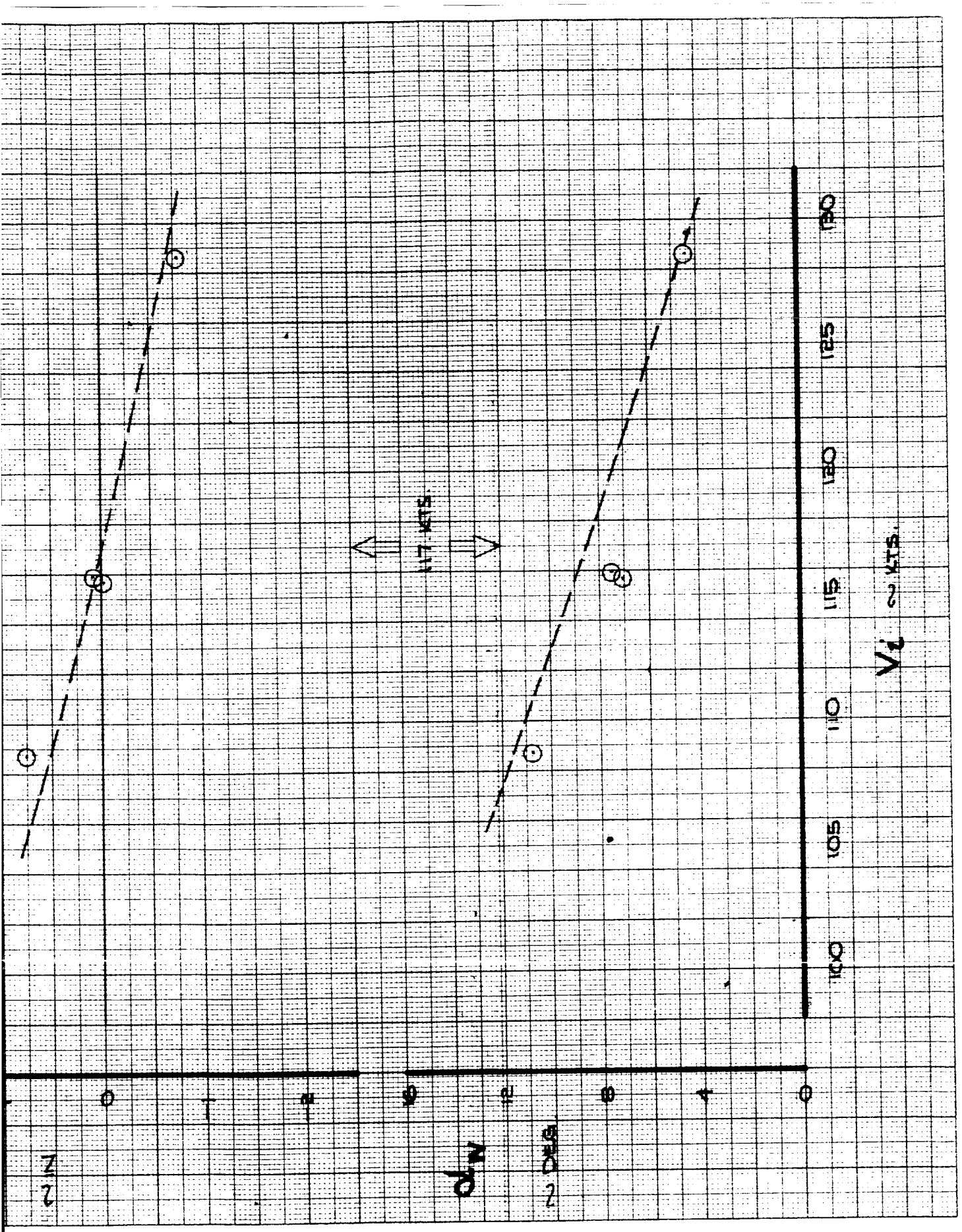

VIII-82
-2

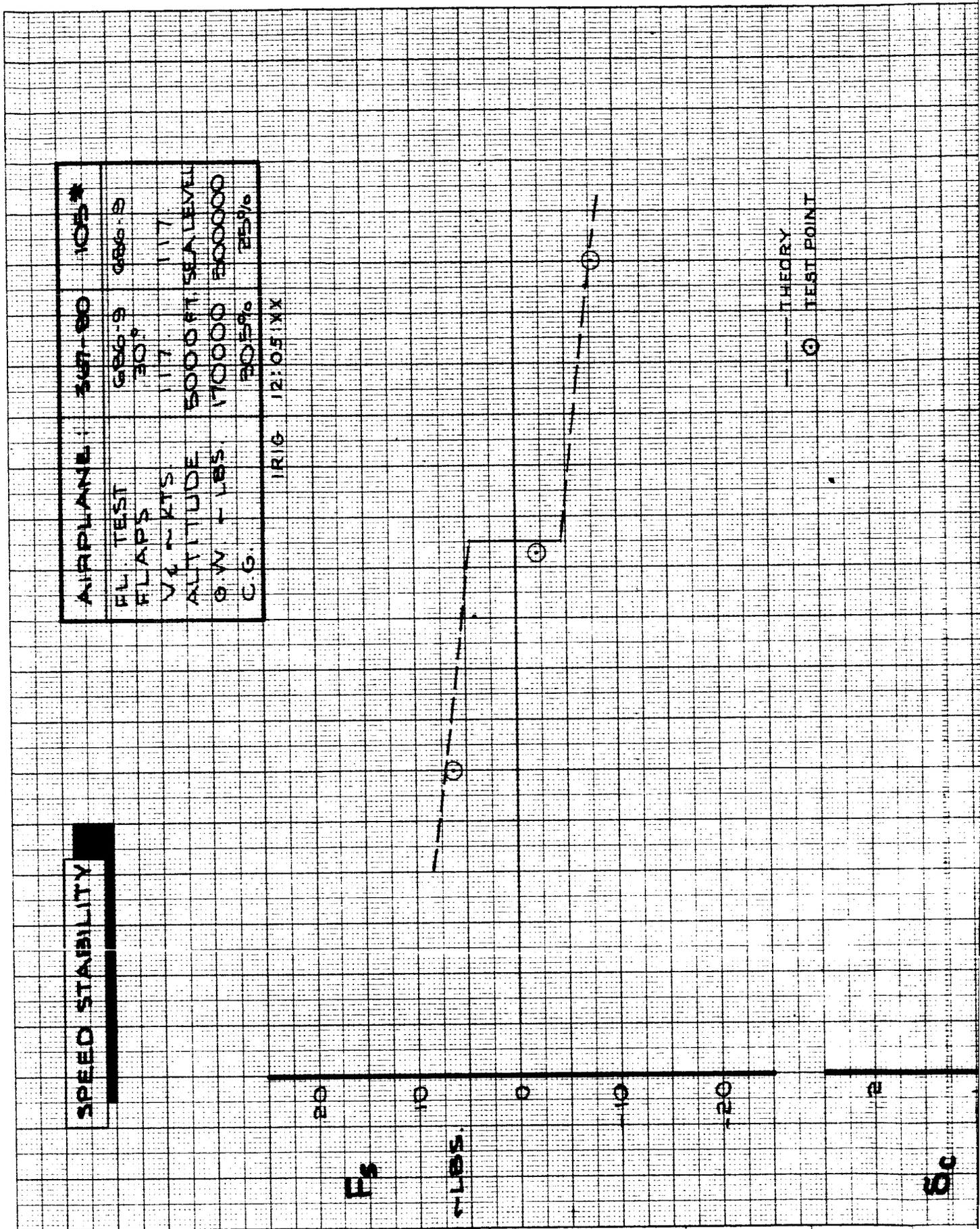

			REVISED	DATE
CALC				
CHECK				
APPD.				
APPD.				

SPEED STABILITY
FL. TEST : 686-9
CONFIG. : 105*

THE BOEING COMPANY D6-15000

367-80
FIG. 58
PAGE VII-33

TD 1053-R5

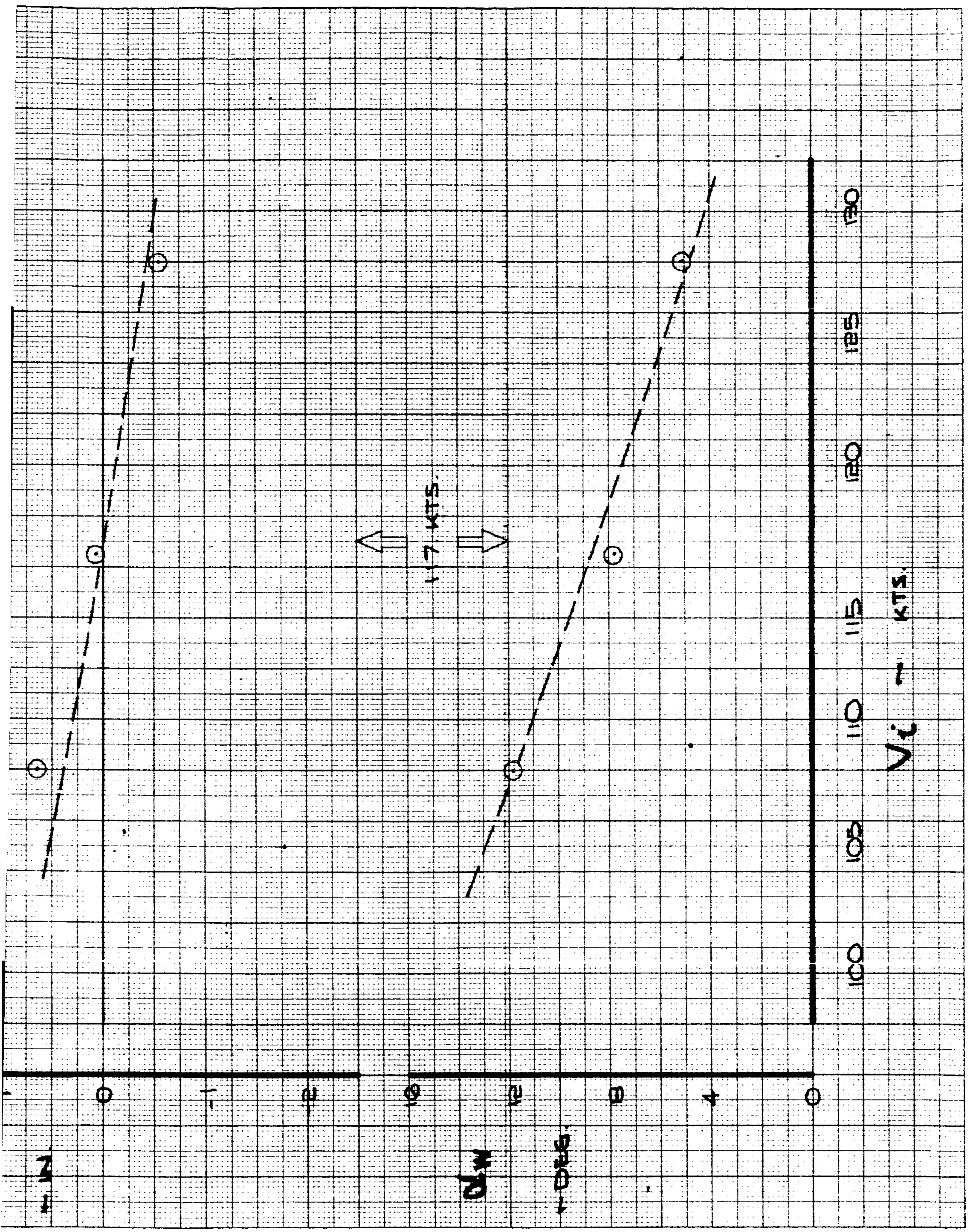

VIII-83-2

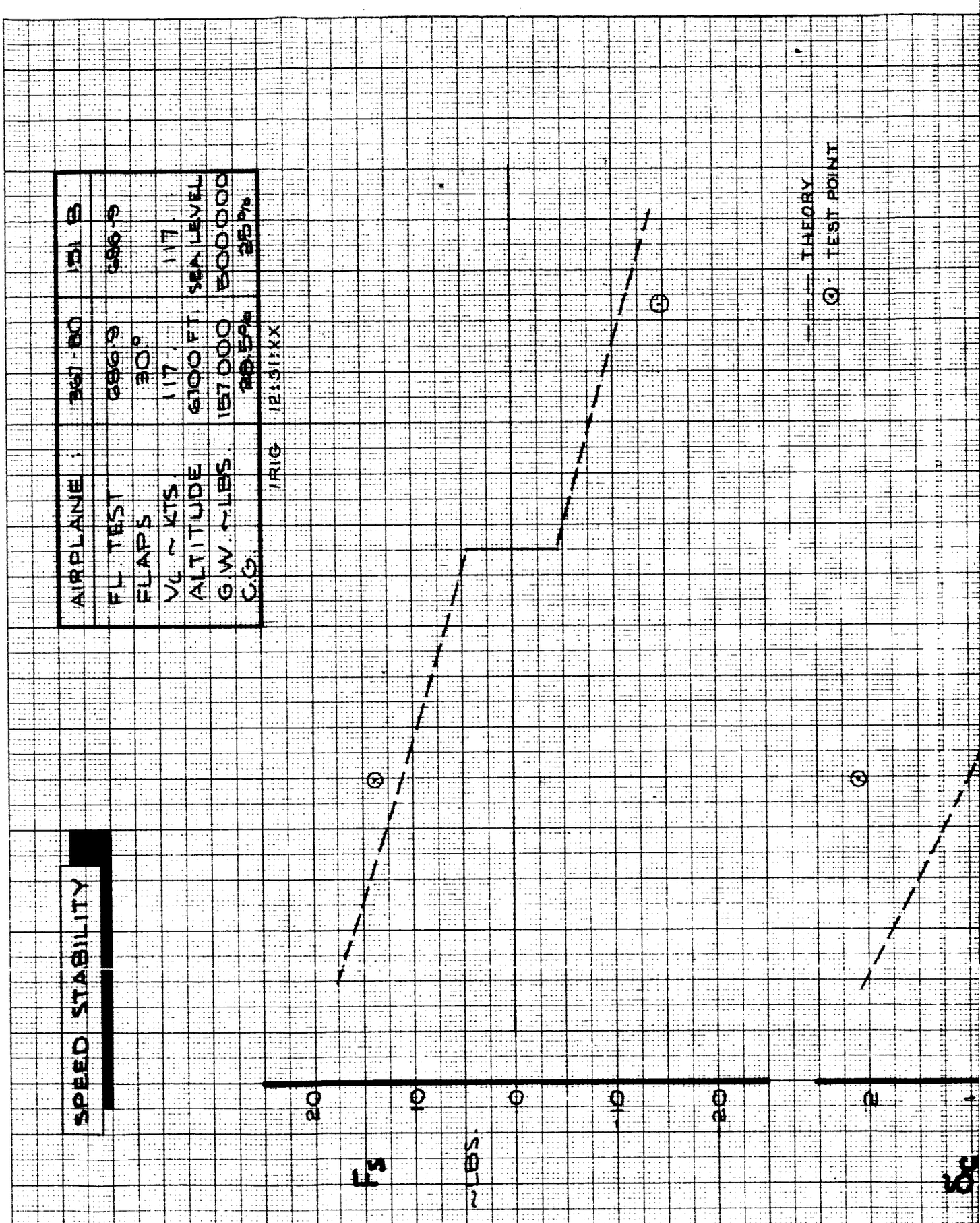

CALC			REVISED	DATE	SPEED STABILITY	367-80
CHECK					FL. TEST : 686-9	FIG. 59
APPD.					CONFIG. : 151-B	
APPD.					THE BOEING COMPANY D6-15000	PAGE VII-34

TD 1053-R5

III-84-2

			REVISED	DATE
CALC				
CHECK				
APPD.				
APPD.				

SPEED STABILITY
FL. TEST : 686-8
CONFIG. : 151C

367-80
FIG. 60

THE BOEING COMPANY D6-15000

TD 1053-R5

III-85-2

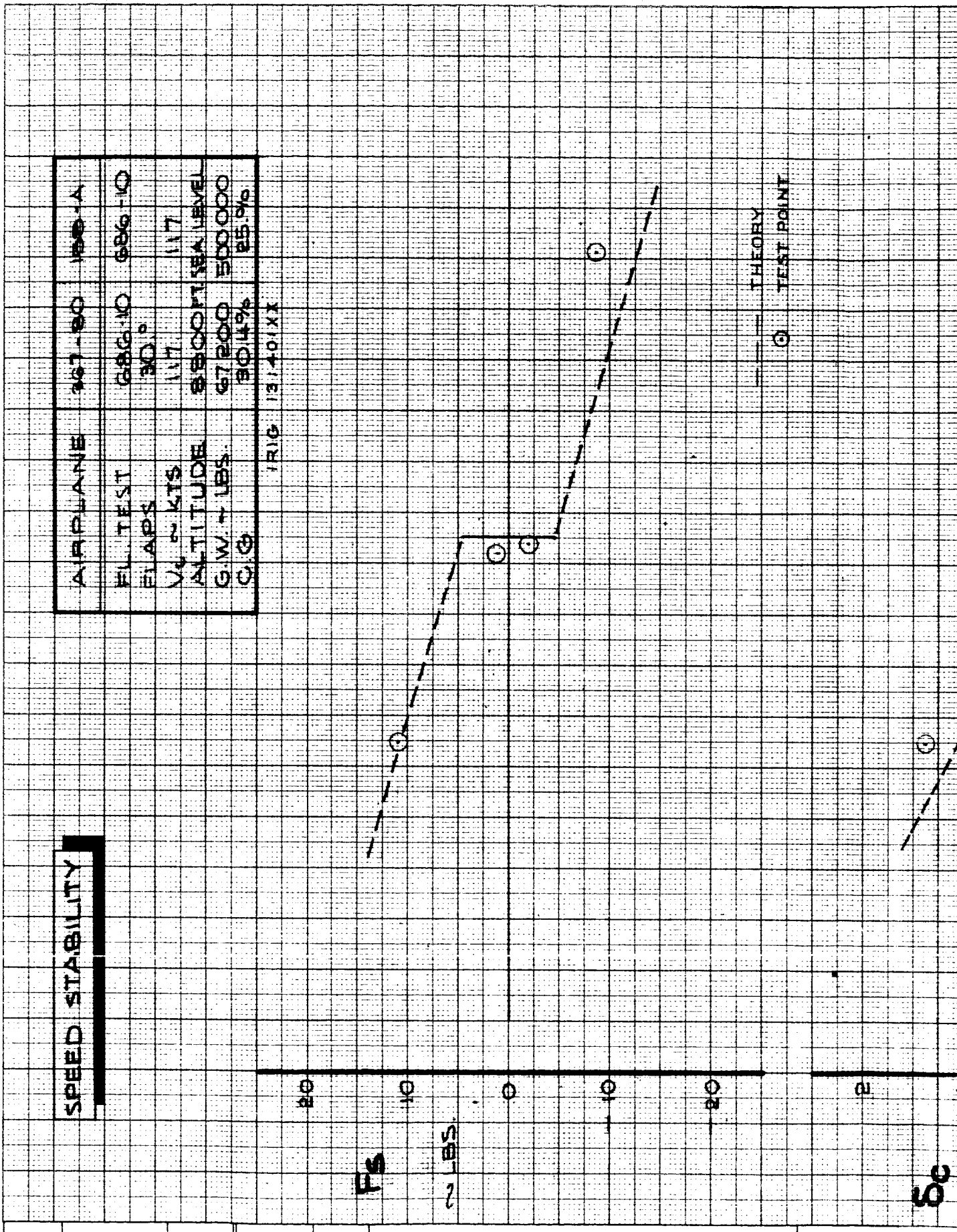

				REVISED	DATE	SPEED STABILITY	367-80
CALC						FL. TEST : 686-10	FIG. 61
CHECK						CONFIG. : 158-A	
APPD.						THE BOEING COMPANY D6-15000	PAGE VII-30
APPD.							

TD 1053-R5

III-86-2

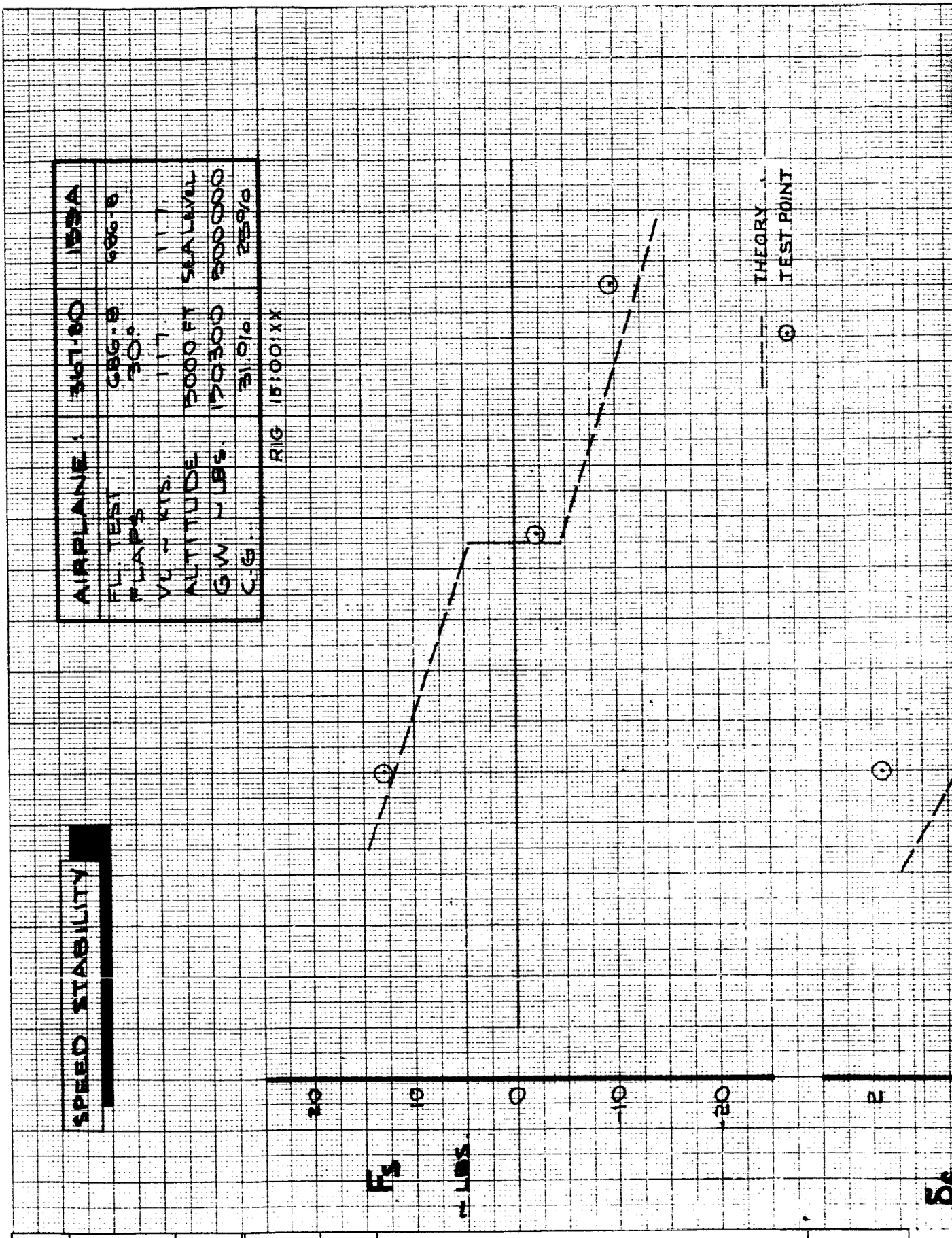

CALC			REVISED	DATE	SPEED STABILITY	367-80
CHECK					FL. TEST : 686-8	FIG. 62
APPD.					CONFIG. : 159 A	
APPD.					THE BOEING COMPANY	PAGE
					DG-15000	VII- 7

TD 1053-R5

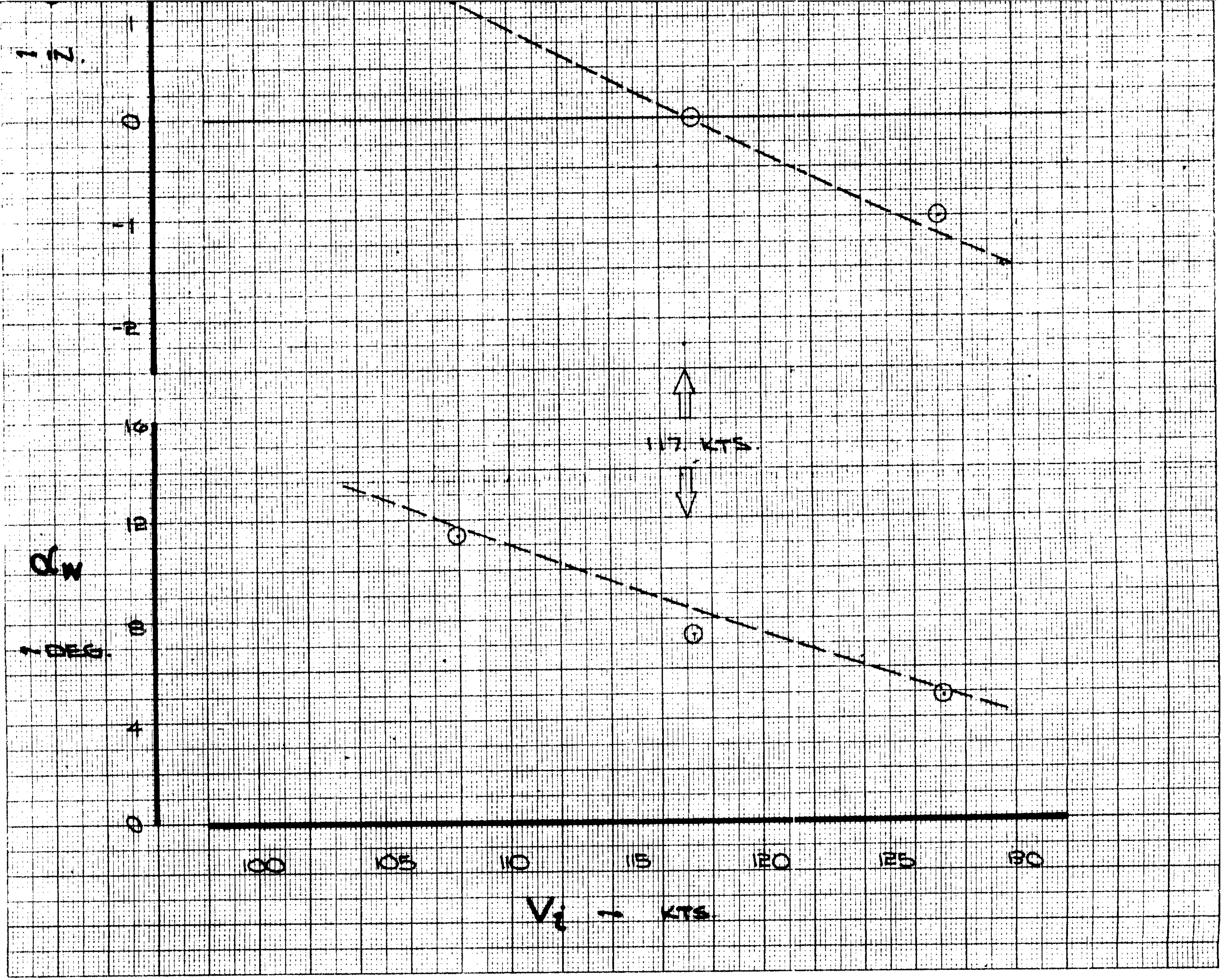

$\frac{1}{Z}$
α_W
- DEG.
117 KTS.
V_i - KTS.
0
4
8
12
16
-2
-1
0
1
100
105
110
115
120
125
130

III-84-2

			REVISED	DATE
CALC				
CHECK				
APPD.				
APPD.				

SPEED STABILITY
FL. TEST : 686-10
CONFIG. : 161 B

THE BOEING COMPANY

D6-15000
FIG. 63
PAGE VII-53

TD 1053-R5

V_i - KTS
130
125
120
115
110
105
100
±11.7 KTS
$\Delta\psi$
DEG
2
1
0
-1
-2
-3
-4
-5
Z

VII-88-2

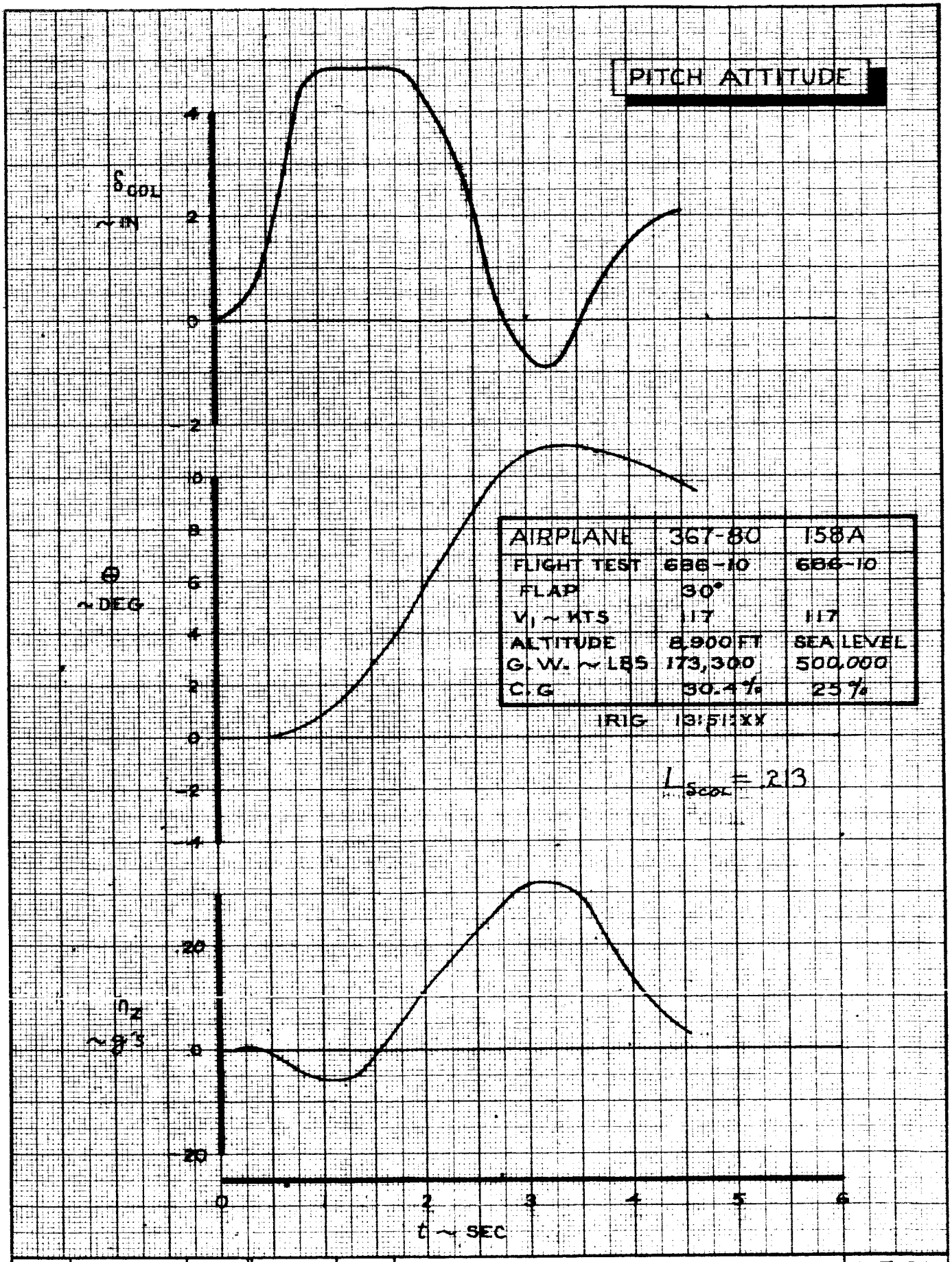

			REVISED	DATE
CALC				
CHECK				
APR				
APR				

PITCH ATTITUDE
FLIGHT TEST 686-10
CONFIGURATION 158A

367-80

FIG. 64

THE BOEING COMPANY D6-15000

PAGE VII-89

TD 661 C-R4

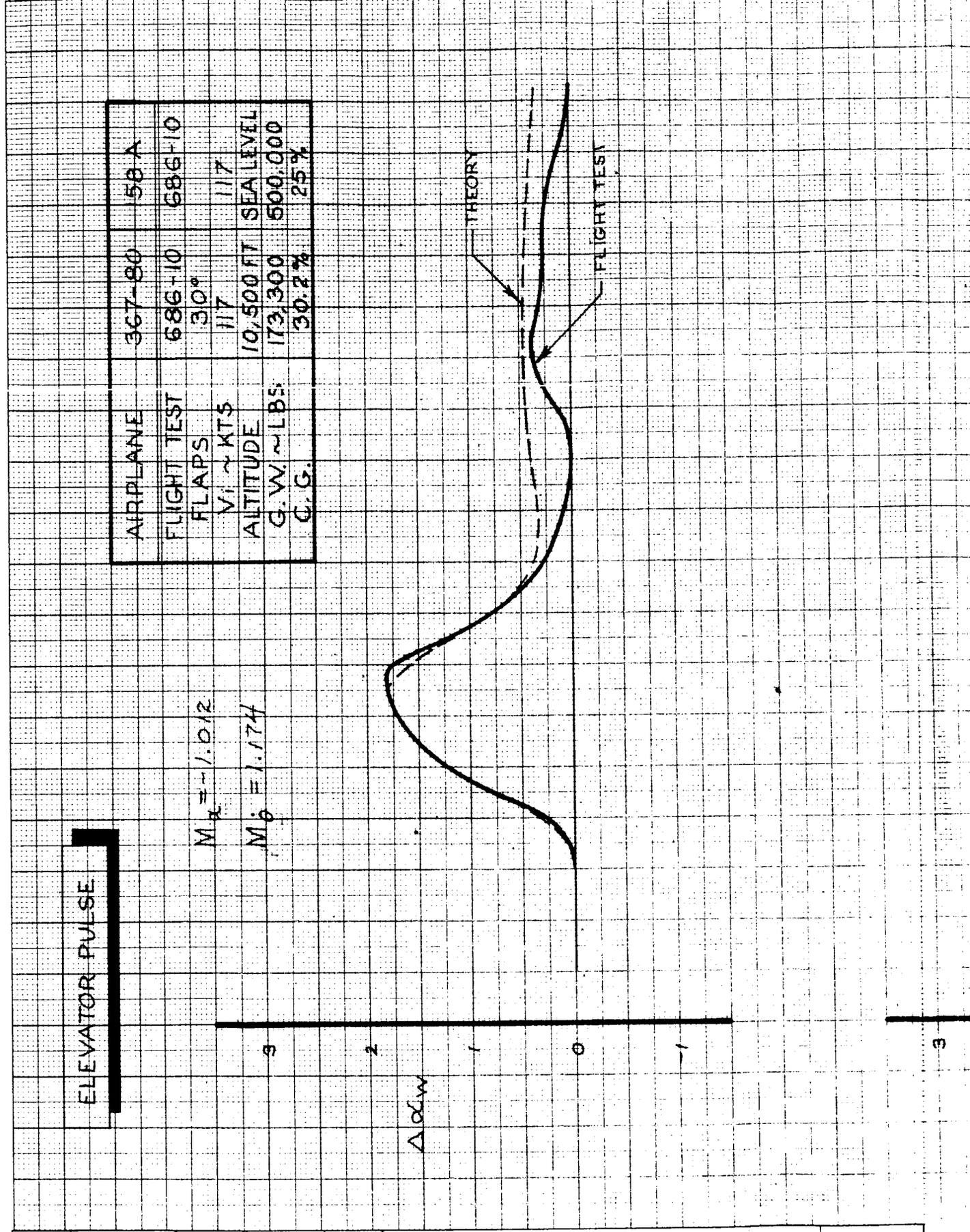

CALC			REVISED	DATE	ELEVATOR PULSE FLIGHT TEST 686-10 CONFIGURATION 158 A
CHECK					
APPD.					
APPD.					
					THE BOEING COMPANY D6-15000

367-80
FIG. 65
PAGE VII-[illegible]

TD 1053-R5

93

VII-90-2

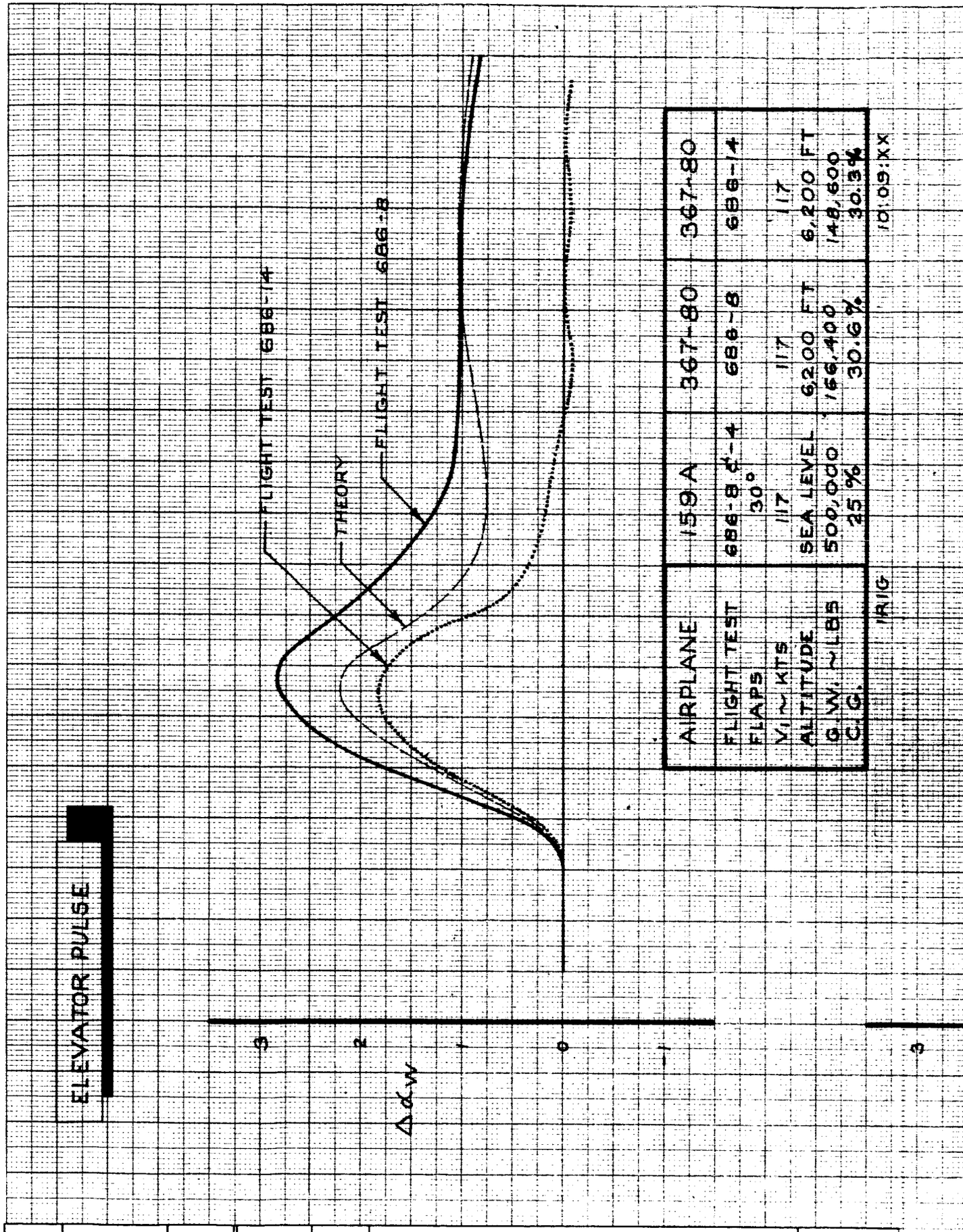

CALC			REVISED	DATE	ELEVATOR PULSE FLIGHT TEST 686-8 ε-14 CONFIGURATION 159 A	367-80
CHECK						FIG. 66
APPD.						
APPD.					THE BOEING COMPANY D6-15000	PAGE VII-31

TD 1083-R5

$M_\alpha = -.506$
$M_\dot{\theta} = -.174$
2
1
0
1
θ
δE
4
2
0
0
2
4
6
8
10
12
14
16
$t \sim$ SEC

VII-91-2

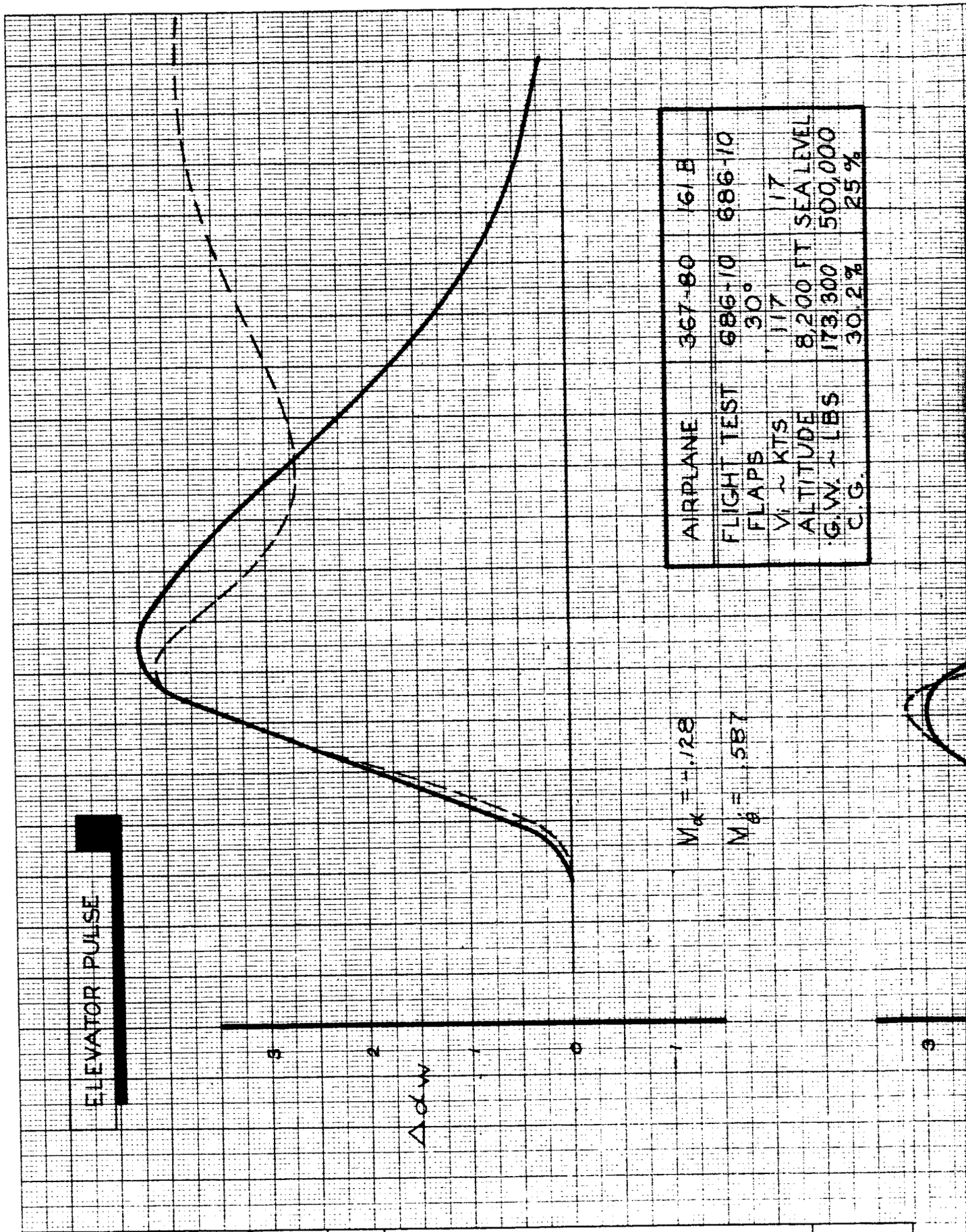

			REVISED	DATE
CALC				
CHECK				
APPD.				
APPD.				

ELEVATOR PULSE
FLIGHT TEST 686-10
CONFIGURATION 161 B

367-80

FIG. 67

THE BOEING COMPANY D6-15006

PAGE VII-92

TD 1053-R5

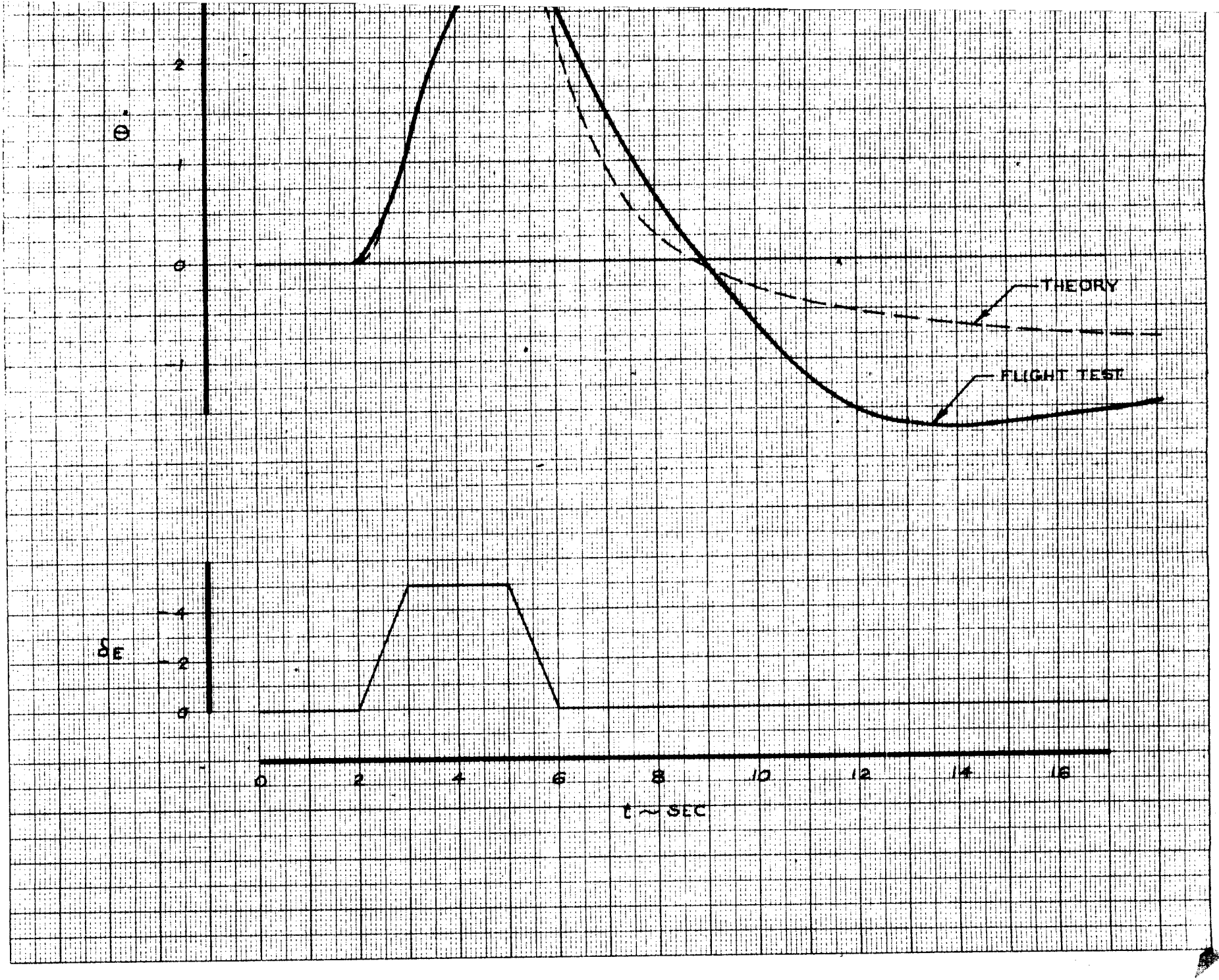
2
θ̇
1
0
-1
THEORY
FLIGHT TEST
-4
δE
-2
0
0
2
4
6
8
10
12
14
16
t ~ SEC

B. Ground Based Simulation

The longitudinal characteristics of all the configurations evaluated on the ground based simulator are presented in Table 3. The longitudinal aerodynamic coefficients used to obtain these characteristics are listed in Appendix 1. The effect of elevator lift on pitch response during a step column maneuver is shown for the basic configuration in Fig. 23 (page VI-43). The response of configurations with no elevator lift ($L_{\delta_E} = 0$) and elevator lift opposite the basic configuration (L_{δ_e} = - basic value) are shown in Figs. 68 and 69 for comparison. The effect of changes in static stability and damping are presented in Figs. 70, 71, and 72 for an elevator pulse. These are comparable to the typical response shown in Fig. 26 (page VI-46).

AD 1040C-R3

6-7000

CALC R. Root	APR	APR	CHECK
12-66			
REVISED			
DATE			

GROUND BASED SIMULATION

LONGITUDINAL RUN LOG

THE BOEING COMPANY
RENTON, WASHINGTON D6-15000

TABLE 3

PAGE VII-94

GROUND BASED CONFIG	L_α	M_α	M	$L_{\delta_{col}}$	$M_{\delta_{col}}$	M_ϕ	F_{col}/δ_{col}	SHORT PERIOD		PHUGOID		δ_E/δ_{col}
								ω_n	ζ	ω_n	ζ	
G-	1/SEC·RAD	1/SEC²	RAD/SEC²	1/SEC·IN	RAD/SEC²·IN	1/SEC	LB/IN	RAD/SEC	—	RAD/SEC	—	DEG./IN
100	.571	-.506	.166	-.00195	.0219	-.585	4.4¢5.7	.928	.707	.177	.142	-3.29
100A			.332		.0439		4.4					
100X			.166	-.00391	.0219		5.7					
101A			.240	-.00195	.0316		4.4¢5.7					
102			.133		.0176		4.4					
103			.107		.0141							
103A				-.00391	.0281							-6.58
105			.166		.0438							
105A			.245		.0646		5.7					
105*			.166	-.00588	.0658							-9.87
105*X				-.01175								
106		-.245		-.00195	.0219		4.4	.772	.843	.148	.205	-3.29
107		0.						.575	1.100	—	—	
108			.107		.0141							
109			.213		.0282							
109A			.166	-.00391	.0438							-6.58
110		+.245		-.00195	.0219			.295	2.200			-3.29
111	.302	-.506						.834	.629	.137	.116	
112		-.735						.957	.546	.206	.119	
112A		-.980						1.075	.485	.212	.124	
113		-.343						.737	.716	.184	.124	
113A						-.296		.666	.580	.203	.083	
115		0.				-.585		.420	1.340	—	-	
120	.571	-.506				-.242		.817	.605	.201	.081	

4

8b

TD 1040C - R3

8-7000

APR	APR	CHECK	CALC
			R. Root
			2-2-66
			REVISED
			DATE

GROUND BASED SIMULATION
LONGITUDINAL RUN LOG.

THE BOEING COMPANY
RENTON, WASHINGTON D6-15000

PAGE VII-95

TABLE 3

GROUND BASED CONFIG.	L_α	M_α	$M_{\dot\alpha}$	$L_{\delta_{COL}}$	$M_{\delta_{COL}}$	M_θ	F_{COL}/δ_{COL}	SHORT PERIOD		PHUGOID		δ_E/δ_{COL}
								ω_n	ζ	ω_n	ζ	
G~	1/SEC. RAD	1/SEC²	RAD/SEC²	1/SEC. IN	RAD/SEC²·IN	1/SEC.	LB/IN	RAD/SEC.	—	RAD/SEC.	—	DEG/IN
122A	.571	-.980	.166	-.00195	.0219	-.585	4.4	1.151	.569	.198	.130	-3.29
123	.925	-.506						1.036	.799	.158	.170	
123A				-.00391	.0438							-6.58
123B			.245		.0646		5.7					
124		-.122	.166	-.00195	.0219		4.4	.805	1.000	.099	.416	-3.29
125		.098						.660	1.24	—	—	
126		-.245	.107		.0141			.883	.93	.127	.260	
126A			.166	-.00391	.0438							-6.58
127		0	.107	-.00195	.0141			.73	1.115	—	—	-3.29
128		-.245				-.245		.725	.92	.160	.091	
129		0.						.520	1.195	—	—	
130			.166		.0219	-.585		.695	1.115			
131		-.122				-.245		.635	1.040	.128	.169	
132		-.506	.107		.0141			.882	.762	.184	.073	
150	.571		.166		.0219	-.585		.927	.716	C_{D_α} =	1.77 × BASIC	
151				+.00195						.177	.140	
151B			.245	+.00165	.0273		5.7					-2.78
151C				0.								
151C*			.166		.0219							-3.29
151D			.245	+.00391	.0646							-6.58
152		-1.420	.166	-.00195	.0219	-1.173	4.4	1.466	.645	.190	.155	-3.29
153			.332		.0439							
154		-.506	.166		.0219			1.089	.865	.151	.225	
155			.332		.0439							

1.b

TD 1040C - R3

6-7000

CALC	APR	APR	CHECK	R. Root	2-2-66	REVISED	DATE

GROUND BASED SIMULATION
LONGITUDINAL RUN LOG.

THE BOEING COMPANY
RENTON, WASHINGTON D6-15000

TABLE 3

PAGE VII-96

GROUND BASED CONFIG.	L_α	M_α	M	$L_{\delta_{COL}}$	$M_{\delta_{COL}}$	$M_{\dot\theta}$	F_{COL}/δ_{COL}	SHORT PERIOD		PHUGOID		δ_E/δ_{COL}
								ω_n	ζ	ω_n	ζ	
G~	1/SEC · RAD	1/SEC²	RAD/SEC²	1/SEC · IN	RAD/SEC² · IN	1/SEC.	LB/IN	RAD/SEC	—	RAD/SEC.	—	DEG/IN
156	.571	-.980	.332	-.00195	.0439	-.585	4.4	1.151	.569	.198	.130	-3.29
157			.166		.0219	-1.173		1.290	.733	.177	.169	
157A						-.585		1.151	.569	.198	.130	
158				-.00391	.0438	-1.173		1.290	.733	.177	.169	-6.58
158A			.245				5.7					
158A*			.166			-.585	4.4	1.151	.569	.198	.130	
158X			.245		.0646		5.7					
159		-.506	.166		.0438	-1.173	4.4	1.290	.733	.177	.169	
159A			.245	-.00165	.0273		5.7					-2.78
159B				-.00391	.0646							-6.58
160		-1.470	.166		.0438		4.4	1.466	.645	.190	.155	
161		-.122				-.585		.675	.958	—	—	
161B			.245		.0646		5.7					
162		-.049	.166		.0438		4.4	.618	1.045			
163	.925	-.980						1.242	.668	1.83	.139	
163A				-.00195	.0219							-3.29

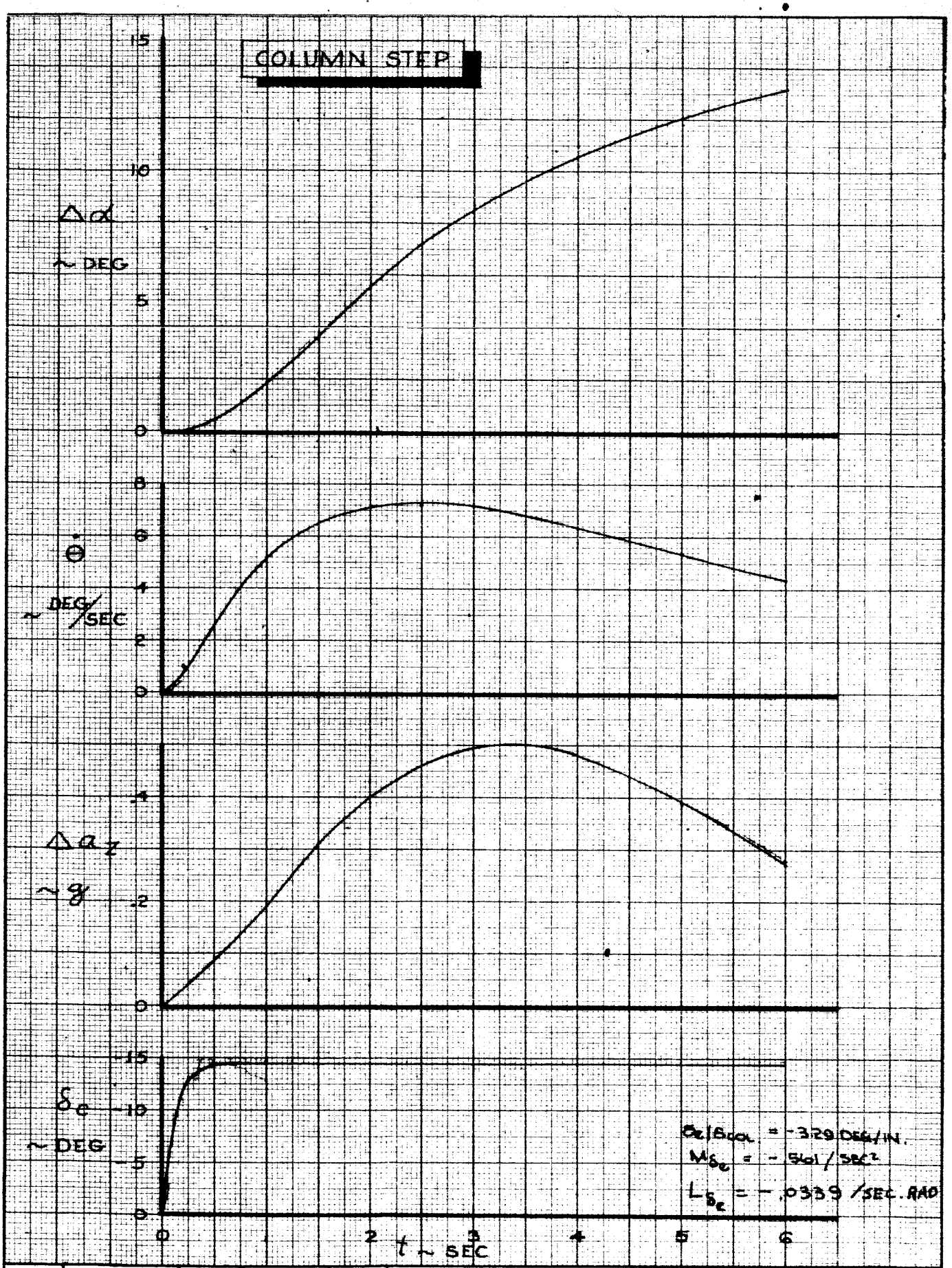

CALC	R. Root	2-2-66	REVISED	DATE	COLUMN STEP GROUND BASED SIMULATOR CONFIGURATION G151 B
CHECK					
APR					
APR					
					THE BOEING COMPANY

D6-15000

FIG. 68

PAGE VII-97

TD 461 C-R4

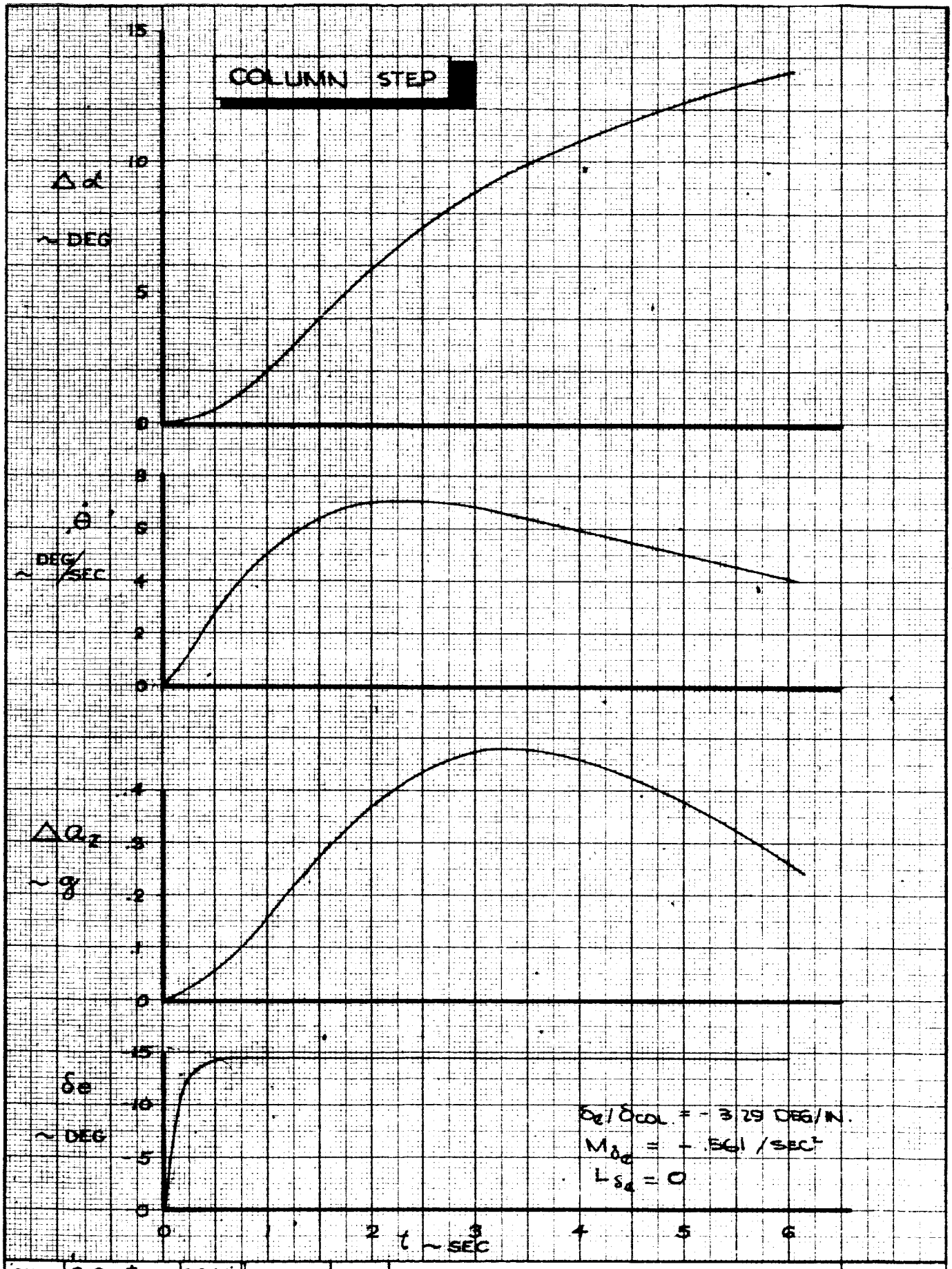

CALC	R. Root	2-2-66	REVISED	DATE
CHECK				
APR				
APR				

COLUMN STEP
GROUND BASED SIMULATOR
CONFIGURATION G151C

D6-15000
FIG. 69

THE BOEING COMPANY

PAGE VII-98

TD 461 C-R4

101

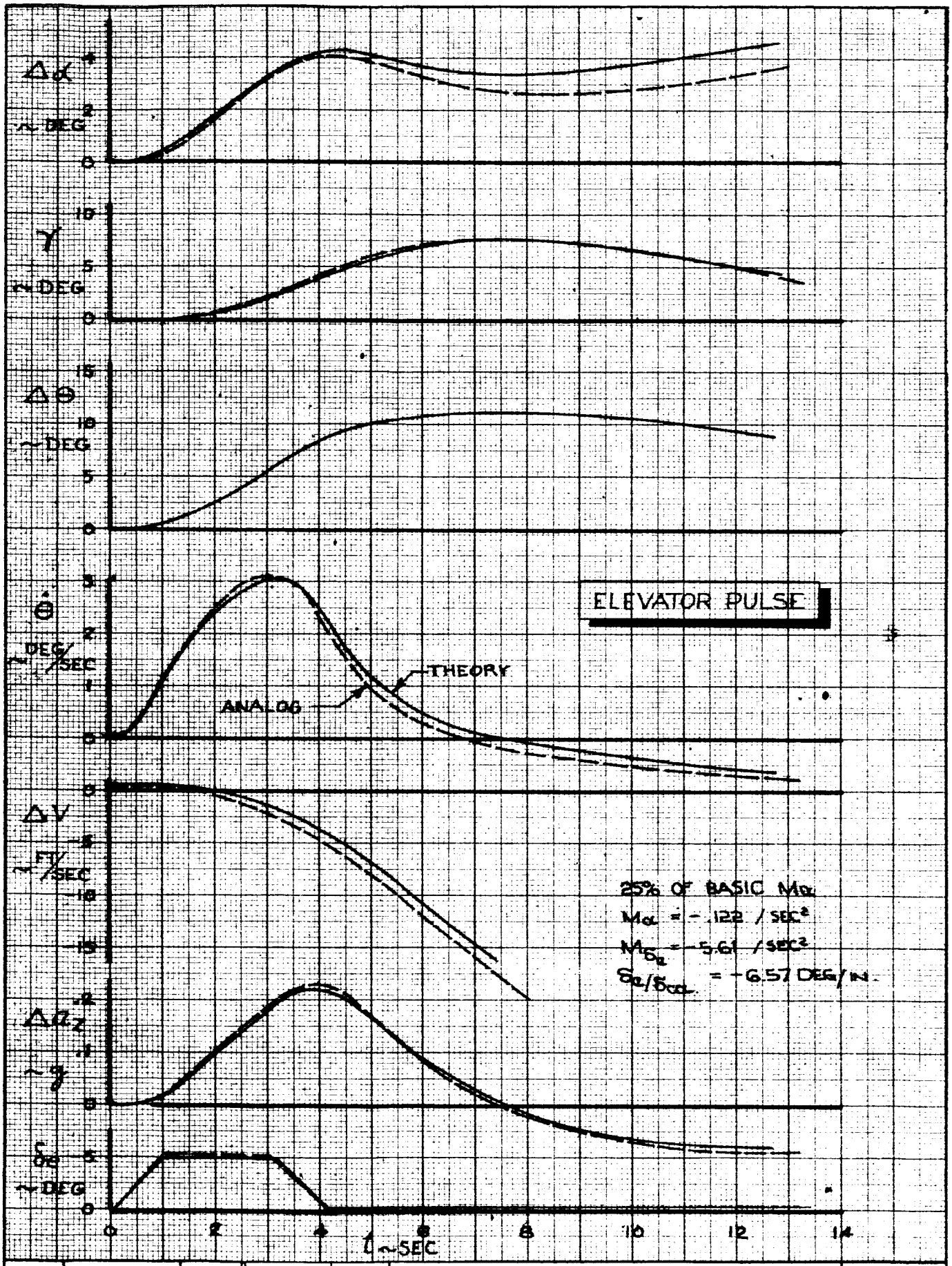

CALC	R. Root	2-2-66	REVISED	DATE	ELEVATOR PULSE GROUND BASED SIMULATOR CONFIGURATION G161B
CHECK					
APR					
APR					
					THE BOEING COMPANY

D6-15000

FIG. 70

PAGE VII-99

TD 461 C-R4

161 B

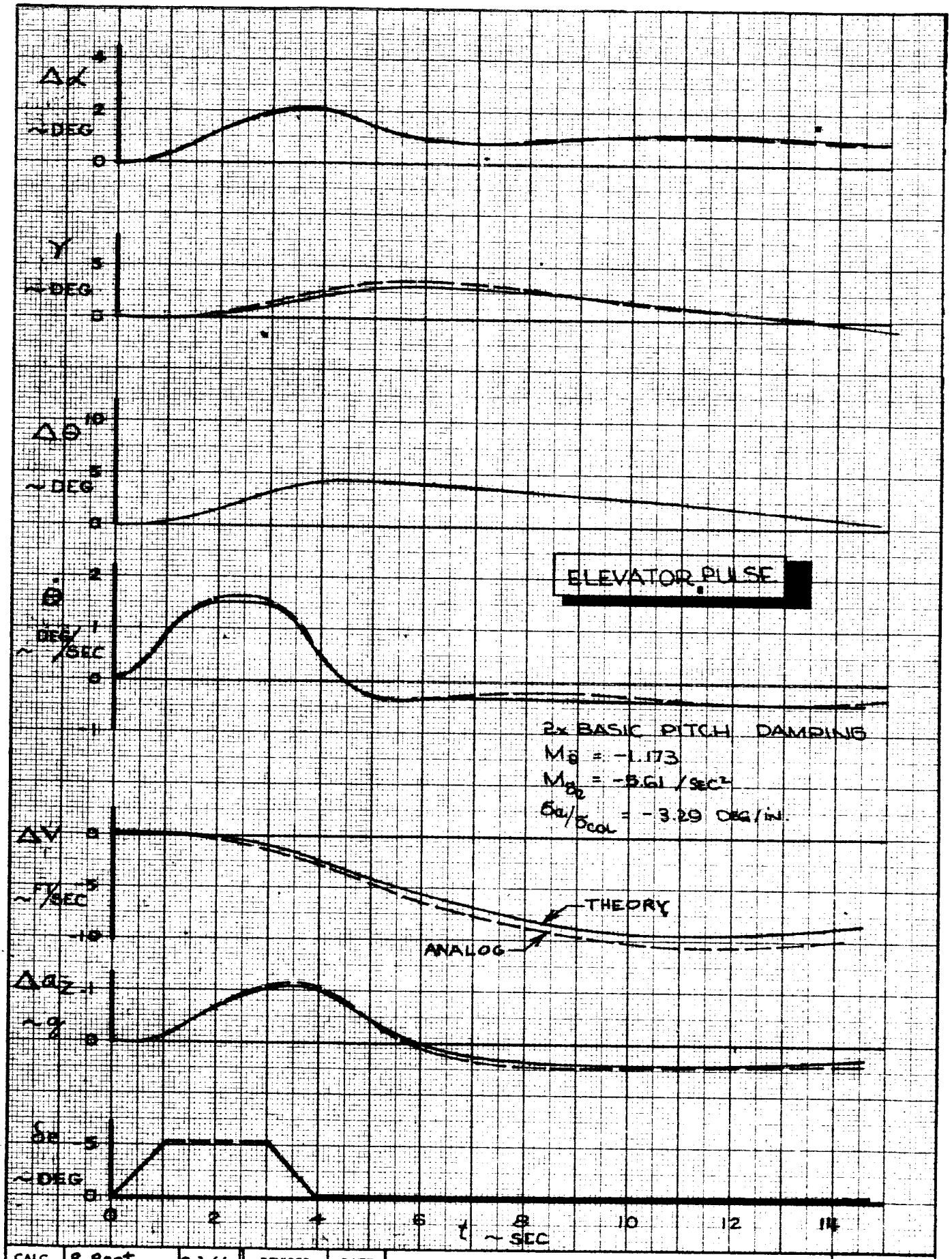

CALC	R. Root	2-2-66	REVISED	DATE	ELEVATOR PULSE GROUND BASED SIMULATOR CONFIGURATION G159A
CHECK					D6-15000
APR					FIG. 71
APR					THE BOEING COMPANY
					PAGE VII-100

TD 461 C-R4

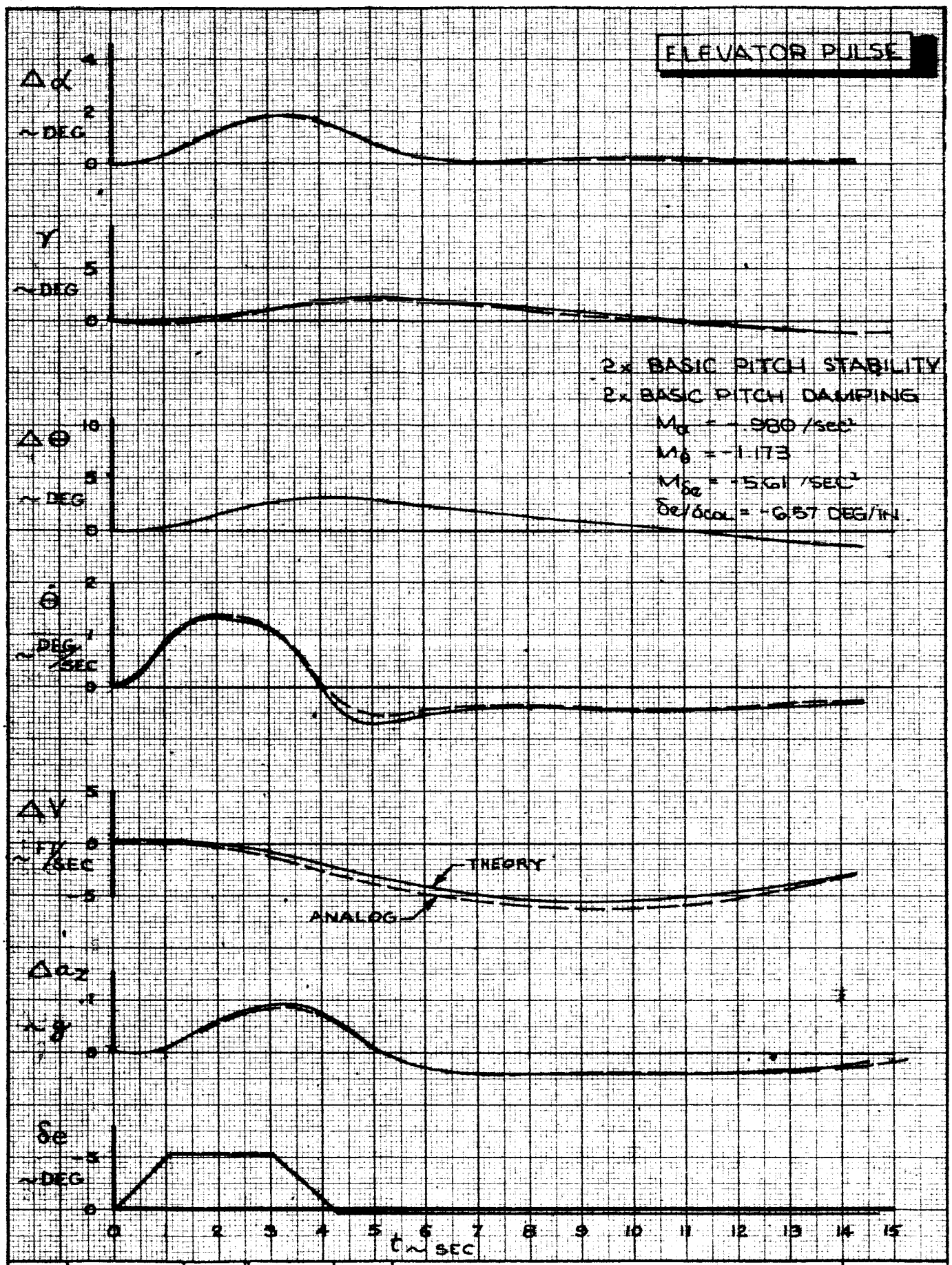

CALC	R. Root	2-2-66	REVISED	DATE	ELEVATOR PULSE GROUND BASED SIMULATOR CONFIGURATION G158A	D6-15000
CHECK						FIG. 72
APR					THE BOEING COMPANY	PAGE VII-101
APR						

TD 461 C-R4

158A

VIII. LATERAL CONFIGURATION CHARACTERISTICS

A. Airborne Simulation

The characteristics of the four lateral directional configurations evaluated on the airborne simulation which are different from the basic 1209 configuration are documented in this section.

The responses to the documentation maneuvers are summarized or eliminated when there is negligible change from the basic configuration. During all the lateral flight test documentation and evaluation the longitudinal configuration was the basic 101A configuration.

Table 4 contains a summary of the lateral directional configurations evaluated on the Airborne Simulation. The lateral-directional aerodynamic coefficients used to obtain these characteristics are listed in Appendix 1. A summary plot of the steady roll rate maneuver is shown in Fig. 73 for several configurations. The maximum steady state roll rate available agrees farily well with the theoretical value.

The roll rate reversal data is shown in Figs. 74 thru 77 for four configurations. Comparison of these configurations with the basic, 1209 (Fig. 13), and with each other shows the effect of roll control sensitivity (slope) and total roll control power ($\ddot{\phi}$ max). The roll control power available in flight test is generally lower than theory predicts whereas the sensitivity is accurately predicted.

CONFIG.	L	$\delta_{W_{EFF.}}$	$L_{\delta W}$	$t_{\delta a_{MAX.}}$	τ_{3D}	P_{SS}	ϕ_1	ϕ_2	DUTCH ROLL		COMMENTS
									ω_n	ζ	INCREASED (+) DECREASED (−)
	RAD/SEC²	DEG	1/SEC²	SEC	SEC	RAD/SEC	DEG	DEG	RAD/SEC	−	
1209	.267	50	.306	.48	1.14	.348	RT 2.10 LT 2.10	11.3 13.0	.508	.329	BASIC
1203A	.240	30	.458	↓	↓	.358	1.89	10.02	↓	↓	+ ROLL CONTROL SENSITIVITY
1207A	.150	30	.286	↓	↓	.196	1.20	7.25	↓	↓	− ROLL CONTROL POWER
1235	.267	30	.511	↓	.60	.167	1.90	8.95	.533	.380	+ DAMPING IN ROLL + ROLL SENSITIVITY
1237	.250	50	.286	.84	1.14	.326	1.40	9.10	.508	.329	+ TIME TO MAX. AILERON
−80BLC	.323	NON LINEAR	1.200	.48	NON LINEAR	NON LINEAR	4.00	20.72	.513	.564	++ ROLL SENSITIVITY & POWER + DAMPING

MEASURED DURING FLIGHT TEST

ENGR. | CHECK | APR | APR | REVISED | DATE

AIRBORNE SIMULATION LATERAL RUN LOG

THE BOEING COMPANY
RENTON, WASHINGTON

TABLE 4

D6-15000

VIII-103

AD 1017-R6

6-7000

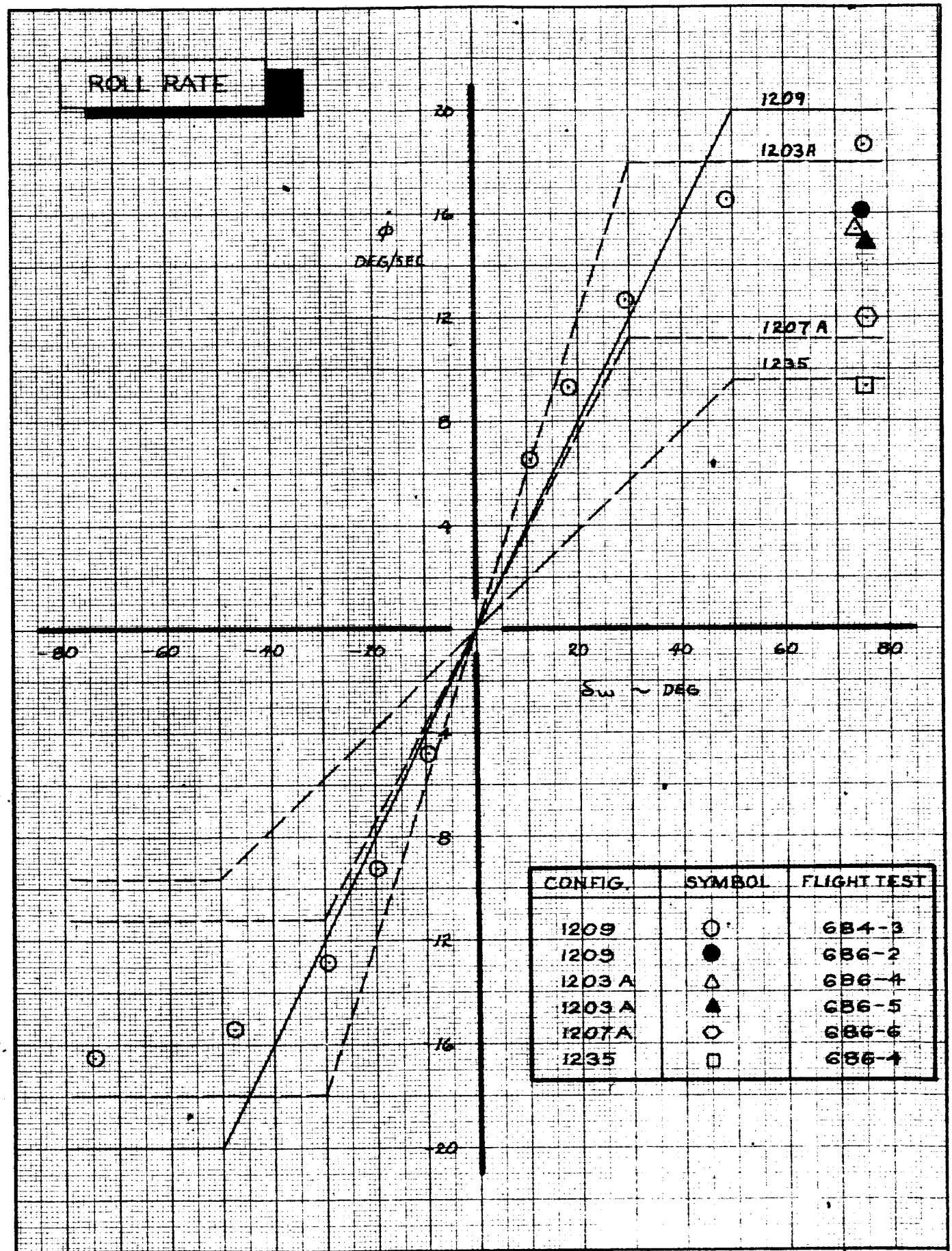

CONFIG.	SYMBOL	FLIGHT TEST
1209	○	686-3
1209	●	686-2
1203A	△	686-4
1203A	▲	686-5
1207A	⬡	686-6
1235	□	686-1

			REVISED	DATE
CALC				
CHECK				
APR				
APR				

SUMMERY OF STEADY ROLL RATES

367-80

FIG. 73

THE BOEING COMPANY D6-15000

PAGE VIII-104

TD 461 C-R4

107

A 20° heading change is presented for configuration 1235 in Fig. 78. The high roll damping of this configuration is evident when the time history of the wheel activity is compared to that of the basic 1209 configuration. (Fig. 19).

Table 5 shows the results of wheel steps.

TABLE 5

WHEEL STEP

CONFIG.	ϕ_1	ϕ_2	β_1	β_2	δw_1	δw_2
1203A	1.89	10.02	.23	1.76	75.6	75.6
1207A	1.20	7.25	.16	1.00	75.6	75.6
1209 Left	2.10	11.3	.30	1.96	75.6	75.6
1209 Right	2.10	13.0	.41	2.03	75.6	75.6
1235	1.90	8.95	.07	1.12	75.6	75.6
1237	1.40	9.1	.11	1.28	75.6	75.6
-80 BLC	4.00	20.72	.74	2.11	75.6	75.6

ROLL RATE REVERSAL

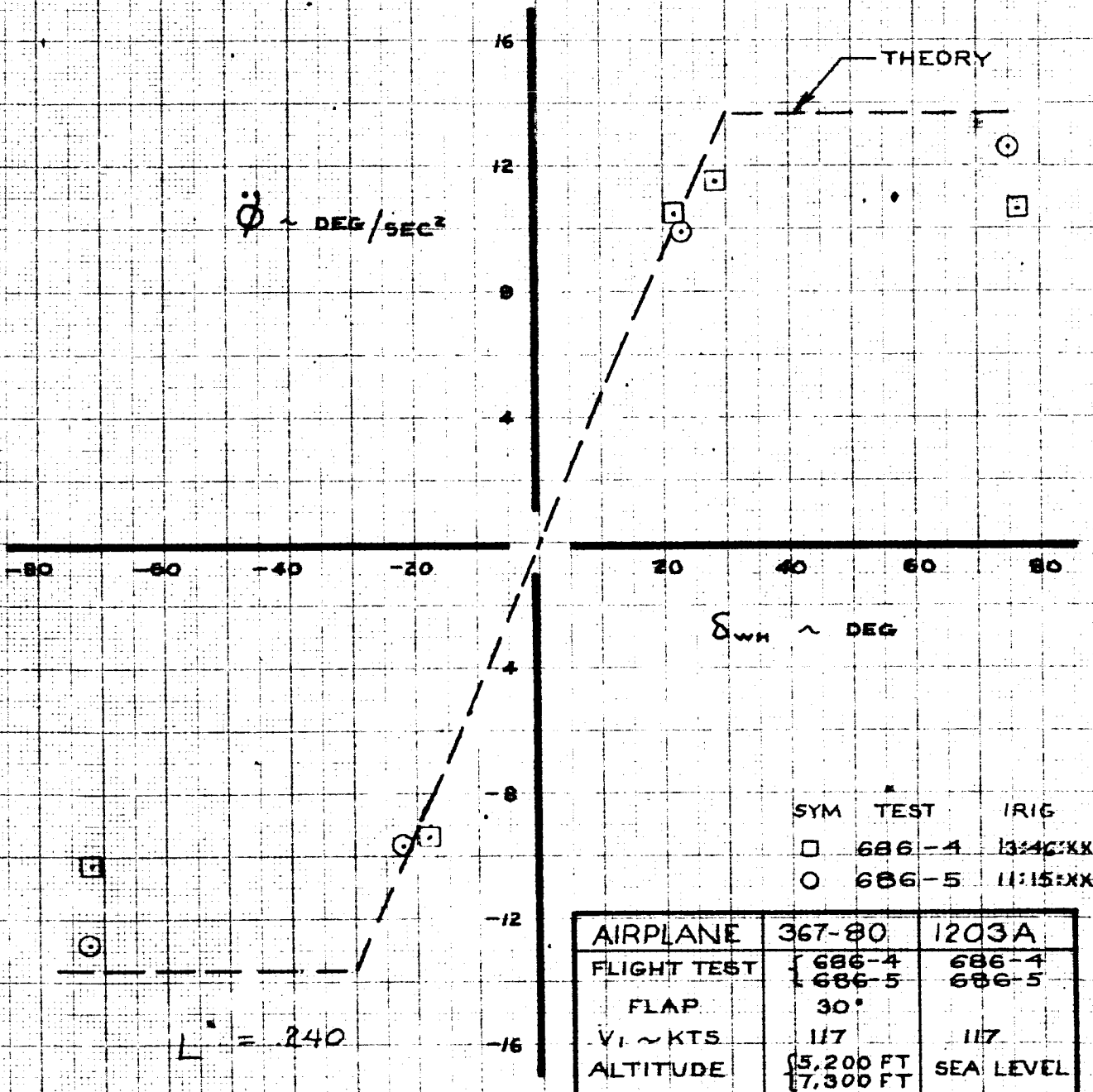

AIRPLANE	367-80	1203A
FLIGHT TEST	686-4 686-5	686-4 686-5
FLAP	30°	
V_1 ~ KTS	117	117
ALTITUDE	5,200 FT 7,300 FT	SEA LEVEL
G.W. ~ LBS	161,900 163,800	500,000
C.G.	30.7% 30.8%	25%

			REVISED	DATE
CALC				
CHECK				
APR				
APR				

ROLL RATE REVERSAL
FLIGHT TEST 686-4 & -5
CONFIGURATION 1203A

367-80

FIG. 74

THE BOEING COMPANY D6-15000

TD 461 C-R4

ROLL RATE REVERSAL

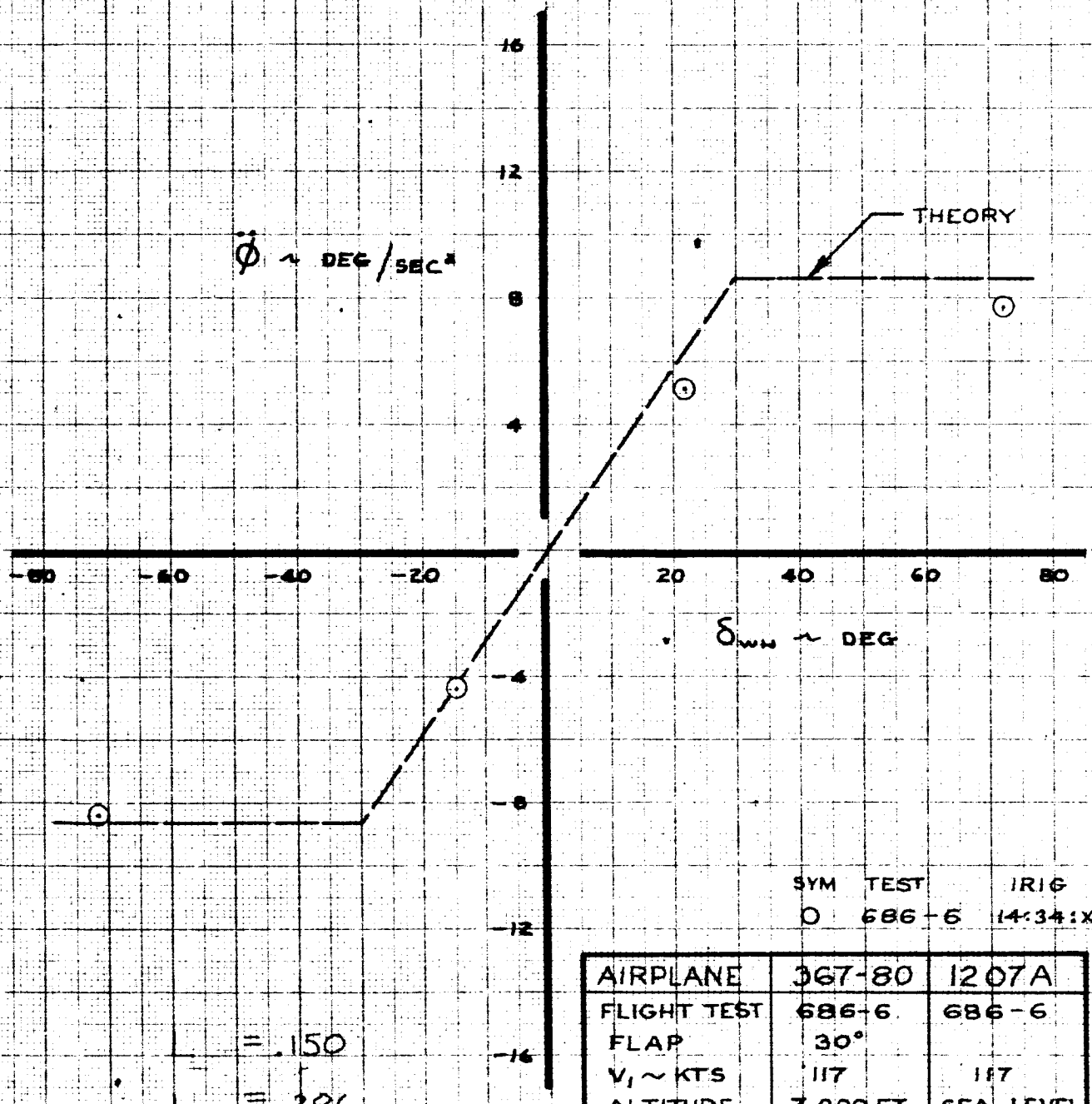

SYM TEST IRIG
○ 686-6 14:34:XX

$\frac{\dot{\phi}}{\delta_{WH}} = .150$

$\frac{\ddot{\phi}}{\delta_{WH}} = .286$

AIRPLANE	367-80	1207A
FLIGHT TEST	686-6	686-6
FLAP	30°	
V_i ~ KTS	117	117
ALTITUDE	7,000 FT	SEA LEVEL
G.W. ~ LBS	158,900*	500,000
C.G	30.7%	25%

			REVISED	DATE
CALC				
CHECK				
APR				
APR				

ROLL RATE REVERSAL
FLIGHT TEST 686-6
CONFIGURATION 1207A

367-80

FIG. 75

THE BOEING COMPANY D6-15000

TD 461 C-R4

ROLL RATE REVERSAL

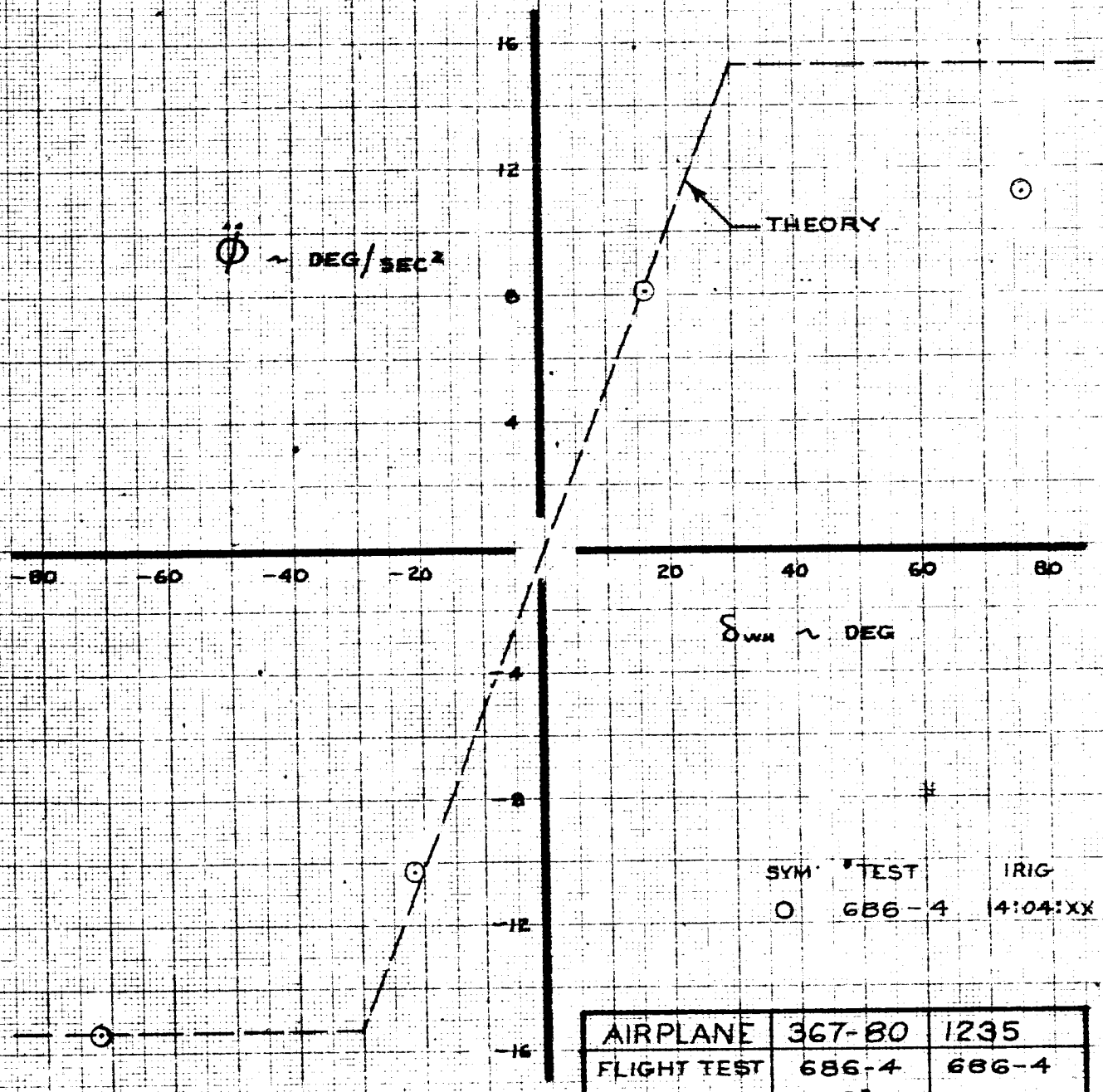

SYM	TEST	IRIG
O	686-4	4:04:XX

$L_{\delta_{WH}} = .511$

$L = .267$

AIRPLANE	367-80	1235
FLIGHT TEST	686-4	686-4
FLAP	30°	
V_I ~ KTS	117	117
ALTITUDE	5,200 FT	SEA LEVEL
G. W. ~ LBS	158,500	500,000
C. G.	29.3%	25%

			REVISED	DATE
CALC				
CHECK				
APR				
APR				

ROLL RATE REVERSAL
FLIGHT TEST 686-4
CONFIGURATION 1235

367-80

FIG. 76

THE BOEING COMPANY D6-15000

TD 461 C-R4

ROLL RATE REVERSAL

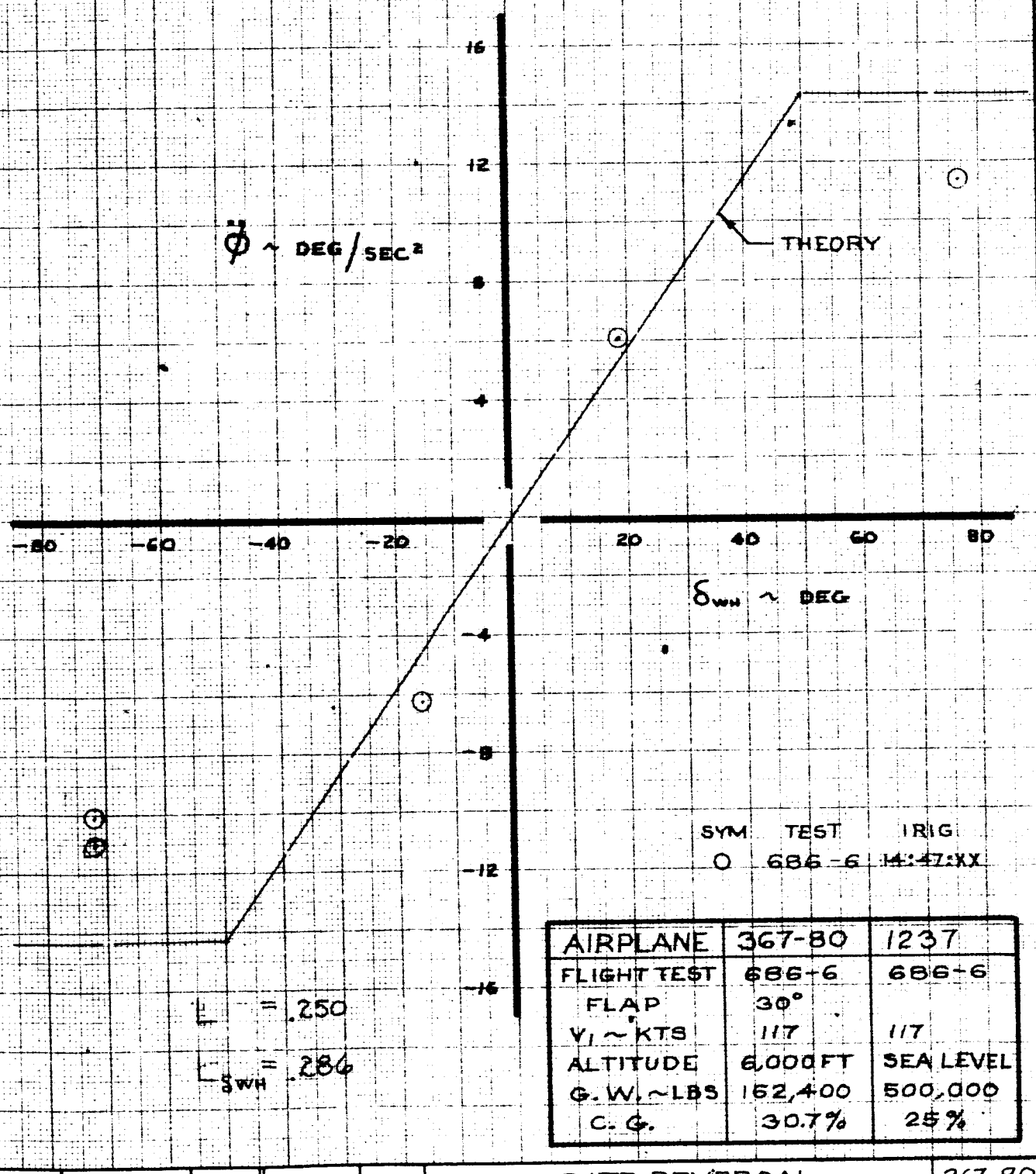

AIRPLANE	367-80	1237
FLIGHT TEST	686-6	686-6
FLAP	30°	
V_i ~ KTS	117	117
ALTITUDE	6,000 FT	SEA LEVEL
G.W. ~ LBS	162,400	500,000
C.G.	30.7%	25%

			REVISED	DATE
CALC				
CHECK				
APR				
APR				

ROLL RATE REVERSAL
FLIGHT TEST 686-6
COFIGURATION 1237

367-80

FIG. 77

THE BOEING COMPANY D6-15000

PAGE VIII-109

TD 461 C-R4

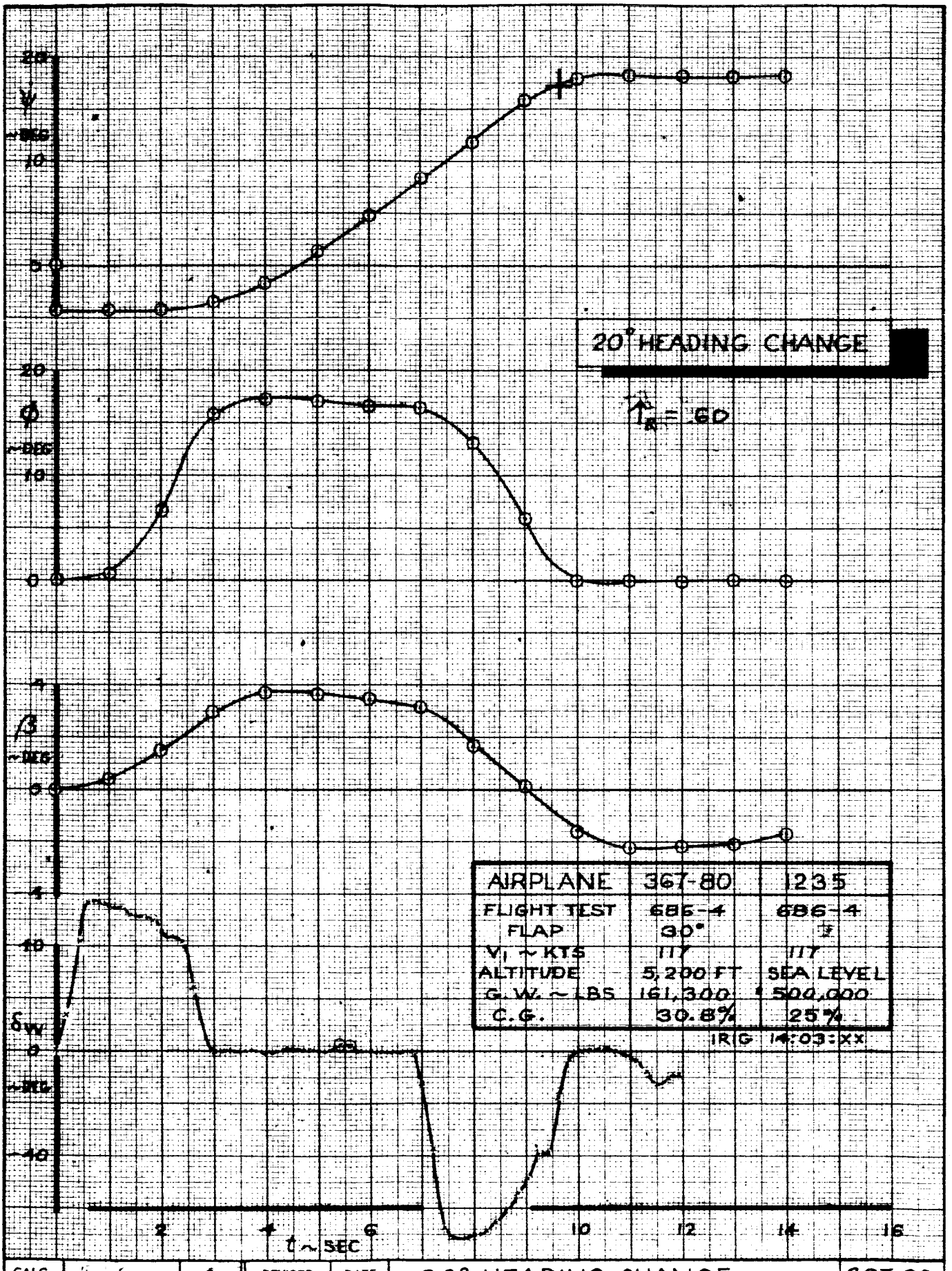

			REVISED	DATE
CALC				
CHECK				
APR				
APR				

20° HEADING CHANGE
FLIGHT TEST 686-4
CONFIGURATION 1235

367-80
D6-15000
FIG. 78

THE BOEING COMPANY

PAGE
VIII-110

TD 461 C-84

B. Ground Based Simulation

The lateral-directional characteristics of all the configurations evaluated on the ground based simulator are presented in Table 6. The aerodynamic coefficients and augmentation system used to obtain these characteristics are listed in Appendix 1. Lateral-Directional aerodynamic characteristics which are equivalent to the basic values with augmentation are also presented. Figures 79, 80, and 81 present roll response ϕ_1 and ϕ_2 as a function of control power for the three augmentation systems used (described in Appendix 1). The effect of roll time constant (τ_R) on roll response is presented in Fig. 82 for a step wheel and Fig. 83 for step aileron. Figs. 84 and 85 give roll response for typical configurations with augmentations 2 and 3. A typical roll response with augmentation 1 was presented in Fig. 36 (page VI-57). Figure 86 presents roll response of a configuration with low available aileron rate (60 °/sec).

S11

TD 1040C - R3

6-7000

APR	APR	CHECK	CALC	R. Root	2-2-66	REVISED	DATE

GROUND BASED SIMULATION
LATERAL RUN LOG.

THE BOEING COMPANY
RENTON, WASHINGTON

TABLE G
D6-15000
PAGE VIII-112

GROUND BASED CONFIG	L	δ_{WH} EFF.	$L_{\delta_{WH}}$	$t_{\delta_{a_{MAX}}}$	τ_{ROLL}	$\dot{\varphi}_{SS}$	ϕ_1	ϕ_2	F_W/δ_W	AUG. SYSTEM	DUTCH ROLL ω_n	DUTCH ROLL ζ	SPIRAL $T_{1/2}$	ϕ/β
G2	RAD/SEC	DEG.	$1/SEC^2$	SEC.	SEC.	DEG/SEC.	DEG	DEG	LB/DEG		RAD/SEC.		SEC.	
1	.20	50	.229	.10	1.42	16.3	4.4	14.2	.28	2	.449	.339	2.5	
1					1.14	13.1	4.1	15.8		3	.508	.329	18.3	1.33
1h					1.42	16.3	4.4	14.2	.14	2	.449	.339	2.5	
2	.30		.344			24.4	6.5	21.2	.28					
3	.40		.458			32.6	8.7	28.1						
4	.50		.573			40.7	10.8	35.0						
5	.60		.688			48.9	13.0	42.0						
5A	.80		.917			65.1	17.4	56.2						
5B	1.0		1.146			81.5	21.6	70.						
5C	.15		.172			12.2	3.3	10.9						
5C					1.14	9.8	3.0	12.0		3	.508	.329	18.3	1.33
5D	.125		.143		1.42	10.2	2.8	9.0		2	.449	.339	2.5	
5E	.9		1.031			73.2	19.5	63.						
5F	.10		.115			8.1	2.2	6.8						
5G	.05		.057		1.14		1.0	4.0		3	.508	.329	18.3	1.33
5H		90	.032											
5J		30	.096											
6	.15		.286		1.42	12.2	3.3	10.9		2	.449	.339	2.5	
6					1.14	9.8	3.0	12.0		3	.508	.329	18.3	1.33
7A	.10		.191		1.42	8.1	2.2	6.8		2	.449	.339	2.5	
8	.30	75	.229			24.4	6.5	21.2						
8A	.15		.115		1.14	9.8	3.0	12.0		3	.508	.329	18.3	1.33
9	.40		.306		1.42	32.6	8.7	28.1		2	.449	.339	2.5	
10		90	.255											

GROUND BASED SIMULATION

LATERAL RUN LOG.

THE BOEING COMPANY

RENTON, WASHINGTON

APR	APR	CHECK	CALC	R. Root	2-2-66	REVISED	DATE

GROUND BASED CONFIG. G2	L RAD/SEC²	δ_{WH} EFF. DEG.	$L_{\delta_{WH}}$ 1/SEC²	$t_{\delta_{aMAX}}$ SEC.	τ_{ROLL} SEC.	$\dot{\varphi}_{SS}$ DEG/SEC	ϕ_1 DEG	ϕ_2 DEG	F_W/δ_W LB/DEG	AUG. SYSTEM	DUTCH ROLL ω_n RAD/SEC	DUTCH ROLL ζ	SPIRAL $T_{1/2}$ SEC.	ϕ/β
11	.30	90	.191	.10	1.42	24.4	6.5	21.2	.28	2	.449	.339	2.5	
12	.20		.127			16.3	4.4	14.2						
13	.125		.080			10.2	2.8	9.0						
14	.15		.0955		1.14	9.8	3.0	12.0		3	.508	.329	18.3	1.33
16		50	.172	.18	1.42	12.2	3.1	10.2		2	.449	.339	2.5	
16					1.14	9.8	2.9	11.5		3	.508	.329	18.3	1.33
17	.25		.287		1.42	20.4	5.2	17.0		2	.449	.339	2.5	
18	.35		.401			28.5	7.2	24.0						
19	.15		.172	.30		12.2	2.7	9.4		2				
19					1.14	9.8	2.5	10.7		3	.508	.329	18.3	1.33
20	.25		.287		1.42	20.4	4.6	15.8		2	.449	.339	2.5	
21	.35		.401			28.5	6.2	22.0						
22	.30		.344	.18	—	—	6.8	24.8			.403	.223	—	
23	.20		.229				4.4	16.5						
23A	.15		.172				3.4	12.3						
24	.30		.344		1.03	17.7	5.9	18.6			.474	.377	3.8	
25	.15		.172			8.9	3.0	9.2						
25A	.20		.229			11.8	3.9	12.3						
26				.10	1.42	16.3	4.4	14.2	.21		.449	.339	2.5	
27									.42					
28									.64					

TABLE 6

D6-15000

TD 1040C - R3

6-7000

APR	APR	CHECK	CALC	GROUND BASED CONF.	L	δ_{WH} EFF.	$L_{\delta_{WH}}$	$t_{\delta_{\alpha MAX.}}$	τ_{ROLL}	$\dot{\varphi}_{SS}$	Φ_1	Φ_2	F_W/δ_W	AUG. SYST.	DUTCH ROLL ω_n	DUTCH ROLL ζ	SPIRAL $T_{1/2}$	Φ/β
					RAD/SEC²	DEG.	1/SEC²	SEC.	SEC.	DEG/SEC	DEG	DEG	LB/DEG		RAD/SEC		SEC	
				202A	.25	50	.287	.20	1.14	16.35	5.	19.2	.28	3	.508	.329	18.3	1.33
				205C	.15		.172			9.8	2.9	11.5						
				205F	.10		.115			6.54	1.9	7.6						
				207A	.15	30	.286			9.8	2.9	11.5						
			REVISED	216		50	.172	.36			2.5	10.8						
				219				.60			1.7	9.5						
			DATE	219A	.10		.115			6.54	1.1	4.9						
				224A	.50		.573	.36	.93	26.6	8.0	31.0			.519	.346	23.5	1.11
				231	.16		.184	.20	1.59	14.6	3.4	14.5			.479	.305	11.7	1.70
				232A	.26		.298		.72	10.7	4.8	18.2			.529	.367	31.2	.87
				233A	.43		.493			17.7	8.0	30.7						
				234A	.15		.173			6.19	2.8	10.5						
				236	.25		.287	.50	1.14	16.35	4.1	17.9			.508	.329	18.3	1.33
				237				.75			3.5	16.3						
				1202	.30	50	.344	.20	1.14	19.6	5.7	20.1	.19	1	.508	.329	18.3	1.33
				1202A	.25		.287			16.35	4.8	16.7	.19 & .28					
				1203	.40		.458			26.1	7.5	26.8	.28					
				1203A	.24	30	.459			15.7	4.6	16.0	.19					
				1203A*	.25		.478			16.35	4.8	16.7						
				1205C	.15	50	.172			9.80	2.8	10.0	.28					
				1205D	.25	75	.191			16.35	4.8	16.7	.19					
				1205F	.10	50	.115			6.54	1.9	6.6						

GROUND BASED SIMULATION
LATERAL RUN LOG.

THE BOEING COMPANY
RENTON, WASHINGTON

811

TD 1040C - R3

6-7000

CALC APR	APR	CHECK		GROUND BASED CONFIG.	L_{δ}	δ_{WH} EFF.	$L_{\delta_{WH}}$	$t_{\delta_{0MAX}}$	τ_{ROLL}	ρ_{SS}	Φ_1	Φ_2	F_W/δ_W	ANG. SYS.	DUTCH ROLL ω_n	DUTCH ROLL ζ	SPIRAL $T_{1/2}$	SPIRAL Φ/β
			R. Root	G 2	RAD/SEC²	DEG.	1/SEC²	SEC.	SEC.	DEG/SEC	DEG.	DEG.	LB/DEG		RAD/SEC.		SEC.	
			2-2-66	1206	.10	30	.191	.2	1.14	6.54	1.9	6.6	.28	1	.508	.329	18.9	1.33
				1207A	.15	↓	.286			9.8	2.8	10.0	.19					
				1209A	↓	75	.115			↓	↓	↓	.19 & .28					
			REVISED	1209B	.40	↓	.306	↓	↓	26.2	7.5	26.8	.28		↓	↓	↓	↓
				1222	.30	50	.344	0	1.59	27.4	8.0	27.0			.479	.305	11.7	1.7
				1223					1.14	19.6	7.5	22.5			.508	.329	18.3	1.33
			DATE	1224					.93	16.0	5.6	20.0			.519	.346	23.5	1.11
				1230	.15		.172	.2	1.59	13.7	3.1	12.0			.479	.305	11.7	1.7
				1231	.16		.184		↓	14.6	3.3	12.9			↓	↓	↓	↓
				1232	.28		.321		.72	11.5	4.6	15.1			.529	.367	31.2	.87
				1233	.47		.539		↓	19.4	7.8	24.4	↓		↓	↓	↓	↓
				1233B	↓		↓		.60	16.2	7.4	22.8	.19 & .28		.533	.380	38.2	.73
				1234B	.15		.172		.72	6.18	2.5	8.0	.28		.529	.367	31.2	.87
				1235	.267		.306	↓	.60	9.2	4.2	13.3	.19		.533	.380	38.2	.73
				1236	.25	↓	.287	.5	1.14	16.35	8.5	16.0	.28		.508	.329	18.3	1.33
				1236B	.43	30	.821	.2	.60	14.8	6.8	21.0	.19		.533	.380	38.2	.73
				1237	.25	50	.287	.75	1.14	16.35	3.2	13.0	.28		.508	.329	18.3	1.33
				1237A	↓	↓	↓	0	↓	↓	5.3	18.5	↓	↓				

GROUND BASED SIMULATION

LATERAL RUN LOG.

THE BOEING COMPANY

RENTON, WASHINGTON

TABLE 2

D6-15000

PAGE VIII-114

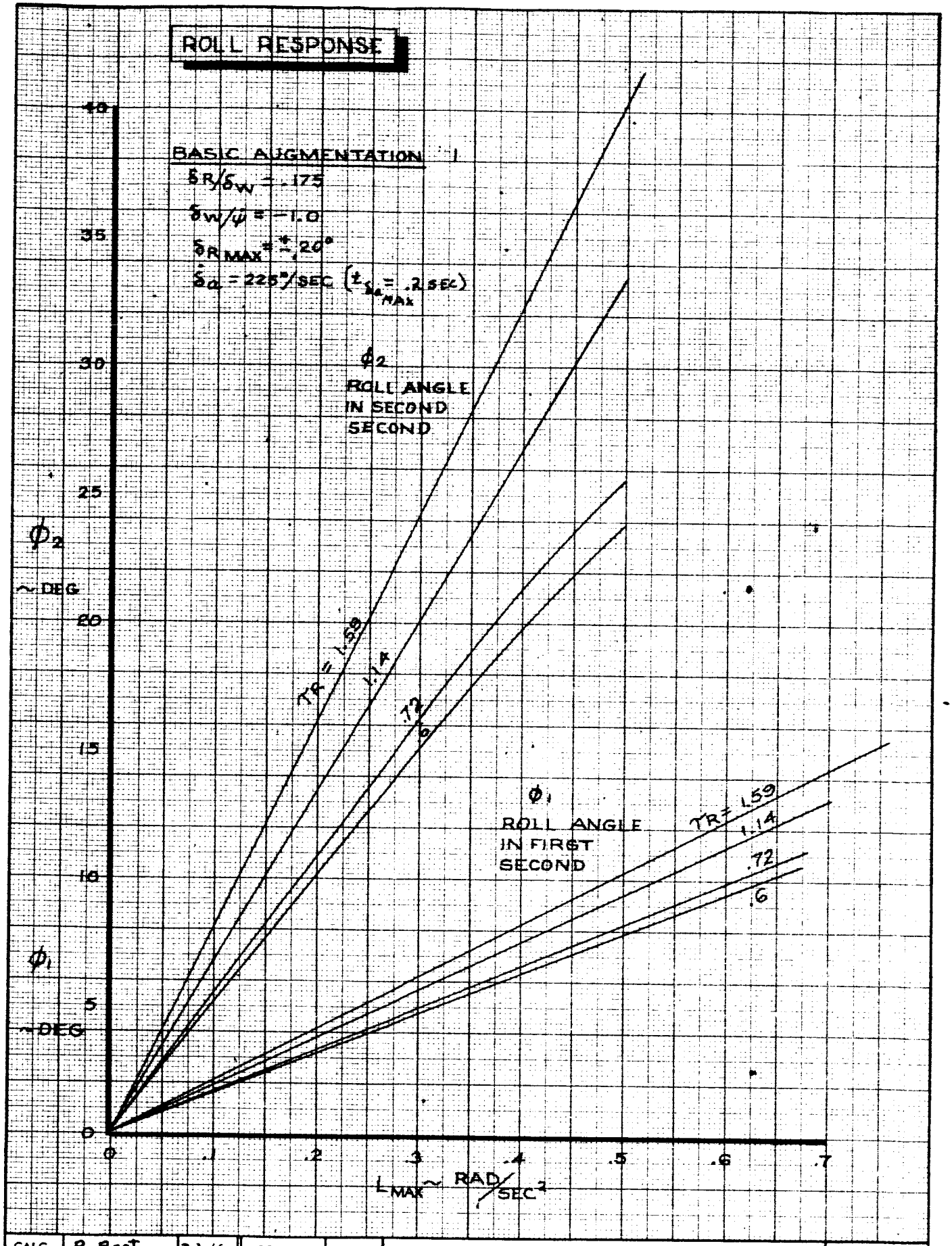

CALC	R. Root	2-2-66	REVISED	DATE	ROLL RESPONSE - WHEEL STEP GROUND BASED SIMULATOR AUGMENTATION 1
CHECK					
APR					
APR					
					THE BOEING COMPANY

FIG. 79

D6-15000

PAGE VIII-115

TD 461 C-R4

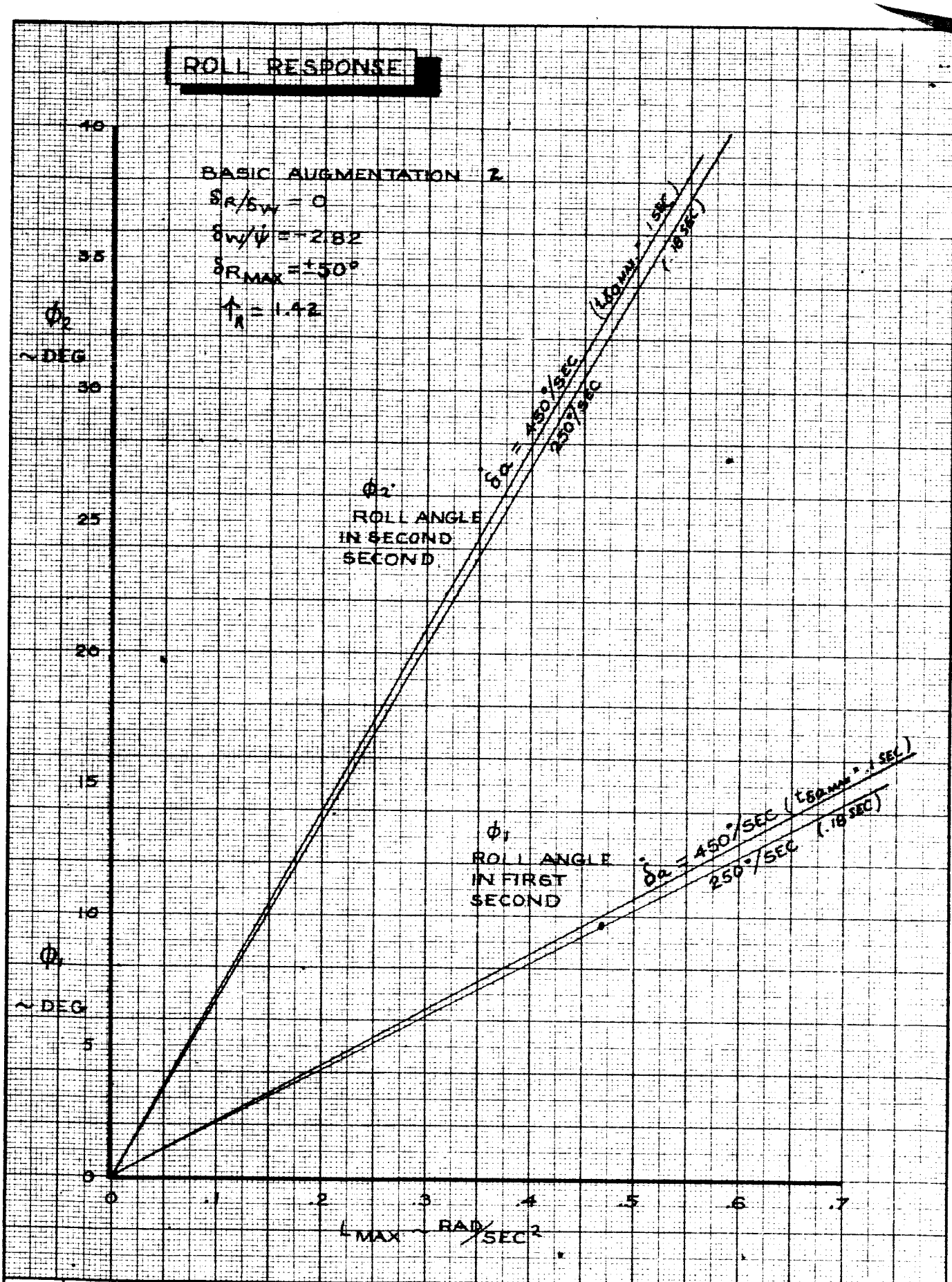

CALC	R. Root	2-2-66	REVISED	DATE	ROLL RESPONSE - WHEEL STEP GROUND BASED SIMULATION AUGMENTATION 2
CHECK					
APR					
APR					
					THE BOEING COMPANY

FIG. 80

D6-15000

PAGE VIII-116

TD 461 C-R4

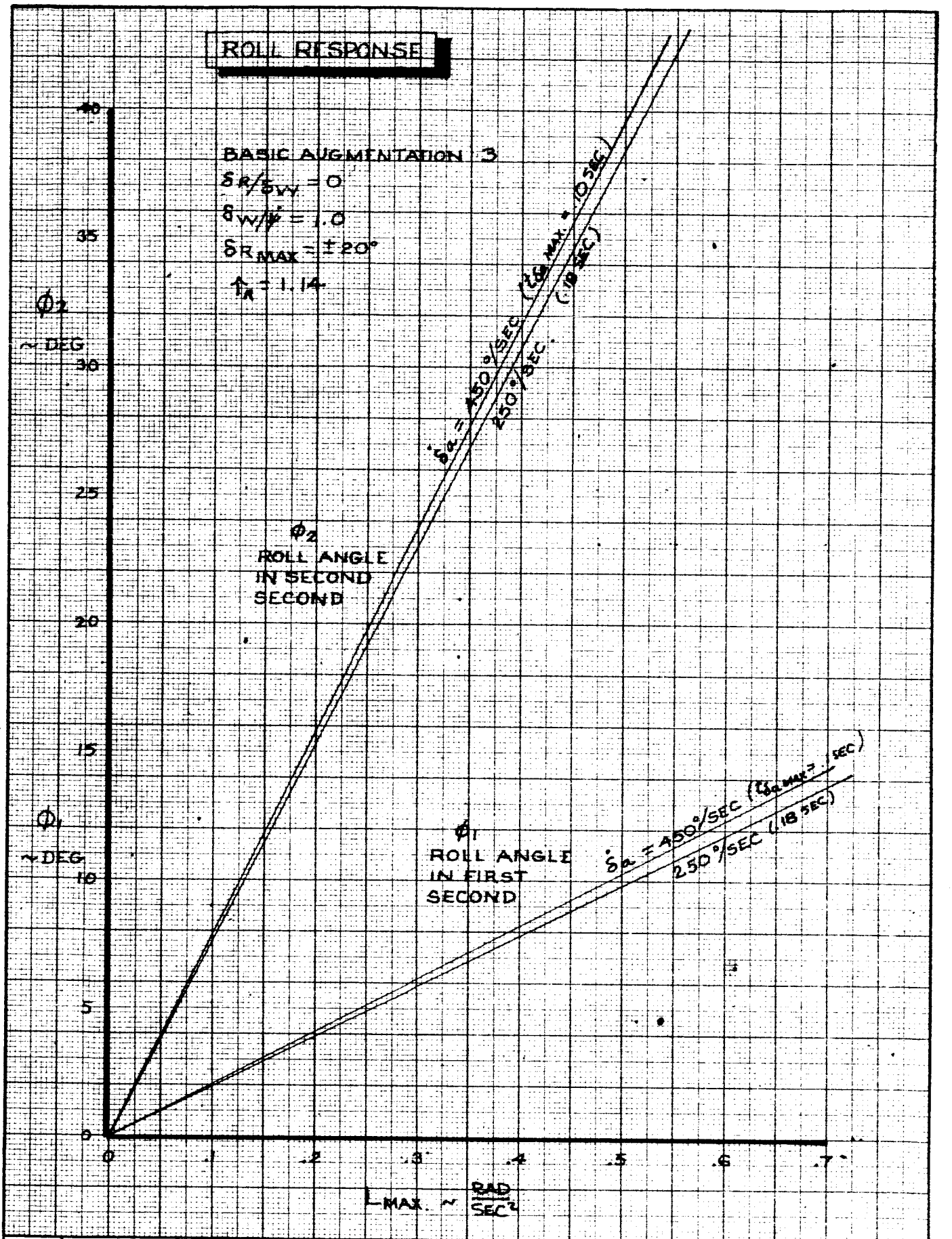

CALC	R. Root	2-2-66	REVISED	DATE
CHECK				
APR				
APR				

ROLL RESPONSE - WHEEL STEP GROUND BASED SIMULATOR AUGMENTATION 3

FIG. 81

D6-15000

THE BOEING COMPANY

TD 461 C-R4

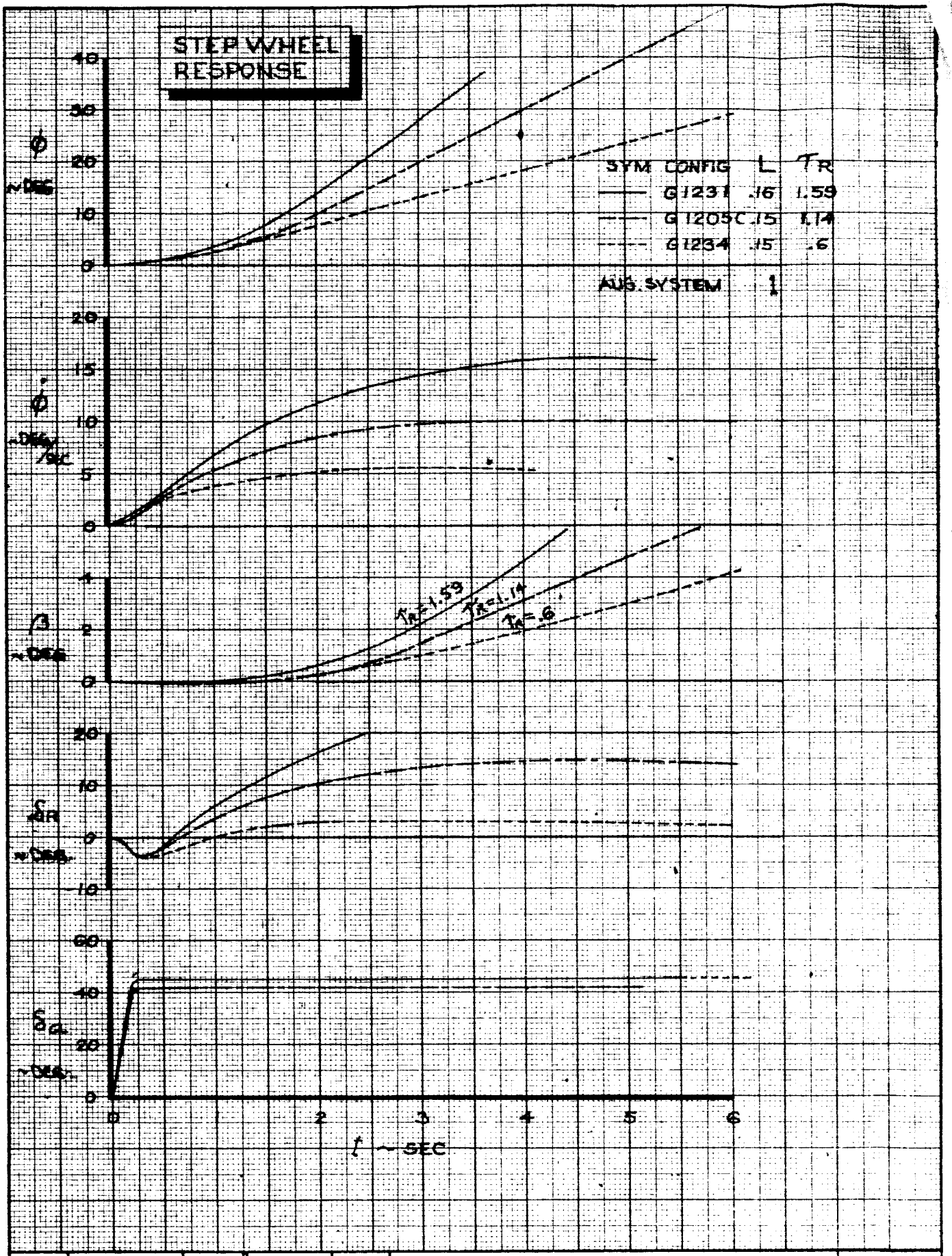

CALC	R. Root	2-2-66	REVISED	DATE	STEP WHEEL RESPONSE GROUND BASED SIMULATOR EFFECT OF T_R
CHECK					
APR					
APR					

FIG. 82

D6-15000

THE BOEING COMPANY

TD 461 C-R4

192

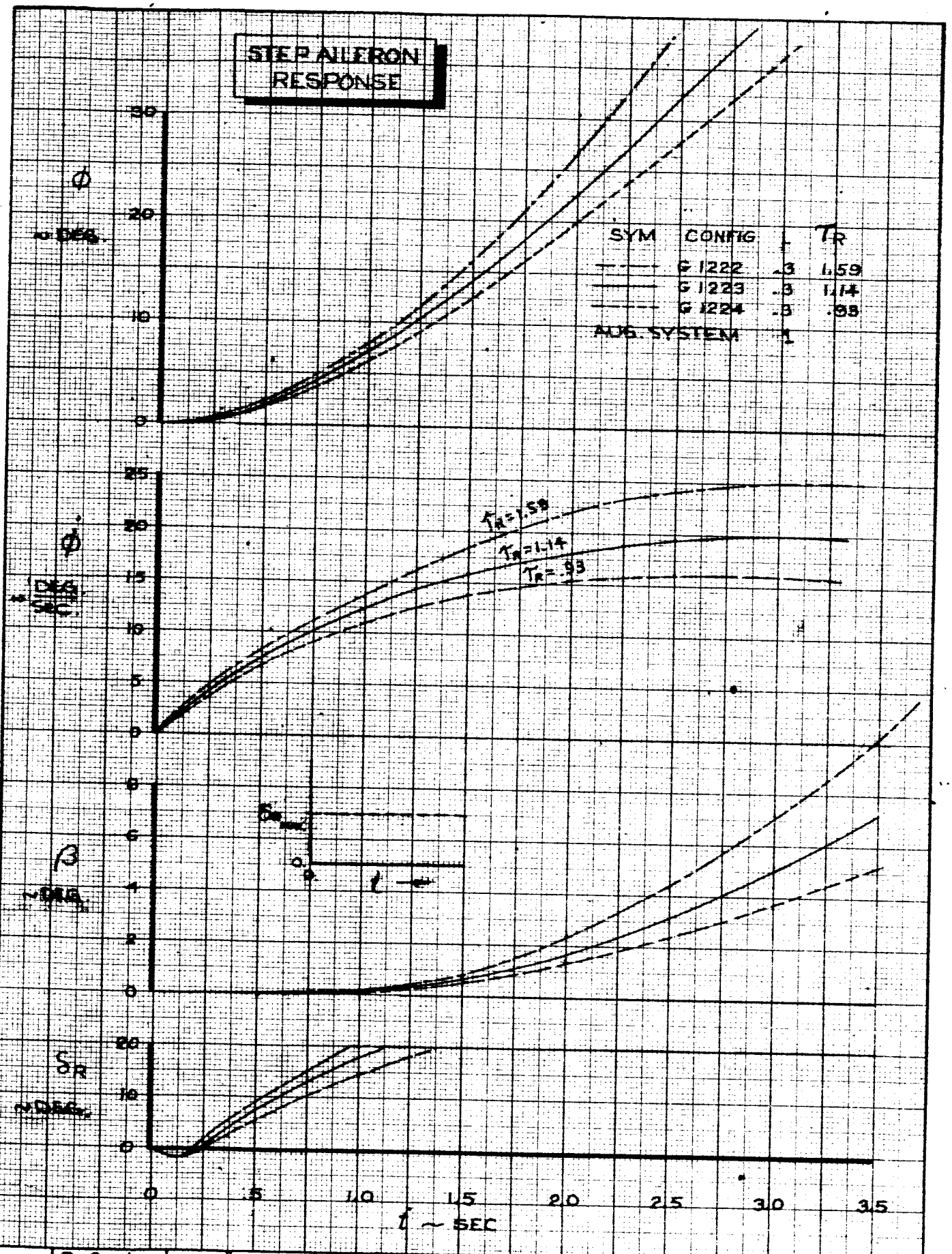

CALC	R. Root	2-2-66	REVISED	DATE	STEP AILERON RESPONSE GROUND BASED SIMULATOR EFFECT OF T_R
CHECK					
APR					
APR					
					THE BOEING COMPANY

FIG. 83

D6-15000

PAGE VIII-119

TD 461 C-R4

129

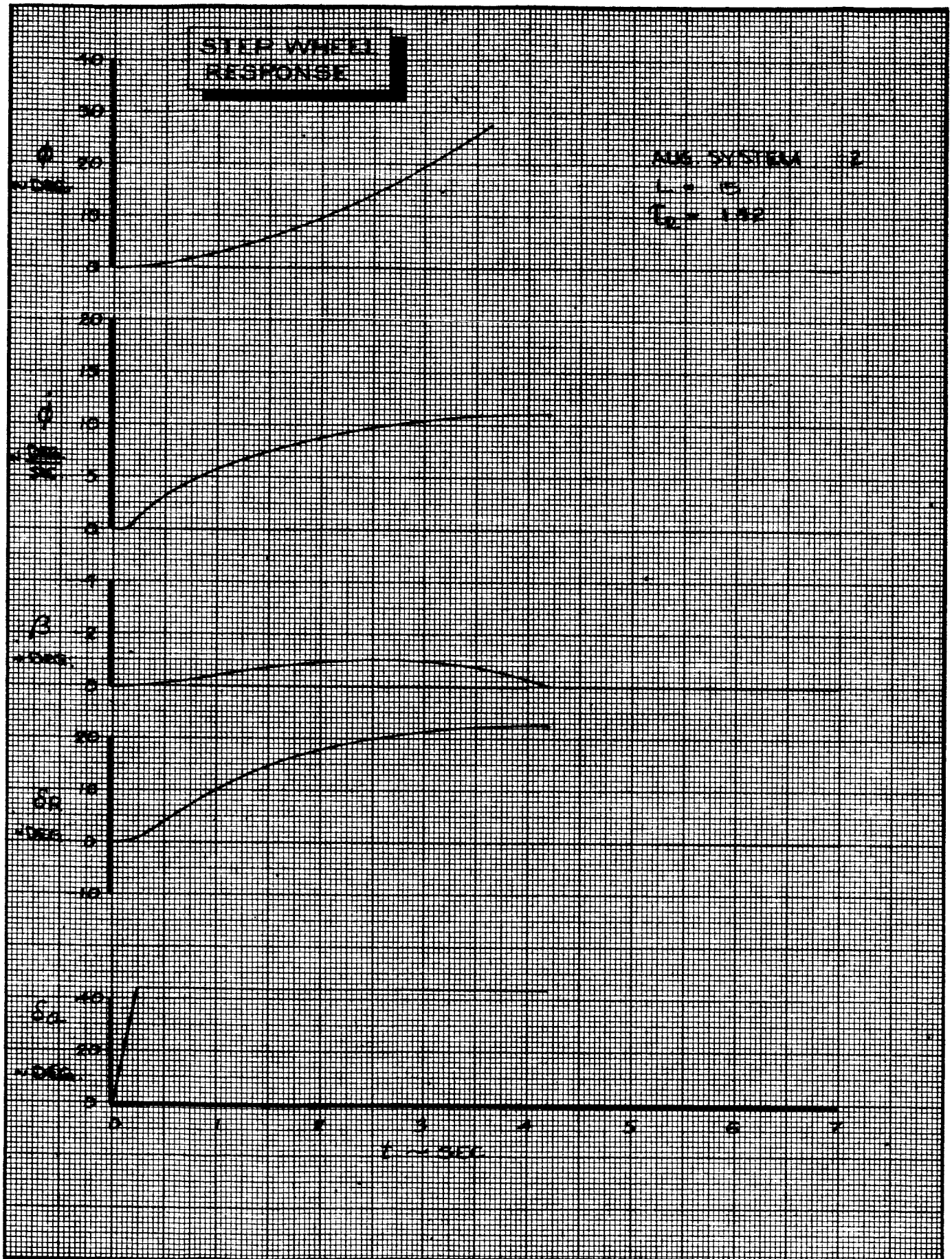

CALC	R. Root	2-2-66	REVISED	DATE	STEP WHEEL RESPONSE GROUND BASED SIMULATOR CONFIGURATION G16	FIG. 84
CHECK						D6-15000
APR					THE BOEING COMPANY	PAGE VIII-120
APR						

TD 461 C-R4

K+E ALBANENE TRACING PAPER

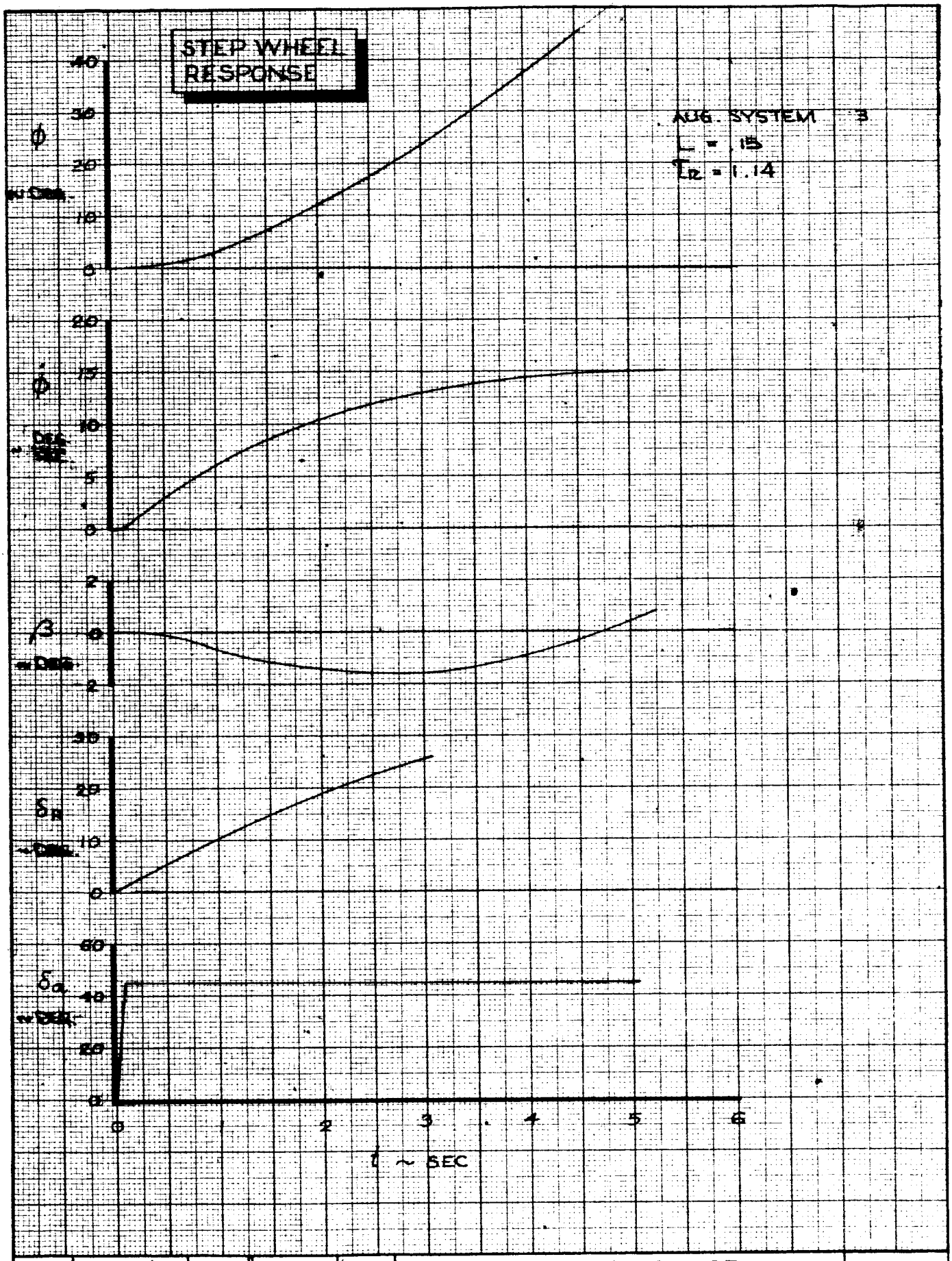

CALC	R. Root	2-2-66	REVISED	DATE	STEP WHEEL RESPONSE GROUND BASED SIMULATOR CONFIGURATION G205 C
CHECK					
APR					
APR					

FIG. 85

D6-15000

THE BOEING COMPANY

TD 461 C-R4

125

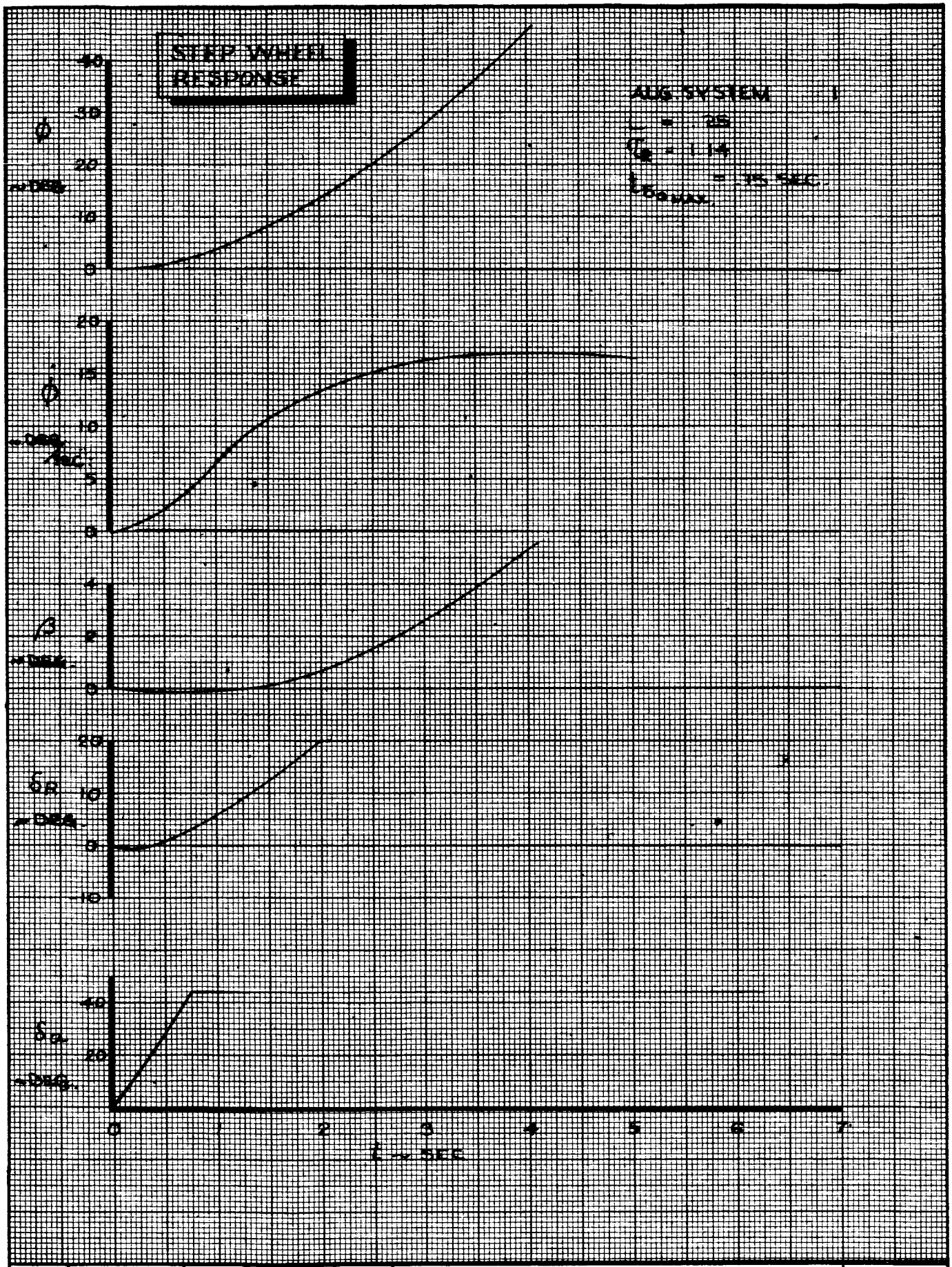

CALC	R. Root	2-2-66	REVISED	DATE	STEP WHEEL RESPONSE GROUND BASED SIMULATOR CONFIGURATION G1237
CHECK					
APR					
APR					

FIG. 86

D6-15000

THE BOEING COMPANY

126

TD 461 C-R4

K•E ALBANENE® TRACING PAPER

IX. DOCUMENTATION OF THE 367-80 WITH BOUNDARY LAYER CONTROL

The longitudinal and lateral characterisitcs of the 367-80 with Boundary Layer Control (BLC) are documented in Figs. 87 [illegible] 64. The dynamic characteristics are included in Tables 1 and 4 (pages VII 59 and VIII 103). A description in terms of aerodynamic coefficients is given in Appendix 1.

The purpose of going to the BLC configuration was to create the large roll control power required for evaluation. It should be noted, however, that this configuration has many characteristics other than roll control power which are different from the basic 1209 and 101A configuration. The 367-80 (BLC) should not be compared directly to the basic (1209) configuration with the intent of isolating the effects of increased roll control power.

Comments on the flight test and theoretical response to the documentation maneuvers performed are listed below.

	Longitudinal
Pitch Rate Reversal	Fig. 87. The pitch control sensitivity is accurately predicted by theory
Wind Up Turn	Figs. 88 & 89. Wind up turn data agrees quite well with the theoretical calculation when the data is shifted to allow for mis-trim.
Speed Stability	Fig. 90. A mis-trim in the flight test data is evident when compared to the theory.
Pitch Attitude	Fig. 91. Approximately 3 seconds are required for a pitch attitude change of 9 degrees.

PITCH RATE REVERSAL

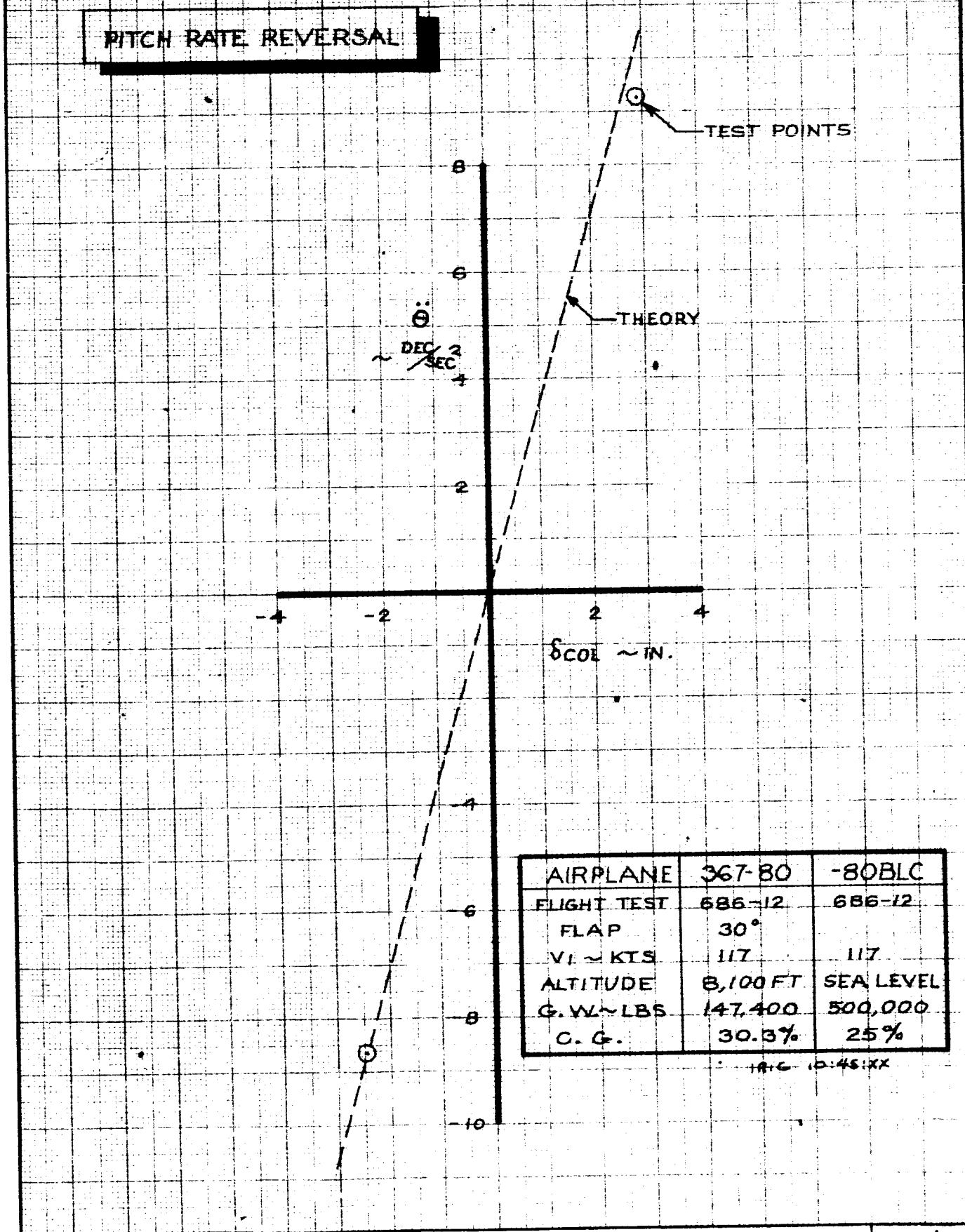

AIRPLANE	367-80	-80BLC
FLIGHT TEST	686-12	686-12
FLAP	30°	
Vi ~ KTS	117	117
ALTITUDE	8,100 FT	SEA LEVEL
G.W. ~ LBS	147,400	500,000
C.G.	30.3%	25%

1A:C 10:45:XX

CALC			REVISED	DATE
CHECK				
APR				
APR				

PITCH RATE REVERSAL
FLIGHT TEST 686-12
CONFIGURATION -80BLC

THE BOEING COMPANY

367-80
D6-15000
FIG. 87
PAGE
IX-124

TD 461 C-R4

WINDUP TURN

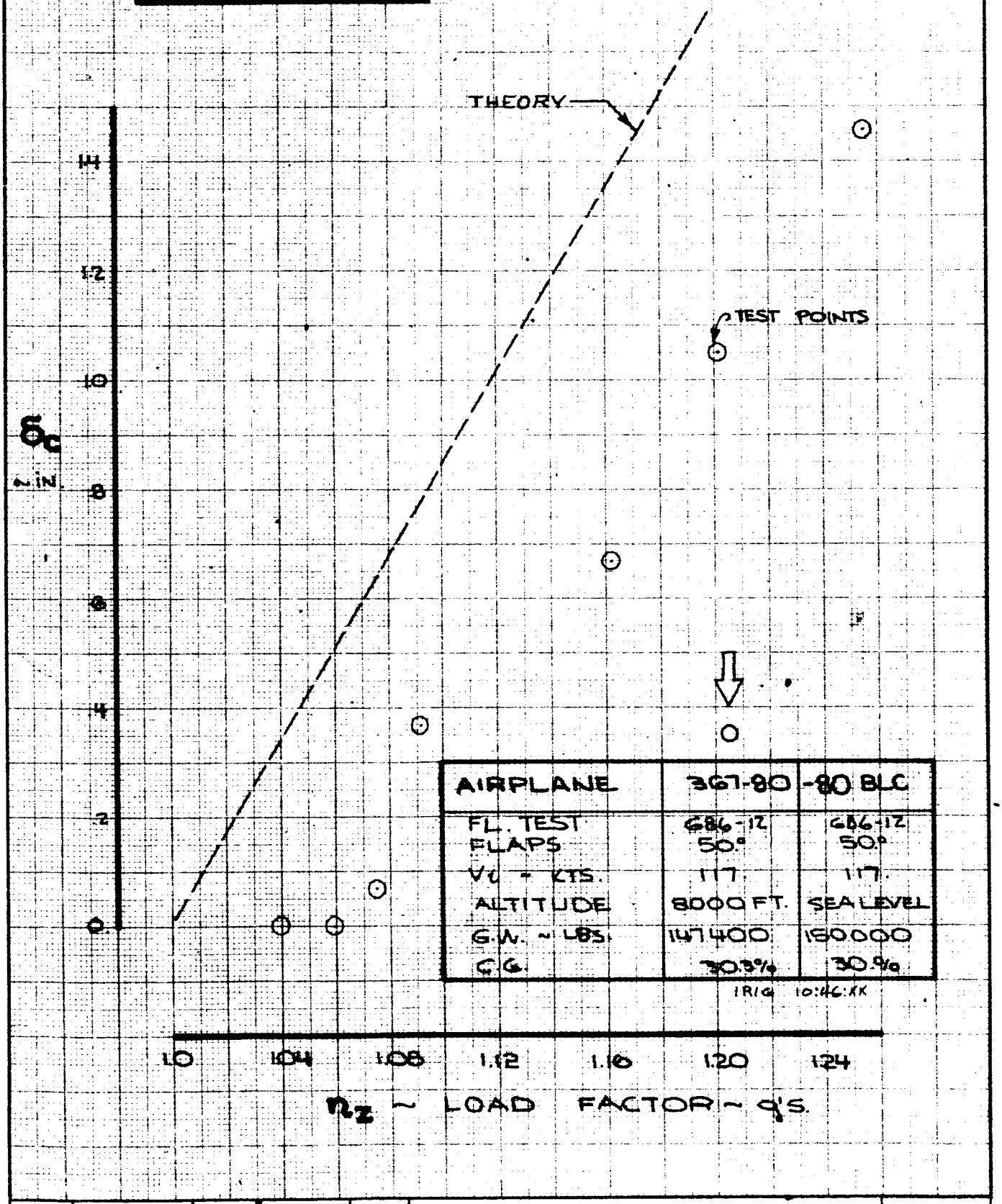

AIRPLANE	367-80	-80 BLC
FL. TEST	686-12	686-12
FLAPS	50°	50°
Vc ~ KTS.	117.	117.
ALTITUDE	8000 FT.	SEA LEVEL
G.W. ~ LBS.	147400	160000
C.G.	30.3%	30.%

IRIG 10:46:44

			REVISED	DATE
CALC				
CHECK				
APR				
APR				

WINDUP TURN
FL. TEST : 686-12
CONFIG. : -80 BLC

THE BOEING COMPANY

367-80
D6-15000
FIG. 88
PAGE
IX-125

TD 461 C-R4

WINDUP TURN

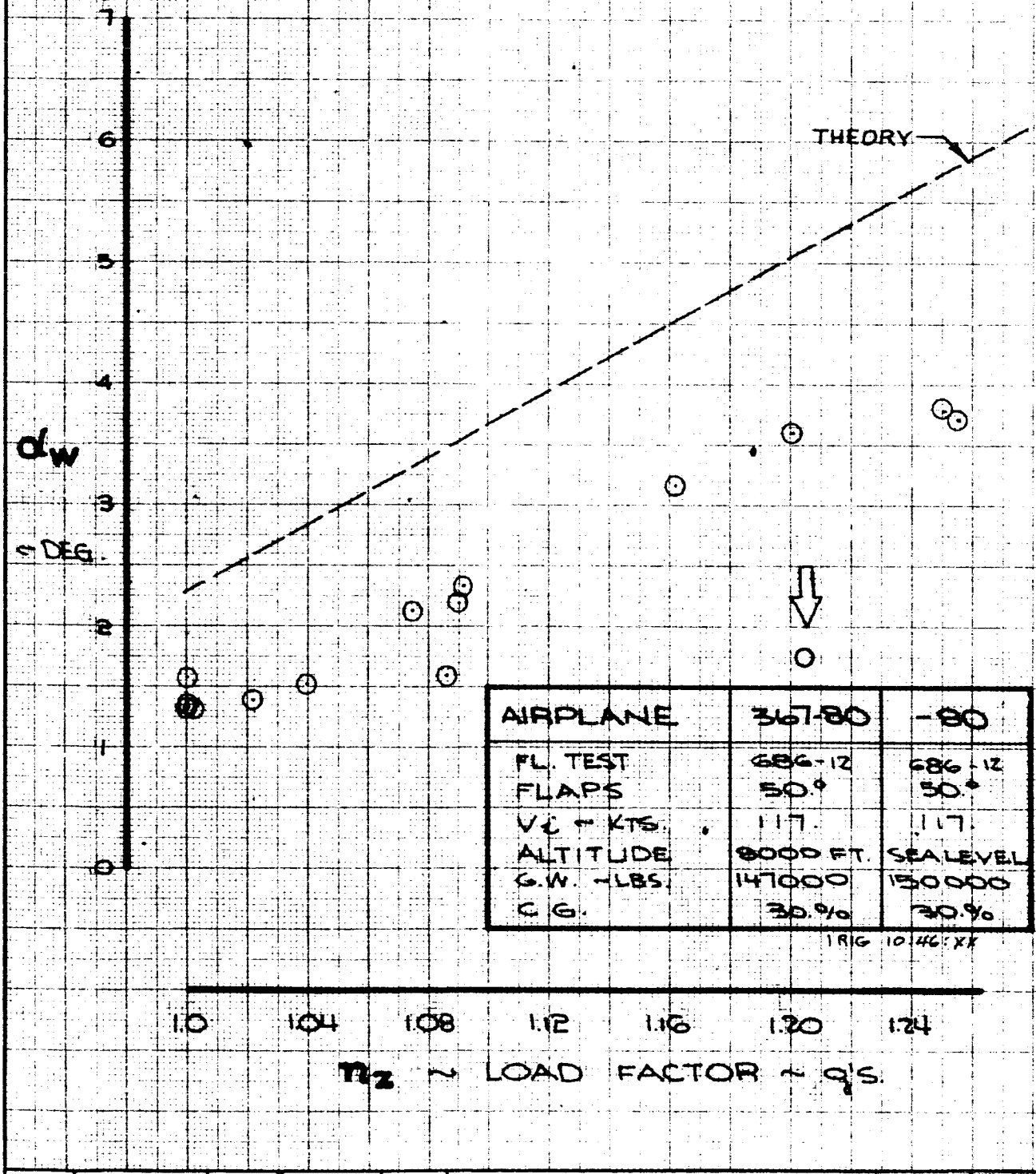

AIRPLANE	367-80	-80
FL. TEST	686-12	686-12
FLAPS	50.°	50.°
V_i ~ KTS.	117.	117.
ALTITUDE	8000 FT.	SEA LEVEL
G.W. ~LBS.	147000	150000
C.G.	30.%	30.%

TRIG 10:46:XX

CALC			REVISED	DATE
CHECK				
APR				
APR				

WINDUP TURN
FL. TEST : 686-12
CONFIG. : -80

THE BOEING COMPANY

-80
D6-15000
FIG. 89
PAGE
IX-126

TD 461 C-R4

130

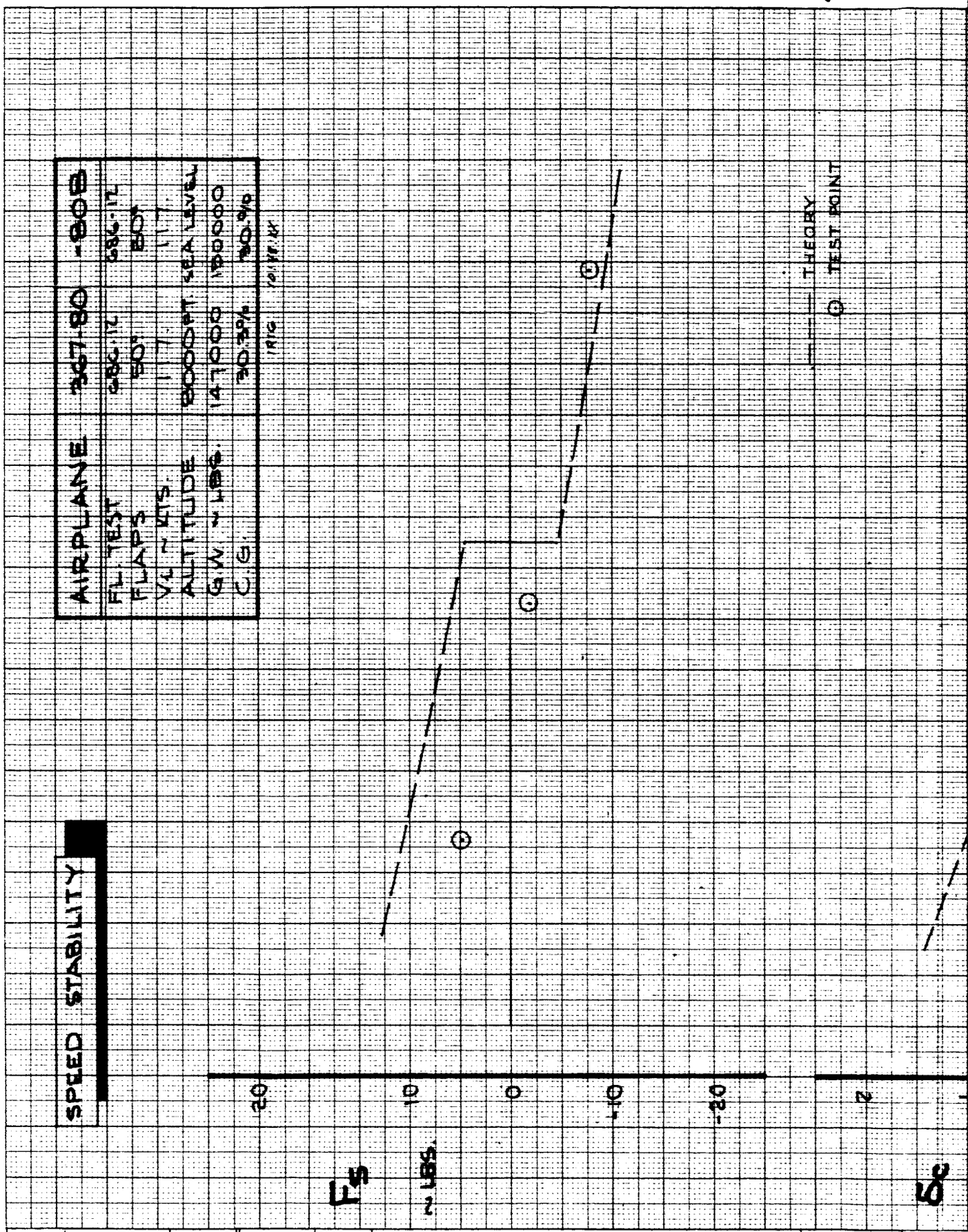

CALC			REVISED	DATE	SPEED STABILITY FL. TEST : 686-12 CONFIG. : -80B
CHECK					
APPD.					
APPD.					
					THE BOEING COMPANY

367-80
D6-15000
FIG. 90
PAGE
IX-127

TD 1053-R5

131

E-12-7-2

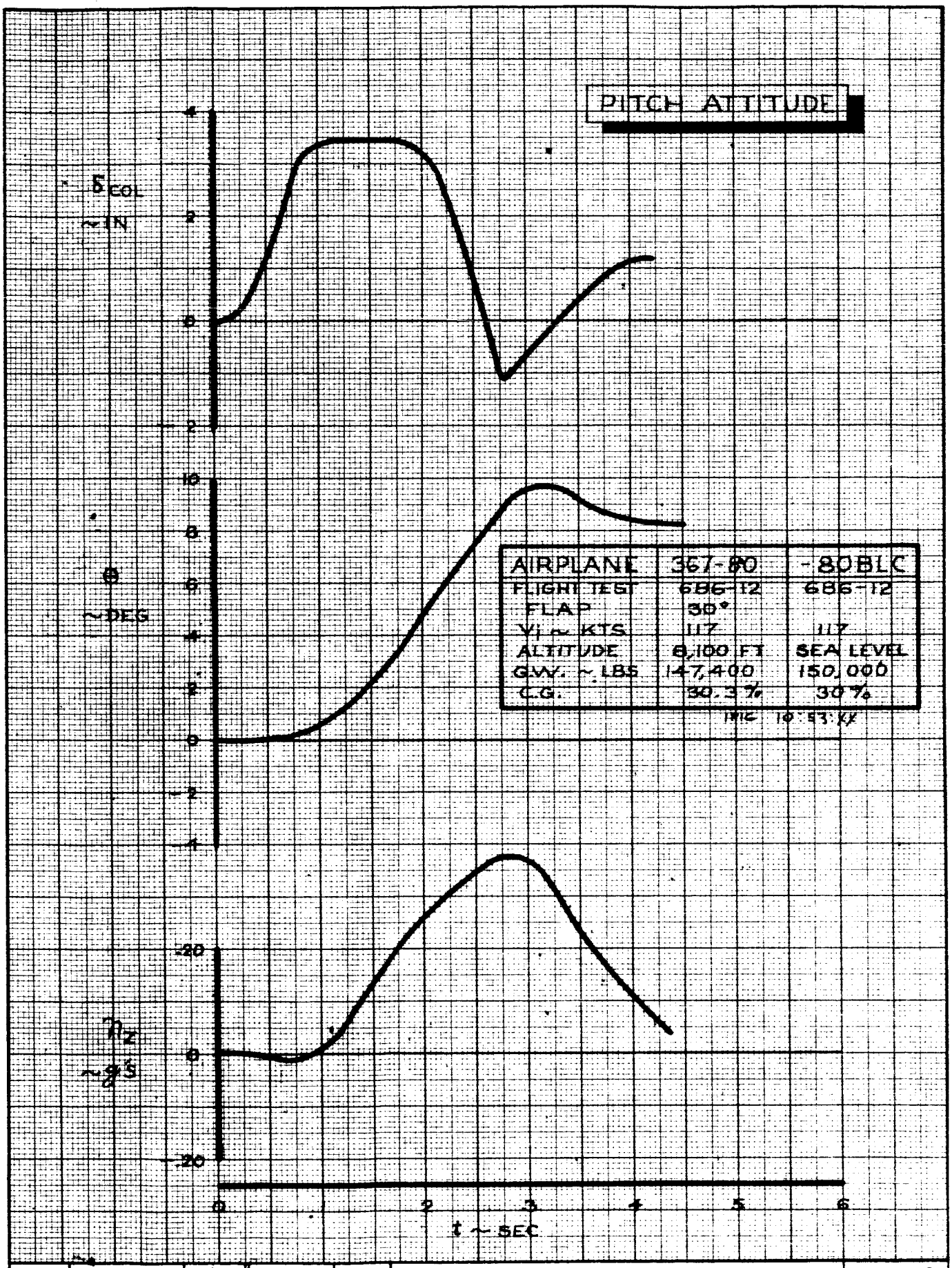

AIRPLANE	367-80	-80BLC
FLIGHT TEST	686-12	686-12
FLAP	30°	
V_i ~ KTS	117	117
ALTITUDE	6,100 FT	SEA LEVEL
G.W. ~ LBS	147,400	150,000
C.G.	30.3%	30%
		I.M.C. 10·53·XX

			REVISED	DATE
CALC				
CHECK				
APR				
APR				

PITCH ATTITUDE
FLIGHT TEST 686-12
CONFIGURATION -80BLC

367-80
D6-15000
FIG. 91

THE BOEING COMPANY

PAGE
IX-128

TD 461 C-R4

132

Lateral

Steady Roll Rate	Fig. 92. The theoretical and flight test data agree for the steady roll rate.
Roll Rate Reversal	Fig. 93. The theoretical roll acceleration matches the flight test data for small wheel deflections but non-linearity in the airplane characteristic causes inaccuracies for wheel deflections greater than about 15°.
Yaw Rate Reversal	Fig. 94. The yaw rate reversal data agrees fairly well with the theoretically calculated line.
Steady Sideslip	Fig. 95. The steady sideslip characteristics of the 367-80 BLC configuration agree with theory.
Spiral Stability	Fig. 96. The theoretical time to half amplitude in the spiral mode is 124 seconds. The flight test time to half amplitude is 16.3 seconds.
Wheel Step	Fig. 96A. The wheel step took approximately .35 seconds to maximum wheel. The sideslip angle was small in the first second and the roll angle after one second was 3.8°.

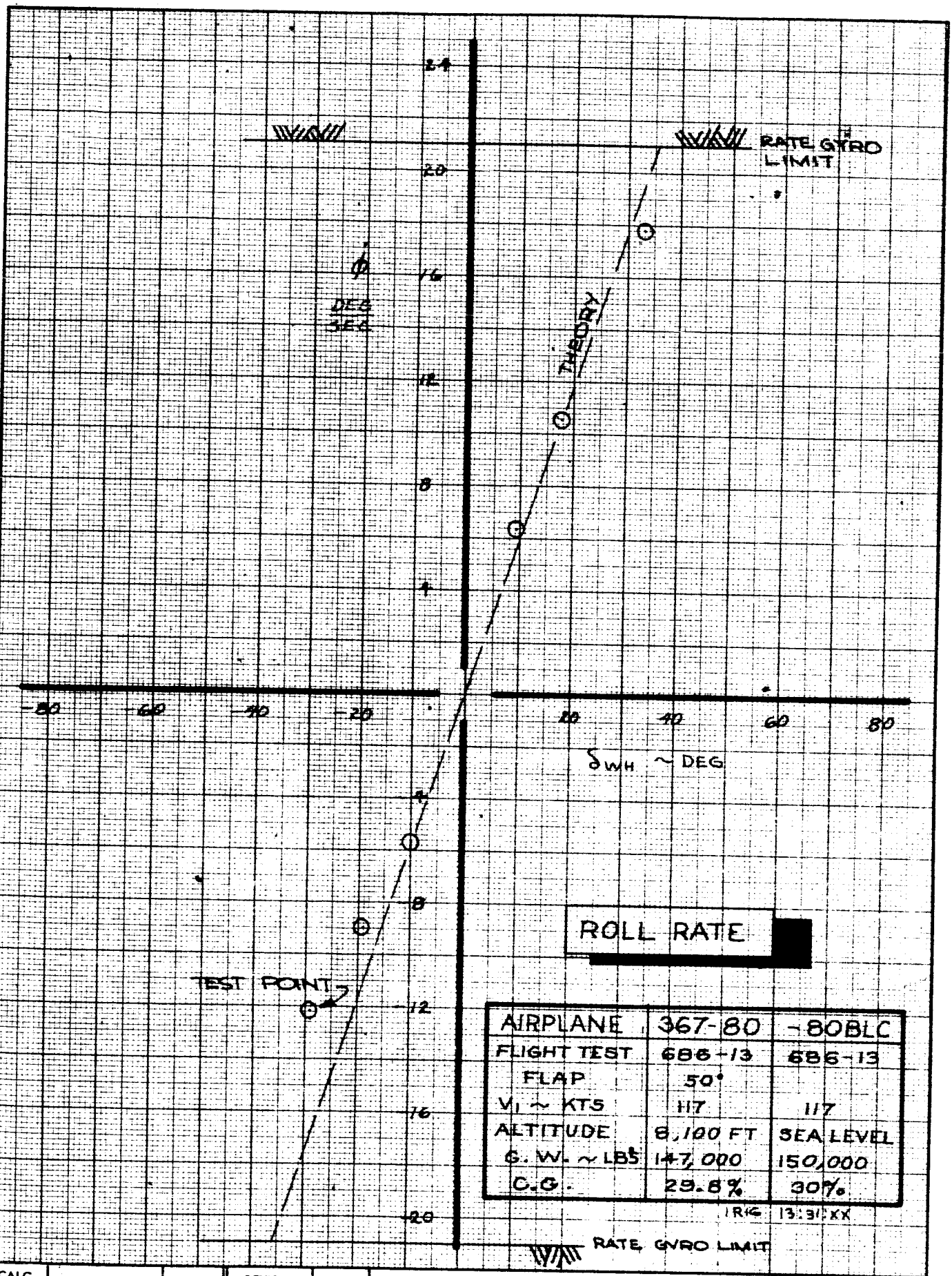

ROLL RATE

AIRPLANE	367-80	-80BLC
FLIGHT TEST	686-13	686-13
FLAP	50°	
V_I ~ KTS	117	117
ALTITUDE	8,100 FT	SEA LEVEL
G. W. ~ LBS	147,000	150,000
C.G.	29.8%	30%

IRIG 13:31:XX

CALC			REVISED	DATE
CHECK				
APR				
APR				

STEADY ROLL RATE
FLIGHT TEST 686-13
CONFIGURATION -80BLC

367-80
D6-15000
FIG. 92

THE BOEING COMPANY

PAGE IX-130

TD 461 C-R4

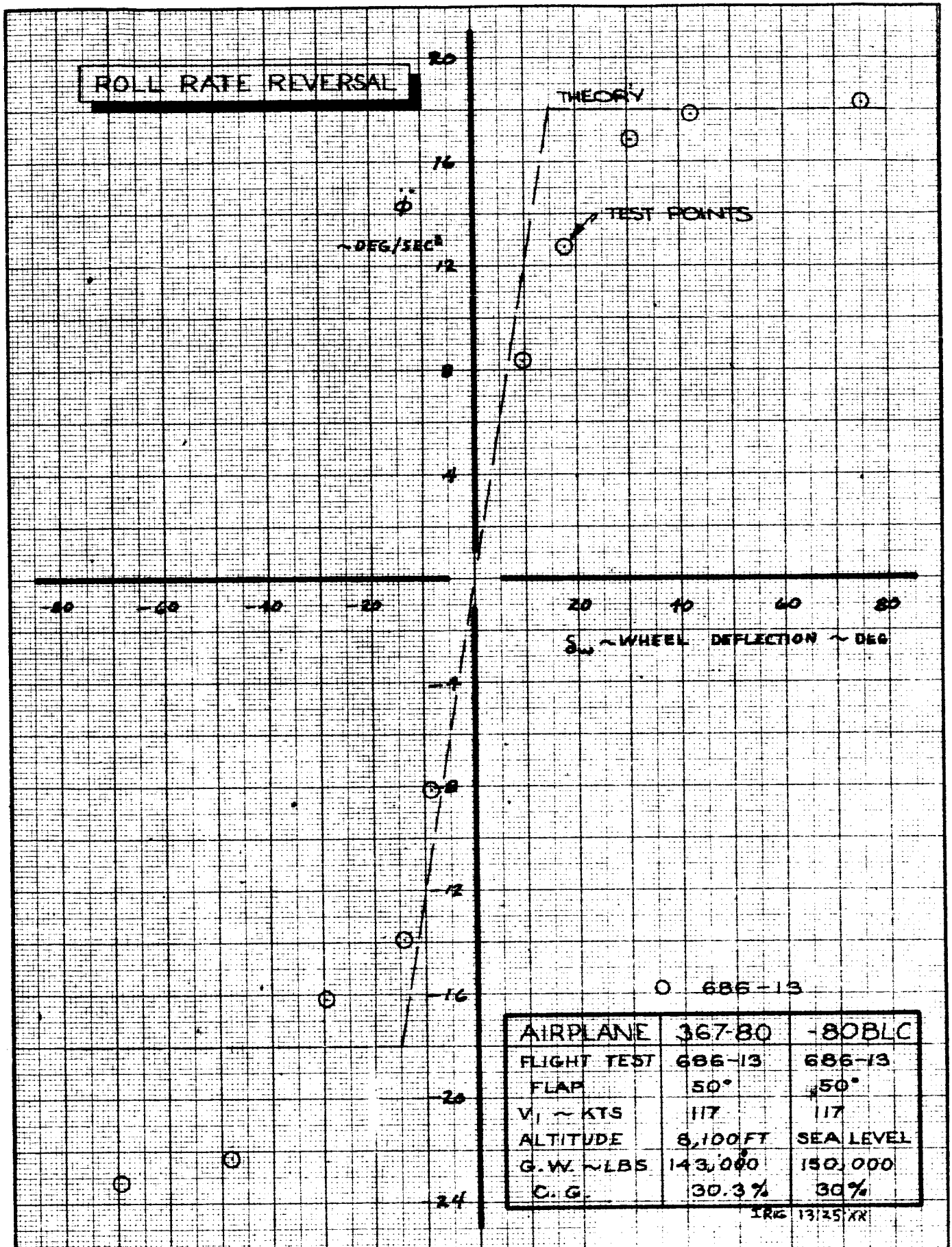

AIRPLANE	367-80	-80BLC
FLIGHT TEST	686-13	686-13
FLAP	50°	50°
V_I ~ KTS	117	117
ALTITUDE	8,100 FT	SEA LEVEL
G.W. ~ LBS	143,000	150,000
C.G.	30.3%	30%

IRG 13125 XX

CALC			REVISED	DATE
CHECK				
APR				
APR				

ROLL RATE REVERSAL
FLIGHT TEST 686-13
CONFIGURATION -80 BLC

367-80
D6-15000
FIG. 93

THE BOEING COMPANY

PAGE IX-131

TD 461 C-R4

YAW RATE REVERSAL

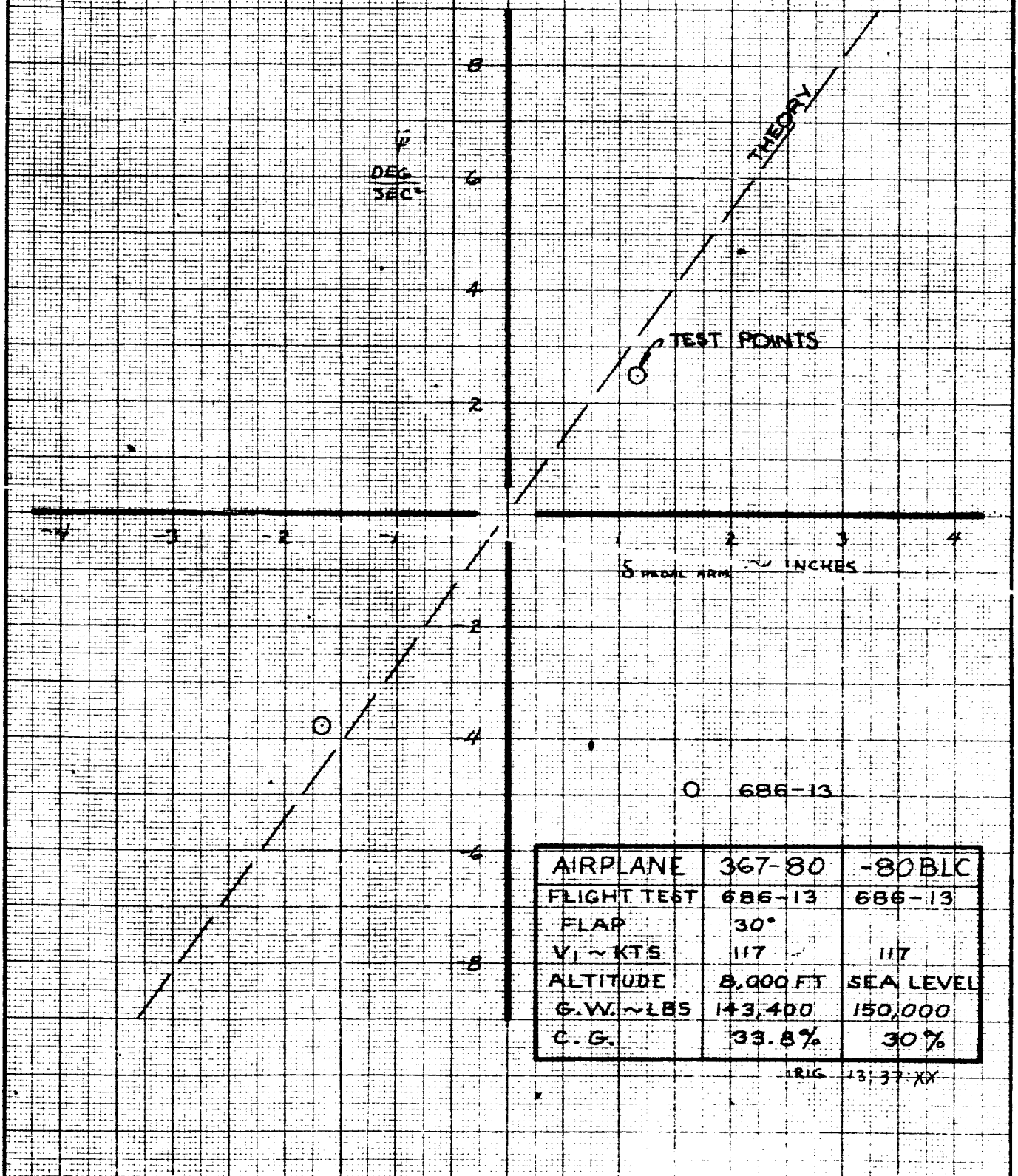

AIRPLANE	367-80	-80 BLC
FLIGHT TEST	686-13	686-13
FLAP	30°	
V_i ~ KTS	117	117
ALTITUDE	8,000 FT	SEA LEVEL
G.W. ~ LBS	143,400	150,000
C.G.	33.8%	30%

RIG 13:37:XX

CALC			REVISED	DATE	YAW RATE REVERSAL FLIGHT TEST 686-13 CONFIGURATION -80 BLC
CHECK					
APR					
APR					THE BOEING COMPANY

367-80
D6-15000
FIG. 94
PAGE IX-132

TD 461 C-R4

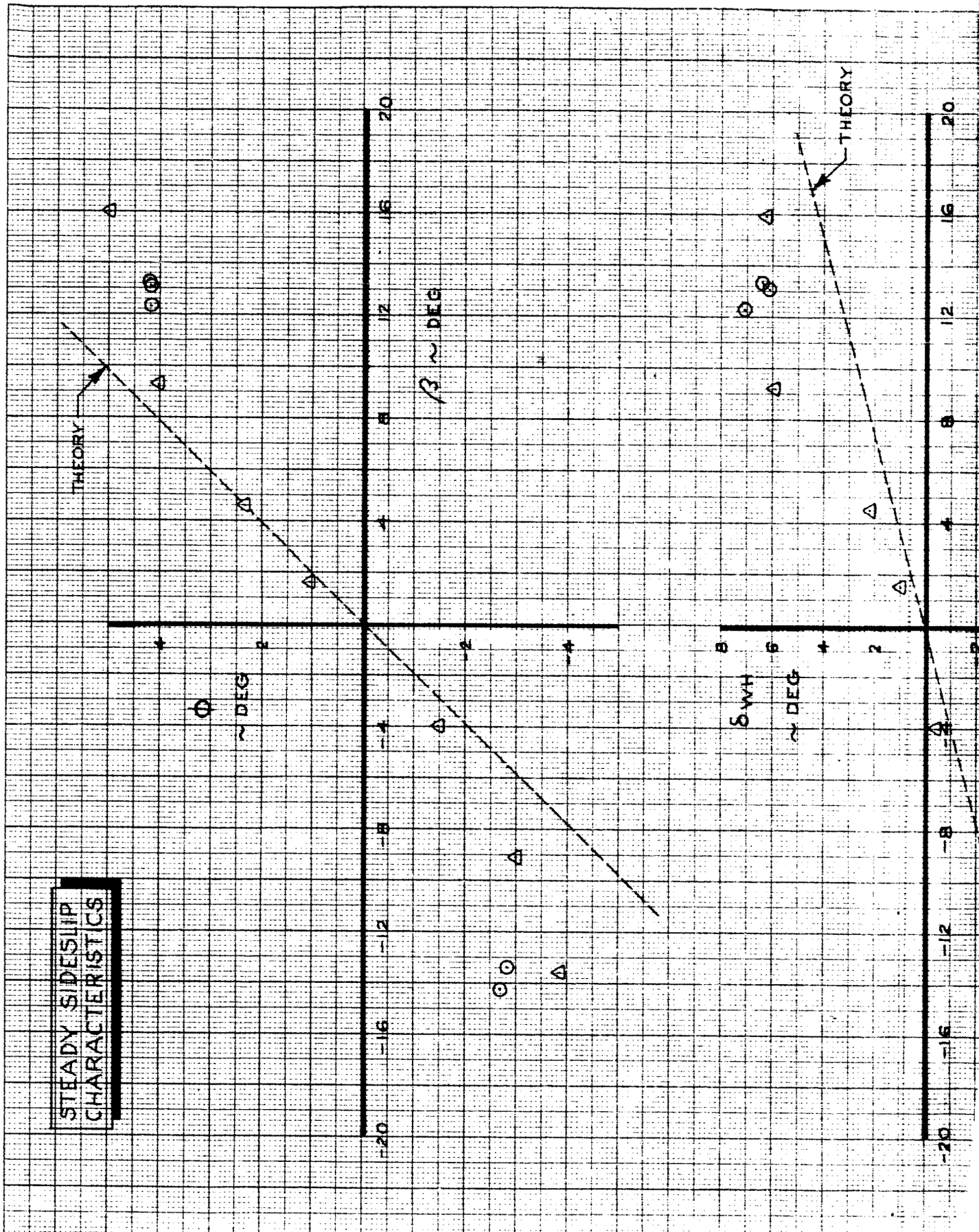

CALC			REVISED	DATE	STEADY SIDESLIP CHARACTERISTICS FLIGHT TEST 686-12 CONFIGURATION -80 BLC
CHECK					
APPD.					
APPD.					
					THE BOEING COMPANY

367-80
D6-15000
FIG. 95
PAGE IX-133

TD 1053-R5

AIRPLANE BASIC 367-80 367-80 -80 BLC
FLIGHT TEST 659-E 686-12 686-12
FLAP 50° 30°
ALTITUDE 3,300 FT 8,100 FT SEA LEVEL
G.W. ~ LBS 161200 143,400 150,000
C.G. 31.5% 30.3% 30
IRIG 17:30:XX 11:06:XX
β ~ DEG
δp ~ IN
THEORY

IX-1332

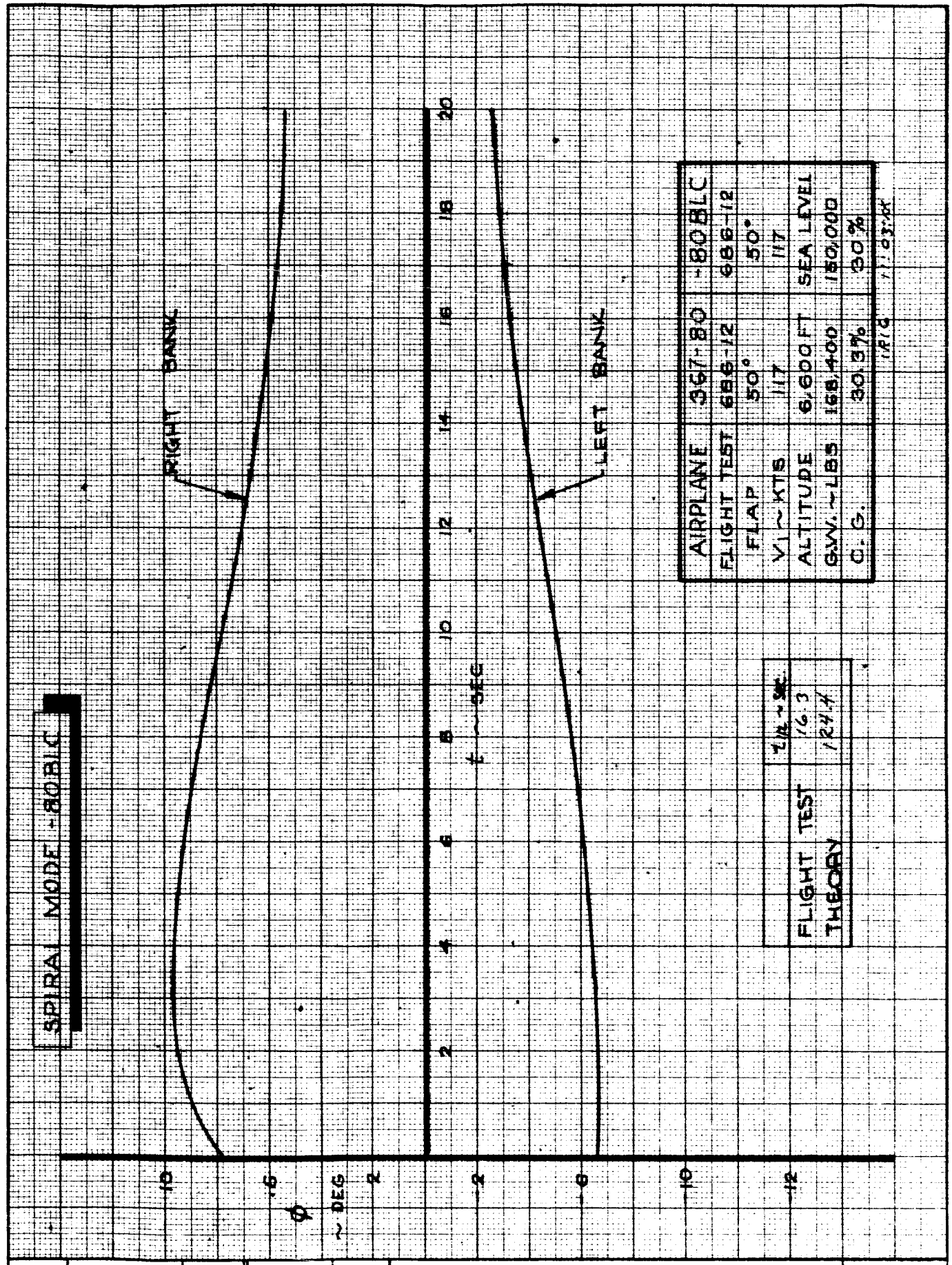

CALC			REVISED	DATE	SPIRAL MODE FLIGHT TEST 686-12 CONFIGURATION -80BLC
CHECK					
APR					
APR					THE BOEING COMPANY

367-80
D6-15000
FIG. 96
PAGE IX-134

TD 441 C-R4

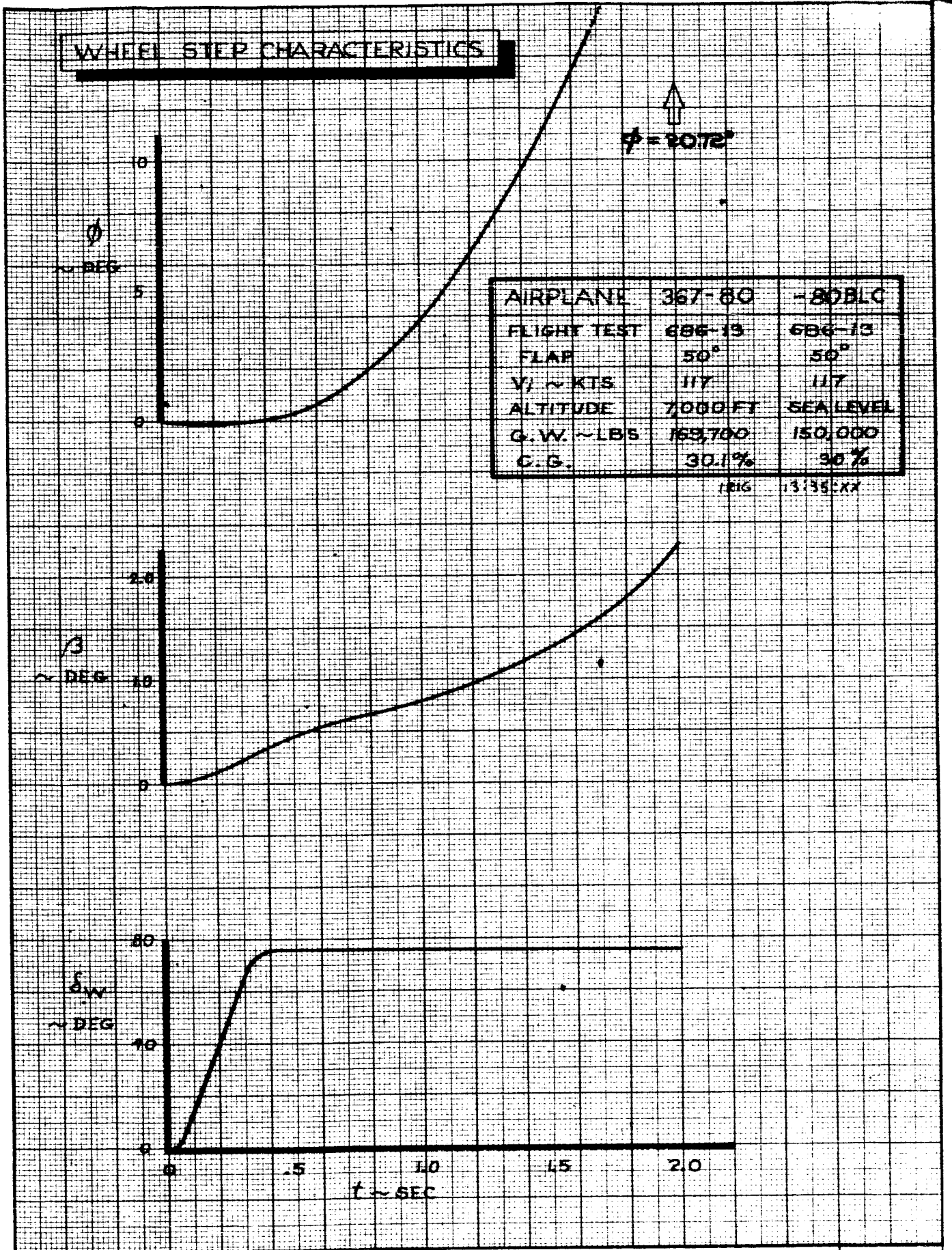

CALC			REVISED	DATE	WHEEL STEP CHARACTERISTICS FLIGHT TEST 686-13 CONFIGURATION -80 BLC
CHECK					
APR					
APR					THE BOEING COMPANY

367-80
D6-15000
FIG. 96A
PAGE
IX-135

TD 461 C-R4

139

X. INFLIGHT - GROUND-BASED SIMULATOR COMPARISON

Dynamic characteristics of similar configurations evaluated on the ground based and inflight simulators are presented herein. Figs. 97 and 98 present wheel step and wheel pulse response characteristics comparing configurations G1202A (ground based) and 1209 (inflight). These are similar configurations but the numbers are different because of changes in the in-flight simulator parameters after program initiation. Response differences are due to the different initial response characteristics of the in-flight simulation caused by control surface nonlinearities and aerodynamic lags and a somewhat differently shaped roll control input. The pilot was requested to input a step wheel. The control input shown was the result. Response of these configurations to a rudder pulse is shown in Fig. 99.

Longitudinal response characteristics are presented in Fig. 100 for an elevator pulse and Fig. 101 for a column step comparing similar configurations. Fig. 101 compares the dynamic characteristics of configurations G151C and 151B. These configurations have similar stability, elevator lift and control power and slightly different lift curve slope and lift due to pitch rate ($C_{L_{\dot{\theta}}}$). They have similar dynamic characteristics. The configuration numbers are different because of changes in the in-flight simulator parameters after program initiation. The responses to a column step of three configurations (101A, 151B, and 151C) evaluated on the inflight simulation are shown in Fig. 102. This figure presents the effect of elevator lift on longitudinal response. Fig. 103 presents the longitudinal response of three configurations (G101A, G151B, G151C), evaluated on the ground based simulator showing the effect of elevator lift.

Figs. 104, 105, and 106 compare configurations 101A, 151B, and 151C with G101A, G151B, and G151C as evaluated on the inflight and ground based simulators. Response differences are due to changes in the characteristics as listed in Table 1 and Table 3. Most of the increment in response shown on these curves is due to the difference in elevator lift between the two simulators for a given configuration number.

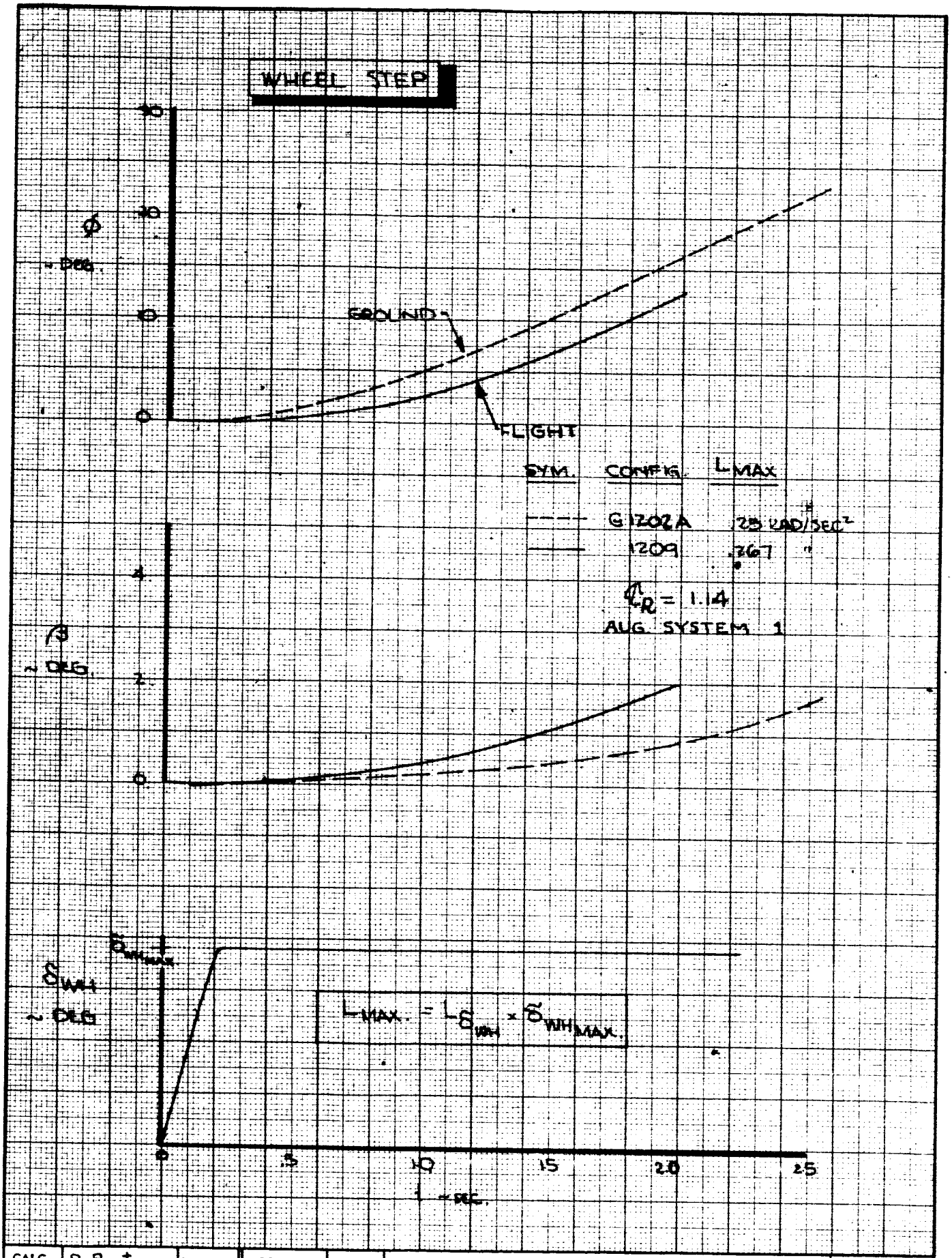

CALC	R. Root	2-1-66	REVISED	DATE	WHEEL STEP GROUND - FLIGHT COMPARISON CONFIG.: G1202A & 1209
CHECK					
APR					
APR					
					THE BOEING COMPANY

D6-15000
FIG. 97
PAGE X-138

TD 461 C-R4

142

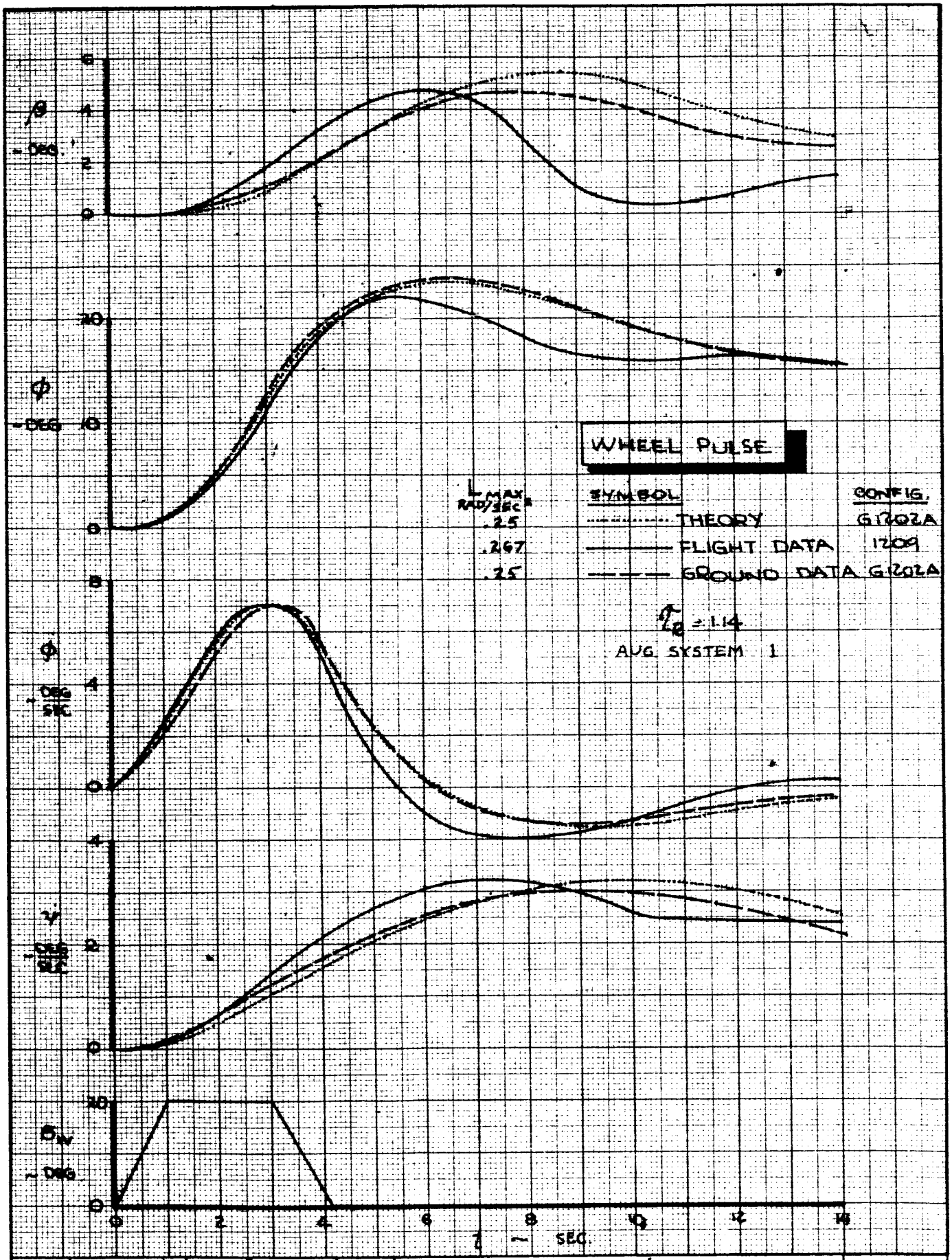

CALC	R. Root	2-1-66	REVISED	DATE
CHECK				
APR				
APR				

CONFIG. G1202A & 1209
WHEEL PULSE
DATA COMPARISON

D6-15000
FIG. 98

THE BOEING COMPANY

PAGE X-139

TD 461 C-R4

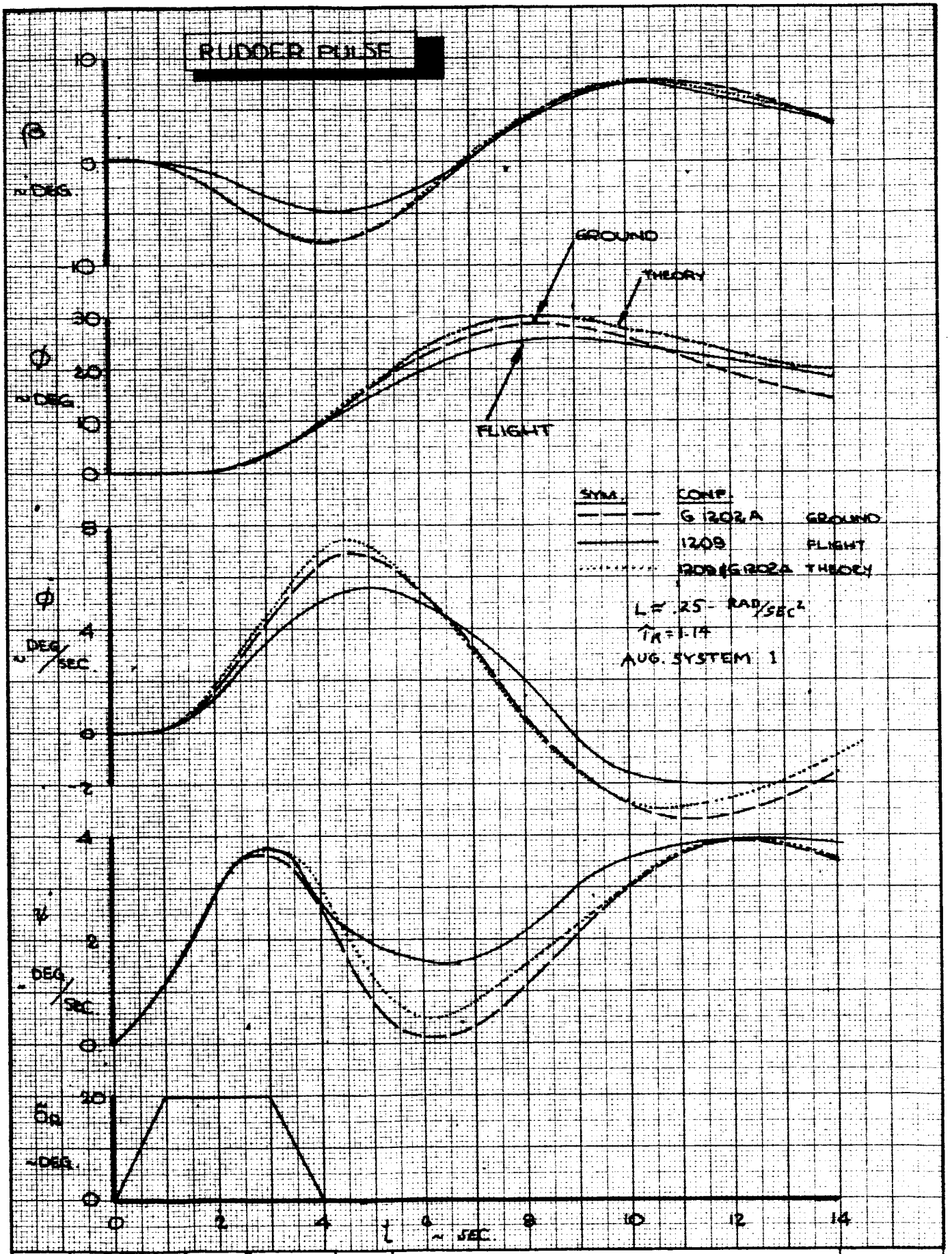

CALC	R. Root	2-1-66	REVISED	DATE	RUDDER PULSE GROUND ~ FLIGHT COMPARISON CONFIG. : G1202A & 1209	D6-15000
CHECK						FIG. 99
APR						
APR					THE BOEING COMPANY	PAGE X-140

TD 461 C-R4

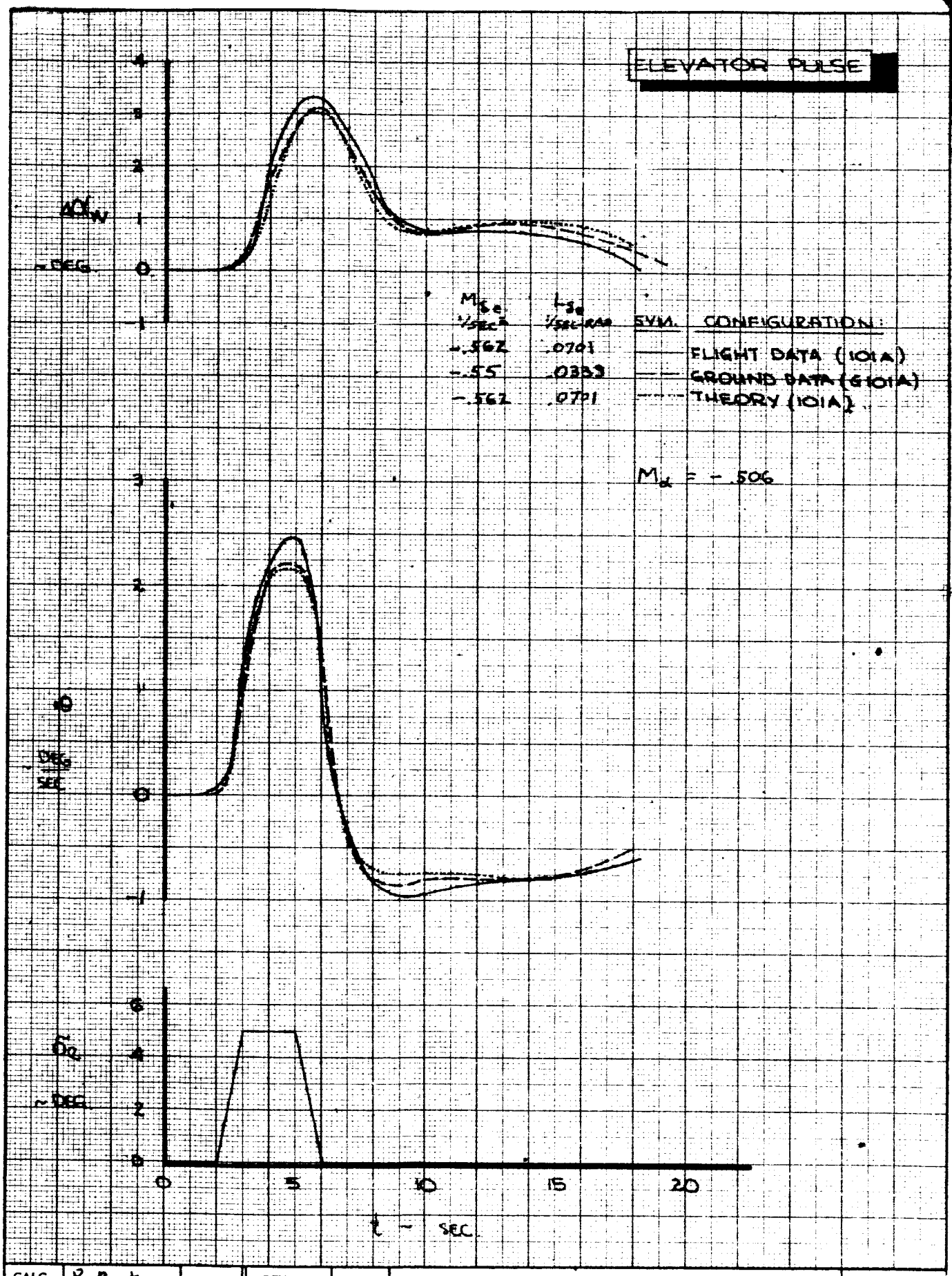

CALC	R. Root	2-2-66	REVISED	DATE	ELEVATOR PULSE GROUND-FLIGHT DATA COMPARISON CONFIG. G101A & 101A
CHECK					
APR					
APR					

D6-15000
FIG. 100
THE BOEING COMPANY
PAGE X-141

TD 461 C-R4

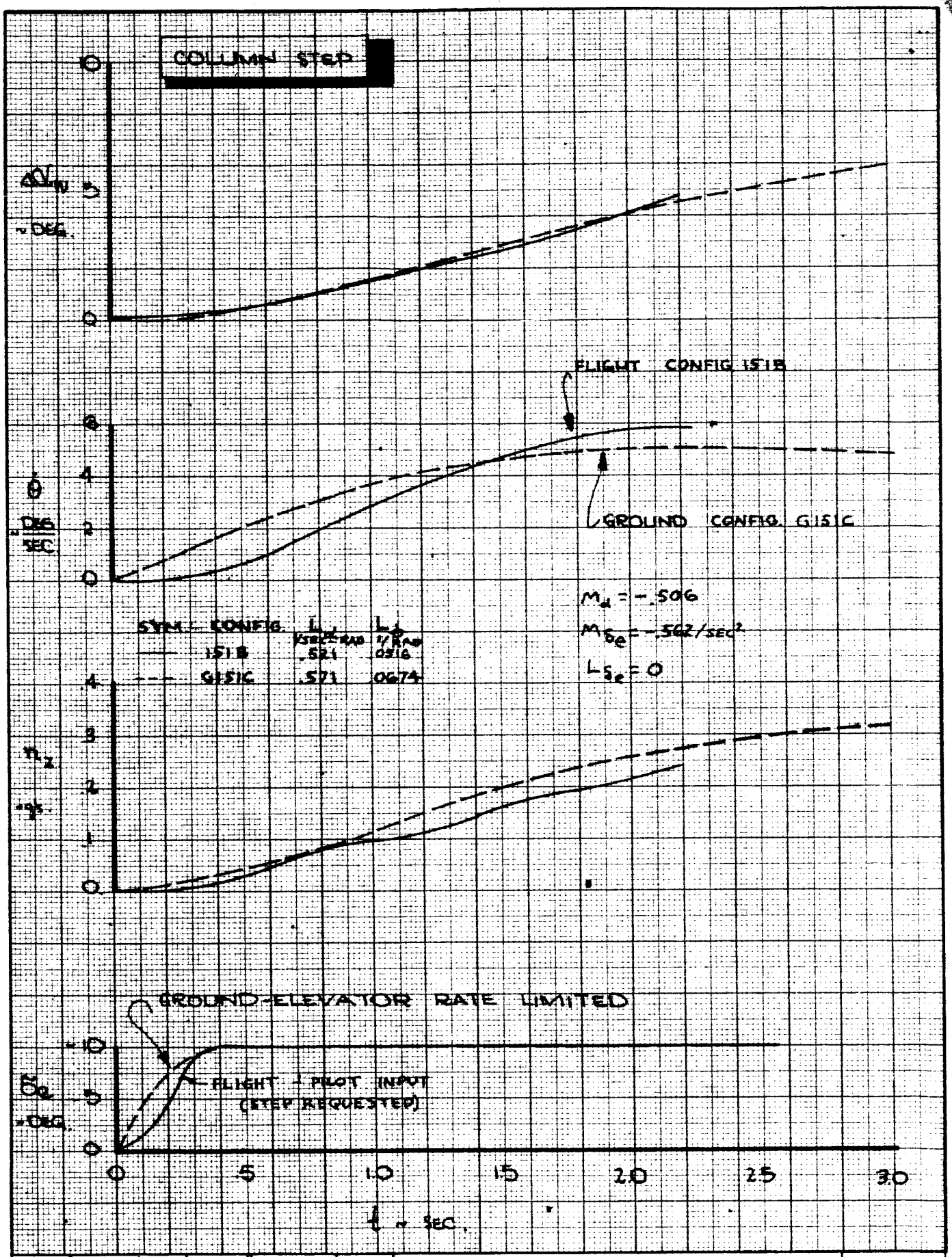

CALC	R. Root	2-2-66	REVISED	DATE	COLUMN STEP GROUND - FLIGHT COMPARISON CONFIG.: G151C & 151B	D6-15000 FIG. 101
CHECK						
APR						
APR					THE BOEING COMPANY	PAGE X-142

TD 461 C-R4

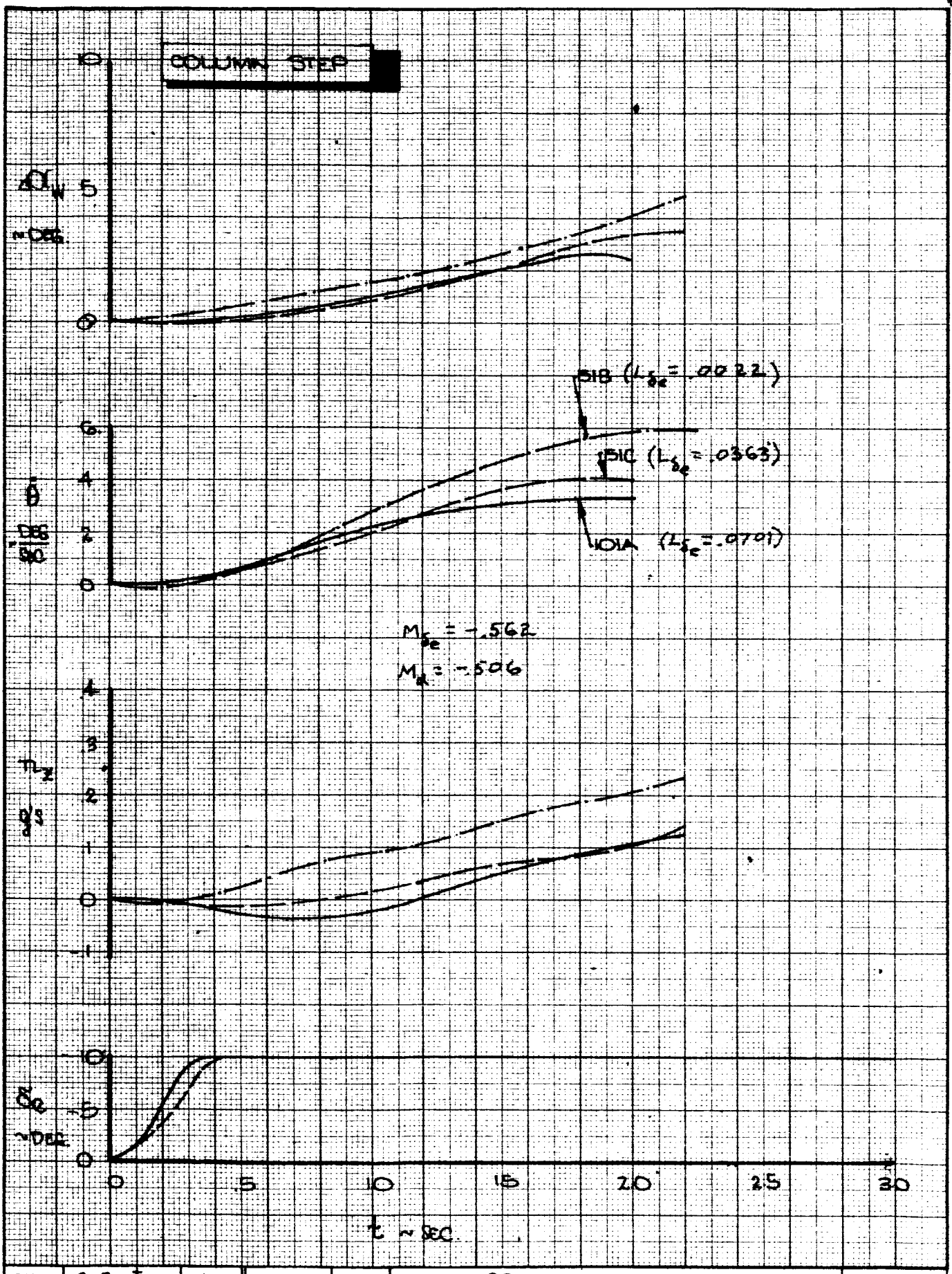

CALC	R. Root	2-9-66	REVISED	DATE	COLUMN STEP FLIGHT DATA COMPARISON CONFIG. 151C, 151B & 101A	D6-15000
CHECK						FIG. 102
APR					THE BOEING COMPANY	PAGE X-143
APR						

TD 461 C-R4

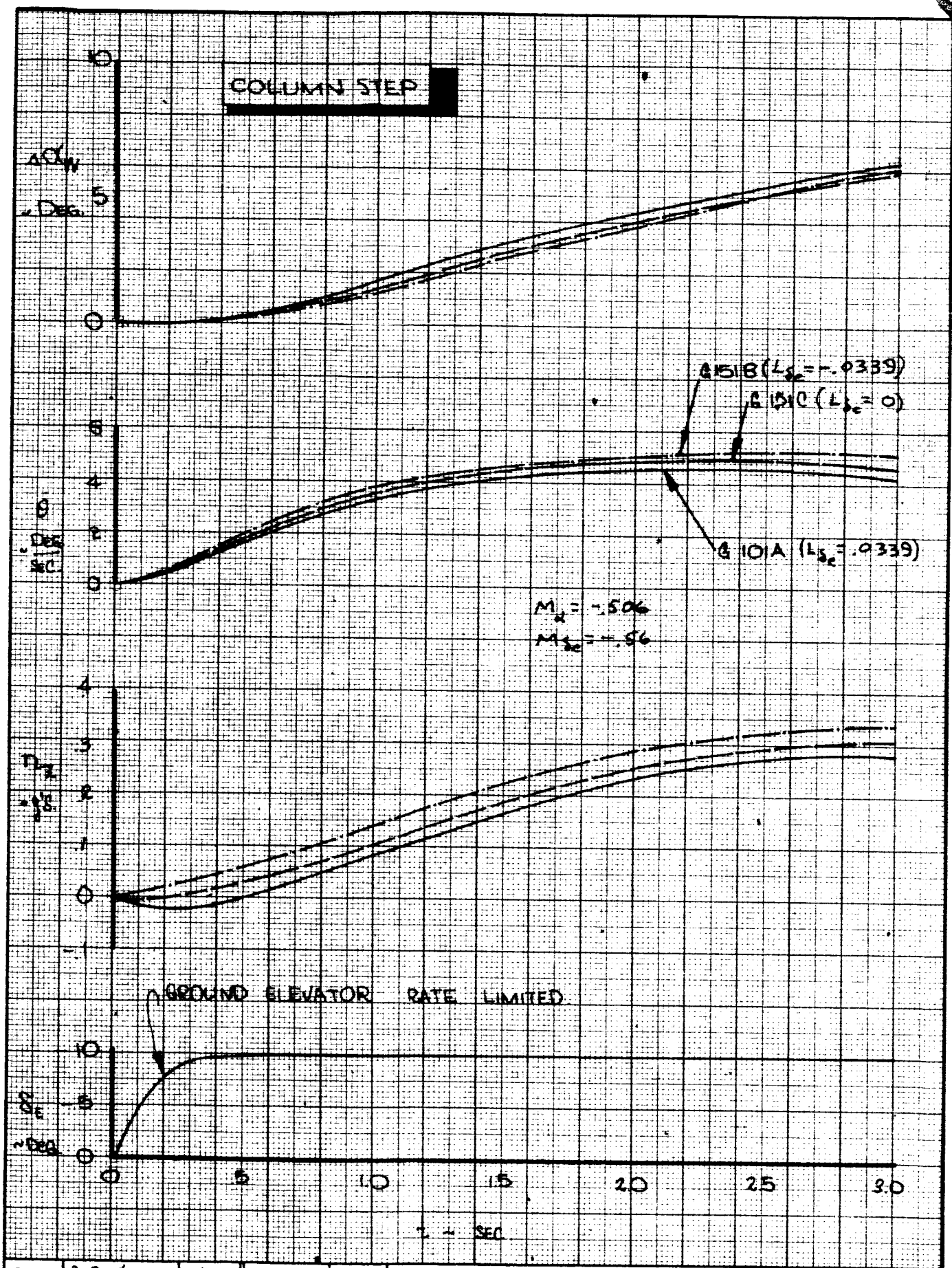

CALC	R. Root	2-4-66	REVISED	DATE	COLUMN STEP GROUND DATA COMPARISON CONFIG. G101A, G151B & G151C
CHECK					
APR					
APR					
					THE BOEING COMPANY

D6-15000
FIG. 103
PAGE X-144

TD 461 C-R4

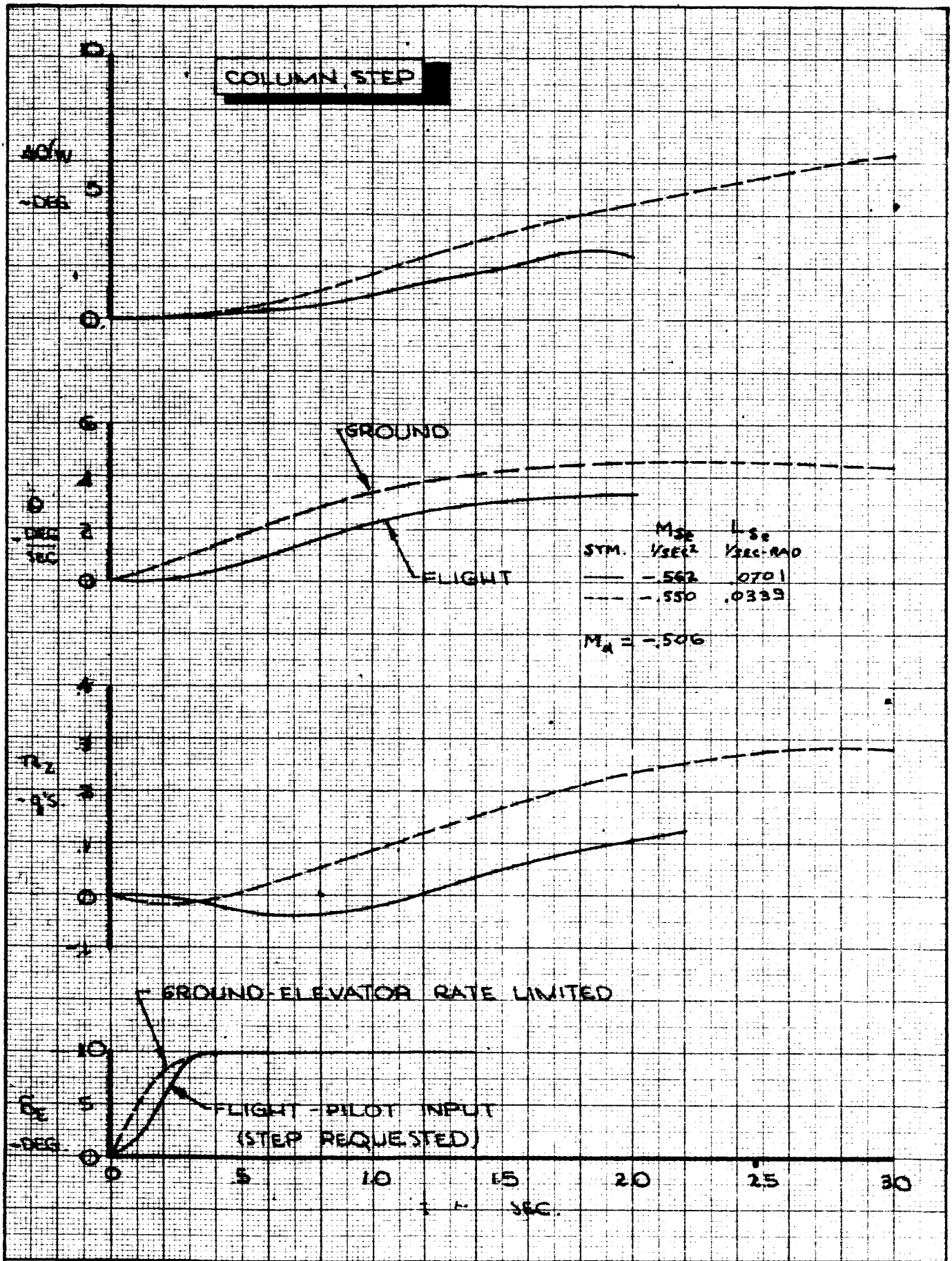

CALC	R. Root	2-2-66	REVISED	DATE	COLUMN STEP GROUND - FLIGHT COMPARISON CONFIG. G101A & 101A	D6-15000
CHECK						FIG. 104
APR						
APR					THE BOEING COMPANY	PAGE X-145

TD 461 C-R4

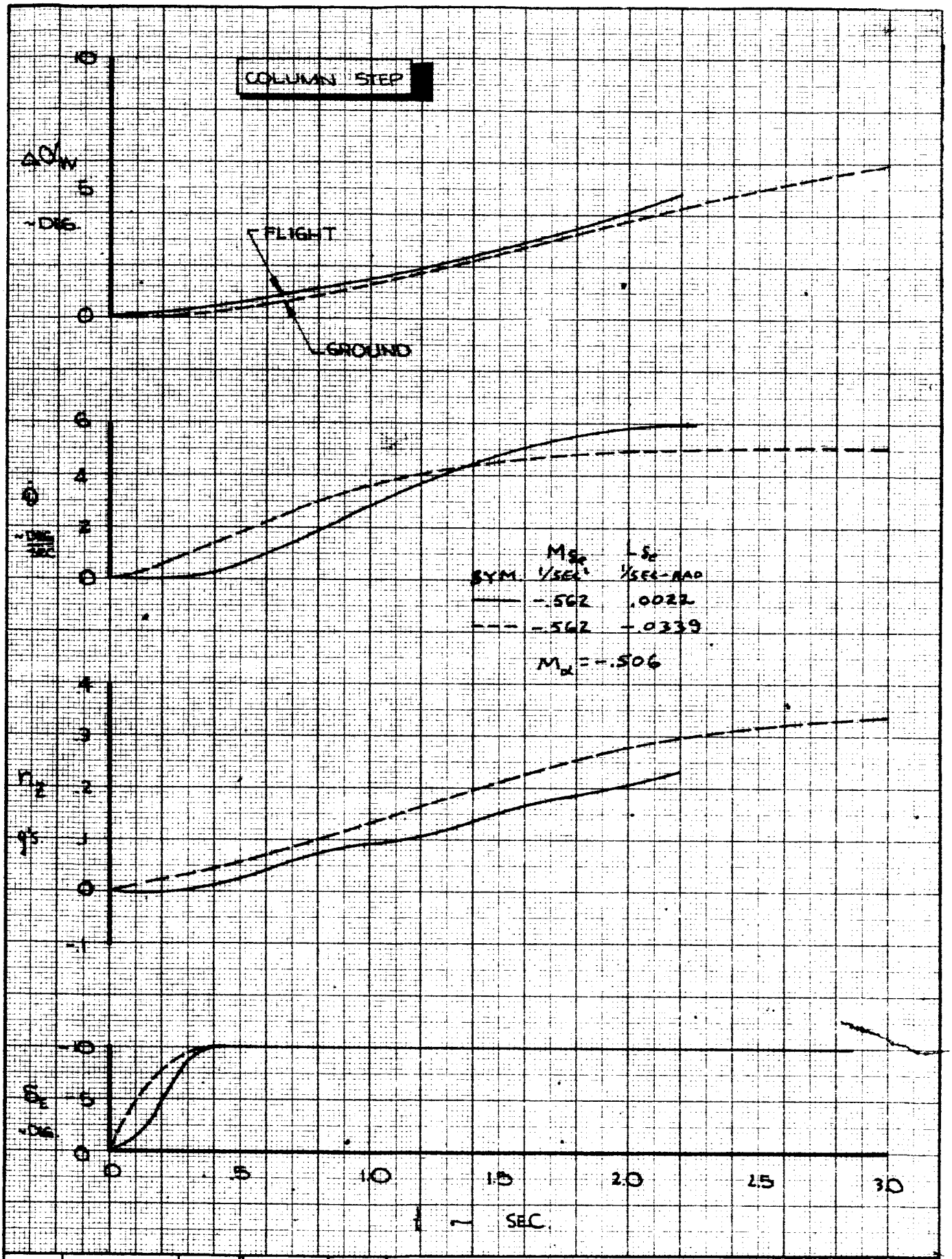

CALC	R. Root	2-2-66	REVISED	DATE	COLUMN STEP GROUND - FLIGHT COMPARISON CONFIG. G151B & 151B
CHECK					
APR					
APR					

D6-15000

FIG. 105

THE BOEING COMPANY

PAGE X-146

TD 461 C-R4

951

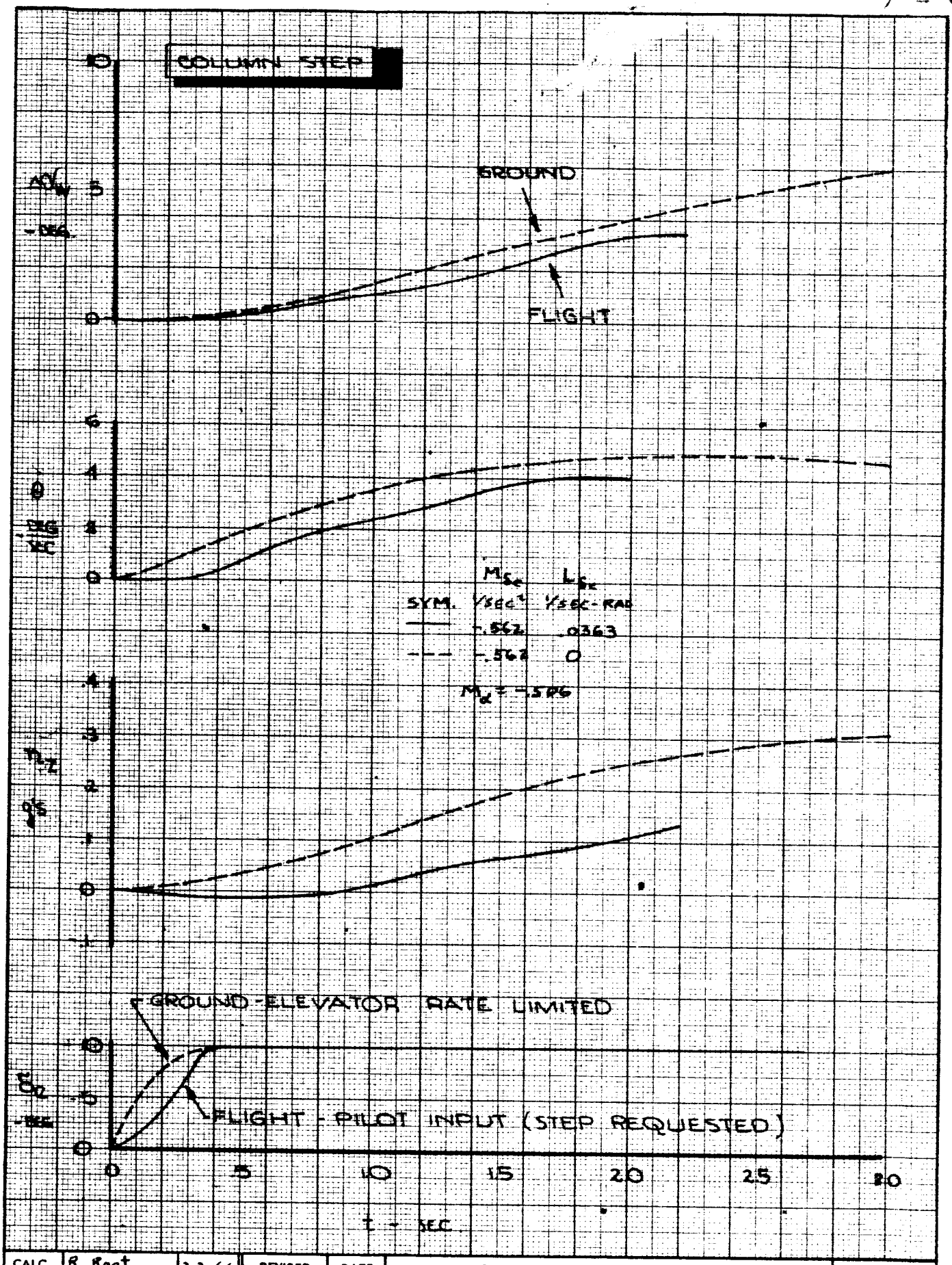

CALC	R. Root	2-2-66	REVISED	DATE	COLUMN STEP GROUND - FLIGHT COMPARISON CONFIG. : G15IC & 15IC.	D6-15000
CHECK						FIG. 106
APR					THE BOEING COMPANY	PAGE X-147
APR						

TD 461 C-R4

151

APPENDIX 1

DESCRIPTION OF THE AMES LARGE TRANSPORT CONFIGURATIONS

A. Airborne Simulator

A description of the basic Ames large transport configuration is given in Table A1-1 and variations from the basic are shown in Table A1-2.

TABLE A1-1

Basic 101A Longitudinal Characteristics

Flight Condition

V_e	117 Kts
Gross Weight	500,000 lbs.
C. G. Location	25% MAC

Airplane Constants

Wing Area	5500 sq. ft.
Wing Span	215 ft.
MAC	28.75 ft.

Lift Derivatives

$C_{L_{Trim}}$	1.94
$\alpha_{Trim_{wcp}}$	4.7°
C_{L_α}	6.2 /rad
$C_{L_{\dot{\alpha}}}$	-.537 /rad/sec
$C_{L_{\dot{\theta}}}$	.613 /rad/sec
$C_{L_{\delta e}}$	.835 /rad

Drag Derivatives

$C_{D_{Trim}}$	.45
C_{D_α}	1.07 /rad

TABLE A1-1 (CONT.)

Pitching Moment Derivatives

C_{m_α}	-2.07 /rad	
$C_{m_{\dot{\alpha}}}$	-.555 /rad/sec	
$C_{m_{\dot{\theta}}}$	-2.387/rad/sec	
$C_{m_{\delta_E}}$	-2.30 /rad	
I_y	30.0 x10^6	slug- FT^2

Longitudinal Dynamic Characteristics

Short Period

Damped Natural Frequency	.645	rad/sec
Undamped Natural Freuqnency	.907	rad/sec
Damping Ratio	.703	

Phugoid

Damped Natural Frequency	.170	rad/sec
Undamped Natural Frequency	.172	rad/sec
Damping Ratio	.149	

TABLE A1-1 (CONT.)

Basic 1209 Lateral - Directional Characteristics

Side Force Derivatives

C_{y_β}	-.9773	/rad
$C_{y_{\dot\phi}}$	.06	/rad/sec
$C_{y_{\dot\psi}}$	.1105	/rad/sec
$C_{y_{\dot\beta}}$	-.074	/rad/sec
$C_{y_{\delta_R}}$	.2464	/rad
$C_{y_{\delta_W}}$	-.0366	/rad

Rolling Moment Derivatives

C_{l_β}	-.1955	/rad
$C_{l_{\dot\phi}}$	-.2442	/rad/sec
$C_{l_{\dot\psi}}$	.1955	/rad/sec
$C_{l_{\delta_R}}$	.00229	/rad
$C_{l_{\dot\beta}}$	-.00069	/rad/sec
$C_{l_{\delta_W}}$	.0975	/rad
I_{X_B}	17.5×10^6	slug-FT^2

TABLE AI-1 (CONT.)

Yawing Moment Derivatives

C_{n_β}	.218	/rad
$C_{n_{\dot{\phi}}}$	.0905	/rad/sec
$C_{n_{\dot{\psi}}}$	-.2883	/rad/sec
$C_{n_{\dot{\beta}}}$	.036	/rad/sec
$C_{n_{\delta_R}}$	-.12	/rad
$C_{n_{\delta_W}}$	-.0001	/rad
I_{Z_B}	45.0 x10^6	slug-FT^2
$I_{X_{Z_B}}$	.95 x10^6	slug-FT^2

Spiral Divergence

Time Constant	26.5	sec
Time to Half Amplitude	18.3	sec

Roll Covergence

Time Constant	1.14	sec

Dutch Roll

Damped Natural Frequency	.479	rad/sec
Undamped Natural Frequency	.508	rad/sec
Damping Ratio	.329	
$\frac{\lvert\phi\rvert}{\lvert\beta\rvert}$	1.33	

151

CONFIG.	$C_{m\delta e}$ 1/RAD	$C_{L\delta e}$ 1/RAD	$\delta e/\delta c$	$C_{m\alpha}$ 1/RAD	$C_{L\alpha}$ 1/RAD	$C_{m\dot{\theta}}$ 1/RAD/SEC	$C_{L\dot{\theta}}$ 1/RAD/SEC	$C_{l\delta w}$ 1/RAD	$C_{l\dot{\phi}}$ 1/RAD/SEC	$\delta w_{EFF.}$ DEG	
101A	-2.30	.835	-1.5	-2.07	6.2	-2.4	.613				
100	-1.56	.705	-1.5	-2.07	6.2	-2.4	.613				
105A	-2.30	.835	-3.0	-2.07	6.2	-2.4	.613				
105 *	-1.56	.705	-4.5	-2.07	6.2	-2.4	.613				
151B	-2.30	.026	-1.5	-2.07	6.2	-2.4	.613				
151C	-2.30	.435	-1.5	-2.07	6.2	-2.4	.613				
151D	-2.30	.026	-3.0	-2.07	6.2	-2.4	.613				
158A	-2.30	.844	-3.0	-4.14	6.57	-4.8	1.17				
159A	-2.30	.844	-1.5	-2.07	6.2	-4.8	1.17				
159B	-2.30	.844	-3.0	-2.07	6.2	-4.8	1.17				
161B	-2.30	.844	-3.0	-.52	5.91	-2.4	.613				
-80 BLC	-.917	.297	-2.2	-1.917	5.46	-.5131	0	.180	-.3064		
1209								.0975	-.2442	50	
1203A								.1460	-.2442	30	
1207A								.0914	-.2442	30	
1235								.1630	-.5100	30	
1237								.0914	-.2442	50	

ENGR. | CHECK | APR | APR

REVISED | DATE

AIRBORNE SIMULATION AERODYNAMIC CHARACTERISTICS

THE BOEING COMPANY
RENTON, WASHINGTON

TABLE A1-2

D6-15000

A1-6

AD 1017-R6

6-7000

A description of Boeing 367-80 with boundary layer control (used as a large transport configuration) is shown in Table A1-3.

TABLE A1-3

367-80 BLC Longitudinal Characteristics

Flight Condition

V_e	117 Kts
Flap Angle	50°
BPR	4:1
Gross Weight	150,000 lbs.
C. G. Location	30% MAC
Speed Brake Trim Angle	6°

Airplane Constants

Wing Area	2821 sq. ft.
Wing Span	130.8 ft.
MAC	20.1 ft.

Lift Derivatives

$C_{L_{Trim}}$	1.14
$\alpha_{Trim_{wcp}}$	2.3°
C_{L_α}	4.53 /rad
$C_{L_{\delta_E}}$	.297
$\frac{\partial C_L}{\partial v}$	-.001875 /ft/sec

Drag Derivatives

$C_{D_{Trim}}$	.183
C_{D_α}	.63 /rad

TABLE A1-3 (CONT.)

Pitching Moment Derivatives

C_{m_V}	-.0012	/ft/sec
C_{m_α}	-1.197	/rad
$C_{m_{\dot{\alpha}}}$	-.1283	/rad/sec
$C_{m_{\dot{\theta}}}$	-.5131	/rad/sec
$C_{m_{\delta_E}}$	-.8124	/rad
I_y	2.25×10^6	slug- FT^2

Longitudinal Dynamic Characteristics

Short Period

Damped Natural Frequency	1.147	rad/sec
Undamped Natural Frequency	1.30	rad/sec
Damping Ratio	.5245	

Phugoid

Damped Natural Frequency	.1342	rad/sec
Undamped Natural Frequency	.1352	rad/sec
Damping Ratio	.1244	

TABLE A1-3 (CONT.)

367-80 BLC Lateral - Directional Characteristics

Side Force Derivatives

C_{y_β}	-.773	/rad
$C_{y_{\dot\phi}}$	.3376	/rad/sec
$C_{y_{\dot\psi}}$	.1035	/rad/sec
$C_{y_{\dot\beta}}$	-.259	/rad/sec
$C_{y_{\delta_R}}$	.1992	/rad
$C_{y_{\delta_W}}$	-.032	/rad

Rolling Moment Derivatives

C_{l_β}	-.1507	/rad
$C_{l_{\dot\phi}}$	-.1951	/rad/sec
$C_{l_{\dot\psi}}$	.1407	/rad/sec
$C_{l_{\dot\beta}}$	-.0268	/rad/sec
$C_{l_{\delta_R}}$	.0206	/rad
C_W	.180	/rad
I_{x_B}	2.57×10^6	slug-FT^2

Yawing Moment Derivatives

C_{n_β}	.0555	/rad
$C_{n_{\dot\phi}}$	-.0207	/rad/sec
$C_{n_{\dot\psi}}$	-.0677	/rad/sec
$C_{n_{\dot\beta}}$	.0484	/rad/sec
$C_{n_{\delta_R}}$	-.0777	/rad

TABLE A1-3 (CONT.)

Yawing Moment Derivatives (cont'd)

$C_{n_{\delta_W}}$	.0125	/rad
I_{Z_B}	4.73 x10^6	slug-FT^2
I_{XZ_B}	0	slug-FT^2

367-80 BLC Stability Augmentation System

	Gain	Time Constant
$\frac{\delta_R}{\delta_{WH}}$	0	0
$\frac{\delta_R}{\beta}$	0	0
$\frac{\delta_R}{\dot{\beta}}$	-1.3	.27 sec
$\frac{\delta_R}{\phi}$	- .5	1.0 sec
$\frac{\delta_A}{\dot{\psi}}$	- .9	0.1 sec
$\frac{\delta_A}{\beta}$	1.0	0.1 sec
$\frac{\delta_A}{\phi}$	-1.2	0.1 sec

Lateral Dynamic Characteristics

Spiral Divergence

Time Constant	180.0	sec
Time to Half Amplitude	124.4	sec

Roll Convergence

Time Constant	Non-linear	sec

TABLE A1-3 (CONT.)

Dutch Roll

Damped Natural Frequency	.423	**rad/sec**
Undamped Natural Frequency	.513	**rad/sec**
Damping Ratio	.564	
$\frac{\lvert\phi\rvert}{\lvert\beta\rvert}$	.468	

B. Ground Based Simulation

Following is a description of the aerodynamic and physical characteristics of the configurations evaluated on the ground based simulation.

The following information is included:

a. Basic configuration description (Table A1-4)

b. Longitudinal changes (Table A1-5)

c. Lateral Directional changes (Table A1-6)

d. Lateral Directional Stability Augmentation System (Table A1-7)

e. Equivalent coefficients (aerodynamic coefficients equivalent to the basic configuration with augmentation) (Table A1-8).

CONFIGURATION DESCRIPTION
AMES LARGE TRANSPORT
GROUND BASED SIMULATION

BASIC AERODYNAMIC COEFF'S

DRAG:	$C_{D_{TRIM}}$	= .45
	C_{D_α}	= 1.07 1/RAD
LIFT:	$C_{L_{TRIM}}$	= 1.94
	$C_{L_{\dot\theta}}$	= .8043 SEC/RAD
	$C_{L_{\dot\alpha}}$	= -.3959 SEC/RAD
	C_{L_α} & $C_{L_{\delta_e}}$	VARIED
PITCH:	$C_{m_{\dot\alpha}}$	= -.555 SEC/RAD
	$C_{m_{i_H}}$	= -.0545 1/RAD
	C_{m_α}, $C_{m_{\delta_e}}$ & $C_{m_{\dot\theta}}$	VARIED
ROLL: (UNAUG.)	C_{l_β}	= -.395 1/RAD.
	C_{l_p}	= .3045 SEC/RAD
	$C_{l_{\delta_r}}$	= .00229 1/RAD
	C_{l_p} & $C_{l_{\delta_w}}$	VARIED
YAW (UNAUG.)	C_{n_β}	= .179 1/RAD.
	C_{n_p}	= -.1579 SEC/RAD
	C_{n_r}	= -.267 SEC/RAD
	$C_{n_{\delta_a}}$	= .0213 1/RAD
	$C_{n_{\delta_r}}$	= -.120 1/RAD
SIDE FORCE (UNAUG.)	C_{Y_β}	= -.83 1/RAD
	C_{Y_ϕ}	= .572 SEC/RAD
	C_{Y_r}	= .02895 SEC/RAD
	$C_{Y_{\delta_a}}$	= -.0805 1/RAD
	$C_{Y_{\delta_r}}$	= .2464 1/RAD

PHYSICAL CHARACTERISTICS

WEIGHT		= 500000 LBS.
CENTER OF GRAVITY		.25 $\bar{c}$
WING AREA	,S	= 5,500 FT^2
M.A.C.	,$\bar{c}$	= 28.75 FT.
SPAN	,b	= 215.0 FT.
VELOCITY	,V	= 117.0 KTS. = (197.5 FT/SEC)
α_{TRIM}	,α_T	= 2.7 DEG.
(SEA LEVEL)	,q	= 46.4 LB/FT^2

I_{xx} = 17.5 × 10^6 SLUG/FT^2

I_{yy} = 30.0 × 10^6 SLUG/FT^2

I_{zz} = 45.0 × 10^6 SLUG/FT^2

I_{xz} = .95 × 10^6 SLUG/FT^2

ENGR.	R. Root	2-1-66	REVISED	DATE	CONFIGURATION DESCRIPTION	TABLE A1-4
CHECK						D6-15000
APR					THE BOEING COMPANY RENTON, WASHINGTON	A1-14
APR						

AD 1040C-R3

6-7000

CALC	APPR	APPR	CHECK	GROUND BASED CONFIG.	C_{L_α}	C_{m_α}	$C_{m_{\dot\theta}}$	$C_{L_{\delta e}}$	$C_{m_{\delta e}}$	$\delta e/\delta_{COL}$
R. Root				G~	1/RAD	1/RAD	SEC/RAD	1/RAD	1/RAD	DEG/IN
2-2-66				100	6.81	-2.07	-2.39	.409	-1.56	-3.29
				100A					-3.12	
				100X				.818	-1.56	
REVISED				101A				.409	-2.25	
				102					-1.25	
DATE				103					-1.0	
				103A						-6.58
				105					-1.56	
				105A					-2.3	
				105*					-1.56	-9.87
				105*X				.818		
				106		-1.0		.409		-3.29
				107		0				
				108					-1.0	
				109					-2.0	
				109A					-1.56	-6.58
				110		+1.0				-3.29
				111	3.6	-2.07				
				112		-3.00				
				112A		-4.00				
				113		-1.40				
				113A		-1.40	-1.21			
				115		0	-2.39			
				120	6.81	-2.07	-1.00			

GROUND BASED SIMULATION
LONGITUDINAL RUN LOG

THE BOEING COMPANY
RENTON, WASHINGTON

TABLE A1-5
D6-15000

PAGE A1-15

L-91

TD 1040C - R3

6-7000

CALC	APR	APR	CHECK
R. Root			
2-2-66			
REVISED			
DATE			

GROUND BASED SIMULATION
LONGITUDINAL RUN LOG

THE BOEING COMPANY
RENTON, WASHINGTON D6-15000

TABLE A1-5

PAGE A1-16

GROUND BASED CONFIG	C_{L_α}	C_{m_α}	$C_{m_{\dot\theta}}$	$C_{L_{\delta_e}}$	$C_{m_{\delta_e}}$	δ_e/δ_{COL}	
G~	1/RAD	1/RAD	SEC/RAD	1/RAD	1/RAD	DEG/IN	
122A	6.81	-4.00	-2.39	.409	-1.56	-3.29	
123	11.0	-2.07	↓	↓	↓	↓	
123A	↓	↓	↓	↓	↓	-6.58	
123B	↓	↓	↓	↓	-2.30	↓	
124	↓	-.50	↓	↓	-1.56	-3.29	
125	↓	.40	↓	↓	-1.56	↓	
126	↓	-1.00	↓	↓	-1.00	↓	
126A	↓	-1.00	↓	↓	-1.56	-6.58	
127	↓	0	↓	↓	-1.00	-3.29	
128	↓	-1.00	-1.00	↓	↓	↓	
129	↓	0	-1.00	↓	↓	↓	
130	↓	0	-2.39	↓	-1.56	↓	
131	↓	-.50	-1.00	↓	-1.56	↓	
132	↓	-2.07	-1.00	↓	-1.00	↓	
150	6.81	↓	-2.39	↓	-1.56	↓	C_{D_α} = 1.9
151	↓	↓	↓	-.409	-1.56	↓	
151B	↓	↓	↓	↓	-2.30	-2.78	
151C	↓	↓	↓	0.	-2.30	↓	
151C*	↓	↓	↓	↓	-1.56	-3.29	
151D	↓	↓	↓	-.409	-2.30	-6.58	
152	↓	-6.00	-4.80	.409	-1.56	-3.29	
153	↓	-6.00	↓	↓	-3.12	↓	
154	↓	-2.07	↓	↓	-1.56	↓	
155	↓	-2.07	↓	↓	-3.12	↓	

TD 1040C - R3

6-7000

GROUND BASED CONFIG.	C_{L_α}	C_{m_α}	$C_{m_{\dot\theta}}$	$C_{L_{\delta e}}$	$C_{m_{\delta e}}$	δ_e/δ_{COL}
G-	1/RAD	1/RAD	SEC/RAD	1/RAD	1/RAD	DEG/IN
156	6.81	-4.00	-2.39	.409	-3.12	-3.29
157	↓	↓	-4.80	↓	-1.56	↓
157A	↓	↓	-2.39	↓	↓	↓
158	↓	↓	-4.80	↓	↓	-6.58
158A	↓	↓	-4.80	↓	-2.3	↓
158A*	↓	↓	-2.39	↓	-1.56	↓
158X	↓	↓	-2.39	↓	-2.30	↓
159	↓	-2.07	-4.80	↓	-1.56	↓
159A	↓	↓	↓	↓	-2.30	-2.78
159B	↓	↓	↓	↓	-2.30	-6.58
160	↓	-6.00	↓	↓	-1.56	↓
161	↓	-.50	-2.39	↓	-1.56	↓
161B	↓	-.50	↓	↓	-2.30	↓
162	↓	-.20	↓	↓	-1.56	↓
163	11.00	-4.00	↓	↓	↓	↓
163A	11.00	-4.00	↓	↓	↓	-3.29

CALC R. Root 2-2-66 CHECK APR APR

REVISED DATE

GROUND BASED SIMULATION
LONGITUDINAL RUN LOG

THE BOEING COMPANY
RENTON, WASHINGTON D6-15000

TABLE A1-5

691

AD 1040C-R3

6-7000

CALC R. Root	APR	APR	CHECK	GROUND BASED CONFIG	Cl_{δ_w}	$\delta_{w_{EFF}}$	Cl_p	AUG.
				G~	1/RAD	DEG	SEC/RAD	
				1	.073	50	-.239	2
2-2-66				1	↓	↓	↓	3
				1h	↓	↓	↓	2
REVISED				2	.110	↓	↓	↓
				3	.146	↓	↓	↓
DATE				4	.183	↓	↓	↓
				5	.219	↓	↓	↓
				5A	.293	↓	↓	↓
				5B	.365	↓	↓	↓
				5C	.054	↓	↓	↓
				5C	.054	↓	↓	3
				5D	.046	↓	↓	2
				5E	.330	↓	↓	↓
				5F	.037	↓	↓	↓
				5G	.018	↓	↓	3
				5H	.010	90	↓	↓
				5J	.030	30	↓	↓
				6	.091	↓	↓	2
				6	.091	↓	↓	3
				7A	.061	↓	↓	2
				8	.073	75	↓	2
				8A	.037	↓	↓	3
				9	.098	↓	↓	2
				10	.082	90	↓	2

GROUND BASED SIMULATION
LATERAL RUN LOG

THE BOEING COMPANY
RENTON, WASHINGTON D6-15000

TABLE A1-6

PAGE A1-18

AD 1040C-R3

8-7000

CALC	APR	APR	CHECK	R. Root	2-2-66	REVISED	DATE

GROUND BASED SIMULATION
LATERAL RUN LOG

THE BOEING COMPANY
RENTON, WASHINGTON D6-15000

TABLE A1-6

PAGE A1-19

GROUND BASED CONFIG	$C_{l_{\delta_W}}$	$\delta_{W_{EFF}}$	C_{l_p}	AUG.
G~	'/RAD	DEG	SEC/RAD	
11	.061	90	-.239	2
12	.040			
13	.026			
14	.030			3
16	.055	50		2
16	.055			3
17	.091			2
18	.128			2
19	.055			2
19	.055			3
20	.091			2
21	.128			
22	.109		-.153	
23	.073			
23A	.055			
24	.109		-.306	
25	.055			
25A	.073			
26			-.239	
27				
28				

121

AD 1040C-R3

8-7000

CALC	APR	APR	CHECK
R. Root			
2-2-66			
REVISED			
DATE			

GROUND BASED SIMULATION
LATERAL RUN LOG

THE BOEING COMPANY
RENTON, WASHINGTON D6-15000

TABLE A1-6

PAGE A1-20

GROUND BASED CONFIG	$Cl_{\delta w}$	δw_{EFF}	Cl_p	AUG
G~	1/RAD	DEG	SEC/RAD	
202A	.091	50	-.239	3
205C	.055	↓	↓	↓
205F	.036	↓	↓	↓
207A	.091	30	↓	↓
216	.055	50	↓	↓
219	.055	↓	↓	↓
219A	.036	↓	↓	↓
224A	.183	↓	-.306	↓
231	.059	↓	-.153	↓
232A	.095	↓	-.411	↓
233A	.158	↓	↓	↓
234A	.055	↓	↓	↓
236	.091	↓	-.239	↓
237	.091	↓	-.239	↓
1202	.109	50	-.239	1
1202A	.091	↓	↓	↓
1203	.146	↓	↓	↓
1203A	.147	30	↓	↓
1203A*	.155	30	↓	↓
1205C	.055	50	↓	↓
1205D	.061	75	↓	↓
1205F	.036	50	↓	↓

AD 1040C-R3

8-7000

GROUND BASED CONFIG	$C_{l_{\delta_W}}$	$\delta_{W_{EFF}}$	C_{l_p}	AUG.
G~	1/RAD	DEG	SEC/RAD	
1206	.061	30	-.239	1
1207A	.091	30		
1209A	.037	75		
1209*	.098	75		
1222	.109	50	-.154	
1223	↓	↓	-.239	
1224	↓	↓	-.306	
1230	.055	↓	-.154	
1231	.059	↓	-.154	
1232	.103	↓	-.410	
1233	.172	↓	-.410	
1233B	.172	↓	-.505	
1234B	.055	↓	-.410	
1235	.098	↓	-.505	
1236	.091	↓	-.239	
1236B	.264	30	-.505	
1237	.091	50	-.239	
1237A	.091	50	-.239	↓

CALC R. Root 2-2-66
CHECK
APR
APR
REVISED
DATE

GROUND BASED SIMULATION
LATERAL RUN LOG

THE BOEING COMPANY
RENTON, WASHINGTON D6-15000

TABLE A1-6

PAGE A1-21

LATERAL DIRECTIONAL STABILITY AUGMENTATION SYSTEM

BASIC SYSTEM

RUDDER : $\delta r = [\frac{\delta r}{\dot{\beta}}]\dot{\beta} + [\frac{\delta r}{\dot{\phi}}]\dot{\phi} + [\frac{\delta r}{\delta w}]\delta w$

WHEEL : $\delta w = [\frac{\delta w}{\dot{\beta}}]\dot{\beta} + [\frac{\delta w}{\dot{\psi}}]\dot{\psi}$

WHERE : $\dot{\beta} = [\frac{g}{V}]\phi - \dot{\psi} = .163\,\phi - \dot{\psi}$

BASIC GAINS

$[\frac{\delta r}{\dot{\beta}}] = -.3$

$[\frac{\delta r}{\dot{\phi}}] = -2.07$

$[\frac{\delta w}{\beta}] = 1.83$

AUG. SYSTEM 1

$[\frac{\delta r}{\delta w}] = .178$

$[\frac{\delta w}{\dot{\psi}}] = -1.00$

$[\delta r_{MAX}] = \pm 20°$

AUG. SYSTEM 2

$[\frac{\delta r}{\delta w}] = 0$

$[\frac{\delta w}{\dot{\psi}}] = -2.82$

$[\delta r_{MAX}] = \pm 50°$

AUG. SYSTEM 3

$[\frac{\delta r}{\delta w}] = 0$

$[\frac{\delta w}{\dot{\psi}}] = -1.0$

$[\delta r_{MAX}] = \pm 50°$

ENGR.	R. Root	2-1-66	REVISED	DATE	LATERAL DIRECTIONAL STABILITY AUGMENTATION SYSTEM	TABLE A1-7
CHECK						D6-15000
APR					THE BOEING COMPANY RENTON WASHINGTON	A1-22
APR						

EQUIVALENT LATERAL-DIRECTIONAL AERODYNAMIC COEFFICIENTS

YAWING MOMENT

$$C_{n_{\dot\beta}} = C_{n_{\dot\beta\,BASIC}} + C_{n_{\delta_r}}\left(\frac{\delta_r}{\dot\beta}\right) = .036 \text{ SEC./RAD}$$

$$C_{n_{\dot\phi}} = C_{n_{\dot\phi\,BASIC}} + C_{n_{\delta_r}}\left(\frac{\delta_r}{\dot\phi}\right) = .0905 \text{ SEC./RAD}$$

$$C_{n_\beta} = C_{n_{\beta\,BASIC}} + C_{n_{\delta_w}}\left(\frac{\delta_w}{\beta}\right) = .218 \text{ 1/RAD}$$

$$C_{n_{\dot\psi}} = C_{n_{\dot\psi\,BASIC}} + C_{n_{\delta_w}}\left(\frac{\delta_w}{\dot\psi}\right) = -.267 + .0213\left(\frac{\delta_w}{\dot\psi}\right) \text{ SEC/RAD}$$

$$C_{n_{\delta_w}} = C_{n_{\delta_{w\,BASIC}}} + C_{n_{\delta_r}}\left(\frac{\delta_r}{\delta_w}\right) = .0213 - .12\left(\frac{\delta_r}{\delta_w}\right) \text{ 1/RAD}$$

ROLLING MOMENT

$$C_{\ell_{\dot\beta}} = C_{\ell_{\dot\beta\,BASIC}} + C_{\ell_{\delta_r}}\left(\frac{\delta_r}{\dot\beta}\right) = -.00069 \text{ SEC/RAD}$$

$$C_{\ell_{\dot\phi}} = C_{\ell_{\dot\phi\,BASIC}} + C_{\ell_{\delta_r}}\left(\frac{\delta_r}{\dot\phi}\right) = C_{\ell_{\dot\phi}} + .00229\left(\frac{\delta_r}{\dot\phi}\right) \text{ SEC/RAD}$$

$$C_{\ell_\beta} = C_{\ell_{\beta\,BASIC}} + C_{\ell_{\delta_{w\,BASIC}}}\left(\frac{\delta_w}{\beta}\right) = -1955$$

$$C_{\ell_{\dot\psi}} = C_{\ell_{\dot\psi\,BASIC}} + C_{\ell_{\delta_{w\,BASIC}}}\left(\frac{\delta_w}{\dot\psi}\right) = .3045 + .109\left(\frac{\delta_w}{\dot\psi}\right) \text{ SEC/RAD}$$

$$C_{\ell_{\delta_w}} = C_{\ell_{\delta_{w\,BASIC}}} + C_{\ell_{\delta_r}}\left(\frac{\delta_r}{\delta_w}\right) = C_{\ell_{\delta_w}} + .00229\left(\frac{\delta_r}{\delta_w}\right) \text{ 1/RAD}$$

SIDE FORCE

$$C_{y_{\dot\beta}} = C_{y_{\dot\beta\,BASIC}} + C_{y_{\delta_r}}\left(\frac{\delta_r}{\dot\beta}\right) = -.074 \text{ SEC/RAD}$$

$$C_{y_{\dot\phi}} = C_{y_{\dot\phi\,BASIC}} + C_{y_{\delta_r}}\left(\frac{\delta_r}{\dot\phi}\right) = .060 \text{ SEC/RAD}$$

$$C_{y_\beta} = C_{y_{\beta\,BASIC}} + C_{y_{\delta_w}}\left(\frac{\delta_w}{\beta}\right) = -.9773 \text{ 1/RAD}$$

$$C_{y_{\dot\psi}} = C_{y_{\dot\psi\,BASIC}} + C_{y_{\delta_w}}\left(\frac{\delta_w}{\dot\psi}\right) = .02995 - .0805\left(\frac{\delta_w}{\dot\psi}\right) \text{ SEC/RAD}$$

$$C_{y_{\delta_w}} = C_{y_{\delta_{w\,BASIC}}} + C_{y_{\delta_r}}\left(\frac{\delta_r}{\delta_w}\right) = -.0805 + .2464\left(\frac{\delta_r}{\delta_w}\right) \text{ 1/RAD}$$

ENGR.	R. Root	2-1-66	REVISED	DATE	EQUIVALENT LATERAL - -DIRECTIONAL AERODYNAMIC COEFFICIENTS.	TABLE A1-8
CHECK						D6-15000
APR					THE BOEING COMPANY RENTON, WASHINGTON	A1-23
APR						

APPENDIX 2

BASIC 367-80 DESCRIPTION

The aerodynamic characteristics of the unaugmented 367-80 inflight simulator are described in Table A2-1 and in Figures A2-1 thru A2-5. Characteristics presented are those used in the control command equations presented in Ref. 1. These equations are used to determine the control gains necessary to augment the aerodynamic characteristics of the 367-80 to the proposed Ames large transport configurations.

Figure A2-1 shows the pitching moment characteristics of the spoilers. The calibration of the inboard to outboard spoilers is presented in Figure A2-2. The lift and drag characteristics of the speed brakes are presented in Figures A2-3 and A2-4. The pitching moment characteristics of the thrust reversers are shown in Figure A2-5.

Several parameters varied during the test flights due to fuel consumption The center of gravity of the 367-80 airplane varied from 29-31%. The weight varied from approximately 172,000 lbs at take-off to 137,000 at touchdown. The lateral directional moments of inertia vary ±15 percent from the values shown in Table A2-1. The pitch moment of inertia varies ±3.3 percent from those presented in Table A2-1.

TABLE A2-1

367-80 Longitudinal Characteristics

Flight Condition

V_e	117 Kts
Flap Angle	30°
BPR	1
Gross Weight	150,000 lbs.
C. G. Location	30% MAC
Speed Brake Trim Angle	6°

Airplane Constants

Wing Area	2821 sq. ft.
Wing Span	130.8 ft.
MAC	20.1 ft.

Lift Derivatives

$C_{L_{Trim}}$	1.146	
$\alpha_{Trim_{wcp}}$	8.5°	
C_{L_α}	5.45	/rad
$C_{L_{\delta_E}}$	.52	/rad

Drag Derivatives

$C_{D_{Trim}}$	.139	
C_{D_α}	.544	/rad

176

TABLE A2-1 (CONT.)

Pitching Moment Derivatives

C_{m_α}	-1.11	/rad
$C_{m_{\dot\alpha}}$	-.272	/rad/sec
$C_{m_{\dot\theta}}$	-.710	/rad/sec
$C_{m_{\delta_E}}$	-.975	/rad
I_y	2.25 $\times 10^6$	slug- FT^2

Speed Brakes

$C_{L_{\delta_{SB}}}$	1.11	/rad
$C_{m_{\delta_{SB}}}$	See Fig.	/rad

Longitudinal Dynamic Characteristics

Short Period

Damped Natural Frequency	1.04	rad/sec
Undamped Natural Frequency	1.42	rad/sec
Damping Ratio	.68	

Phugoid

Damped Natural Frequency	.157	rad/sec
Undamped Natural Frequency	.157	rad/sec
Damping Ratio	.0906	

TABLE A2-1 (CONT.)

367-80 Lateral - Directional Characteristics

Side Force Derivatives

C_{y_β}	-.838	/rad
$C_{y_{\dot{\phi}}}$	.270	/rad/sec
$C_{y_{\dot{\psi}}}$	.0727	/rad/sec
$C_{y_{\dot{\beta}}}$	0	/rad
$C_{y_{\delta_R}}$	.211	/rad
$C_{y_{\delta_{WH}}}$	-.0252	/rad

Rolling Moment Derivatives

C_{ℓ_β}	-.1743	/rad
$C_{\ell_{\dot{\phi}}}$	-.120	/rad/sec
$C_{\ell_{\dot{\psi}}}$	.104	/rad/sec
$C_{\ell_{\dot{\beta}}}$	0	/rad
$C_{\ell_{\delta_R}}$	.0149	/rad
$C_{\ell_{\delta_{WH}}}$	.06	/rad
I_{X_B}	2.57 $\times 10^6$	slug-FT^2

Yawing Moment Derivatives

C_{n_β}	.0909	/rad
$C_{n_{\dot{\phi}}}$	-.0179	/rad/sec
$C_{n_{\dot{\psi}}}$	-.1071	/rad/sec

TABLE A2-1 (CONT.)

Yawing Moment Derivatives (cont'd)

$C_{n_{\dot{\beta}}}$	-.0747	/rad
$C_{n_{\delta_R}}$	-.0749	/rad
$C_{n_{\delta_{WH}}}$	.0030	/rad
I_{Z_B}	4.73×10^6	slug-FT^2
$I_{X_{Z_B}}$	$.156 \times 10^6$	slug-FT^2

Lateral Dynamic Characteristics

Spiral Divergence

Time Constant	15.7	sec
Time to Half Amplitude	10.87	sec

Roll Convergence

Time Constant	1.04	sec

Dutch Roll

Damped Natural Frequency	.77	rad/sec
Undamped Natural Frequency	.77	rad/sec
Damping Ratio	.018	
	1.584	

TD 441 C-84

	CALC	CHECK	APR	APR
	F.S.			
	11/65			
	REVISED			
	DATE			

PITCHING MOMENT CHARACT. OF SPOILERS.

THE BOEING COMPANY D6-15000

PAGE A2-6

FIG. A2-1

367-80

FLAPS	30°
BPR	1.0
G.W.	144,000 LBS
C.G.	29.0 %
TEST NO.	675-3, 675-1

$\alpha_{WCP} = 6.3°$

$V_e = 120$ KTS

⊙ FROM CONSTANT ANGLE OF ATTACK TEST

△ " " AIRSPEED TEST

NOTE:

1.) α AND V CHANGES CORRECTED

2.) THIS CURVE REPLACES FIGURES 5 AND 6 OF AERO COORD. SHEET # 176

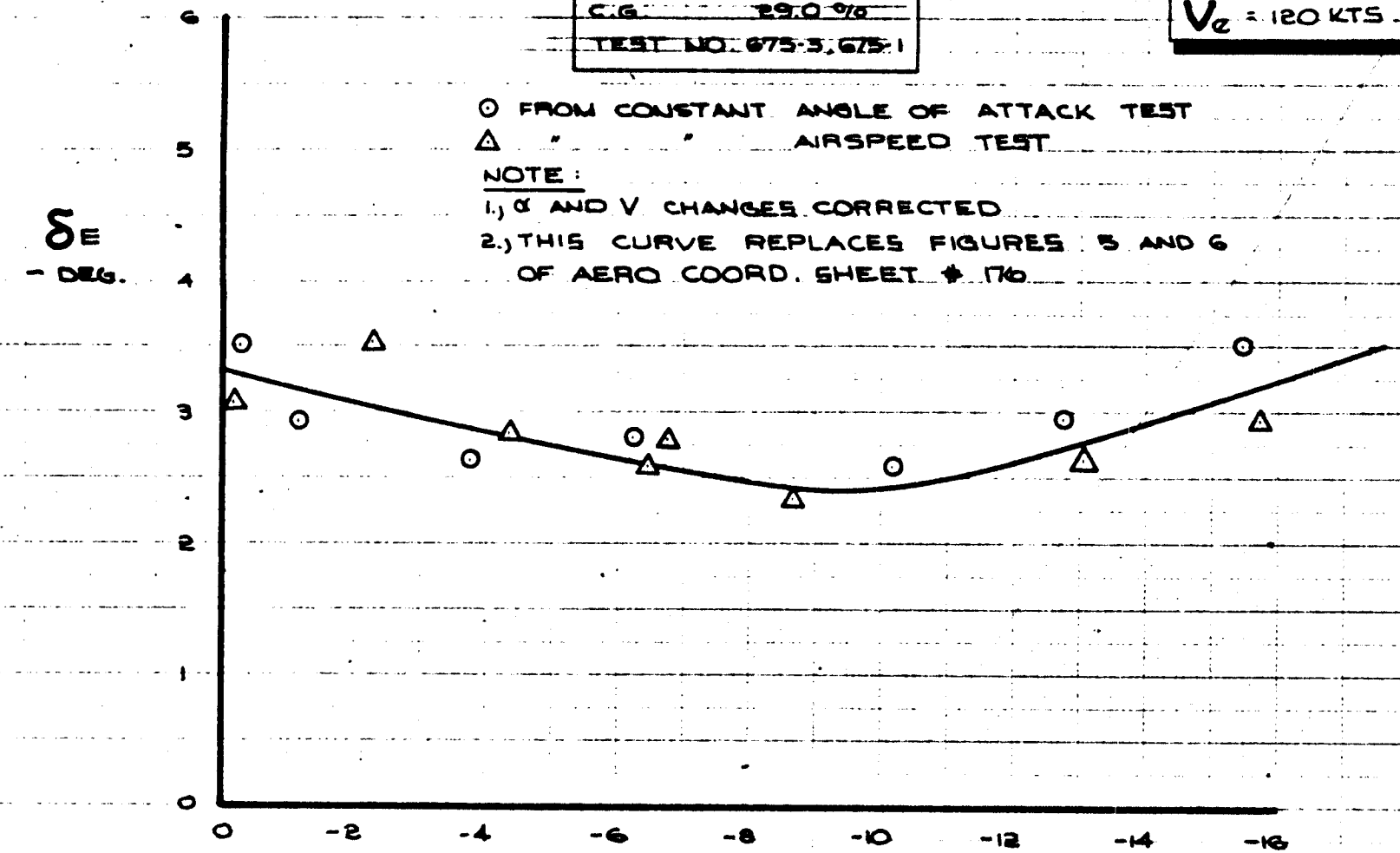

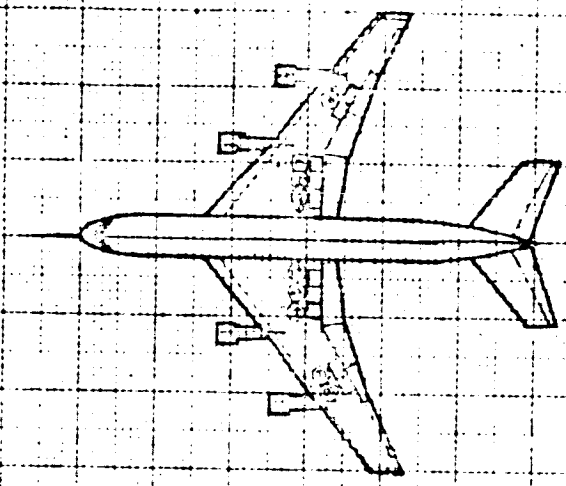

δSB_{AVG} INBOARD ~DEG

-12
-10
-8
-6
-4
-2
0

0 -2 -4 -6 -8 -10 -12 -14

$\delta SB_{AVG.}$ OUTBOARD ~DEG

②⑤⑧⑪ OUTB'D SPOILERS
③⑥⑨⑫ INB'D SPOILERS

TEST 675-2, -3

CALC	W.M.E.	11-1-65	REVISED	DATE
CHECK				
APR				
APR				

SPEED BRAKE OPERATION
CALIBRATION TESTS

367-80

FIG. A2-2

THE BOEING COMPANY D6-15000

PAGE A2-7

TD 461 C-64

K•E ALBANENE® TRACING PAPER

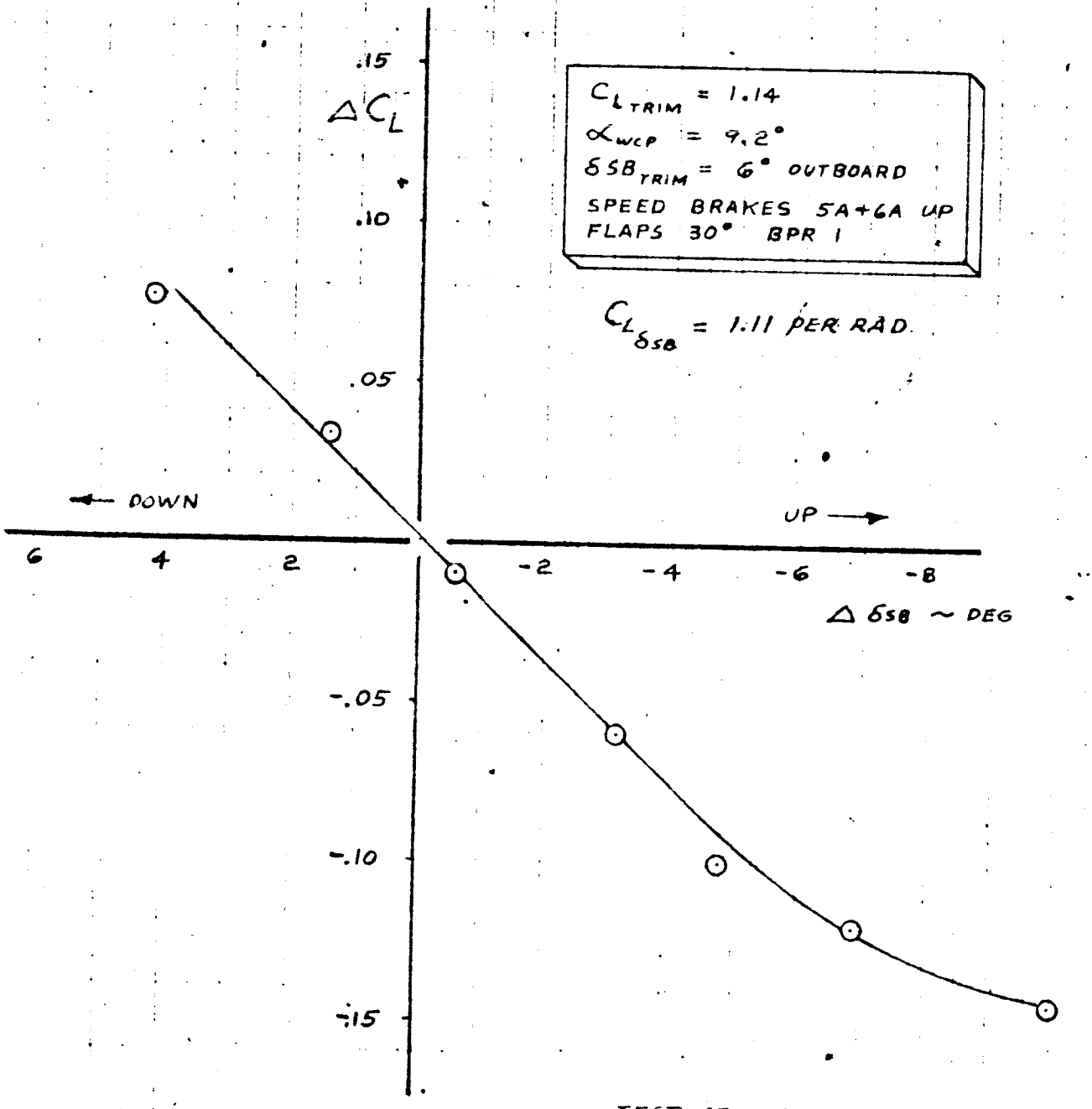

CALC	W.M.E.	10-29-65	REVISED	DATE	SPEED BRAKE CHARACTERISTICS LIFT	367-80
CHECK						FIG. A2-3
APR						
APR					THE BOEING COMPANY D6-15000	PAGE A2-8

TD 461 C-R4

$C_{L_{TRIM}} = 1.14$

$\alpha_{WCP} = 9.2°$

$\delta_{SB_{TRIM}} = 6°$ OUTBOARD

SPEED BRAKES 5A+6A UP

FLAPS 30° BPR 1

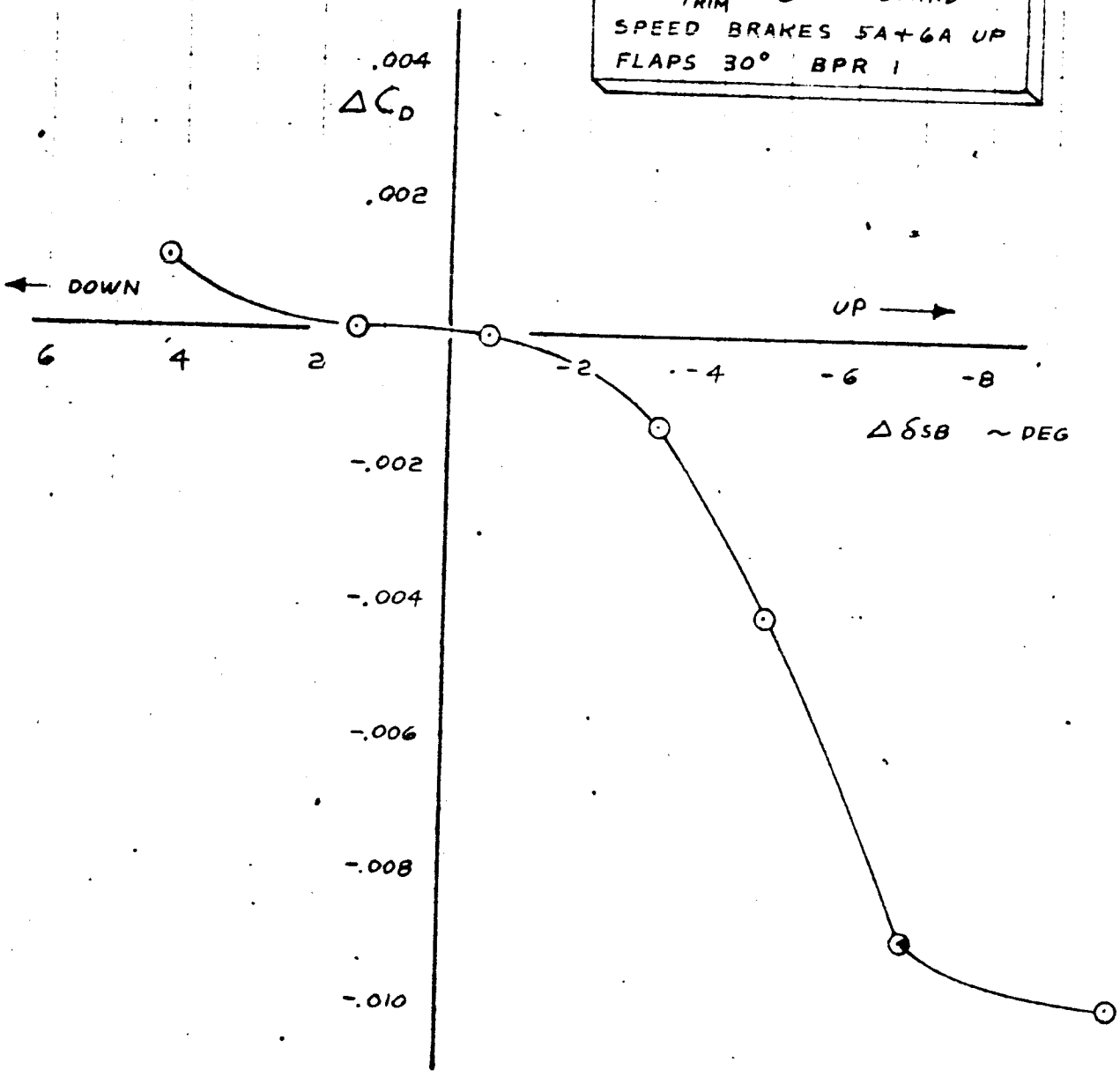

TEST 675-2, -3

CALC	W. M. E.	10-29-65	REVISED	DATE	SPEED BRAKE CHARACTERISTICS DRAG	367-80
CHECK						FIG A2-4
APR					THE BOEING COMPANY D6-15000	PAGE A2-9
APR						

TD 441 C-84

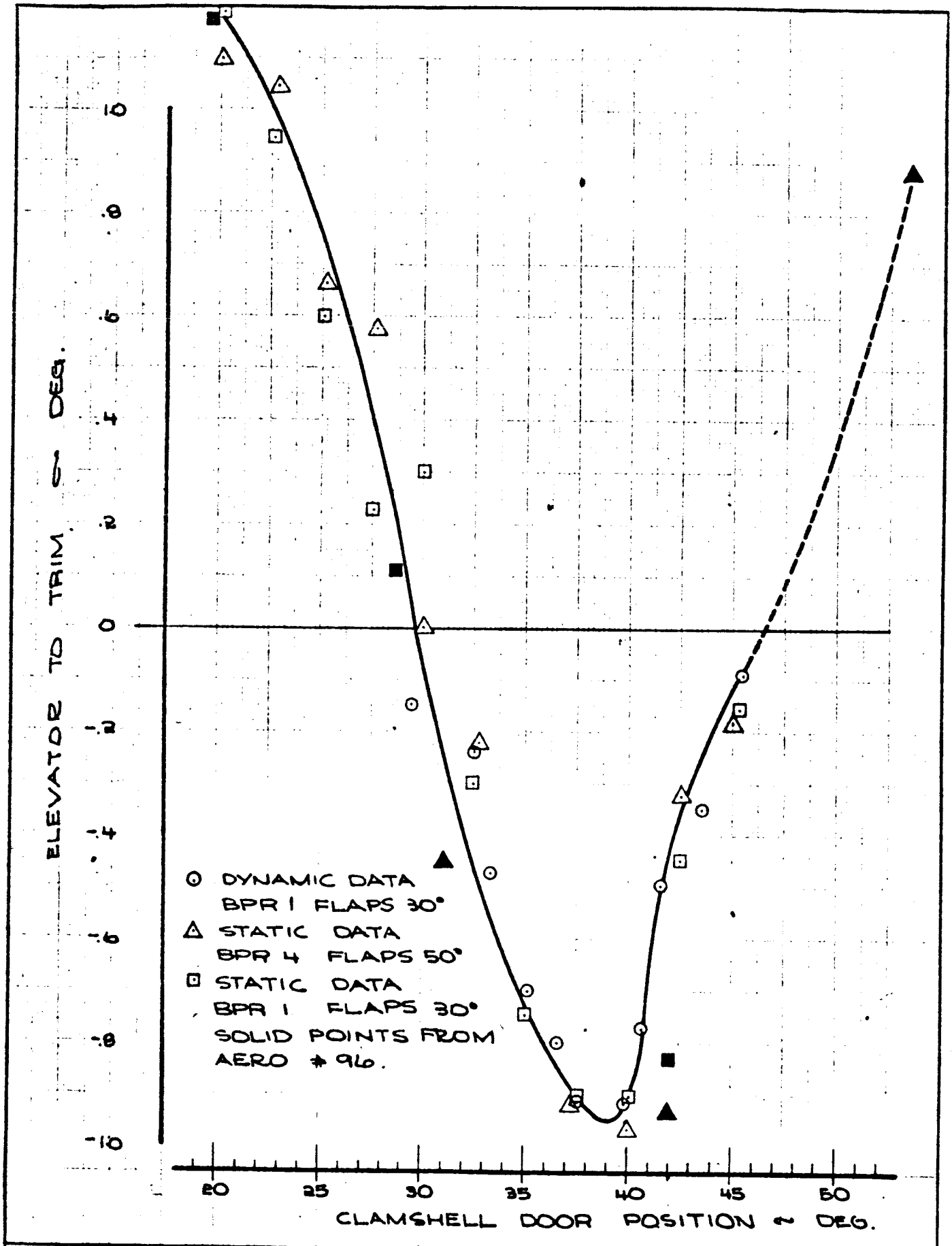

CALC				REVISED	DATE	FLIGHT TEST DATA THRUST REVERSER PITCH. M.
CHECK						
APR						
APR						

3867-80

FIG. A2-5

THE BOEING COMPANY D6-15000

PAGE A2-10

TD 461 C-84

APPENDIX 3

Typical control system force characteristics for the ground based and airborne simulations are presented in Fig. A3-1, for column, wheel, and rudder pedals. Wheel and Column forces were varied on the ground based simulation during the evaluations. These variations are listed in Tables 3 and 6 of section VII and VIII. Forces were kept constant on the airborne simulation. The pilots had the capability of varying column force characteristics in flight, but little variation was noted.

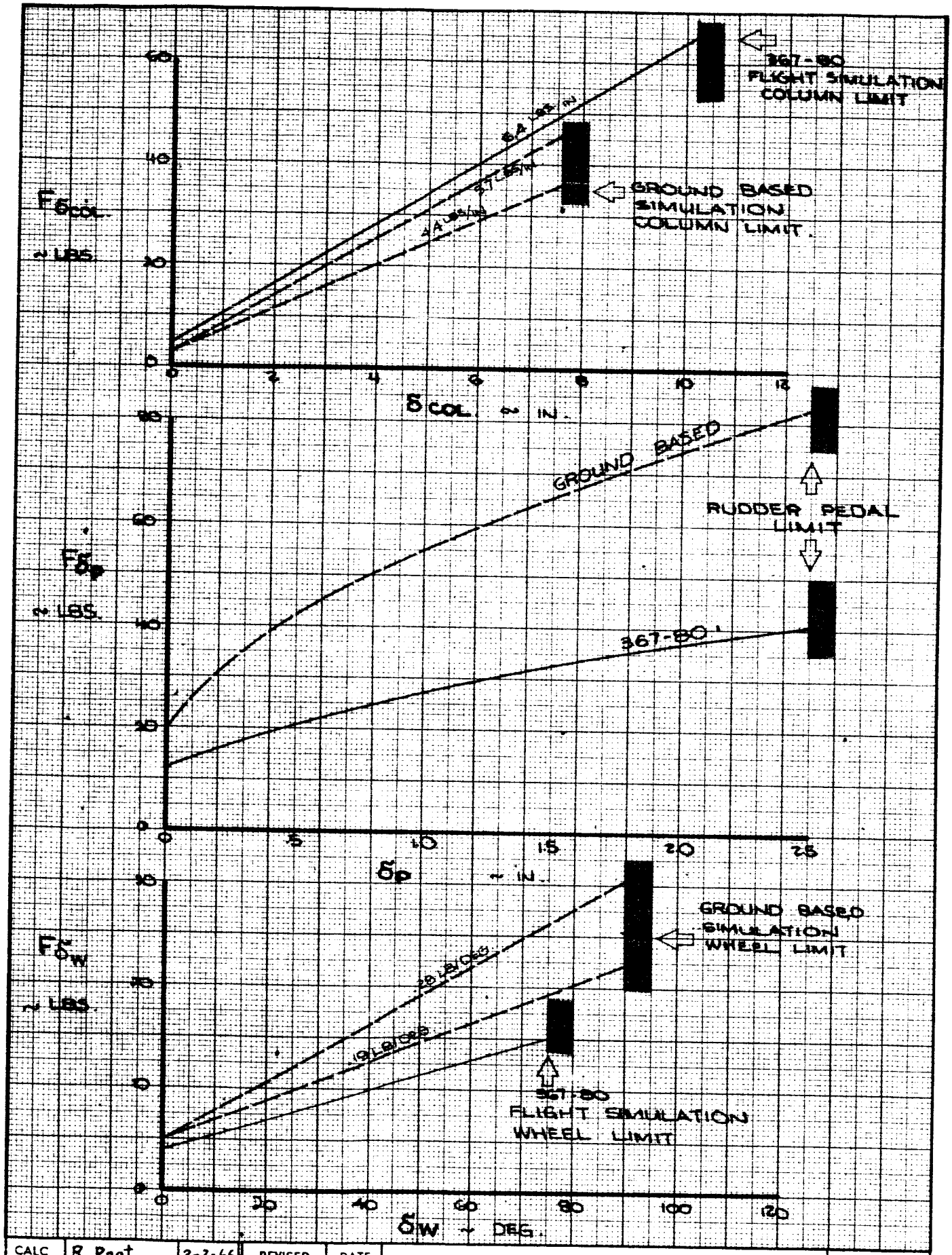

CALC	R. Root	2-2-46	REVISED	DATE
CHECK				
APR				
APR				

CONTROL SYSTEM FORCE CHARACTERISTICS

FIG. A3-1

D6-15000

THE BOEING COMPANY

PAGE A3-2

TD 461 C-R4

APPENDIX 4

Derivation of Theory

The theoretical characteristics presented for the control pulses and steps were obtained from 6-degree-of-freedom digital computer programs. The theoretical equations involved can be found in Reference 2.

The theoretical characteristics of the documentation maneuvers performed other than the pulses and steps are derived on the following pages.

APPENDIX 4

THEORETICAL CALCULATIONS

Speed Stability

$$C_L = C_{L_0} + C_{L_\alpha}\Delta\alpha + C_{L_{\dot\alpha}}\dot\alpha + C_{L_{\dot\theta}}\dot\theta + C_{L_V}\Delta V + C_{L_{\delta_E}}\delta E \quad (1)$$

and

$$C_M = C_{M_0} + C_{M_\alpha}\Delta\alpha + C_{M_{\dot\theta}}\dot\theta + C_{M_{\dot\alpha}}\dot\alpha + C_{M_V}\Delta V + C_{M_{\delta_E}}\delta E \quad (2)$$

For the steady state case $\dot\theta = \dot\alpha = 0$ and equations (1) and (2) become

$$C_L = C_{L_0} + C_{L_\alpha}\Delta\alpha + C_{L_V}\Delta V + C_{L_{\delta_E}}\delta E \quad (3)$$

and

$$C_M = C_{M_0} + C_{M_\alpha}\Delta\alpha + C_{M_V}\Delta V + C_{M_{\delta_E}}\delta E. \quad (4)$$

Differentiating equation (3)

$$\frac{dC_L}{dV} = C_{L_\alpha}\frac{d\Delta\alpha}{dV} + C_{L_V} + C_{L_{\delta_E}}\frac{d\delta E}{dV} \quad (5)$$

Rearranging terms in equation (5) gives

$$\frac{d\alpha}{dV} = \frac{1}{C_{L_\alpha}}\left[\frac{dC_L}{dV} - C_{L_V} - C_{L_{\delta_E}}\frac{d\delta E}{dV}\right] \quad (6)$$

Differentiating equation (4)

$$0 = C_{M_\alpha}\frac{d\Delta\alpha}{dV} + C_{M_V} + C_{M_{\delta_E}}\frac{d\delta E}{dV} \quad (7)$$

Substituting equation (6) into equation (7) gives

$$0 = \frac{C_{M_\alpha}}{C_{L_\alpha}}\left[\frac{dC_L}{dV} - C_{LV} - C_{L\delta E}\frac{d\delta E}{dV}\right] + C_{MV} + C_{M\delta_E}\frac{d\delta E}{dV} \quad (8)$$

Solving for $\frac{d\delta E}{dV}$ in equation (8)

$$\frac{d\delta E}{dV} = \frac{C_{M\alpha}C_{L_V} - C_{M_\alpha}\frac{dC_L}{dV} - C_{M_V}C_{L\alpha}}{C_{L_\alpha}C_{M\delta E} - C_{M\alpha}C_{L\delta_E}} \quad (9)$$

Speed Stability

The lift equation is

$$L_0 = \frac{1}{2} \rho V^2 S C_{L_0}. \tag{10}$$

Differentiating equation (10)

$$0 = \frac{1}{2} \rho S (C_{L_0} 2V dV + V^2 d C_L).$$

Solving this for $\frac{d C_L}{d V}$ gives

$$\frac{d C_L}{d V} = - \frac{2 C_{L_0}}{V}. \tag{11}$$

Substituting equation (11) into equation (9)

$$\frac{d \delta E}{dV} = \frac{C_{M_\alpha} C_{L_V} + C_{M\alpha} \frac{2 C_{L_0}}{V} - C_{M_V} C_{L_\alpha}}{C_{L_\alpha} C_{M\delta E} - C_{M_\alpha} C_{L\delta E}}. \tag{12}$$

Substituting equation (11) into equation (6) gives

$$\frac{d\alpha}{dV} = \frac{1}{C_{L_\alpha}} \left[\frac{-2 C_{L_0}}{V} - C_{L_V} - C_{L\delta E} \frac{d\delta E}{d V} \right] \tag{13}$$

Integrating equation (12) yields

$$\delta E = \int_{Vo}^{V} \frac{d\delta E}{d V} d V = \frac{C_{M_\alpha} C_{L_V} - C_{M_V} C_{L_\alpha}}{C_{L_\alpha} C_{M\delta E} - C_{M_\alpha} C_{L\delta E}} \int_{V_0}^{V} dV + \frac{C_{M_\alpha} 2 C_{L_0}}{C_{M\delta E} C_{L_\alpha} - C_{M_\alpha} C_{L\delta E}} \int_{Vo}^{V} \frac{dV}{V}$$

$$\delta E = + \frac{2 C_{L_0} C_{M_\alpha}}{C_{M\delta E} C_{L_\alpha} - C_{M_\alpha} C_{L\delta E}} \ln \frac{V}{V_o} - \frac{C_{M_V} C_{L_\alpha} - C_{L_V} C_{M_\alpha}}{C_{M\delta E} C_{L_\alpha} - C_{M_\alpha} C_{L\delta E}} (V - V_o) \tag{14}$$

$$\delta_{COL.} = \left(\frac{1}{\delta E / \delta_{COL}} \right) \delta E$$

$$F_S = \left(\frac{F_S}{COL} \right) \delta_{COL}$$

Speed Stability

Integrating equation (13) yields

$$\alpha = \int \frac{d\alpha}{dV}\, dV = -\frac{1}{C_{L_\alpha}} \left[\int_{V_0}^{V} \frac{2 C_{L_0}}{V}\, dV + \int_{V_0}^{V} C_{L_V}\, dV + \int_{V_0}^{V} C_{L_{\delta_E}} \frac{d\delta_E}{dV}\, dV \right]$$

$$= -\frac{2 C_{L_0}}{C_{L_\alpha}} \ln V/V_0 - \frac{C_{L_V}}{C_{L_\alpha}} (V - V_0) - C_{L_{\delta_E}} \delta_E$$

THEORETICAL CALCULATIONS

Wind Up Turn

$$C_L = C_{L_o} + C_{L_\alpha}\alpha + C_{L_{\dot\theta}}\dot\theta + C_{L_{\dot\alpha}}\dot\alpha + C_{L_V} V + C_{L_{\delta_E}}\delta_E \quad (1)$$

and

$$C_m = C_{m_o} + C_{m_\alpha}\alpha + C_{m_{\dot\theta}}\dot\theta + C_{m_{\dot\alpha}}\dot\alpha + C_{m_V} V + C_{m_{\delta_E}}\delta_E \quad (2)$$

The increments from trim are

$$\Delta C_L = C_L - C_{L_o} = (n-1)C_{L_o} \quad (3)$$

and

$$\Delta C_m = C_m - C_{m_o} = 0.$$

For the steady state case V = constant and $\dot\alpha = 0$. Solving for the steady state $\Delta\delta_E$ in equation (2) gives

$$\Delta\delta_E = -\frac{C_{m_\alpha}\Delta\alpha + C_{m_{\dot\theta}}\dot\theta}{C_{m_{\delta_E}}} \quad (4)$$

and solving for $\Delta\alpha$ in equation (1) gives

$$\Delta\alpha = \frac{C_L - C_{L_o} - C_{L_{\dot\theta}}\dot\theta - C_{L_{\delta_E}}\Delta\delta_E}{C_{L_\alpha}} \quad (5)$$

Substituting equation (3) into equation (5)

$$\Delta\alpha = \frac{(n-1)C_{L_o} - C_{L_{\dot\theta}}\dot\theta - C_{L_{\delta_E}}\delta_E}{C_{L_\alpha}} \quad (6)$$

Equations (4) and (6) can be combined with $\dot\theta = \frac{(n^2-1)}{n}\, g/v$ (chapter 9, page 301, Reference 2) for a wind up turn to give

$$\frac{\Delta\delta_E}{(n-1)} = \frac{-C_{m_\alpha} C_{L_o} + \frac{(1+n)}{n}\left(C_{L_{\dot\theta}} C_{m_\alpha} - C_{L_\alpha} C_{m_{\dot\theta}}\right) g/v}{C_{m_{\delta_E}} C_{L_\alpha} - C_{L_{\delta_E}} C_{m_\alpha}} \quad (7)$$

$$\frac{\Delta\delta_c}{(n-1)} = \frac{\Delta\delta_E}{(n-1)} \cdot \frac{(\delta_c)}{(\delta_E)} \quad (8)$$

Wind Up Turn

From Equation 6

$$\frac{\Delta\alpha}{(n-1)} = \frac{C_{L_o} - C_{L_{\dot{\theta}}} \frac{(n+1)}{n} \frac{q}{v} - C_{L_{\delta_E}} \frac{\delta_E}{(n-1)}}{C_{L_\alpha}}$$

or

$$\frac{(n-1)}{\Delta\alpha} = \frac{C_L}{C_{L_o} - C_{L_{\dot{\theta}}} \frac{(n+1)}{n} \frac{q}{v} \quad C_{L_{\delta_E}} \frac{(\delta_E)}{(n-1)}}$$

192

THEORETICAL CALCULATIONS

Steady Sideslip

The yawing moment equation is

$$C_n = C_{n_o} + C_{n_\beta}\beta + C_{n_{\dot\beta}}\dot\beta + C_{n_{\dot\psi}}\dot\psi + C_{n_{\dot\phi}}\dot\phi + C_{n_{\delta_R}}\delta_R + C_{n_{\delta_{WH}}}\delta_{WH} \qquad (1)$$

The side force equation is

$$C_y = C_{y_o} + C_{y_\beta}\beta + C_{y_{\dot\beta}}\dot\beta + C_{y_{\dot\phi}}\dot\phi + C_{y_\phi}\phi + C_{y_{\delta_{WH}}}\delta_{WH} + C_{y_{\delta_R}}\delta_R + C_{y_{\dot\psi}}\dot\psi \qquad (2)$$

The rolling moment equation is

$$C_\ell = C_{\ell_o} + C_{\ell_\beta}\beta + C_{\ell_{\dot\beta}}\dot\beta + C_{\ell_{\dot\phi}}\dot\phi + C_{\ell_{\dot\psi}}\dot\psi + C_{\ell_{\delta_{WH}}}\delta_{WH} + C_{\ell_{\delta_R}}\delta_R \qquad (3)$$

For the steady state case equation (1), (2) and (3) become

$$0 = C_{n_\beta}\beta + C_{n_{\delta_R}}\delta_R + C_{n_{\delta_{WH}}}\delta_{WH}, \qquad (4)$$

and

$$0 = C_{y_\beta}\beta + C_{y_{\delta_R}}\delta_R + C_{y_\phi}\phi + \cancel{C_{y_{\delta_{WH}}}}\ \text{negligible}\ \delta_{WH} \qquad (5)$$

$$0 = C_{\ell_\beta}\beta + C_{\ell_{\delta_{WH}}}\delta_{WH} + C_{\ell_{\delta_R}}\delta_R \qquad (6)$$

Combining equations (4) and (6) yields

$$\frac{\delta_R}{\beta} = \frac{-C_{n_\beta}\ C_{\ell_{\delta_{WH}}} + C_{\ell_\beta}\ C_{n_{\delta_{WH}}}}{C_{n_{\delta_R}}\ C_{\ell_{\delta_{WH}}} - C_{n_{\delta_{WH}}}\ C_{\ell_{\delta_R}}}$$

and

$$\frac{\delta_{WH}}{\beta} = \frac{-C_{n_{\delta_R}}\ C_{\ell_\beta} + C_{n_\beta}\ C_{\ell_{\delta_R}}}{C_{n_{\delta_R}}\ C_{\ell_{\delta_{WH}}} - C_{n_{\delta_{WH}}}\ C_{\ell_{\delta_R}}}$$

also

$$\frac{\delta_P}{\beta} = \frac{\delta_R}{\beta}\ \frac{\delta_P}{\delta_R}$$

Steady Sideslip

From equation (2)

$$\frac{\dot{\phi}}{\beta} = -\frac{1}{C_{Y_\phi}}\left[C_{Y_\beta} + C_{Y_{\delta_R}}\frac{\delta_R}{\beta}\right] \qquad (6)$$

Substituting $C_L = C_{Y_\phi}$ in equation (6)

$$\frac{\dot{\phi}}{\beta} = -\frac{1}{C_L}\left[C_{Y_\beta} + C_{Y_{\delta_R}}\frac{\delta_R}{\beta}\right]$$

THEORETICAL CALCULATION

Steady Roll Rate

The rolling moment equation is

$$C_\ell = \frac{I_{xx}}{qsb}\ddot{\phi} = C_{\ell_\beta}\beta + C_{\ell_{\dot\beta}}\dot\beta + C_{\ell_{\dot\phi}}\dot\phi + C_{\ell_{\dot\psi}}\dot\psi + C_{\ell_{\delta_{WH}}}\delta_{WH} + C_{\ell_{\delta_R}}\delta_R \quad (1)$$

For a steady state roll rate $\ddot{\phi} = 0$, so equation (1) becomes

$$0 = C_{\ell_\beta}\beta + C_{\ell_{\dot\beta}}\dot\beta + C_{\ell_{\dot\phi}}\dot\phi + C_{\ell_{\dot\psi}}\dot\psi + C_{\ell_{\delta_{WH}}}\delta_{WH} + C_{\ell_{\delta_R}}\delta_R \quad (2)$$

If the flight test maneuver to determine steady roll rate is performed correctly then $\delta_R = \beta = \dot\psi = \dot\beta = 0$. The flight test data was adjusted to fit these conditions so

$$0 = C_{\ell_{\dot\phi}}\dot\phi_{SS} + C_{\ell_{\delta_{WH}}}\delta_{WH}$$

$$\frac{\dot\phi_{SS}}{\delta_W} = \frac{C_{\ell_{\delta_{WH}}}}{C_{\ell_{\dot\phi}}}$$

THEORETICAL CALCULATION

Roll Acceleration

The rolling moment equation is

$$C_\ell = \frac{I_{xx}}{qsb}\ddot{\phi} = C_{\ell_\beta}\beta + C_{\ell_{\dot\beta}}\dot\beta + C_{\ell_{\dot\phi}}\dot\phi + C_{\ell_{\dot\psi}}\dot\psi + C_{\ell_{\delta_{WH}}}\delta_{WH} + C_{\ell_{\delta_R}}\delta_R \quad (1)$$

The roll rate reversal data was measured at a point where $\phi = \psi = \beta = \delta_R = \dot\beta = 0$

so equation (1) becomes

$$\frac{I_{xx}}{qsb}\ddot{\phi} = C_{\ell_{\delta_{WH}}}\delta_{WH} .$$

solving for $\ddot\phi / \delta_{WH}$

$$\frac{\ddot\phi}{\delta_{WH}} = C_{\ell_{\delta_{WH}}}\frac{qsb}{I_{xx}}$$

THEORETICAL CALCULATIONS

Yaw Acceleration

The yawing moment equation is

$$C_n = \frac{I_{zz}}{qsb}\ddot{\psi} = C_{n_\beta}\beta + C_{n_{\dot\beta}}\dot\beta + C_{n_{\dot\psi}}\dot\psi + C_{n_{\dot\phi}}\dot\phi + C_{n_{\delta_R}}\delta_R + C_{n_{\delta_{WH}}}\delta_{WH} \quad (1)$$

The roll rate reversal data was measured at a point where $\beta = \dot\beta = \dot\psi = \dot\phi = \delta_{WH} = 0$

so equation (1) becomes

$$\frac{I_{zz}}{qsb}\ddot\psi = C_{n_{\delta_R}}\delta_R$$

solving for $\ddot\psi/\delta_R$

$$\ddot\psi/\delta_R = C_{n_{\delta_R}}\frac{qsb}{I_{zz}}$$

Multiplying equation (2) by the pedal to rudder gearing gives

$$\ddot\psi/\delta_P = C_{n_{\dot\delta_R}}\frac{qsb}{I_{zz}}\left(\frac{\delta_R}{\delta P}\right)$$

THEORETICAL CALCULATIONS

Pitch Acceleration

The pitching moment equation is

$$C_M = \frac{I_{yy}}{qsc}\ddot{\theta} = C_{M_\alpha}\Delta\alpha + C_{M_{\dot\theta}}\dot\theta + C_{M_{\dot\alpha}}\dot\alpha + C_{M_U}\Delta U + C_{M_{\delta_E}}\delta E \qquad (1)$$

The pitch acceleration was measured at a point where $\Delta\alpha = \dot\theta = \dot\alpha = dU = 0$

so equation (1) becomes

$$\frac{\ddot\theta}{\delta E} = C_{M_{\delta_E}}\frac{q\bar{sc}}{I_{yy}} \qquad (2)$$

Multiplying equation (2) by the column to elevator gearing gives

$$\frac{\ddot\theta}{\delta_{COL}} = C_{M_{\delta_E}}\frac{q\bar{sc}}{I_{yy}}\left(\frac{\delta e}{\delta COL}\right)$$

APPENDIX 5

A. Ground Based Analog Simulation Description

The ground-based flight simulator used for these studies was the Ames Research Center, moving-base transport simulator with a color TV visual scene. The visual scene, projected to simulate daylight flying, was produced by the Ames Research Center landing-approach color image generator. The simulation solved the six degree of freedom equations of motion of the airplane and presented the solutions in cab motions, instrument readings, and visual display changes. Linearized aerodynamic coefficients were used in the equations of motion. The equations of motion are given in Table A5-1.

The moving-base transport simulator utilized a transport-type (C-130) cab with conventional seating, instrumentation, and controls for two pilots. The left hand seat was used for these tests. A hydraulic feel system allowed for variation of the control system parameters. The instrument panel included the following instruments:

1. Air-speed
2. Altitude
3. Rate of climb
4. Angle of attack
5. Angle of sideslip
6. Turn and slip
7. Heading
8. Attitude
9. Localizer and glide slope error.

TABLE A5-1

Ground Based Simulation Equations of Motion:

DRAG

$$C_D = C_{D_{\alpha=0.}} + C_{D_\alpha}\alpha$$

$$\dot{V} = \frac{1}{m}(T_N - qSC_D - W\sin\gamma)$$

$$V = V_T = \int \dot{V}dt + V_0 \qquad (V_0 = \text{initial velocity})$$

$$x = x_0 + \int (V\cos\gamma \cdot \cos\psi)dt \qquad (X_0 = \text{initial distance from runway threshold})$$

$$V_e = \sqrt{\sigma}\, V + V_{GUST}$$

$$q = \frac{V_e^2}{295}$$

$$T_N = T_{N_0} + \frac{\partial T_N}{\partial V} u \qquad (T_{N_0} = \text{initial net thrust for trim})$$

$$u = V - V_0$$

PITCH

$$C_m = C_{m_q} q + C_{m_{\dot{\alpha}}}\dot{\alpha} + C_{m_{\alpha=0}} + C_{m_\alpha}\alpha + C_{m_{\delta_e}}\delta_e + C_{m_{i_H}} i_H$$

$$I_{YY}\frac{\dot{q}}{57.3} = qS\bar{c}\,C_m$$

$$q = \int \dot{q}\,dt$$

TABLE A5-1 (CONT.)

$$Cn_W = Cn_{\delta_s}\delta s + Cn_{\delta a}\delta a + Cn_{\delta r}\delta r + Cn_{\beta_w}\beta_w + Cn_p(P) + Cn_r(r)$$

$$I_{xx}\frac{\dot{r}}{57.3} = I_{xz}\left(\frac{\dot{r}}{57.3}\right) + q\,S\,b\,C_l$$

$$I_{zz}\frac{\dot{r}}{57.3} = q\,S\,Cn\,b$$

$$P = \int \dot{P}\,dt$$

$$r = \int \dot{r}\,dt$$

$$\dot{\phi} = P + r\frac{\theta}{57.3}$$

$$\dot{\psi} = r\cos\phi + q\sin\phi$$

$$\phi = \int \dot{\phi}\,dt + \phi_0 \qquad (\phi_0 = \text{initial roll angle})$$

$$\psi = \int \dot{\psi}\,dt + \psi_0 \qquad (\psi_0 = \text{initial yaw angle})$$

SIDE FORCE

$$C_Y = C_{Y\delta_s}\delta s + C_{Y\delta_r}\delta r + C_{Y\beta_w}\beta_w + C_{Y_p}(P) + C_{Y_r}(r) + C_{Y\delta_w}\delta_w$$

$$a_Y = \frac{1}{m}\left(q\,S\,C_Y + W\sin\phi + T\frac{\beta r}{57.3}\right)$$

$$\dot{\beta}_p = P\frac{\alpha}{57.3} - r + \frac{57.3}{V}\,a_y$$

$$\beta_p = \int \dot{\beta}_p\,dt + \beta_0 \qquad (\beta_0 = \text{initial sideslip angle})$$

$$\beta = \beta_p + \beta_{GUST}$$

$$S_Y = S_{Y_0} + \int V\sin\psi_p\,dt \qquad (S_{y_o} = \text{initial lateral distance from runway})$$

$$\psi_p = \int\left(\frac{a_y}{V}\cdot\cos\phi - q\sin\phi\right)dt$$

TABLE A5-1 (CONT.)

$$\alpha_p = \alpha_0 + \int (q + 57.3 \frac{a_z}{V})\, dt \qquad (\alpha_0 = \text{initial } \alpha \text{ for trim})$$

$$\alpha = \alpha_p + \alpha_{GUST}$$

$$\theta = \gamma + \alpha_p$$

LIFT

$$C_L = C_{L_{\alpha=0}} + C_{L_\alpha}\alpha + C_{L_{\delta e}}\delta e + C_{L_{i_H}} i_H + C_{L_{\dot\alpha}}\dot\alpha + C_{L_q} q$$

$$(C_{L_{\alpha=0}} + C_{L_\alpha}\alpha \text{ limited to } C_{L_{MAX.}})$$

$$-a_z = \frac{1}{M}(qSC_L - W\cos\phi\cos\gamma)$$

$$\dot\gamma = -\frac{57.3}{V}(a_z\cos\phi + a_y \sin\phi)$$

$$\gamma = \int \dot\gamma\, dt - \gamma_0 \qquad (\gamma_0 = \text{initial flight path angle})$$

$$\dot h = V\sin\gamma$$

$$h = \int \dot h\, dt + h_0 \qquad (h_0 = \text{initial altitude})$$

ROLL AND YAW

$$C_l = C_{l_W} - C_{n_W}\frac{\alpha}{57.3} \qquad (C_{l_W} \text{ and } C_{n_W} \text{ defined below})$$

$$C_n = C_{n_W} + C_{l_W}\frac{\alpha}{57.3}$$

$$C_{l_W} = C_{l_{\delta s}}\delta_s + C_{l_{\delta a}}\delta a + C_{l_{\delta r}}\delta r + C_{l_{\beta_w}}\beta_w + C_{l_p}(P) + C_{l_r}(r)$$

202

The pilots outside view was limited to the visual TV scene by blocking out all windows not directly in front of him.

Motion of the cab was controlled by three linear hydraulic servo actuators. These were operated differentially or synchroniously for three degrees of motion; roll, pitch, and heave (vertical). The actuators were controlled in a closed loop fashion by the simulation. The roll axis of motion was scaled down by a factor of two so that a simulated roll angle of ten degrees produced five degrees of cab roll motion. This resulted in less side acceleration error apparent to the pilot in a steady turn due to gravity. The pilot received the proper roll cues from the instruments and visual scene. A tabulation of the moving-base transport simulator physical characteristics is shown in Table A5-2.

The visual scene was produced by a closed circuit color television system which utilized a scale contour map including roads, buildings and fields, as well as the runway to which the approaches were conducted. A color television camera was positioned by electric servos and driven closed loop by the simulation. The scope of the simulated airplane movements was limited only by the boundaries of the contour map. Descent through a cloud layer was simulated by obliterating the picture to a pre-selected altitude. The tabulated physical characteristics of the visual display system are shown in Table A5-2.

TABLE A5-2

SYSTEM CAPABILITIES

Ames Moving-Base Transport Simulator

Motions Generated:	Acceleration	Displacement
Roll	1 Rad/Sec^2	± 9°
Pitch	0.5 Rad/Sec^2	+ 14° - 6°
Heave (vertical)	± 0.8g (from ambient)	24 inches

Ames Landing-Approach Color Television Display

Motions Generated	Velocity	Displacement
Roll	0.35 Rad/Sec	--
Pitch	0.52 Rad/Sec	--
Yaw	0.17 Rad/Sec	360°
Lateral	240 Knots	2 1/2 miles
Vertical	6000 ft/min.	1500 ft. to 20 ft.
Longitudinal (runway length)	240 knots --	9 miles 10,000 ft. (model scale 1:1200)

APPENDIX 6

The following is a description of the documentation maneuvers performed by the evaluation pilots:

Longitudinal Maneuvers

Pitch Rate Reversal — The airplane was trimmed by the safety pilot before engaging simulation. After stabilizing in steady flight pitch rate reversals were performed. The maneuver was initiated by applying a sharp column input, then quickly applying a step column input in the opposite direction. The column was stabilized, the airspeed held within 2 knots of trim, and the angle of attack held within 1° of trim when the pitch rate reversed.

Column Step — From a stabilized flight condition, an aft column step was applied with amplitude sufficient to give a 1.2g maneuver. Recover was initiated after peak load factor was reached.

Wind Up Turn — Wind up turns to 45° bank angle were performed, stabilizing in 5° bank increments.

Speed Stability — The safety pilot trimmed the airplane in level flight. From initial trim the speed was increased and decreased in 5 kts increments using elevator only.

Phugoid — The aispeed was decreased 10 kts from trim using elevator only. The controls were released and the phugoid was allowed to continue for two cycles. If the phugoid was divergent the maneuver was repeated with an initial 5 knot decrease in airspeed.

Pitch Attitude	A precision pitch attitude change of 5° to 10° was performed in minimum time, using the flight director for attitude reference.
Elevator Pulse	The airplane was trimmed in the initial configuration by the safety pilot before engaging simulation. The column pulse was then applied from the computer.

Lateral Maneuvers

Steady Roll Rate	The airplane was stabilized in a steady turn and step wheel inputs were applied.
Roll Rate Reversal	The roll rate reversals were initiated by pulsing the wheel sharply, then applying the specified step wheel input in the opposite direction. When done properly the wheel was stabilized and the sideslip angle was less than 2° when the roll rate reversed.
Yaw Rate Reversal	After the safety pilot trimmed the airplane, the yaw rate reversal was initiated by the evaluation pilot with an 8° sharp rudder input followed by an opposite rudder step input as required. When done properly the sideslip was less than 2° and the rudder pedals were stabilized when the yaw rate reversed.
Steady Sideslip	With the airplane in the trimmed condition the evaluation pilot stabilized in a 10° sideslip, released the controls, and re-stabilized in level flight.
Spiral Stability	The configuration was stabilized in a 10° right turn and the controls were released. Recovery was initiated when the bank angle reached either 5° or 20°.

206

20° Heading Change	The evaluation pilot performed a 20° heading change in minimum time.
Wheel Step	With the airplane in level flight a full wheel step was applied rapidly with recovery initiated when the bank angle reached 15°.
Wheel Pulse	The airplane was trimmed in the initial configuration by the safety pilot before engaging simulation. The wheel pulse was applied from the computer.
Rudder Pulse	The airplane was trimmed in the initial configuration by the safety pilot before engaging simulation. The rudder pulse was applied from the computer.